TRANSLATION

INFRARED TECHNOLOGY IN MILITARY MATTERS

By

Yu. A. Ivanov and B. V. Tyapkin

FOREIGN TECHNOLOGY DIVISION

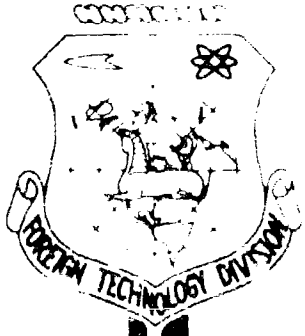

AIR FORCE SYSTEMS COMMAND

WRIGHT-PATTERSON AIR FORCE BASE

OHIO

FTD-MT-

EDITED MACHINE TRANSLATION

INFRARED TECHNOLOGY IN MILITARY MATTERS

BY: Yu. A. Ivanov and P. V. Tyapkin

English Pages: 327

Insert MT-64-121

THIS TRANSLATION IS A RENDITION OF THE ORIGINAL FOREIGN TEXT WITHOUT ANY ANALYTICAL OR EDITORIAL COMMENT. STATEMENTS OR THEORIES ADVOCATED OR IMPLIED ARE THOSE OF THE SOURCE AND DO NOT NECESSARILY REFLECT THE POSITION OR OPINION OF THE FOREIGN TECHNOLOGY DIVISION.

PREPARED BY:

TRANSLATION DIVISION
FOREIGN TECHNOLOGY DIVISION
WP-AFB, OHIO.

Yu. A. Ivanov
B. V. Tyapkin

INFRAKRASNAYA TEKHNIKA V VOYENNOM DELE

Izdatel'stcv "Sovetskoe Radio"

Moskva-1963

Pages 1-359

TABLE OF CONTENTS

In this book are presented basic physical phenomena assumed as a basis for military application of instruments of infrared technology; there are considered certain elements of these instruments, and also there are expounded questions of military application of infrared rays for the solution of separate tactical problems.

Construction and tactically technical data of some instruments of infrared technology are borrowed from the foreign press based on their status in 1960.

This book is calculated basically for the military reader, however it may be useful for a wider circle of readers interested in the development of a means of technology of infrared rays.

MT-64-153,
Infrared Technology in Military Ma ters.
Moscow, Izd. "Sovetskoye Radio," 1963.
Pa es: Co er - 399

PREFACE

The technology of infrared rays is a divisior of contemporary physics and electronics, embracing questions o' radiation, propagation, and registration of infrared rays, and also their practical use in research laboratories, industry, and military matters.

In this book are considered physical phenomena connected with radiation, propagation, and registration of infrared rays; it presents generalized material of works in the re- on of military application of infrared rays and makes an attempt at analysis of the promising developments in this comparatively young region of military technology.

The book consists of two parts. In the first part, including six chapters, are considered questions of physics and technology of radiation, propagation, and registration of infrared rays, and also certain elements of military instruments founded on the use of infrared rays. In this respect the first part is introductory for the second, including six chapters, where an analysis is made of the development and contemporary state of instruments of infrared technology applied by foreign armies.

In the second part the greatest attenti n is given to questions of intelligence, detection, and aiming with help of instruments of infrared technology, which i not sufficiently illuminated in domes ic l teratu e.

The size of the book did not allow authors to consider adjacent questions concerning principles of construction of instruments of infrared technology, luminescence, electronic and geometric optics, the error of these systems during construction of the image, and several other questions. With respect to these questions the authors refer the readers to corresponding courses of optics and physics.

In this book all concrete examples, concerning constructive solutions, technical and tactical appraisals and characteristics, and also prospects of development, are based on material of foreign technical literature. The list of literature used is given at the end of the book.

The authors thank Engineer-Lieutenant Colonel I. F. Usol'tsev for a number of valuable indications during the editing of the book, Doctor of Technical Sciences I. Z. Kriksunov, and Candidate of the Technical Sciences M. A. Bramson, for taking on the labor of reviewing the book, and also Engineer S. V. Yudkevich for attentively examining certain chapters of the manuscript. Their advice was considered during final editing of the manuscript.

During work on the book Chapter IX (Sections 1 - 3) and Chapter X (Sections 1 - 2) were written by B. V. Tyapkin; the remaining chapters by Yu. A. Ivanov

INTRODUCTION

In the period of the Second World War in the arming of armies of the fighting states there began to appear various instruments facilitating the conduct of combat actions at night. Among them, in the first place, one should include radar and heat-direction finding equipment and instruments of night vision. Already the first application of infrared instruments showed promise for the solution of a majority of tactical problems on land, in the air, and on the sea during favorable meteorological conditions. Therefore, in the postwar period the volume of works in the region of military application of infrared instruments has sharply increased. Simultaneously they began to develop tactics of their application in troops and intensely to equip, with infrared equipment, the Army, the Air Force, antiaircraft defense, and the Navy.

Large works in the region of military application of infrared rays are conducted in the United States, England, France, Italy, the Federal Republic of Germany, Sweden, Japan, Switzerland, and in certain other countries.

The significant interest toward infrared instruments is caused by the advantages which infrared radiation possesses as compared to the electromagnetic oscillations of radar and light ranges of wave lengths.

1. Infrared beams are radiated by practically all bodies having a temperature other than a solute zero. Consequently, infrared instruments can be a passive

principle of action and do not require, for detection of target, its irradiation by electromagnetic energy.

2. Infrared rays are not detected by the eye, therefore, both passive and active instruments of infrared technology cannot be detected by an enemy not armed with corresponding equipment.

3. Since the transparency of the atmosphere is better for infrared rays than for visible ones, it allows us to increase the range of infrared instruments as compared to optical and, what is most important, allows us to carry out observation of targets at night in the absence of their visual visibility.

4. With correct selection of range of spectral sensitivity of passive infrared instruments, losses of radiation energy in the atmosphere are proportional to the square of distance, while losses of energy of electromagnetic oscillations of radar instruments are proportional to the fourth degree of distance. This allows us to create infrared instruments which are simpler, with less weight and smaller dimensions than radar of the same purpose and with the same range.

5. Simplicity of construction, naturally, determines higher reliability of infrared instruments as compared to radar equipment.

6. The passive principle of action and the presence of the possibility, by simple means, to free themselves from the hindering effect of the background (selection of target) make infrared instruments less subject to interferences on the part of the enemy as compared with radar stations.

7. Using for their work electromagnetic oscillations of a range of waves between visible light and millimeter waves, infrared instruments, while yielding in resolving power to optical systems, significantly exceed radars in this respect. Thus, for instance, although radar stations with an 8-mm range of waves and with an antenna diameter of 30 cm allow us to resolve from a range of 8,000 m two targets at a distance of 400-500 m, a heat-direction finder with mirror 7.5 cm in diameter and a photoresistor of PbS allows us to observe from the same range separate motors of an aircraft located at a distance of 8 m from each other.

Still higher resolving power have electronic optical systems, ensuring the observation of objects in infrared rays almost with photographic clearness.

However, such fundamental deficiencies of infrared methods of aiming as the practical impossibility of their work in unfavorable meteorological conditions (fog, overcast), and also the difficulty of target range measurement force us to apply them in combination with radar technology.

Nevertheless, in spite of these deficiencies, in the arming of capitalist countries there have appeared, in ever increasing quantities, infrared instruments for solving, in combination with other means, the following problems:

1) Tactical and strategic intelligence,

2) The guiding of rockets and missiles to heat-radiating targets,

3) Noncontact blowing up of ammunition near target,

4) Detection of heat-radiating targets at night and aiming by them,

5) Navigation,

6) Communications and signalling between units,

7) Protection of military objects and the blocking of narrow sections of country.

Along with the solution of these problems there is conducted also intense research in the region of the use of infrared instruments for the needs of antimissile defense, intelligence from space, and communications in space.

P A R T I

PHYSICAL BASES AND ELEMENTS OF INSTRUMENTS OF INFRARED TECHNOLOGY

C H A P T E R I

BASIC IDEAS ABOUT RADIATION

1. Nature of Radiation

Radiation we understand as the transfer in space from one body to other of energy either with the help of particles of matter (β and α -radiation during radioactive decay), or with the help of an alternating electromagnetic field (γ -radiation, x-radiation, light, infrared rays and radio waves).

From all the variety of forms of radiation there will subsequently be considered only the so-called optical radiation, and in it, in turn, - the still narrower region of infrared rays.

As any electromagnetic oscillation, infrared radiation is possible to characterize by frequency ν , wave length λ and speed of propagation v.

Sometimes electromagnetic oscillations are characterized by wave number A, under which we understand a number of wave lengths, packed in a section, equal to one centimeter.

Connection between basic magnitudes of radiation is determined, as is known, by ratios:

$$\lambda = \frac{c}{\nu} . \qquad (I.1)$$

$$v = \frac{\lambda}{T} , \qquad (I.2)$$

where $c = 2.998 \cdot 10^{10}$ cm/sec is the speed of light in a vacuum;

T is the period of oscillations.

In a medium, whose index of refraction is not equal to unity ($n \neq 1$), the speed of propagation of electromagnetic oscillations differs from the speed of light in a vacuum

$$v' = \frac{c}{n}. \qquad (I.3)$$

By comparing (I.2) and (I.3), it is possible to note that for one and the same radiation the wave length will change depending upon the medium, where propagation of electromagnetic oscillations occurs, whereas their frequency remains constant.

The range of waves of electromagnetic oscillations is very great — from 10^{-11} to $3 \cdot 10^{10}$ cm. Therefore, for the measurement of wave length of electromagnetic oscillations, along with well-known units of length, we use the smaller ones: micron (μ), millimicron ($m\mu$), angstron ($\mathring{A}$) and ex (X) (Table I.1).

Table I.1. Connection Between Units of Measurement of the Wave Length of Electromagnetic Oscillations

Units	m	cm	mm	μ	$m\mu$	$\mathring{A}$	X
1 Meter.....	1	10^2	10^3	10^6	10^9	10^{10}	10^{13}
1 Centimeter...	10^{-2}	1	10	10^4	10^7	10^8	10^{11}
1 Millimeter...	10^{-3}	10^{-1}	1	10^3	10^6	10^7	10^{10}
1 Micron.....	10^{-6}	10^{-4}	10^{-3}	1	10^3	10^4	10^7
1 Millimicron..	10^{-9}	10^{-7}	10^{-6}	10^{-3}	1	10	10^4
1 Angstron.....	10^{-10}	10^{-8}	10^{-7}	10^{-4}	10^{-1}	1	10^3
1 x..... ...	10^{-13}	10^{-11}	10^{-10}	10^{-7}	10^{-4}	10^{-3}	1

A wide range of waves of electromagnetic radiation is conveniently presented in the form of a scale broken down into separate regions, including oscillations similar in their properties, methods of obtaining, and methods of registration (Fig. I.1).

As can be seen from scale of electromagnetic oscillations, the region of optical radiation includes oscillation of waves approximately from 10 $m\mu$ to 340 μ , and the range of infrared rays lies within limits of 0.75—340 μ *.

Electromagnetic oscillation have dual character, i.e., possess both wave properties and corpuscular.

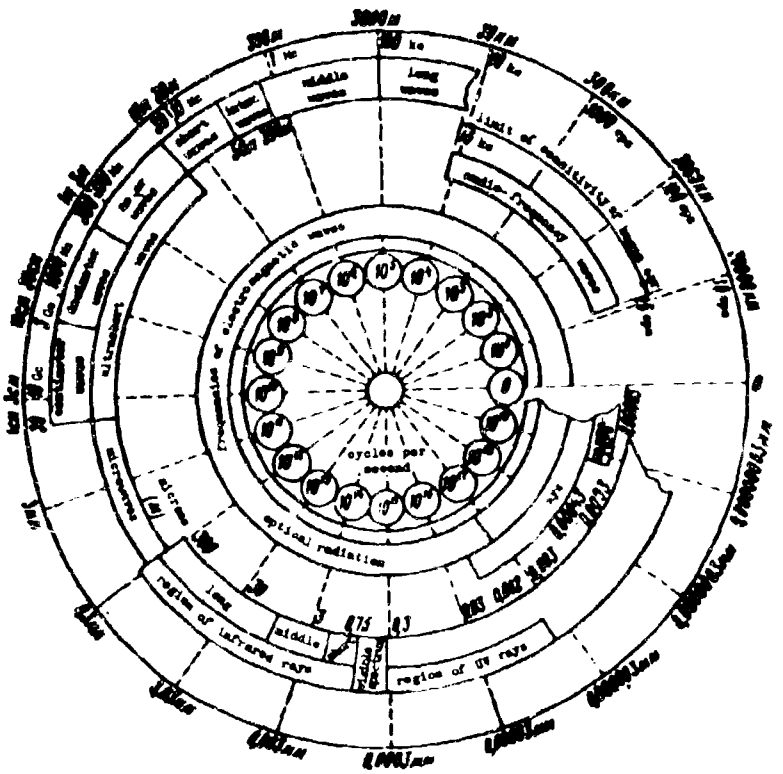

Fig. I.1. Spectrum of electromagnetic oscillations.

*Based on contemporary data, this range can be expanded to 720–750 μ , i.e., up to submillimeter radio waves.—Editors Note.

Wave electromagnetic theory of radiation explains well a series of optical phenomena: interference, diffraction, polarization, reflection, and refraction of light rays. However it is contradicted by experimental data during explanation of phenomena, connected with interaction of radiation with substance; -- distributic of energy in spectrum of radiation of heated bodies, photoelectric effect, light scattering, etc.

Tab e I.2. Energy of Photons of Electromagnetic Oscillations of Different Wave Length

(1 ev = $1.59 \cdot 10^{-12}$erg)

Wave Length, μ	Energy of Photon	
	erg	ev
(	$6.22 \cdot 10^{-12}$	3.9
0.55	$3.4 \cdot 10^{-12}$	2.14
0.76	$2.46 \cdot 10^{-12}$	1.53
1	$1.87 \cdot 10^{-12}$	1.17
1.3	$1.44 \cdot 10^{-12}$	0.91
3	$0.62 \cdot 10^{-12}$	0.39
5	$0.37 \cdot 10^{-12}$	0.23
12	$0.16 \cdot 10^{-12}$	0.10

A way out was found after publicatior in 1900 by Planck of the quantum theory of radiation. This theory carries the idea of iscretion (discontinuity) of the structure of matter to electromagnetic processes of radiation. According to this theory the energy of elementary radiators (atoms and molecules) can change only by jumps, multiples of a certain value constant for a given frequency. Such a minimum (for a given frequency of radiation) portion f energy Planck called a quantum of energy,

$$\varepsilon = h\nu, \qquad (I.4)$$

where $h = 6.6238 \cdot 10^{-27}$erg·sec is the universal Planck's constant.

Later, in 1905, Einstein developed Planck's theory further and carried the idea of discretion of radiation to propagation and absorption of electromagnetic waves. Radiation began to be considered as flux of particles of matter - photons - with energy $h\nu$ and mass

$$m_\phi = \frac{h\nu}{c^2}. \qquad (I.5)^*$$

*The Russian subscript "ф" indicates "photon". -Ed.

Consequently, in accordance with the quantum theory radiation is considered not only as a process of transformation of one form of energy into another, but as a transition of matter from a form of substance into a form of electromagnetic field, and conversely.

In Table I.2 are presented values of energy of photons with different wave lengths.

2. Energy Characteristics of Radiation

Application of instruments of infrared technology is based on registration or quantitative measurement of energy, transferable by electromagnetic wave from the source of radiation to the receiver.

Depending upon receiving devices and spectral composition of the radiation subject to measurement, two systems of units are established - energy and light technology (Table I.3).

First system of units is universal and may be applied to the whole range of spectrum of optical radiation; the second - light technology - may be used only in the region of visible radiation and loses meaning in the region of ultraviolet and infrared rays. Therefore, subsequently there will be considered only magnitudes taken in the energy system of units. Designation of magnitudes is given in the new terminology recommended by the Committee of Technical Terminology of the Academy of Sciences of the USSR.

Radiant flux Φ characterizes power of optical radiation and allows us to judge energy content of radiation hitting optical instruments,

$$\Phi \quad \frac{\Delta W}{\Delta t}, \qquad (I.6)$$

where W is energy of radiation.

In the case of monochromatic radiation radiant flux is estimated by the spectral power of the energy of radiation. For sources of optical radiation having continuous spectrum, the total radiant flux is determined by the area between the

spectral curve of radiation and the axis of abscissas.

$$\Phi = \int_{\lambda_1}^{\lambda_2} \varphi_\lambda d\lambda. \qquad (I.7)$$

Table I.3. Light Technology and Energy Systems of Units of Measurement of Radiation Energy

	Designation of Magnitude	Systems of Units			
		Light Technology		Energy	
		Designation	Unit	Designation	Unit
Radiated Energy	Total energy	Light energy	lu·sec	Energy of Radiation	w·sec
	Energy per unit of time	Luminous flux	lu	Radiant flux	w
	Energy per unit of time and on a unit of solid angle	Luminous intensity	cp	Radiation intensity	$\frac{w}{sterad}$
	Energy per unit of time from a unit of surface	Lightness	$\frac{lu}{m^2}$	Density of Radiation	$\frac{w}{cm^2}$
	Energy per unit of time on a unit of solid angle from a unit of surface	Brightness	stilb	Radiance	$\frac{w}{cm^2 sterad}$
	Energy on a unit of supplied power	Luminous efficiency	lu/w	Radiation yield	—
Incident Energy	Energy on a unit of area	Quantity of illumination	lux·sec	Quantity of Irradiation	$\frac{w \cdot sec}{cm^2}$
	Energy on a unit of area per unit of time	Illuminance	lux	Irradiance	$\frac{w}{cm^2}$

Radiant flux is measured in units of power, and in some cases its power is compared with the power of particle flux, expressed in ev/sec. In this case transition to the usual units of power can be carried out, using the following relationship, 1 w = $6.29 \cdot 10^{20}$ ev/sec.

Table I.4. Connection Between Basic Units of Measurement of Power of Radiant Flux

Designation of unit	erg/sec	w	cal/sec	cal/min
1 erg/sec	1	$0,9997 \cdot 10^{-7}$	$2,389 \cdot 10^{-8}$	$1,434 \cdot 10^{-6}$
1 w	$1,003 \cdot 10^{7}$	1	0,239	14,34
1 cal/sec	$4,185 \cdot 10^{7}$	4,185	1	60
1 cal/min	$6,976 \cdot 10^{5}$	0,06976	0,01667	1

Space character of distribution of radiant flux is determined by radiation intensity J, under which we understand the ratio of radiant flux to magnitude of solid angle, in which radiation is evenly distributed. Therefore, sometimes the idea "radiation intensity" is defined as angular density of radiant flux in a given direction

$$J = \frac{\Delta\Phi}{\Delta\omega}. \qquad (I.8)$$

This idea is valid only in a case of radiation of a point source. However, in practice, with sufficient accuracy, this idea can be used also in a case of sources whose linear dimensions are significantly less than the distances at which their radiation is taken.

Magnitude of solid angle ω may be defined as the ratio of a surface, cut by a cone with a summit in center of sphere, to the square of its radius

$$\omega = \frac{a}{r^2}. \qquad (I.9)$$

For a unit of solid angle is taken steradian - a solid angle, to which on the sphere of the unit radius there corresponds a surface with an area equal to unity. A solid angle, embracing all space around a point source of radiation, is equal to 4π. Therefore, with equal distribution of radiant flux in all directions, radiation intensity in a given direction may be calculated by the formula

$$J = \frac{\Phi}{4\pi}. \qquad (I.10)$$

In the case of nonuniform distribution of radiant flux in space it is necessary to introduce the idea of average-spherical (average-hemispherical) radiation intensity, under which we understand radiation intensity of a source with equal distribution of radiant flux, whose magnitude is equal to the radiant flux of a source with nonuniform distribution.

From the resulting expressions can be made one very important conclusion in order to understand the essence of the work of rources of radiant flux: the magnitude of full radiant flux of a given source of radiation cannot be increased by optical systems. Application of optical systems allows us only to redistribute radiant flux from one direction to another.

When determining radiation of real bodies of different configuration, the calculation of radiant flux and radiation intensity presents well-known difficulties. Therefore, in Table I.5 are given characteristics of radiation of sources of the simplest form, which in a number of cases, by means of combining, can simplify the calculation of radiation of sources even of a more complicated form.

Table I.5. Characteristics of Radiation of Bodies of Simple Form

Form of Source of Radiation	Radiation Intensity	Radiant Flux	Average-Spherical Radiation Intensity
Luminescent Disk	$J = J_0 \cos\alpha$	$\Phi = \pi J_0$	$\frac{1}{4} J_0$
Luminescent Sphere	$J = J_0 = \text{const}$	$\Phi = 4\pi J_0$	J_0
Luminescent Hemisphere	$J = \frac{J_0}{2}(1+\cos\alpha)$	$\Phi = 2\pi J_0$	$\frac{1}{2} J_0$
Luminescent Cylinder	$J = J_{90} \sin\alpha$	$\Phi = \pi^2 J_{90}$	$\frac{\pi}{4} J_{90}$
Luminescent Cylinder with spherical end	$J = \frac{J_0}{2}(1+$ $+\cos\alpha) + J_{90}\sin\alpha$	$\Phi = 2\pi J_0 +$ $+\pi^2 J_{90}$	$\frac{1}{2} J_0 +$ $+\frac{\pi}{4} J_{90}$

NOTE: J_0 is radiation intensity in a direction normal to the radiating surface,

J_{90} is radiation intensity at an angle of 90° to the axis of a cylinder,

J is radiation intensity at angle α to normal.

Density of radiation $\mathcal{R}$ characterizes surface density of radiant flux emitted by the surface of a given source. Quantitatively it is equal to the ratio of total radiant flux inside solid angle 2π to the area of the radiating surface:

$$\mathcal{R} = \frac{\Delta\Phi}{\Delta S}. \qquad (I.11)$$

Radiance $\mathcal{B}$ characterizes surface density of radiation intensity in a given direction or, in other words, this is the ratio of radiation intensity to the area of projection of the radiating surface to a plane (Fig. I.2), perpendicular to a given direction:

$$\mathcal{B} = \frac{\Delta J}{\Delta S \cos\alpha}. \qquad (I.12)$$

For surfaces whose radiation obeys the law of Lambert and, consequently, does not depend on direction, the magnitude of radiance also does not depend on direction. For such bodies, dependency between radiation density and radiance takes the form:

$$\mathcal{R} = \pi\mathcal{B}. \qquad (I.13)$$

Irradiance $\mathcal{E}$ characterizes surface density of radiant flux incident on a given surface. Numerically it is equal to the ratio of radiant flux to the area of irradiated surface, on which it is evenly distributed

$$\mathcal{E} = \frac{\Delta\Phi}{\Delta S}. \qquad (I.14)$$

Expressing radiant flux through radiation intensity, we obtain

$$\mathcal{E} = \frac{J\cos\alpha}{r^2}. \qquad (I.15)$$

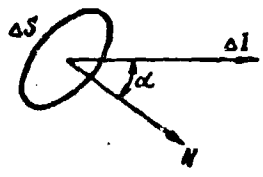

Fig. I.2. Determination of radiance.

The last equality shows that irradiance of a surface, created by a point source, is reciprocal to the square of the distance between irradiated surface and source and depends on the angle between direction of radiant flux and the normal to a given surface (Fig. I.3).

For surfaces whose radiation obeys the law of Lambert, irradiance is connected with radiation density and radiance by the following relationships,

$$\mathcal{E} = \mathcal{R}; \tag{I.16}$$

$$\mathcal{I} = \frac{\mathcal{E}}{\pi}. \tag{I.17}$$

Quantity of irradiation $\mathcal{H}$ determines energy content of radiation falling on an irradiated body for a definite time,

$$\mathcal{H} = \int \mathcal{E} dt. \tag{I.18}$$

This idea finds wide application in different photochemical processes, and, in particular, in photography, where quantity of reacted substance is proportional to the power of incident radiation (irradiance) and the time of action.

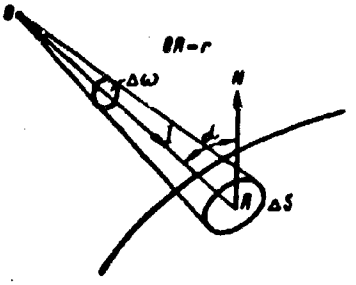

Fig. I.3. Determination of irradiance of a surface.

Radiation yield $\eta_э$ determines effectiveness of one or another source of radiation, in which there occurs transformation of some form of energy into energy of radiation. Quantitatively radiation yield is determined by the ratio of radiant flux radiated by a source to the power supplied to it.

$$\eta_э = \frac{\Phi}{\mathcal{P}} 100\%. \tag{I.19}$$

If one were to determine the effectiveness of a source of radiation with respect to some definite receiver of radiant flux, determining the effectiveness of the use of spectral energy of radiation of a given source, then, considering (I.7) and (I.11), we obtain

$$\eta_э = \frac{S \int_{\lambda_1}^{\lambda_2} S_\lambda r_\lambda d\lambda}{\mathcal{P}}, \tag{I.20}$$

where λ_1 and λ_2 are boundaries of sensitivity of the receiver of radiation,

r_λ is spectral intensity of radiation density of a source in the range of sensitivity of the receiver,

S_λ is spectral sensitivity of the receiver.

3. Spectrum of Optical Radiation and its Image

Under spectrum of optical radiation we understand the ordered location of separate monochromatic radiations by wave lengths. Such location can have the form of a continuous curve and separate lines or bands between which radiation is absent (Fig. I.4).

In the first case they have something to do with a solid (continuous) spectrum of optical radiation, consisting of an infinite number of lines continuously following one after another. This form of spectrum is characteristic for radiation of heated solid and liquid bodies. In certain cases, for instance at very large pressures, a continuous spectrum is created by the radiation of gasiform atoms and molecules.

In the second case the spectrum of radiation will be called either line or band.

Line spectra consist of separate thin lines distinctly divided from each other. Such spectra are radiated by excited atoms or ions, at such a distance from each other that their radiation can be considered independent. Therefore, heated gases or vapor at normal pressure always give line spectra.

Band spectra consist of a large number of closely located lines, forming separate, clearly differentiated bands. These spectra appear during the study of molecules of gases consisting of two or more atoms, with such a distance between molecules that their radiation can be considered independent. Therefore, band spectra are radiated by polyatomic molecules of heated gases, whose temperature still is insufficient for dissociation of their molecules into atoms or ions.

If radiation is formed as a result of several different processes, then mixed spectra can be formed. An example of such a form of spectra is the spectrum of radiation of an electrical arc, gas-discharge tubes of high and super-high pressure, etc.

Besides such division, a spectrum of optical radiation is sometimes conveniently subdivided by the nature of appearance and methods of its registration. Such a classification is shown in Fig. I.5, where, besides the nature of radiation and the receivers for its registration, there are indicated sources of radiation, and also wave lengths, frequency and wave numbers, corresponding to some spectrum of radiation

Fig. I.4. Types of radiation spectra. 1—Line; 2—Band; 3—Continuous; 4—Mixed.

In practical application of infrared instruments there is always actually measured the irradiance of the receiving device, created by the measured radiation. Therefore, it is more correct to talk, not about the spectrum of radiation, but about the distribution of irradiance created by a spectrum of given radiation in the plane of the receiving device. In this case, automatically considered are losses of radiation in the thickness of the medium where measured radiation spreads. If it is necessary to obtain data about the real spectrum of radiation it is necessary to obtain data about the real spectrum of radiation it is necessary to determine losses in a medium at a given distance and to introduce correction in the obtained results of measurement of irradiance.

There can be practically recommended three methods of plotting spectral curves of irradiance.

It is possible to present a continuous spectrum (Fig. I.6) consisting of separate spectral lines located at equal and minute spectral intervals "a". For every such line one can determine irradiance in w/cm^2 and plot it on the graph in the form of an ordinate. The width of spectral intervals depends upon the structure of the spectrum: the thinner the spectrum, the narrower must be the spectral intervals. The sum of all ordinates gives in this case the general irradiance of the receiver, created by all the spectrum of radiation.

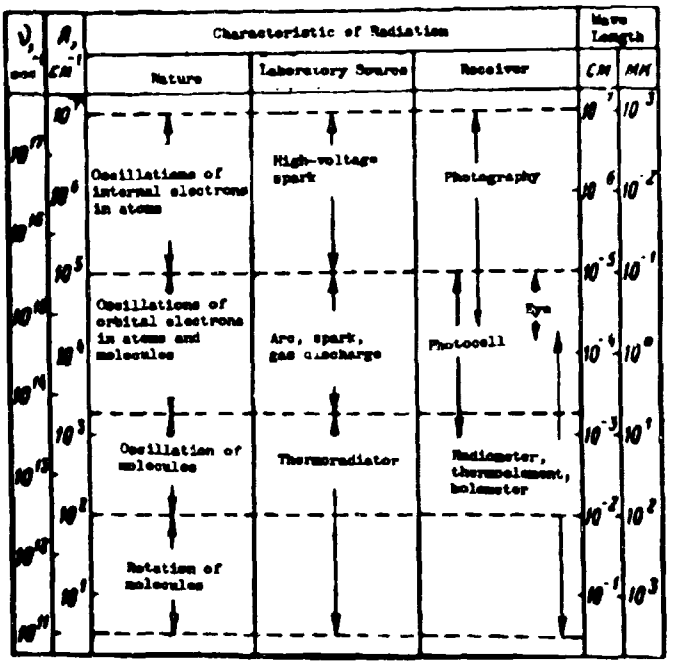

Fig. I.5. Spectrum of optical radiations.

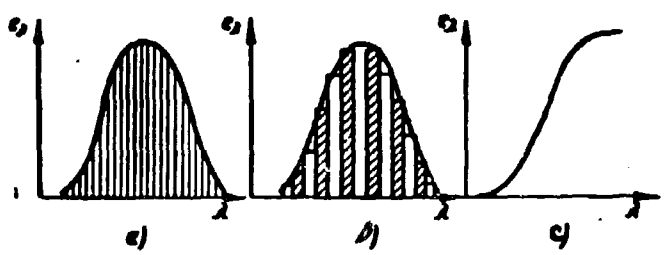

Fig. I.6. Methods of plotting spectral curves of irradiance.

Another method of plotting a spectrum of irradiance consists of plotting irradiance of separate spectral intervals in the form of rectangular plateaus "b". Wave length in this case is taken in linear scale. The area of a rectangle equal to the product of $e_\lambda \Delta\lambda$, is the measure of irradiance created by radiation at a given wavelength interval. Since magnitude $\Delta\lambda$ has a dimension of length, then for the product of $e_\lambda \Delta\lambda$ to have dimension of irradiance (w/cm^2), spectral intensity of irradiance e_λ should have dimension of w/cm^3. Its numerical value depends on the selection of a unit of measurement of length of spectral interval. Thus, if $\Delta\lambda$ is expressed in millimicrons, then in order to recalculate irradiance in

w/cm^2 for a wave length interval expressed in cm, to a magnitude of irradiance in w/cm^2 for a wave length interval in $m\mu$, it is necessary that all ordinates be decreased in 10^7 times. For instance, if $e_\lambda = 10\ w/cm^3$, this corresponds to irradiance 1 microwatt/cm^2 for 1 $m\mu$.

A spectrum, depicted thus, presents rectangles continuously following one after the other. Their sum is the measure of irradiance created by the entire spectrum of radiation. Decreasing the width of spectral intervals, there can be obtained at the end an envelope repeating all the details of the structure of the spectrum. In this case, the measure of irradiance is the area between the circle and the axis of abscissas.

If along the axis of abscissas nonlinear scale is applied, then, for the purpose of preserving elementary rectangles as the measure of irradiance for the corresponding wavelength intervals, it is necessary to change simultaneously in inverse ratio the scale along the axis of the ordinates.

The third, the intergal method of plotting the spectrum of irradiance (Fig. I.6 c) is characterised by the fact that to every wave length will be added the integral value of measured irradiance. Summation is produced from the shortwave boundary to the considered wave length. With such construction a continuous spectrum of irradiance will be depicted in the form of a monotonically increasing curve. This curve allows us to determine the value of irradiance for any spectral interval, but does not allow us to clarify the structure of the spectrum. Limitations in selection of scale with such a method of construction of irradiance spectrum are dropped.

By the above-considered methods it is possible also to depict line, band, and mixed spectra. With an integral method of plotting line spectrum, the latter will be in the form of a broken line.

Mixed spectra are very conveniently depicted by the method of rectangles, since it allows us to estimate energy of continuous and line spectra by means of the comparison of their areas.

CHAPTER II

SOURCES OF RADIATION

1. Classification of Sources of Radiation

From the physical point of view a source of radiation energy may be any system of matter, in which there occurs transformation of the energy supplied to it into energy of radiation. In accordance with this, all sources of radiation energy it is possible to break down into three basic groups - thermal, luminescent and mixed*.

To the first group belong sources for which radiation energy is the result of conversion of thermal energy. It does not matter by what means thermal energy appears: as a result of passage of a current in a medium, by means of chemical reaction, or as a result of the conversion of mechanical energy.

The second group includes sources for which radiation energy appears as a result of excitation of atoms and molecules of a substance by some kind of external exciter. Under luminescent radiation we understand optical radiation of a body above its thermal radiation at that same temperature, lasting more than 10^{-10} sec.

In the third group are sources in which both thermal and luminescent radiation simultaneously assist.

The most widespread group of radiation sources in nature are thermal sources. The power of their radiation depends on temperature, dimension, and surface properties of the radiating body. At a given temperature and surface magnitude the

*Considered are sources of incoherent radiation of the optical range of waves.--Editor's note.

properties of a body from the point of view of radiation can be simply determined by absorbing ability $a_{\lambda T}$. Depending upon the character of the change in magnitude of the absorbing ability during a change in temperature of a body and the wave length of radiation incident on its surface, thermal sources of the radiation can be of three forms:

1. An ideal black body, for which absorbing ability does not depend on wave length of radiation incident on it or on temperature of its surface and remains always equal to unity. Such a body, as compared to other bodies, has the biggest emissive power of radiation at a given temperature for all wave lengths.

2. A gray body, for which absorbing ability, while remaining less than unity, depends on temperature, but does not depend on wave length of incident radiation.

3. A selective-absorbing body, for which absorbing ability, while remaining less than unity, depends on wave length of incident radiation and on temperature of body.

2. Radiation of an Ideal Black Body

An ideal black body (AChT), although it does not exist actually in nature, is of interest for two reasons: first, it, at a given temperature, radiates maximum energy content and, secondly, its radiation may be calculated theoretically.

Furthermore, radiation of an ideal black body possesses properties which are absent in many cases in radiation of real bodies, but are namely;

a) Radiation of an ideal black body is nonpolarized,

b) It will obey the law of Lambert, and, consequently, the magnitude of emissivity of an ideal black body in all directions is identical,

c) Emissivity of an ideal black body is proportional to the square of the refractive index of the medium in which radiant flux spreads,

d) Radiation of an ideal black body depends only on wave length and temperature, for which form of basic functions of radiation $r_\lambda = f(T)$ and $r_\lambda = f_1(\lambda T)$ has universal character.

A model of an ideal black body with a very high degree of approximation can be made in the form of a closed box with a small hole, walls of which are evenly heated to the necessary temperature (Fig. II.1).

Getting into the hole of the box, the radiant flux, after multiple reflection on internal surfaces of the box is practically completely absorbed and only accidentally, with vanishingly minute energy, can emerge from the hole.

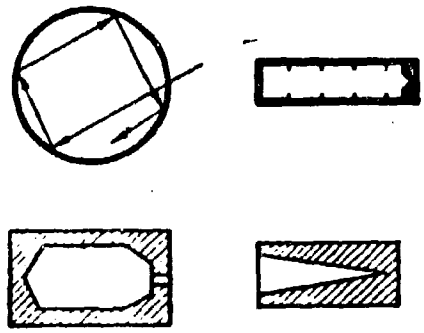

Fig. II.1. Diagram of models of an ideal black body.

If, however, we heat the walls of the box, then its hole will behave as an ideal black body with an area equal to the area of the hole. Besides, in spite of the fact that the internal surface of the walls of the box will radiate in accordance with the properties of the material, full radiation of the box through the hole will not depend on the material and properties of the walls, if the temperature of its separate parts is identical.

Radiation of an ideal black body may be calculated in accordance with the following laws.

Kirchhoff's Law

Kirchhoff's law indicates that the ratio of radiation and absorbing abilities of the same point of a body, for the same wave length of radiation, the same direction, and at a given temperature for all bodies is constant magnitude

$$\frac{e_{\lambda T}}{a_{\lambda T}} = \frac{e'_{\lambda T}}{a'_{\lambda T}} = \ldots = \text{const.} \qquad \text{(II.1)}$$

In the case of an ideal black body ($a_{\lambda T} = 1$) equality (II.1) will take the form

$$\frac{e_{\lambda T}}{a_{\lambda T}} = E_{\lambda T}. \qquad \text{(II.2)}$$

Equality (II.2) mathematically connects radiation of an ideal black body with the radiation of real bodies. As can be seen, emissivity of any body is equal to the product of emissivity of an ideal black body and the absorbing ability of a given body.

Kirchhoff's law is valid for any bodies, including gases, if they create a purely thermal radiation, however, i dill not apply, if onto thermal radiation is added luminescent.

The Stefan - Boltzmann Law

Integral density of radiation of an ideal black body is proportional to the fourth degree of its temperature

$$\mathcal{R} = \sigma T^4. \qquad \text{(II.3)}$$

where $\sigma = 5.672 \cdot 10^{-12} \frac{w}{cm^2 \cdot deg^4}$ is the radiation constant (Boltzmann constant).

$T = t^\circ C + 273$ is absolute temperature of the body.

For a body with area S (in cm^2) density of radiation will be determined by relationship

$$\mathcal{R} = \sigma S T^4. \qquad \text{(II.4)}$$

From formula (II.3) it is clear that the temperature of a body renders a decisive influence on the magnitude of radiation density of an ideal black body; thus, for example, an increase of absolute temperature of a body 2 times leads to growth of its radiation 16 times.

Expression (II.3) determines radiation density of an ideal black body with surface $S = 1\ cm^2$ within limits of a hemisphere. For determining radiance of ideal black body $\mathcal{R}$ within limits of solid angle ω, the axis of which constitutes angle α with normal to heat-radiating surface S, it is necessary to use expression

$$\mathcal{R} = \frac{\omega}{\pi} S \sigma T^4 \cos\alpha. \qquad \text{(II.5)}$$

Planck's Law

Distribution of energy in the radiation spectrum of an ideal black body is described by Planck's law, whose mathematical expression has the form

$$r_{\lambda T} = c_1 \lambda^{-5} \left(e^{\frac{c_2}{\lambda T}} - 1 \right)^{-1}, \qquad \text{(II.6)}$$

where λ is wave length,

T is absolute temperature,

$c_1 = 3.740 \cdot 10^{-12}$ w $\cdot$ cm^2,

$c_2 = 1.438$ cm $\cdot$ degree.

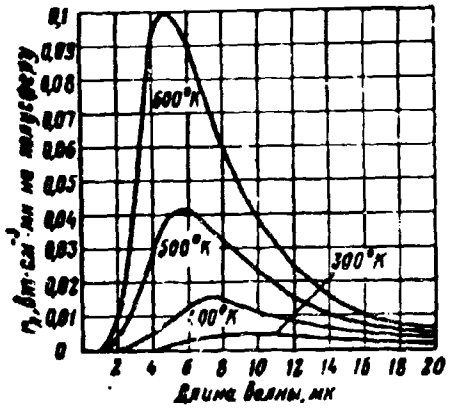

Fig. II.2. Spectral intensity of radiation density of an AChT (Ideal Black Body) at various temperatures.
KEY: (a) w$\cdot$cm^{-3} μ; (b) Wave length μ.

The course of curves of spectral density of radiation of an ideal black body (AChT), calculated by the formula of Planck, for certain temperatures is shown in Fig. II.2.

Wien's Law

The position of maximum of a curve of radiation at different temperatures of an ideal black body is determined by Wien's law (law of displacement).

$$\lambda_{\text{макс}} T = 2896 \quad \mu \cdot \text{deg}. \qquad \text{(II.7*)}$$

where $\lambda_{\text{макс}}$ is expressed in μ.

*The Russian subscript "макс" indicates "maximum".--Ed.

Finding from (II.7) value $\lambda_{макс}$ in cm and substituting it in (II.6) the value can be obtained of spectral density of radiation at a point, corresponding to $\lambda_{макс}$

$$r_{макс} = 1{,}301 \cdot 10^{-16} T^5 \ \frac{w}{cm^3} \qquad (II.8)$$

3. Radiation of Real Bodies

Radiation of real bodies differs from the radiation of an ideal black body. Therefore, they are called "nonblack", implying with this term both bodies with selective radiation and gray bodies.

As already was noted, radiation of these bodies, in the first place, is determined by the behavior of the absorbing ability with a change of temperature of the body and the wave length of incident radiation. Furthermore, when calculating radiation of real bodies it is necessary to consider that they are not isolated from each other and that, due to this, fluxes of their radiation energy consist of proper temperature radiation and reflected fluxes of energy radiated by neighboring bodies.

How closely radiation of a real body with a given wave length and at a given temperature coincides with radiation of an ideal black body can be judged if one were to introduce the concept of coefficient of emissivity $\varepsilon_{\lambda T}$:

$$\varepsilon_{\lambda T} = \frac{r^{c}_{\lambda T} + r^{o}_{\lambda T}}{(r_{\lambda T})_{АЧТ}}, \qquad (II.9)$$

where $r^{c}_{\lambda T}$ is spectral density of proper emission of body,

$r^{o}_{\lambda T}$ is spectral density of radiation reflected by body,

$(r_{\lambda T})_{АЧТ}$ is spectral density of radiation of an ideal black body.

From the resulting expression it is clear that in a case of only proper emission of body ($r^{o}_{\lambda T} = 0$) the coefficient of emissivity is equal to the absorbing ability of a given body

$$\varepsilon_{\lambda T} = a_{\lambda T}. \qquad (II.10)$$

In the presence of proper and reflected radiation it is possible to introduce the concept of a coefficient of blackness γ_T, under which we understand the ratio

of full radiation of a given body to its temperature radiation

$$\gamma_T = \frac{r_T}{r_T^c} = 1 + \frac{r_T^o}{r_T^c}. \qquad \text{(II.11)}$$

Comparing the resulting expressions, we will obtain

$$\varepsilon_T = \gamma_T a_T. \qquad \text{(II.12)}$$

From expression (II.12) it follows that for exposed bodies with high surface temperature ($\gamma_T \approx 1$) the coefficient of emissivity is equal to the absorbing ability of a body, however, in the case of exposed bodies with low temperature or radiation of internal cavities, the coefficient of emissivity and the absorbing ability of a body can significantly differ.

For gray bodies, whose absorbing ability depends only on temperature and does not depend on wave length of radiation, the law of integral radiation may be recorded, taking into account the coefficient of emissivity ε_λ, values of which, for different materials at definite temperatures, are presented in heat technology reference books.

Although with the calculation of the radiation of gray bodies, the matter is comparatively safe, since in this case it is necessary only to determine dependency $\varepsilon_\lambda = f(T)$, nevertheless, when estimating the radiation of selective radiating bodies, it is necessary additionally to consider dependency $\varepsilon_{\lambda T} = f(\lambda)$.

A widespread material in infrared technology with selective radiation is tungsten, whose properties are sufficiently well studied and are presented in special literature [1, 2]. We will note only that very frequently it is required to know the integral value of emissivity at a given temperature. These values can be calculated by empirical formulas,

a) for low temperatures (below 1,000° K)

$$\varepsilon_T = 0{,}571\sqrt{\rho_T T}, \qquad \text{(II.13)}$$

b) for high temperatures (higher than 1,000°K)

$$\varepsilon_T = 0{,}5737\sqrt{\rho_T T} - 0{,}1763\rho_T T. \qquad \text{(II.14)}$$

where ρ_T is specific resistance of tungsten in ohm · cm at temperature T°K.

Since radiation of real bodies differs from radiation of ideal black bodies, in order to be able to compare their radiation we use the concept of apparent temperatures (pseudotemperatures). Under apparent temperature we understand the temperature of an ideal black body whose radiation in a given spectral range gives the same effect as radiation of a given body at its true temperature.

There are three such temperatures: energy $T_э$, luminance $T_я$ and color $T_ц$.

Under energy temperature we understand the temperature of an ideal black body, at which it has a radiation identical with a given body having true temperature T,

$$T = \frac{T_э}{\sqrt[4]{\varepsilon_T}}. \qquad (II.15)$$

Luminance temperature corresponds to the temperature of an ideal black body, at which its brightness for radiation with a wave length of 0.665 μ is equal to the brightness of a radiating body with temperature T with that same wave length

$$T = \frac{c_2}{\lambda} \frac{1}{\ln\left(\varepsilon_{\lambda T} e^{\frac{c_2}{\lambda T_я}}\right)}. \qquad (II.16)$$

From formula (II.16) it is clear that luminance temperature may be determined for radiation with any wave length if the value of the spectral coefficient of blackness is known for it; however, in photometric practice its value is taken to refer to wave length 0.665 μ.

Under color temperature we understand the temperature of an ideal black body, at which colorfulness of its radiation is identical with colorfulness of the radiation of a real body with temperature T,

$$T_ц = \frac{(\lambda_1 - \lambda_2) T_{1я} T_{2я}}{\lambda_1 T_{1я} - \lambda_2 T_{2я}}. \qquad (II.17)$$

The difference between color and true temperatures is the result of selectivity of radiation of different bodies. For gray bodies, for which the course of the curve of spectral density of radiation is like the course of the curve of radiation of an ideal black body, there will be no such difference.

Knowledge of color temperature of real bodies has a large value during appraisal of integral sensitivity of receivers of radiation with selective reaction since it characterizes the qualitative side of radiant flux.

4. Electrical Sources of Radiation

Application of these or other sources of radiation energy as irradiating devices in infrared instruments of active effect (with preliminary irradiation) becomes expedient, if they satisfy definite requirements, the chief of which are:

high efficiency in infrared region of spectrum,

duration of action and stability of radiation,

possibility of using jointly with optical systems,

convenience of adjustment of radiation conditions,

minimum weight and dimensions with sufficient emissive power of radiation.

These requirements are satisfied most fully by electrical incandescent lamps (Table II.1)

Table II.1. Characteristics of Radiation of Certain Radiators in the Infrared Region of Spectrum

Source of Radiation	General Density, w/cm^2	Density in Region 0.8–12 μ w/cm^2	Distribution of Energy in Percents in Region of Spectrum, μ		
			0.8—1.4	1.4—2.4	2.4—12
Gas-filled Tungsten Tube..	0.0125	0.007	3.2	20.5	51.6
Electrical Arc.....	0.034	0.024	12.8	54	26
Mercury Vapor Tube.....	0.026	0.01	39	21	—
Helium Tube.....	0.021	—	100	—	—
Pin Tube.....	0.0007	0.0005	60	20	—

Electrical Incandescent Lamps

In electrical incandescent lamps the energy supplied to the body of incandescence is expended on light and invisible radiation and losses on the bulb, gas,

and holders. Numerical values of these magnitudes for contemporary tubes of different power are presented in Table II.2 and show that electrical incandescent lamps are economical and sufficiently powerful sources of radiation.

Table II.2. Energy Balance of Electrical Incandescent Lamps

P, Watt	T, °K	η lu/w	Energy Tapped by Holders, %	Losses in Gas, %	Losses on Bulb, %	Radiation Outside Bulb, %	Visible Radiation, %
25	2535	10.2	1.8	—	7.0	91.2	7
40	2710	11.1	1.6	24.5	7.1	66.8	6.8
60	2767	12.8	1.6	22.2	7.1	69.1	7.6
100	2837	15.4	1.7	18.5	7.0	72.8	9.3
200	2878	17.0	1.7	13.7	7.2	77.4	10.2
500	2340	19.6	1.8	9.2	6.7	82.3	11.4
1000	2395	20.5	4.8	6	7.1	82.1	12.0

Spectral characteristics of the radiation of certain types of tubes are shown in Fig. II.3 and II.4.

At present, industry is releasing a great assortment of electrical incandescent lamps, data on which can be found in corresponding catalogs and light technology reference books. When selecting them as sources of radiation energy in infrared instruments, it is necessary to consider the character of operation of the instruments, the necessary force of radiation, the time of operation, the possibility of supplying electric power by available sources, etc. One should give special attention to the selection of electrical incandescent lamps if they are intended for joint work with optical systems, since in this case an important, and sometimes decisive factor, is the size of the tube and its thermal conditions. This, first, is connected with the placement of the body of incandescence in focus of the optical

system and, secondly, with the cooling of the bulb of the tube inside a comparatively small volume of air in the fittings, closed, as a rule, by the infrared filter. Furthermore, such tubes are required to have high dimensional brightness, i.e., ratio of luminous intensity of tube to area of incandescence.

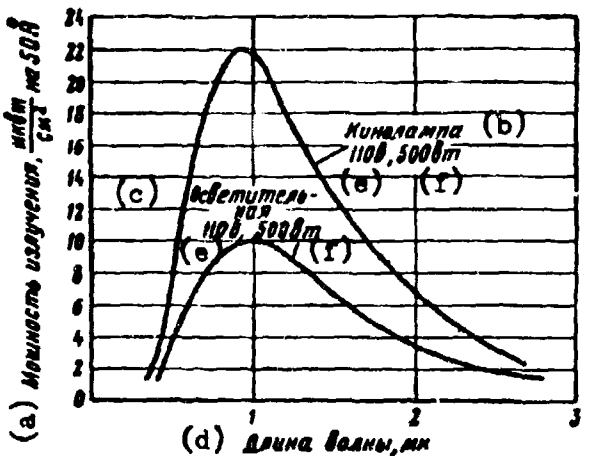

Fig. II.3. Spectral intensity of radiation of illuminating and movie projection tubes 110 v, 500 w.
KEY: (a) Emissive power of radiation $\frac{\mu w}{cm^2}$ per 50 Å; (b) Movie projection tube; (c) Illuminating tube; (d) Wave length, μ; (e) Volt; (f) Watt.

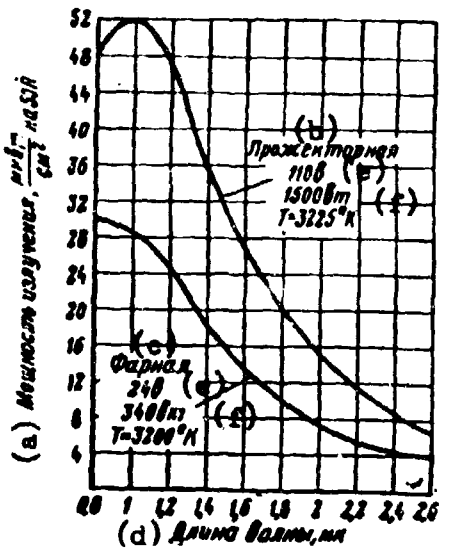

Fig. II.4. Spectral intensity of radiation of headlight and searchlight tubes.
KEY: (a) Emissive power of radiation $\frac{\mu w}{cm^2}$ per 50 Å; (b) Searchlight; (c) Headlight; (d) Wave length, μ; (e) Volt; (f) Watt.

Electrical Arcs

In irradiation installations where it is required to obtain high radiation intensity, simple and high-intensity electrical arcs are used (Fig. II.5).

A simple arc will be formed between two graphite electrodes, whose cathode is source of electrons, and on whose anode, as a result of bombardment of electrons, there will be formed a heated crater with temperature of an order of 4,000°K. Radiation of such an arc is determined mainly by temperature of the crater, which radiates nearly 85% of the energy, while the cathode radiates nearly 10%, and the flame - 5% of the energy.

Brightness of simple arcs attains 18,000-20,000 stilb when fed by direct current and 12,000 stilb when fed by alternating current. Luminous efficiency is 12-14 lu/w.

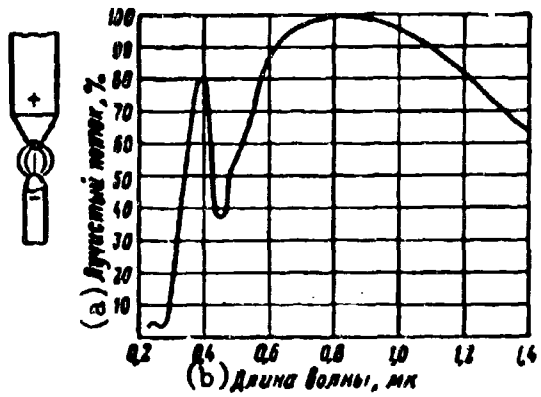

Fig. II.5. Spectral radiation flux level of simple arc.
KEY: (a) Radiant flux, %; (b) Wave length, μ .

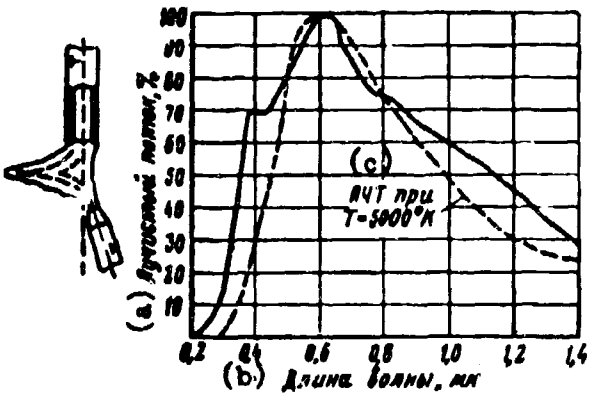

Fig. II.6. Spectral radiation flux level of high-intensity arc.
KEY: (a) Radiant flux, %; (b) Wave length, μ ; (c) Ideal black body at T = 5000°K.

For improvement of light characteristics of arc it is necessary to increase density of current between its electrodes. In such arcs, having the name high-intensity, electrodes have a soft wick, i.e., core, consisting of 30-60% mixture of fluoride salts of rare-earth metals, soot or graphite and up to 4% boric acid (Fig. II.6).

Brightness of high tensity arcs attains 80,000 stilb due to adding the radiation of a crater with a temperature of nearly 5,000°K to the pure temperature of the luminescent radiation of heated vapors of rare-earth metals.

In connection with the higher temperature of a crater of such an arc, the spectrum of its radiation will shift as compared to the spectrum of radiation of a simple arc in the direction of shorter waves ($\lambda_{макс} \approx 0.6\ \mu$) . This also explains the almost identical effectiveness of both types of arcs in the infrared region of the spectrum.

5. Radiation of Industrial and Military Objects

The activity of the overwhelming majority of industrial and military objects is connected with the application of energy installations, as a result of whose operation a large quantity of thermal energy and, consequently, radiation energy is released. These objects have a definite thermal contrast relative to the surrounding background, due to which they can be revealed by instruments of infrared technology.

In their properties and characteristics industrial and military objects can pertain both to extended and to point sources of radiation. But in both the first and second case the radiation of these objects depends on temperature, configuration, and area of radiating surfaces, their mutual location and degree of blackness. This causes a large variety in the radiations of effective objects both in power and in spectral composition and space distribution of radiation energy.

It is natural that with such a variety of heat-radiating objects a general criterion for appraising their radiation cannot be formulated. It is expedient to estimate in each specific case the radiation of objects which occupy a large area and have a very large quantity of sources of thermal radiation differing in characteristics. Moreover the relative location of sources of radiation on an industrial site can essentially change tentative calculations. Calculation of thermal radiation should be made by analogy with calculation of radiation of non-black bodies, considering these objects, with sufficient accuracy for practice, to be gray and diffusely radiating bodies. Such simplification allows the comparatively simple estimation not only of integral radiation of an object, but also distribution of radiation energy by spectrum.

Sometimes it is expedient to separate from a group of heat-radiating objects in a considered territory one or two of the most powerful sources of radiation and take their radiation as the radiation of an object on the whole. Error in

appraising radiation will be, in this case, less the more the difference between temperatures of surfaces of selected objects and the remaining sections, and also the smaller the area and the coefficient of emissivity of the latter. Such a method of appraisal gives comparatively good results when determining radiation of industrial objects of the metallurgical and metal-working industry, coke-chemical, etc. factories, thermal electric power stations, and railroad junctions. On these objects, as a rule, it is possible to separate separate objects: blast furnaces, hot-blast stoves, coke batteries, furnaces for firing ore, cupola furnaces, open-hearth furnaces, dumps of hot slag, pipe, basins for discharging water, open boiler units, locomotives, etc., whose radiation sometimes exceeds radiation of surrounding objects many times.

If it is not possible to separate separate heat-radiating objects on an industrial site, then it is necessary to apply the "zone method".

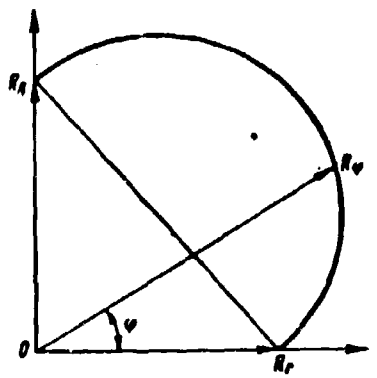

Fig. II.7. To calculate radiation of objects in a vertical plane.

The essence of this more tedious method of calculation consists in the fact that the entire industrial site is broken down into separate sections (zones) with objects having approximately identical temperatures and blackness coefficients of their surfaces.

For these objects is determined the density of radiation in horizontal and vertical planes (sometimes this is necessary to produce also from different directions). Having arranged in a definite scale radiation densities of a given zone in two mutually perpendicular planes, we connect their ends by a straight line, on which, as on diameter, we construct a semi-circle (Fig. II.7). Then any straight line conducted at angle φ from point O to intersection with semicircle will determine in that same scale the radiation density in the vertical plane at an

angle. Density of radiation of all of the industrial objective on the whole, to whatever interesting direction, may be determined by means of geometric summation of vectors of radiation densities of separate heat-radiating objects in a given direction,

$$\mathcal{R}_{\varphi}=\sqrt{\mathcal{R}_{1\varphi}^2+\mathcal{R}_{2\varphi}^2+\ldots+\mathcal{R}_{n\varphi}^2}. \qquad \text{(II.18)}$$

It is possible similarly to estimate radiation and objects of military technology. Calculation in this case is significantly simplified by the fact that heat-radiating surfaces of military objects are concentrated in a small area and are, as it were, local sources of radiation.

Actually, on ships basic sources of radiation are pipes and gas torches, radiating radiant flux in the direction of the upper hemisphere; on tanks - the rear armor plating under which is located the motor and exhaust branch pipe, for cannons - the barrel heated during firing; for aircraft - motors and exhaust gases ; and for objects flying with supersonic speed (aircraft and rockets) there is the skin, heated up to high temperatures as will be shown below, due to aerodynamic drag.

As an example we will consider the peculiarity of radiation of aircraft (aircraft and rockets), which are in this respect the most characteristic military objects since in them are concentrated high energy capacity in a comparatively small volume and there occurs radiation of both the motors and exhaust gases and the sheathing of the apparatus.

For aircraft with piston motors basic sources of infrared radiation are exhaust branch pipes, gases outgoing from branch pipes, and hoods of motors. Their radiation intensity is determined, as in earlier considered examples, by temperature, dimensions of surfaces, degree of their blackness, and also fullness of combustion of fuel. Distribution of radiation energy in space is determined also by the degree of shielding of heat-radiating surfaces by other parts of the aircraft.

Hoods of motors have comparatively low temperature (80 - 100°C) and a small coefficient of blackness (0.2 - 0.45) which causes the low intensity of their

radiation. However, depending upon type of aircraft, or more correctly on the structural distribution of units of the power plant, radiation of hoods can spread both to the front and to the rear of the hemisphere upward and downward.

Exhaust gases of piston motors include a large quantity of fine hard particles of carbon heated to a temperature of 1,000-1,100°C. Their appearance in gas flow is the result of incomplete combustion working, as a rule, with a mixture insufficiently enriched with air. The presence of such particles in gas flow significantly increases its emissivity and ensures a practically continuous spectrum of radiation of exhaust gases of a piston motor. The indicatrix of the radiation of exhaust gases, as a rule, is extruded in the direction of the rear hemisphere and along the transverse axis of the aircraft.

In the total balance of radiation of an aircraft with piston motors the fraction of radiation of exhaust gases and hoods of motors oscillates from 35 to 45%. The remaining part (65-55%) is apportioned to radiation of exhaust branch pipes.

Exhaust branch pipes of motors are disposed either under the center section of an aircraft or above it, along the longitudinal axis of an aircraft. Therefore, propagation of radiation energy from the heated branch pipes can occur either in the direction of upper or lower hemispheres with a maximum of radiation along the transverse axis of the aircraft. Propagation of radiation in the direction of front and rear hemispheres, will depend on the degree of change of visible dimensions of surface of branch pipes and dimensions of surfaces of elbow and branch pipes exit.

Temperature of branch pipes attains values of an order of 800-700°C near collector, being lowered, by measure of approach to cut off to 250-350°C. Material, from which a branch pipe is prepared is heat-resisting steel oxidized in the process of operating the aircraft. Therefore, the blackness coefficient of the surfaces of branch pipes is sufficiently great, attaining values of 0.8-0.9.

The presented data allow us in the example of a C-47, to estimate radiation of an aircraft with a comparatively low capacity power installation.

On the C-47 two exhaust branch pipes with a diameter of 15 cm and a length of nearly 100 cm are placed under the center section from the external side of each of the two motors. Radiation of one branch pipe along the transverse axis of the aircraft will be equal to $1.94 \cdot 10^3$ w, and it spreads in horizontal or vertical planes only to one side. The radiation intensity in a direction perpendicular to the surface of the branch pipe will constitute a magnitude of the order of 620 w/sterad.

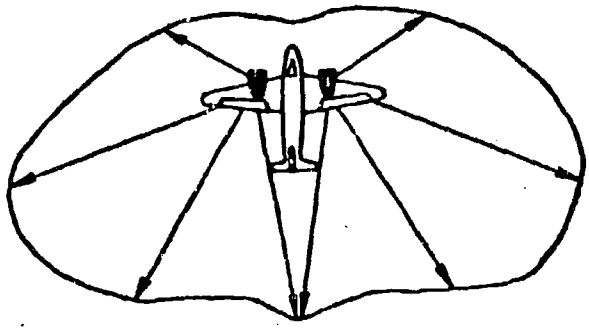

Fig. II.8. Indicatrix of the radiation of a C-47 in the horizontal plane.

During appraisal of total radiation capacity of an aircraft it is necessary to consider radiation of the two branch pipes to all sides. Then the total radiant flux due to radiation of only the cylindrical part of two branch pipes will constitute

$$\Phi' = 2\pi D l \varepsilon \sigma T^4 = 13 \cdot 10^3 \text{ w}$$

Consequently, the radiation of all the C-47 will be equivalent to the radiation of a point source with a power of

$$\Phi = \frac{\Phi'}{0,6} = 22 \cdot 10^3 \text{ w}$$

Approximate distribution of radiation intensity of a C-47 in a horizontal plane due to the radiation of branch pipes, exhaust gases, and hoods of motors is shown in Fig. II.8.

For jet aircraft at subsonic speeds of flight a basic source of radiation is the jet engine together with the extension pipe and exhaust cone (if there is one), and also the jet of gases outgoing from the nozzle. In distinction from a piston motor the specific gravity of the radiation of gases here is significantly less due to a fuller combustion of fuel at a surplus of oxygen and the absence, due to this, in the gas stream of hard heated particles of carbon. Radiation of the gas fraction,

in the form of two-three atomic molecules, has a band spectrum coinciding with the absorption spectrum of analogous molecules in the air. Therefore, radiation of heated vapors of water and carbon dioxide, separated in the biggest quantity during full combustion of carbohydrates, does not play any noticeable role in the total balance of radiation of the gas stream at low altitudes. However, it can render noticeable influence at great heights where contents of CO_2 and H_2O are small (Fig. II.9).

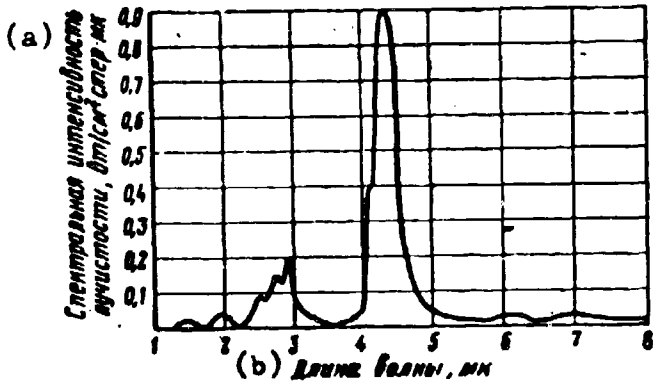

Fig. II.9. Spectral intensity of radiance of a jet of gases during combustion of kerosene fuel.
KEY: (a) Spectral intensity of radiance, $w/cm^2 \cdot$ sterad $\cdot \mu$;
(b) Wave length.

In literature [3, 4] is indicated that radiation of a gas stream of a jet engine with a temperature of 1,200°K has a maximum near 2 μ. During emissivity $\varepsilon = 0.1$ total radiation intensity of gas stream constitutes $6.8 \cdot 10^{-15}$ $w \cdot m^{-2} \cdot deg^{-4}$.

Form of the jet of gas stream and distribution of temperature in it are shown in Fig. II.10 [5].

In connection with this, radiation of jet aircraft basically is conditioned by radiation of the internal cavity of the extension pipe, the walls of which have a temperature of the order of several hundreds of degrees, and open parts of the motor (blades of the turbines, the exhaust cone).

Blades of the turbines are washed by the gas flow with a temperature of 700-750°C at a exhaust velocity of 300-400 m/sec. Therefore, if one were to consider aerodynamic heating, temperature of the blades of a gas turbine can exceed 800°C, since with such a speed increase of temperature in places of full braking of gas constitutes a magnitude of an order of 45-80°C [6].

In Fig. II.11 are given experimental data [7] on temperature increase of air in the compressor at altitudes of 11,000 - 25,000 m, which show that blades of

turbines, on the end of it and examined through the exhaust nozzle exit of the extension pipe of the motor, can have a significant temperature.

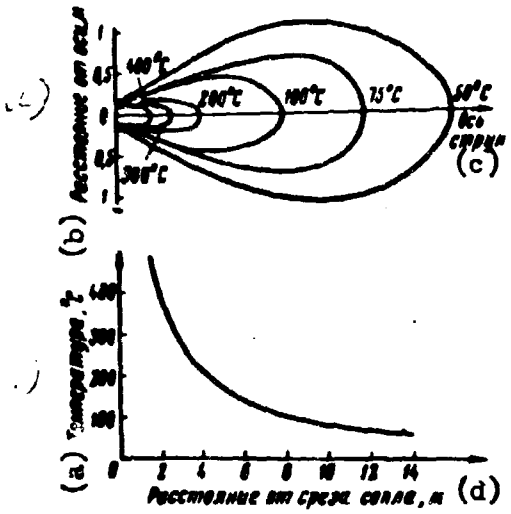

Fig. II.10. Form of jet a) and distribution of temperature in the gas stream of a jet engine with traction of 300 kg b).
KEY: (a) Temperature; (b) Distance from axis, m; (c) Axis of stream; (d) Distance from nozzle exit, m.

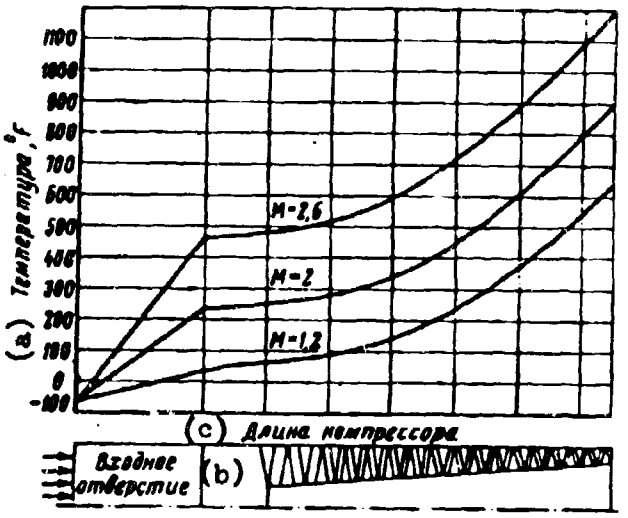

Fig. II.11. Temperature increase of air along the axis of the compressor at heights of 11,000--25,000 m.
Transition from Fahrenheit temperature scale to centigrate scale is carried out by the formula

$$t°C=\frac{5}{9}(t°F-32).$$

KEY: (a) Temperature, °F; (b) Inlet; (c) Length of compressor.

In connection with this the indicatrix of the radiation of a jet engine, and also the jet aircraft on the whole, in distinction from the indicatrix of radiation of an aircraft with piston motors, has a sharply directed character. Basic radiation must be in the direction of the rear hemisphere. The character of the radiation indicatrix for each type of jet aircraft will be determined by thermal conditions of the motors, their number, and also the geometric relationships between length and diameter of the extension pipe, the base between motors and the length of the fuselage.

With transition to supersonic speeds of flight a source of thermal radiation of an aircraft is the sheathing of the airframe where specific gravity of radiation of sheathing in the total balance of radiation intensity of the aircraft continuously increases with growth in speed of flight. Besides, increase of speed of

flight requires application of higher energy propellants and, consequently, radiation of the propulsion system also will be increased.

Now much work is conducted on the creation of new, more chemically active fuels. In particular, fuels are being developed with inclusion of powdery metal which during combustion would separate a large quantity of heat (for instance, aluminum, beryllium, lithium and others). In this case radiation of the gas stream will be sharply increased due to radiation of heated particles of metal oxides and increase of the radiation factor of the stream. Another direction in the creation of highly active particles of metal oxides and increase of radiation factor consists of the development of synthetic compounds of hydrogen with certain elements (boron, lithium, and others). Obtained thus, the fuel pentaborane (a compound of boron with hydrogen) at combustion separates 1.5 times more heat than the usual fuels. This undoubtedly will lead to an increase of emissive power of radiation both of the motor and the gas stream.

During supersonic flight sheathing of aircraft brakes the encountered air flow, its kinetic energy passes into heat, causing heating of the boundary layer and the sheathing to a temperature of T_0, the magnitude of which may be calculated by the formula

$$\Delta T = T_0 - T_\infty = A\frac{v^2}{2gc_p} = \frac{v^2}{2000} = \frac{M^2 T_\infty}{5}, \qquad \text{(II.19)}$$

where T_0 is temperature of the braked layer of air, °K;

T_∞ is temperature of the air flowing around the body, °K;

v is speed, m/sec;

M is Mach number.

The relationship of the absolute temperature of the undisturbed air flow and the temperature of the flow braked to zero speed at different Mach numbers is given in Table II.3.

Table II.3. The Ratio of the Temperature of Undisturbed Air Flow to the Temperature of Air Braked to Zero Speed at Various Mach Numbers.

M	0	1	2	2.5	3	4	5	10
T/T_*	1	0.883	0.556	0.444	0.357	0.238	0.167	0.048

In Fig. II.12 are given computed heating curves of the surface of an aircraft due to braking of air flow, with supersonic speed of flow at altitudes up to 1 km, without calculation of losses in radiation. For higher speeds of flight at heights from 11 to 25 km the heating curve of the sheathing of an aircraft at places of full braking is presented in Fig. II.13 [7].

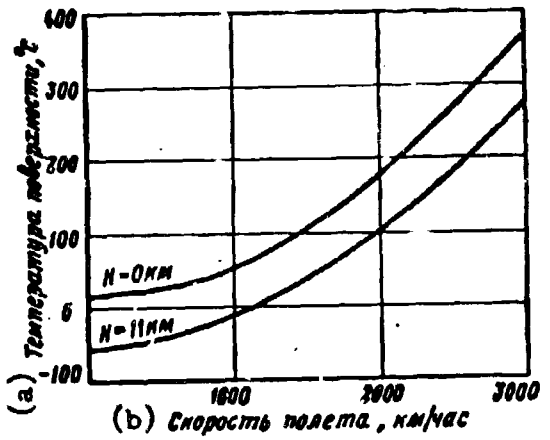

Fig. II.12. Temperature of the surface of an aircraft at point of braking, depending upon speed of flight.
KEY: (a) Temperature of surface, °C; (b) Speed of flight, km/hr.

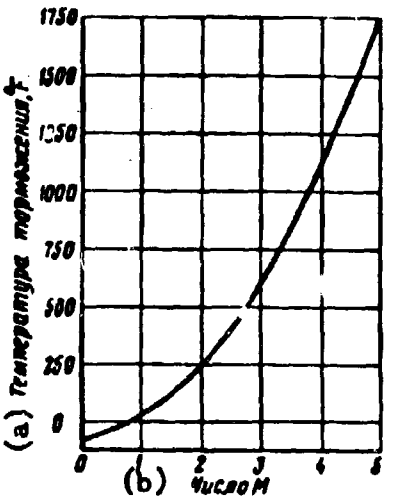

Fig. II.13. Temperature of braking depending upon Mach number at heights of flight 11,000 - 25,000 m.
KEY: (a) Temperature of braking, °F; (b) Mach number.

The given curves, obtained by means of calculation by the formula (II.19), give satisfactory agreement with experimental data, although losses of thermal energy due to radiation were not considered. These losses will be higher the higher the temperature of the surface and the more its emissivity coefficient ε. This dependency [8] is shown in Fig. II.14.

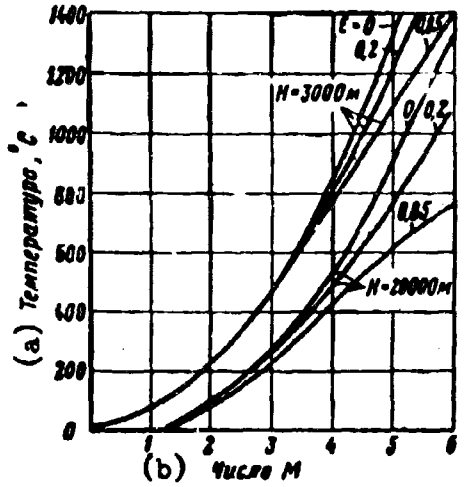

Fig. II.14. Equilibrium temperature of a body during aerodynamic heating, taking into account radiation.
KEY: (a) Temperature, °C; (b) Mach number.

Besides heating of the aircraft's sheathing due to aerodynamic braking of the air, its heating occurs also due to friction in the boundary layer. The magnitude of aerodynamic increase of temperature in this case may be calculated from relationship (II.9), taking into account Prandtl number (Pr)

$$\Delta T = A\frac{v^2}{2gc_p}\sqrt{\Pr} = 0{,}85\frac{v^2}{2\,000}. \qquad \text{(II.20)}$$

Temperature of heating of sheathing of certain contemporary aircraft in flight (the United States) is presented in Table II.4.

Table II.4. Experimental Data on Heating of Sheathing of Certain Aircraft [9]

Type of Aircraft	M	Temperature of Sheathing	
		°C	°K
Convair F-106.....	1.5	60	333
MacDonald F-101.....	1.6	62	335
Lockheed F-104A.....	2.0	122	395
Martin XB-68.....	2.5	214	487
Bell X-2.....	3	333	606

Established or, as it is otherwise called, equilibrium temperature of aircraft sheathing sets in not at once. For that a definite time is required, depending on thermal conduction of the sheathing material, its emissivity, and height of flight of the aircraft. As an example in Fig. II.15 are presented curves of skin heating

of aircraft during supersonic flight with speed corresponding to Mach 4, at heights of 6,100 and 36,600 m [10].

As can be seen from Fig. II.15, at a height of 6,100 m an equilibrium temperature of aircraft sheathing, equal to 630°C, is established in less than 1.5 min of flight with a speed of Mach 4, whereas at height 36,600 m it is established only after 20 minutes.

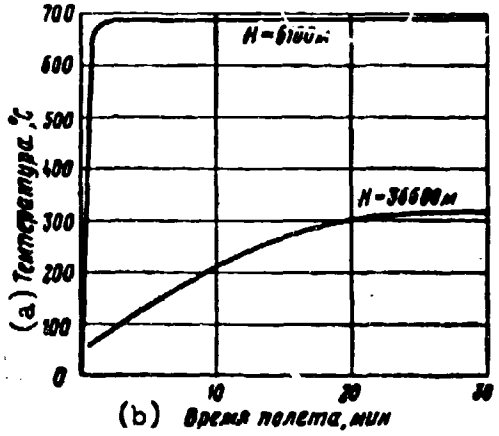

Fig. II.15. Growth of surface temperature of aircraft in time during flight speed of Mach 4. KEY: (a) Temperature, °C; (b) Time of flight, minutes.

Heating of aircraft sheathing during supersonic flight permits the aircraft to become a source of intense radiation of infrared rays, the flux of which practically spreads to all sides within limits of solid angle 4π. This omnidirectional radiation, the magnitude of which in a given direction will depend on dimensions of projection of the surface of the aircraft, its emissivity and temperature, will be added to the ever-increasing, sharply directed radiation of jet engines and will make aircraft more vulnerable to detection and destruction (target-seeking guidance and exploding of rockets) by means of infrared technology.

To lower thermal radiation of the airframe of supersonic aircraft is virtually possible only by the application of materials for sheathing with very low emissivity. However, this requirement is in contradiction with the requirement of high emissivity of sheathing material for its intense cooling in order to increase the durability of aircraft during supersonic flight (the problem of the thermal barrier).

Still more powerful sources of thermal radiation are rockets, whose speed of flight significantly exceeds sonic. For rockets, the basic causes of appearance of thermal radiation are the heating of the body during operation of the motor,

aerodynamic heating during flight in dense layers of atmosphere, and heating of the body of the rocket due to solar radiation during its flight in space. Furthermore, in the initial stage of flight, a powerful, although brief, source of radiation is the jet of heated gases ejected by the motor.

Due to the operation of the motor, the body of a rocket and especially its tail part can be heated to significant temperatures, since temperature in the combustion chamber attains 2,000-3,000°C; however, the most intense heating of the body occurs due to the flight of a rocket in dense layers of atmosphere.

Thus, for instance, it is known that the German rocket the FAU-2 (A-4), due to friction against air at a flight speed near 5,600 km/hr, was heated to red incandescence. Calculation of the body temperature of the FAU-2 rocket by the formula (II.20) shows that its temperature constituted a magnitude of the order of 950°C.

If one were to consider dimensions of a rocket (length near 14 m, maximum diameter 1.65 m) and its form, then it is possible to estimate its radiation as a magnitude of the order of 4,000-5,000 kilowatt.

Space rockets additionally are heated by solar rays during flight in space [11].

The heat balance of space rockets (burning of fuel, aerodynamic heating and heating by solar rays), in the final result, determines the resultant temperature. Heating of the body of a rocket due to its irradiation by solar rays should be considered only during its flight in space, where heating due to friction is practically absent, and the motor of the rocket has ceased its work. Appraisal of this radiation can be conducted in an example of a hypothetical space body of spherical form, having a shell from material with emissivity $\varepsilon = 1$ (ideal conductor of heat). Solar constant is 1,200 w/m^2. Under the action of this irradiation the surface of a sphere turned to the Sun will be evenly heated proportionally to the product of the solar constant by the area of projection of the sphere (area of great circle)

and inertialessly will transmit heat to that part of the sphere which is turned from the Sun. Such a state of heating of sphere will continue as long as radiation from all of the surface is not balanced by radiation incident from the Sun. For a sphere, the total surface and area of projections are connected by ratio 4 : 1. Consequently, a heated sphere will radiate 290 w/m^2 only due to solar irradiation, which corresponds to radiation of a shell with a temperature of 290-300°K.

Literature

1. A. P. Ivanov. Electrical sources of light. State Power Engineering Publishing House, 1955.

2. JOSA, 1946, Oct., Vol. 36, No. 10.

3. Aviation Age, 1957, Mar.

4. Aviation Week, 1957, May, Vol. 13.

5. I. Goshek. Aerodynamics of high speeds. Publishing House of Foreign Literature, 1954.

6. Ya. I. Levinson. Physical bases of aerodynamics of high speeds, 1942.

7. Flying Safety, 1958, Nov.

8. J. Royal Aeronautical S., 1958, Vol. 62, No. 566.

9. American Aviation, 1956, Vol. 20, No. 11.

10. Translation No. 7469, BNT.

11. Missiles and Rockets, 1958, Jun., No. 5.

C H A P T E R III

PROPAGATION OF RADIATION ENERGY IN THE ATMOSPHERE

The air envelope of Earth - the atmosphere - is that medium, in which there occurs transfer of radiation energy from source to receiver. Composition and property of the atmosphere, in many respects, predetermine effectiveness of application of infrared instruments.

1. Composition of the Atmosphere

Atmosphere of Earth constitutes a mechanical mixture of gases and fine solid particles in it in suspension. Such a mixture is called aerosol.

Table III.1. Basic Solid, Liquid, and Gasiform Impurities in the Atmosphere

Impurity	Dimension, cm	Number in 1 dm^3	Rate of drop, cm/sec
Molecules of Gases....	10^{-8}	$2.8 \cdot 10^{19}$	—
Ions: light.....	$2.5 \cdot 10^{-8}$	$5 \cdot 10^{2}$	—
average.....	10^{-7}	10^{3}	—
heavy.....	10^{-6}	10^{3}	—
Dust: cosmic.....	10^{-5}—10^{-4}	—	—
terrestrial.....	10^{-4}—10^{-2}	10^{2}—10^{4}	10^{-3}
Condensation nuclei...	10^{-6}—10^{-5}	10^{2}—10^{5}	10^{-7}
Drops: haze.....	10^{-5}—10^{-4}	10^{2}—10^{3}	10^{-3}—10^{-2}
fog.....	10^{-4}—10^{-3}	10—10^{3}	10^{-3}—10^{-2}
drizzle.....	10^{-2}	1—10	10^{2}
rain.....	10^{-1}	1—4	$5 \cdot 10^{2}$

presence of turbulent mixing, remains constant to heights of the order of 25-30 km. However, in real atmosphere containing water vapor, the percentage of gases changes depending upon the quantity of steam.

In the atmosphere, in variable quantity, are water vapor and solid and liquid impurities (Table III.1). Their quantity in the atmosphere changes, depending upon the geographic medium, the activity of man, and nature. In this group one should include carbon dioxide and ozone, which, along with water vapor, solid, and liquid impurities, affect optical properties of the atmosphere.

Water Vapor

Depending upon temperature and humidity, the atmosphere can contain from 0 to 4% water vapor (in volume). Dimensions of its molecules vary from $11 \cdot 10^{-5}$ to $14 \cdot 10^{-5}$ μ. With a lowering of temperature quantity of water vapor drops (Table III.2). Differing also are average contents of water vapor, depending upon geographic latitude (Table III.3).

Table III.2. Change of Pressure of Saturated Water Vapor E and Absolute Atmospheric Humidity A for Earth, Depending Upon Temperature

t, °C	-20	-15	-10	-5	0	+5	+10	+20	+30	+40	+50
E, mm Hg cm	0.95	1.43	2.14	3.16	4.58	6.54	9.21	17.54	31.82	55.3	92.5
e, mb	1.27	1.91	2.85	4.22	6.1	8.64	12.26	23.28	42.42	73.7	123
A, g/m^3	1.08	1.6	2.35	3.41	4.86	6.32	9.41	17.32	30.38	51.1	82.8

With increase of height, quantity of water vapor sharply decreases, since affecting its distribution are the low temperatures and processes of condensation and also the distance from the surface on which occurs the process of evaporation.

[illegible], g/cm^3	18.5	16.8	13.6	9.8	7.2	5.2	3.4
[illegible], %	79	75	71	70	74	78	82

For average conditions, decrease of absolute humidity with height (water vapor pressure) may be approximately expressed by barometric formula

$$a_H = a_0 \cdot 10^{-\frac{H}{\beta}}, \qquad \text{(III.1)}$$

where β = 5,000 for lower layers of the atmosphere if height is expressed in meters.

Proceeding from expression (III.1), one should expect that water vapor pressure or absolute atmospheric humidity at 2,000 m will be half as much, at 5,000 m will be ten times less, at 10,000 m one hundred times less than at the surface of earth. Research confirms this position and shows that the basic quantity of vapor is concentrated in the lower 5-kilometer layer. The presence of moisture at great heights is connected, as a rule, with vertical displacements of air masses, however, in spite of this, vapor pressure at the boundary of the troposphere (11,000 m) drops to e_{11} = 0.0137 mb.

A number of authors, characterizing the humidity of the atmosphere, operate with an idea of water content under which they understand the quantity of water precipitated in a layer of a single section with extent L

$$W = a_H L, \qquad \text{(III.2)}$$

where a_H is absolute atmospheric humidity at height H.

Water content of a layer may be defined both in mass units (g) and in units of length (mm).

arbon dioxide is present in atmosphere as a result of vital activity of organic nature and emanation from the Earth's crust, however, its contents in the surface layer are nonuniform. Thus, its average content in pure rural air is taken to be 0.03% by volume, whereas above cities its content can reach 0.05%.

Due to the vertical mixing of the atmosphere such concentration of carbon dioxide is kept constant to heights of the order of 20-25 km.

Ozone

Ozone (O_3) in the atmosphere is contained up to 0.00004%. Distribution of ozone in the atmosphere is nonuniform. In lower layers of the atmosphere ozone is contained from 0.000001 to 0.00001%, and at a height of 65-70 km only traces of it are observed.

Solid and Liquid Impurities

Besides water vapor, ozone, and carbon dioxide, in the atmosphere, constantly present, are dust, smoke, particles of salt, pollen of plants, bacteria and microbes, drops of water, and small crystals of ice. The majority of these impurities not only will directly dim atmosphere, but also have a large value in cloud formation and fog, coming forward in the role of condensation nuclei of water vapor.

Distribution of solid and liquid particles by height is intimately connected with their rate of drop, which may be calculated by Stokes' formula

$$v = 1.26 \cdot 10^8 \cdot r^2 \text{ cm/sec} \qquad \text{(III.3)}$$

where r is radius of particle, cm.

This formula agrees well with experimental data for particles having a radius not more than 10^{-3}cm, and shows that particles by dimension less than 1 μ drop with such insignificant speed ($v < 10^{-2}$cm/sec) that they turn out to be in suspension and are easily carried by ascending flows upward.

$$n_h = n_0 e^{-\frac{v}{k}h}, \qquad (III.4)$$

where k is coefficient of turbulence,

n_0 is number of particles in 1 cm^3 of air near earth.

Ratio $\frac{v}{k}$ can lie from 405 (by Vigrand) to 750 (by Zaytsev and Gayvoronskiy).

Atmospheric dust can have cosmic, volcanic, and ground origin.

In the surface layer of the atmosphere the main cause of its turbidity is ground dust, smoke, bacteria, salt, and hydrometeors.

Weight measurements show that in relatively transparent rural air there is contained up to 0.00025 g of dust in 1 cm^3, being increased almost three times in a period of drought and arid winds. In dry clear weather in 1 cm^3 of air there is contained up to 130,000 dust motes, decreasing after rain to 32,000-30,000. Above water surface quantity of dust significantly decreases (Table III.4).

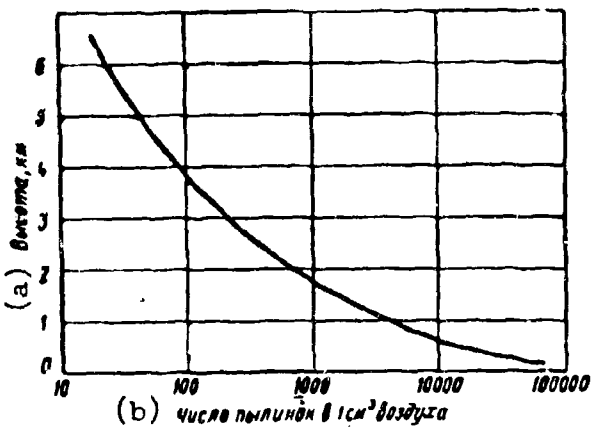

Fig. III.1. Distribution of dust motes by heights.
KEY: (a) Height, km; (b) Number of dust motes in 1 cm^3 of air.

Distribution of dust in atmosphere is determined not only by the state of the weather and the geographic medium, but also by the activity of man, especially in industrial regions. City dust and smoke of industrial enterprises, as a rule, are disposed at heights not higher than 700-500 m, however, in case of intense vertical displacements of air they can be carried to great heights.

The presence of a significant quantity of dust in the surface layer of atmosphere sharply decreases its transparency (Fig. III.2), and the presence in it, additionally, of hydrometeors and water vapor to an even larger degree worsens the transparency of the surface layer.

Distance from shore, km	[illegible]	16	19	21	26
Number of dust motes in 1 cm^3	35,000	2,750	1,250	800	780

Hydrometeors are formed in air upon achievement of a saturating concentration of water vapor (at a given temperature), when vapor pressure attains maximum value. Formation of hydrometeors promotes presence in air of hygroscopic impurities - condensation nuclei.

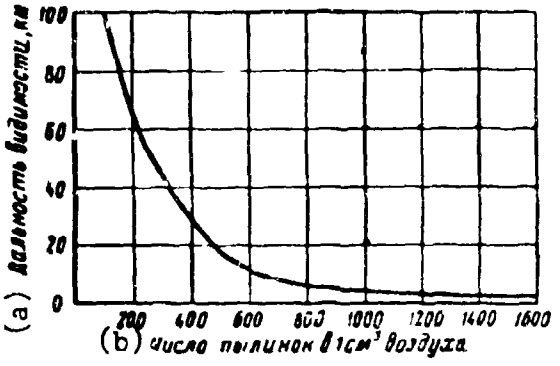

Fig. III.2. Dependency of meteorological visual range on dustiness of atmosphere. KEY: (a) Visual range, km; (b) Number of dust motes in 1 cm^3 of air.

Appearance of hydrometeors causes a sharp turbidity of atmosphere.

Depending upon the degree of turbidity of the atmosphere, they demonstrate:

Haze with visibility 1-10 km;

Fog with visibility less than 1 km.

Observations show that in water fogs drops are encountered with dimensions from 0.1 to 50-60 μ. In this case these drops become visible to the eye and settle on earth in the form of drizzle. The overwhelming majority of drops have a dimension of 7-15 μ during positive temperatures and 2-5 μ during negative. Quantity of drops in 1 cm^3 of air constitutes 50-100 for weak fog and 50-600 for strong.

In haze, which is the initial stage of development of fog, the dimension of drops is less than 1 μ, and their quantity in 1 cm^3 of air does not exceed 10-40.

For the convenience of comparing fogs we characterize them by water content, i.e., quantity of concentrated moisture in a unit of volume. Magnitude of water content of fog depends on quantity and dimension of drops and on temperature of air (Table III.5).

[illegible] at different temperatures

[illegible], °C	-30	-20	-10	0	+10	+20
W, g/m³	0.05–0.18	0.16–0.25	0.18–0.65	0.18–0.7	0.3–1.2	0.5–1.5

Optical properties of fogs in many respects are similar to properties of clouds: they reflect the sunlight well ($\rho \approx 0.8$) and they have selective absorption of radiant flux. Scattering of radiant flux is proportional to the number of drops in a unit of volume and their dimension, i.e., water content of fog.

Therefore, it is comparatively simple to calculate visual range in fog by the formula

$$L = c\frac{r_{cp}}{W}, \qquad \text{(III.5)}$$

where r_{cp} is average dimension of drops of fog,

W is water content of fog,

$c = 2.5$, if r_{cp} is in μ, and W is in g/m^3 (usually in practice we consider $r_{cp} = 15\ \mu$).

2. Weakening of Radiant Flux in Atmosphere

From the point of view of visibility, basic optical phenomena occurring in the atmosphere, lead to a weakening of radiant flux spreading from the observed object to the observer, and a lowering of the brightness contrast of an object relative to the surrounding background.

Weakening of radiant flux in atmosphere can occur in general both due to scattering and absorption of radiation energy. The first shows in the most considerable manner in the visible region of the spectrum; the second shows in the ultraviolet and especially in the infrared region.

It is possible to judge the character of weakening of radiant flux of the atmosphere by Fig. III.3, where there is graphically shown spectral irradiance of the upper layers of atmosphere 1 and the surface of Earth 2 by solar rays at noon.

factor of p[illegible] and an extent of [illegible] can be described by the law of Bouguer - Lambert:

$$\Phi = \Phi_0 e^{-\beta l} = \Phi_0 \tau^l, \qquad \text{(III.6)}$$

where Φ_0 is radiant flux entering the medium,

Φ is radiant flux outgoing from the medium,

$\tau = e^{-\beta}$ is coefficient of transparency of a medium with an extent of 1 km;

$$\beta = \ln \frac{1}{\tau}. \qquad \text{(III.7)}$$

The given formulas are just for nomachromatic radiant flux, spreading horizontally in the atmosphere with a constant attenuation factor on all of the section.

During propagation of radiant flux vertically or at an angle γ to the horizon, the attenuation factor β can endure sharp changes, connected with heterogeneity of the atmosphere at various heights.

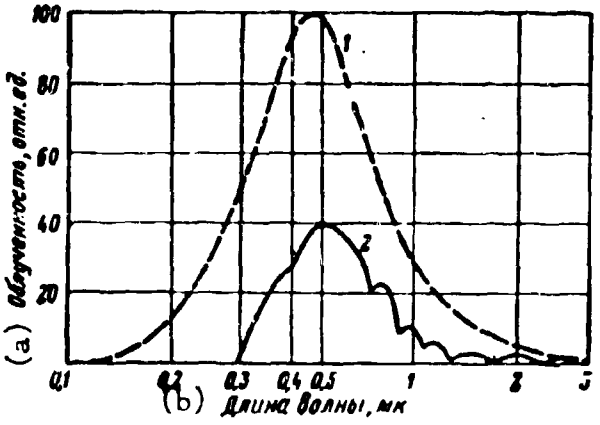

Fig. III.3. Spectral intensity of irradiance of upper layers of the atmosphere (1) and the surface of Earth (2).
KEY: (a) Irradiance, relative units; (b) Wave length, μ.

In this case one should break down by height the thickness of the atmosphere in n equal layers, within limits of which the value of the attenuation factor remains constant, and should determine for each layer the coefficient of transparency. Then total transparency of a layer of atmosphere by height H will be defined as the product of the coefficients of transparency of separate layers:

$$\tau_{H\lambda} = \tau_{(0-H_1)\lambda} \tau_{(H_1-H_2)\lambda} \cdots \tau_{(H_{n-1}-H_n)\lambda}. \qquad \text{(III.8)}$$

If, however, radiant flux spreads slanted at an angle γ to horizon, then

$$\tau_{\lambda\gamma} = \tau_{H\lambda}^{\frac{1}{\sin\gamma}}. \qquad \text{(III.9)}$$

During propagation in the atmosphere of complex polychromatic radiant flux,

it is necessary to determine transmissivity for separate monochromatic fluxes, and then total transmissivity from ratio

$$\tau = \frac{\int_0^\infty \tau_\lambda r_\lambda S_\lambda d\lambda}{\int_0^\infty r_\lambda S_\lambda d\lambda}, \qquad \text{(III.10)}$$

where r_λ is spectral density of intensity of radiation,

S_λ is spectral sensitivity of receiver of radiation.

In simpler cases for approximate calculation we use averaged value of attenuation factor β_{cp} for monochromatic radiant flux within limits of the entire layer of atmosphere, where there occurs a transfer of radiation energy,

$$\Phi = \int_{\lambda_1}^{\lambda_2} \Phi_{0\lambda} e^{-\beta_{cp} L} d\lambda. \qquad \text{(III.11)}$$

Transparency of the atmosphere is a function of scattering and selective absorption of radiation energy in the atmosphere. Therefore, it is possible to present total transparency of atmosphere as the product of the coefficient of transparency caused by the scattering of radiant energy τ_p, and the coefficient of transparency caused by the selective absorption in it $\tau_{s.a}$:

$$\tau = \tau_p \tau_{s.a}. \qquad \text{(III.12)}$$

3. Scattering of Radiation Energy in the Atmosphere

Under energy dissipation of radiation in some medium, including the atmosphere, we understand the process of deflection of radiant flux from its initial direction. In the atmosphere the cause of scattering is its optical heterogeneity and, occurring because of this, the refraction, reflection, and diffraction of radiant flux in these heterogeneities.

Depending upon the relationship between the dimensions of particles of the dispersed phase and the wave length of radiant flux, scattering may be molecular (in particles of minute dimension), diffractional (in particles commensurable with

wave length), and geometric (in particles of large dimensions). In real atmosphere, where there are particles of practically any dimensions, all three forms of scattering exist simultaneously.

For visible light the attenuation factor of radiant flux due to scattering may be determined, if the meteorological visual range is known:

$$L=\frac{3,92}{\beta}, \qquad \text{(III.13)}$$

where β is the attenuation factor for $\lambda = 0.55\ \mu$ [mile^{-1}].

Based on this expression, Zhil'bert [1] obtained attenuation factors of visible radiation due to scattering depending upon the state of the weather, and also compared them with scattering coefficient in pure dry atmosphere β_0, calculated by the formula of Rayleigh (see Table III.6).

Table III.6. Weakening of Visible Radiation ($\lambda = 0.55\ \mu$) During Various Degrees of Turbidity of Atmosphere

L, km	State of Atmosphere	β, Mile^{-1}	β/β_0
< 0.02	Very strong fog	> 85.6	> 6,060
0.05	Strong fog	85.6	6,060
0.2	Moderate fog	21.4	1,515
0.5	Weak fog	8.54	606
1	Strong haze	2.14	151
4	Weak haze	1.07	75.6
10	Clear	0.427	30.2
20	Very clear	0.214	15.1
50	Excellent visibility	0.0713	5.06

For radiation with a wave length other than $0.55\ \mu$, the attenuation factor without calculation of selective absorption may be determined from ratio

$$\frac{\beta_\lambda}{\beta}=\left(\frac{0.55}{\lambda}\right)^n. \qquad \text{(III.14)}$$

This formula coincides well with practical results when appraising the weakening of infrared rays by atmosphere with a meteorological visual range of more than 10 km.

Jebby and other authors [2] determined the transmission of radiant flux in separate windows of transparency of the atmosphere on a route extending 4,200 m, depending upon meteorological visual range. Interpolation of the obtained data allowed them to construct convenient curves for calculation of transparency of atmosphere in the infrared region of the spectrum under different atmospheric conditions due to scattering of radiant flux in it (Fig. III.4). In all cases the equivalent layer of precipitated water was taken as constant (17 mm), and the meteorological visual range was calculated by relationship (III.13).

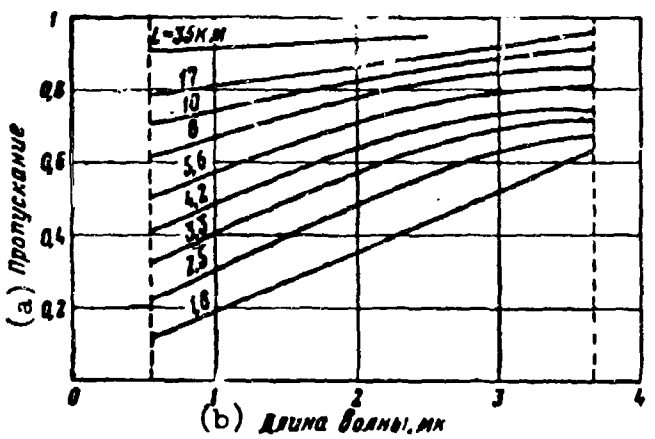

Fig. III.4. Transparency of the atmosphere due to scattering at different distances of meteorological visibility on a base of 1.85 km.
KEY: (a) Transmission; (b) Wave length, μ.

Scattering of radiant flux of dry and pure atmosphere, with which we usually deal at great heights, with a sufficient degree of accuracy, coincides with the laws of molecular scattering, studied in detail by Rayleigh.

Considering the scattering of radiant flux by gas ions and separate bunches of molecules appearing as a result of continuous chaotic motion of the latter, Rayleigh introduced the law, "When light is dispersed by particles, minute as compared to any of the wave lengths, the relation of amplitudes of oscillations in scattered and incident light is reciprocal to the square of the wave length, and the relation of intensities - to their fourth degree".

Mathematically this law may be expressed by the following dependency,

$$s'_\lambda = \frac{\pi^2 (n^2 - 1)^2}{2r^2 \lambda^4 N} (1 + \cos^2 \varphi), \qquad \text{(III.15)}$$

where $\varepsilon_\lambda^\varphi$ is the coefficient of scattering in a given direction; angle φ with direction of incident monochromatic radiant flux is a component;

n is index of refraction of air;

N is number of molecules in 1 cm^3 of volume;

r is distance from dispersing medium.

Rayleigh's law is valid as long as the ratio of diameters of particles and wave length remains significantly less than unity. As shown by the work of M. V. Shuleykin, Rayleigh's law is valid for drops with a diameter of not more than 0.42 μ. With increase in diameter of particles exponent with wave length decreases (Table III.7), changed also is coefficient A:

$$\varepsilon_\lambda = A\lambda^{-k}. \tag{III.16}$$

Table III.7. Change of Coefficient k in Expression (III.16) with Change of Diameter of Dispersing Particles

d, μ	0,42	0,52	0.59	0,64	0,68	0,71
k	4	3,5	3	2,5	2	1,5

In accordance with this, if, for a case of ideal molecular scattering, formula (III.16) takes the form $\varepsilon_\lambda = 0.0082 \cdot \lambda^{-4}$, then in high-altitude conditions for dry atmosphere $\varepsilon_\lambda = 0.012 \cdot \lambda^{-3.68}$, and in the case of moisture content in a quantity of 10 mm of condensed water

$$\varepsilon_\lambda = 0{,}0008 \times \lambda^{-1.75}.$$

Diffractional Scattering

In real atmosphere always present in suspension are solid and liquid particles, the dimensions of which are commensurable or exceed the wave length of the spreading radiation. Energy dissipation of radiation in them is more complex and may be described by the following mathematical dependency:

$$\left.\begin{aligned} \mathcal{R} &= \frac{\lambda^2}{2\pi} f(\alpha\beta), \\ \alpha &= \frac{2\pi\rho}{\lambda}, \quad \beta = \frac{n}{n_0}\alpha, \end{aligned}\right\} \tag{III.17}$$

where $\mathcal{R}$ is intensity of scattered radiation energy;

ρ is radius of dispersing particles;

n, n_0 are indices of refraction of a particle and air.

In distinction from molecular scattering where the polar diagram is symmetrical relative to the primary beam and in a direction perpendicular to it, during diffractional scattering there is observed symmetricalness only relative to the primary beam, and the indicatrix may be expressed by equation

$$R_\varphi = 1 + p\cos\varphi + q\cos^2\varphi. \qquad \text{(III.18)}$$

Coefficients p and q depend on substance of particles and their dimensions. For fog with average water content p = 2.7 and q = 3.

With increase in α, i.e., ratio of ρ to λ, the diagram of scattering is extruded forward. Energy thrown back and to the sides decreases, approaching in limit to 16.8% of all decreased energy (geometric scattering).

Hutton and Stratton found that in the case of diffractional scattering the coefficient of scattering β_ε is function

$$\left.\begin{aligned}\beta_\varepsilon &= 2\pi\rho^2 k,\\ k &= f(\alpha).\end{aligned}\right\} \qquad \text{(III.19)}$$

Since k depends on dimension of particles and wave length, then at λ = const the curve in Fig. III.5 gives dependency of scattering coefficient on dimension of particles, but at ρ = const - on the wave length of the spreading radiant flux.

A particular case of diffractional scattering is the case of the scattering of radiant flux on limiting large particles - geometric scattering. It is characterized by two basic positions:

a) magnitude of scattered energy does not depend on wave length of radiant flux falling on the particle;

b) energy of radiation thrown in the direction of the primary beam is 24 times more than the energy thrown to the opposite side.

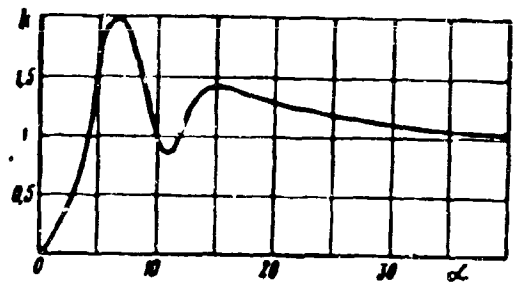

Fig. III.5. Dependency k = f (α) in the formula of Stratton - Hutton.

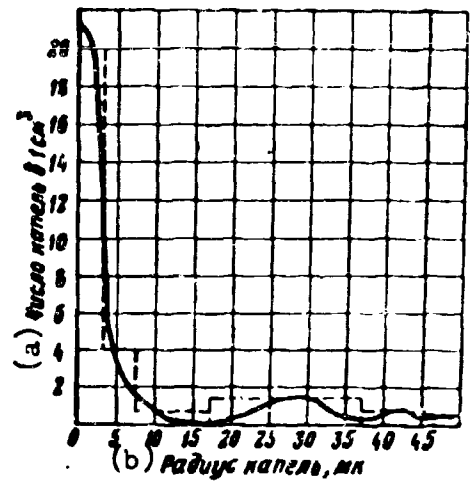

Fig. III.6. Distribution of drops in fog by dimensions.
KEY: (a) Number of drops in 1 cm^3; (b) Radius of drops, μ .

In spite of this, in practice is observed the best passage of long-wave infrared radiation in a turbid atmosphere, where geometric scattering is basic. This is possible to explain, first, by the dependency of refractive index of the reflecting particle on wave length and, secondly, by the presence in atmosphere, along with big particles, of a very large quantity of small particles (Fig. III.6), which on the whole makes atmosphere more transparent for long-wave radiation.

Best passage of turbid atmosphere, including fogs, by long-wave radiation is confirmed by a number of works, in spite of the presence, in this region of the spectrum, of selective absorption.

4. Selective Absorption of Radiant Energy

During absorption of radiant flux in the atmosphere there occurs its weakening due to transition of part of the radiation energy into other forms of energy: thermal, mechanical, and chemical. Characteristic for such weakening is the fact that absorption of radiant flux in the atmosphere is selective and exists only for those waves whose frequency is resonance for molecules of gases composing the atmosphere. As a rule, in such selective absorption of radiant flux participate

polyatomic molecules of gases and in the first place water vapor (H_2O), carbon dioxide (CO_2), and ozone (O_3).

Ozone has the most important absorption bands in the far ultraviolet part of the spectrum between 0.2 and 0.32 μ with $\lambda_{макс} = 0.255\ \mu$; in the visible region — with $\lambda_{макс} = 0.6\ \mu$, where the coefficient of absorption is $\beta = 0.068\ cm^{-1}$; in the infrared region of the spectrum in a range of wave lengths 4.63-4.95 μ ; 8.3-10.6 μ ($\beta = 0.255\ cm^{-1}$) and 12.1-16.4 μ .

Carbon dioxide has a series of absorption bands in the infrared region of the spectrum, from which the strongest are the narrow band 4-4.8 μ and the wide in a range of 12.9-17.1 μ with $\lambda_{макс}^{*} = 14.3\ \mu$.

Water vapor contained in atmosphere in relatively large quantities, has a large number of wide absorptior bands in visible and infrared regions of the spectrum. In the visible region of the spectrum are five relatively weak absorption bands by water vapor, namely: 730.4-682 mμ , 606-586 mμ , 578-567 mμ , 547.8-542 mμ and 511.1-498 mμ . However, even near the infrared region of the spectrum there are strong and wide absorption bands: 0.926-0.970 μ , 1.095-1.165 μ , 1.319--1.498 μ , 1.762-1.977 μ and 2.52-2.845 μ .

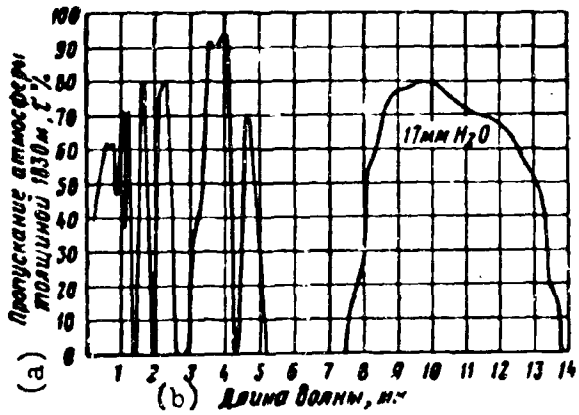

Fig. III.7. Transparency of atmosphere by Jebby.
KEY: (a) Transmission of atmosphere with a thickness of 1830 m, %; (b) Wave length, μ .

In Fig. III.7 is depicted transparency of atmosphere with a thickness of 1,830 m, according to Jebby, for wave lengths to 14 μ .

The fullest and most detailed research of spectral transmittance of the atmosphere in the infrared range of the spectrum was conducted by Taylor and Uayts [Whites, Waites] in 1956 [3]. In this research they studied transparency of a horizontal layer of atmosphere above

*The Russian subscript "makc" indicates "maximum".--Ed.

a water surface. Length of sections corresponded to 305 m; 5.47 and 16.2 km.

As a result of research there was obtained a fine structure of spectrum of transmission of the atmosphere in a wave range of 0.6-15 μ .

The works of Jebby, Taylor, and Uayts [Whites, Waites] allow us, with sufficient accuracy, to determine those sections of spectrum, within the limits of which the atmosphere is more or less transparent for infrared rays. Thus, for air at sea level with a content in the layer of precipitated water 13.7-17 mm there are "windows", i.e., sections transparent for infrared radiation, with the following wave lengths,

0.95-1.05 μ	3.3-4.2 μ
1.15-1.35 μ	4.5-5.1 μ
1.5-1.8 μ	8-13 μ
2.1-2.4 μ	

With increase of height above sea level the passband width of the "windows" of atmosphere is increased (Fig. III.8) due to decrease of air density and quantity of water vapor in it.

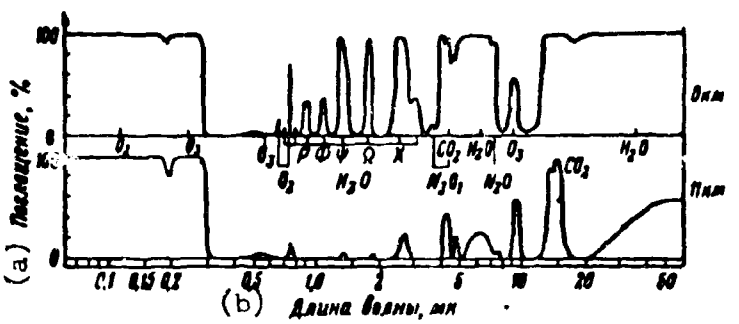

Fig. III.8. Spectral coefficient of absorption of the atmosphere at various heights.
KEY: (a) Absorption, %; (b) Wave length, μ .

A sufficiently simple method of calculating transparency of the atmosphere inside a wide spectral band was offered by Elder and Strong [5]. Their method of calculation is based on the experimentally fixed fact that the more equivalent the layer of absorber W, the less the additional increase of absorption caused an increase in equivalent layer of absorber to magnitude dW. Mathematically this position may be described by approximate empirical equation

$$\tau_{\text{п.п}} = t_0 - k \log W. \qquad \text{(III.20)}$$

Equation III.20 is based on the assumption that spreading radiation occupies a sufficiently wide spectral range, in order to include some absorption bands. Therefore, Elder and Strong broke the spectrum of infrared radiation 0.72-14 μ down into 8 sections, for which values of coefficients t_o and k were determined (Table III.8).

Table III.8. Sections of Infrared Spectrum and the Value of Constants in Equation (III.20)

No. of section	Boundary of Section, μ	k	t_o
I	0.72-0.92	15.1	106.3
II	0.92-1.1	16.5	106.3
III	1.1-1.4	17.1	96.3
IV	1.4-1.9	13.1	81.0
V	1.9-2.7	13.1	72.5
VI	2.7-4.3	12.5	72.3
VII	4.3-5.9	21.5	51.2
VIII	5.9-14	—	—

For the case of atmosphere free from solid and liquid impurities (based on Elder and Strong, over 2-3 km), but containing water vapor, the solution to equation (III.20), depending upon the concentration of water vapor, is shown in Fig. III.9, where, to determine water content of the atmosphere at heights over 3,000 m, Elder and Strong applied expression

$$W = a_0 \cdot 10^{-\left(3 + \frac{H}{5}\right)L}, \qquad \text{(III.21)}$$

where a_0 is absolute humidity for earth, g/cm^3,

H is height, km,

L is distance, m.

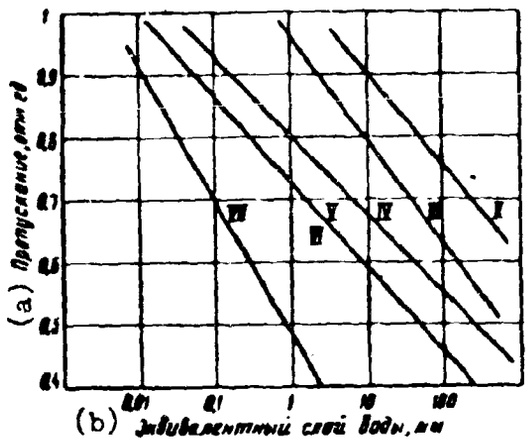

Fig. III.9. Graphic interpretation of equation $\tau_{изл}=t_0-k \log W$.
KEY: (a) Transmission, relative units; (b) Equivalent layer of water, mm.

The graph in Fig. III.9 allowr us, with respect to definite water content, to determine transparency of the atmosphere due to selective absorption of water vapor inside any section of the spectrum at heights over 3 km. However, the equation of Elder and Strong does not consider weakening of radiant flux by haze. Using data of many observations for heights over 2-3 km (pure atmosphere), Elder and Strong (approximating dependency $\tau_p=f(\lambda)$ for equivalent layer of water 1 mm) give a formula of transparency of atmosphere due to scattering in water vapor:

$$\tau_p=(0{,}998)^{\blacktriangledown}, \qquad \text{(III.22)}$$

where W is water content in atmosphere on every kilometer of beam path.

Consequently, in accordance with expression (III.12) total transmissivity of pure atmosphere may be calculated as

$$\tau=\tau_{н.п}\tau_p=(t_0-k \log W)\cdot 0{,}998^{W}. \qquad \text{(III.23)}$$

Literature

1. JOSA, 1941, No. 7.
2. Proc. Roy. Soc. Am., 1951, No. 1084, p. 206.
3. JOSA, 1957, Vol. 47, No. 3.
4. JOSA, 1956, Mar., Vol. 46, No. 3, Apr., No. 4.
5. J. Franklin Inst., 1953, Vol. 255, No. 3, p. 189.

C H A P T E R IV

OPTICAL MATERIALS AND OPTICAL SYSTEMS

I. Materials

1. Infrared Filters

The filter is an optical device, with the help of which a change of spectral composition and magnitude of radiant flux falling on a sensitive element is possible.

The action of filters may be based on different optical phenomena: absorption, interference, selective reflection, polarization, and so forth. Filters can be solid, liquid and gasiform. In technology the most wide-spread are solid filters, founded on the absorption of radiant flux in glass, plastic, special films and artificial or natural crystals.

For absorption of visible radiation and transmission of near-wave infrared radiation (0.8–3 μ) the most widely used are glass filters, colored in their mass by manganese oxide or sulpho-selenide of antimony, and also film and filters on a base of acetyl-cellulose or gelatin (Fig. IV.1 and IV.2).

From filters is required maximum integral transmission in the infrared region of the spectrum and minimum - in the visible. Furthermore, it is desirable that the front edge of the spectral curve of transmission would be, as far as possible, steeper. In this respect film filters are somewhat better than glass, however, the latter are stabler in time, more durable and more heat- and moisture-proof. They are also more technical in production.

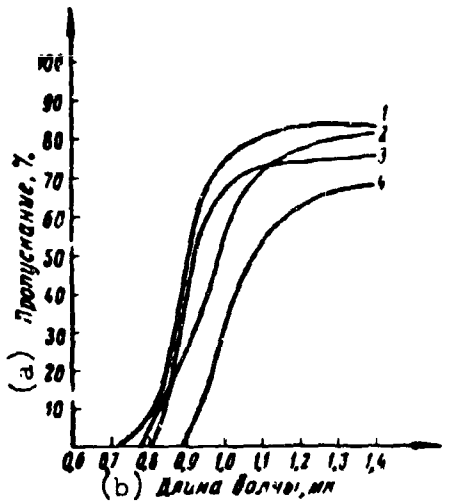

Fig. IV.1. Transmission of infrared filters.
1--KC-13 d = 2 mm; 2--KC-12 d=2mm; 3--Film d = 3 mm; 4--Film d = 4 mm.
KEY: (a) Transmission, %; (b) Wave length, μ .

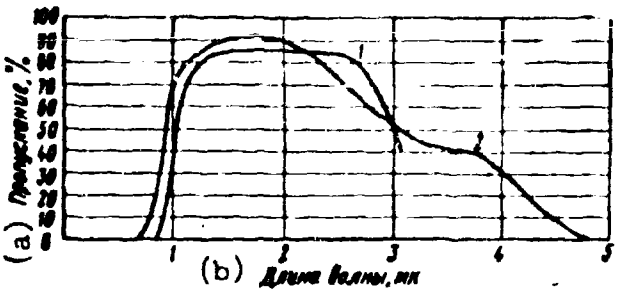

Fig. IV.2. Transmission of glasses IKS-1, d = 2 mm (1) and manganic d = 2 mm (2).
KEY: (a) Transmission, %; (b) Wave length, μ .

For filtration of visible radiation with success gelatin glass filters can be applied (Fig. IV.3). They consist of a layer of colored gelatin placed between two pieces of glass. These filters have a steep front edge of spectral characteristic and a high transparency in the infrared region of the spectrum. However, they are sensitive to change of temperature and possess bad moisture proof characteristics, since they consist of three elements glued together.

In the considered filters visible radiation is absorbed by dye, but absorption of long-wave radiation is determined by the sort glass. Therefore, for filtration of long-wave infrared radiation can be used unpainted glass (Fig. IV.4) which conducts well visible and infrared radiation up to 2.5 μ , and opaque for waves of more than 4.5 μ .

To exclude visible and near-wave infrared radiation powder filters have been used, constituting a base which is transparent in the necessary region of the spectrum (a plate of sylvite or rock salt), on which, by means of evaporation in a vacuum, there is precipitated a layer of metallic or semiconductor powders.

Principle of action of such filters is based on dispersion of visible and near-wave infrared radiation by particles whose dimensions are commensurable with wave length. Such filters will be opaque for radiation with wave length smaller

than dimension of particles of the powdery layer, and transparent for wave lengths larger than dimension of particles. It was determined that for transmission of radiation energy in range of waves 2-7.5 μ particles of a powder filter have to have dimensions from 0.22 to 2.5 μ [2].

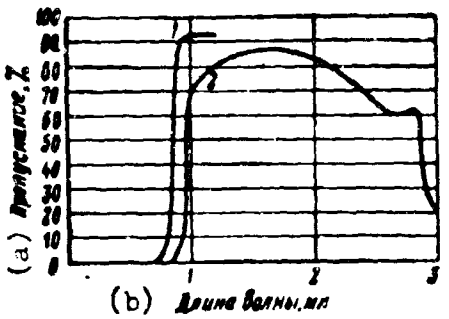

Fig. IV.3. Transmission of gelatin glass filters of the firm of "Worten-Kodak" (1) and State Optical Institute (GOI) No. 2128/6680 d = 4 mm (2).
KEY: (a) Transmission, %; (b) Wave length, μ.

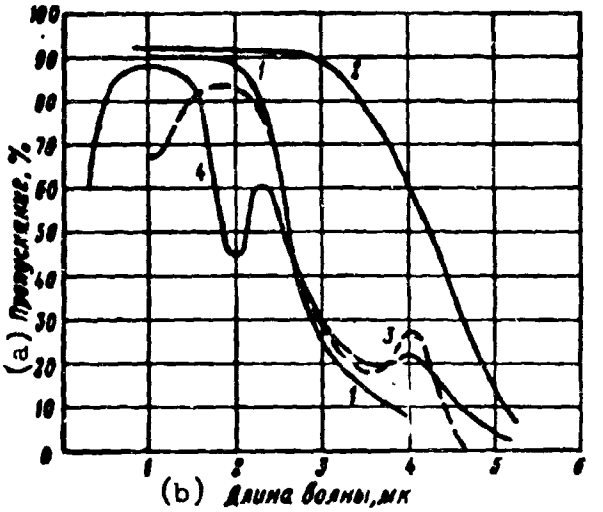

Fig. IV.4. Transmission of glasses, mirror (1), quartz (2), window (3) and single crystal of quartz (4).
KEY: (a) Transmission, %; (b) Wave length, μ.

As a rule, dispersing powder should be transparent to infrared rays, however, as in seen from Fig. IV.5, metallic niello can appear transparent to infrared rays.

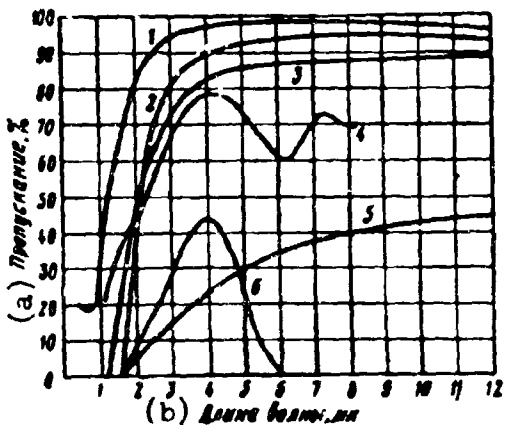

Fig. IV.5. Transmission of powder filters:
1—gold niello on sylvite; 2—selenium on sylvite; 3—telluric niello on sylvite; 4—magnesium oxide on mica; 5—bismuth niello on sylvite; 6—magnesium oxide on glass (d = 0.1 mm).
KEY: (a) Transmission, %; (b) Wave length, μ.

To powder filters one should relate filters of silver chloride with a black layer of silver bromide. They are absolutely opaque for visible rays, but conduct radiation well in the wave range 1-3 μ [3].

As a base for many powder filters is applied mica, if it is desirable to separate radiation with a wave length of 2-8 μ. Spectral transmission of two sorts of mica is shown in Fig. IV.6.

Table IV.1. Basic Properties of Certain Crystals

Material	λ_o, μ	Refractive Index n_D	Solubility in Water, g/100 cm^3	Properties
KBr	27	1.55	53.48	Colorless cubic crystals. Hygroscopic, soft, easily scratch. Dissolved in alcohol and glycerine. Prepared in diameter up to 190 mm. Value average
NaCl	20	1.54	35.7	Colorless cubic crystals. Hygroscopic. Cracked, easily scratch. Dissolved in glycerine. Prepared in diameter up to 190 mm. Value low
LiF	85	1.39	0.27	Colorless cubic crystals. Cracked, easily scratch. During polishing can be scaled off on surface. Dissolved in acids. Prepared in diameter up to 185 mm and larger. Raw material for artificial preparation is deficient. Value average.
CaF_2 (Fluorite)	11	1.43	0.002	Colorless cubic crystals. Cracked, easily scratch. Start to conduct from 0.324 μ. Dissolved in solutions of salts NH_4. Prepared in dimension up to 150 mm. Value average.
KCl (Sylvite)	24	1.49	34.7 (20°c)	Colorless cubic crystals. Hygroscopic. Easily scratch. Dissolved in alkalis, esters, glycerine. Have absorption band near 3 and 7 μ. Good crystals are rarely encountered. Value average.
KI	31	1.67	127.5	Colorless cubic crystals. Are very hygroscopic. Polished with difficulty. Very soft, easily scratch. Dissolved in alcohol and ammonia. Prepared in diameter up to 190 mm. Value average.
CsBr	40	1.7	124.3 (25°C)	Colorless cubic crystals. Hygroscopic. Soft, easily scratch. Dissolved in alcohol. Prepared in diameter up to 45 mm. Value average.
CsI	50	—	—	Colorless cubic crystals. Very hygroscopic.

The above considered filters allow the separation of comparatively narrow sections of the infrared spectrum. If it is necessary to work with long-wave infrared radiation, then it is expedient to apply materials for which the normal frequencies of oscillations of molecules lie in the far infrared region of the spectrum. Such materials are, mainly, crystals: potassium bromide, potassium iodide, rock salt, lithium fluoride, calcium fluoride, potassium chloride, cesium bromide, and others. Their basic properties and spectral curves of transmission are given in Table IV.1 and in Fig. IV.7.

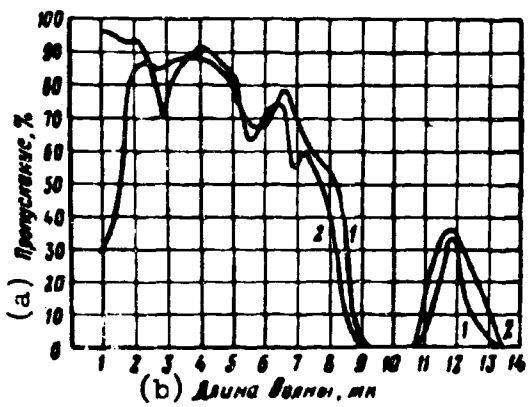

Fig. IV.6. Transmission of black mica d = 0.4 mm (1) and muscovite d = 0.2 mm (2).
KEY: (a) Transmission, %; (b) Wave length, μ .

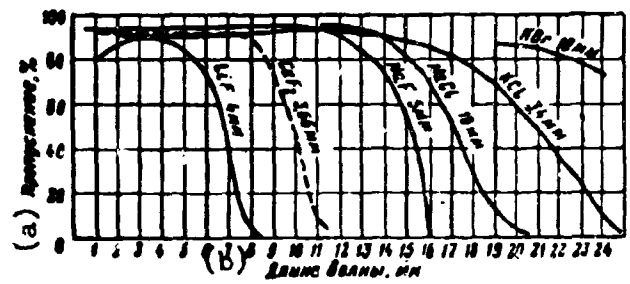

Fig. IV.7. Transmission of certain crystals.
KEY: (a) Transmission, %; (b) Wave length, μ .

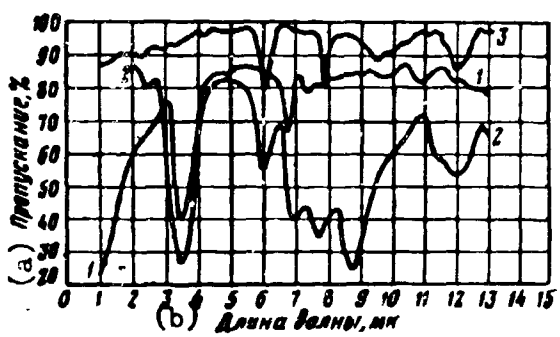

Fig. IV.8. Transmission of protective films.
1--polyethylene d = 0.025 mm; 2--hydrochloride of rubber d = 0.045 mm; 3--nitrocellulose d = 0.5 mm.
KEY: (a) Transmission, %; (b) Wave length, μ .

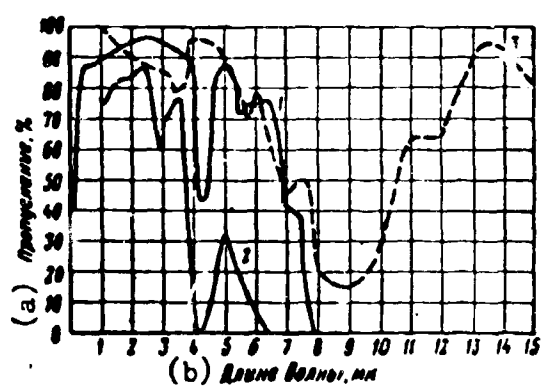

Fig. IV.9. Transmission of teflon. 1--thickness 0.? mm; 2--thickness 4 mm; and 3--vinyl varnish d = 20 μ .
KEY: (a) Transmission, %; (b) Wave length, μ .

The characteristic peculiarity of the enumerated crystals is high hygroscopicity, for which it is necessary to cover them by protective films, introducing noticeable absorption of infrared radiation and worsening the optical properties of parts of the instruments. As protective films, the most frequently used are films of hydrochloride, rubber, polyethylene, teflon, vinyl varnish, and other materials [5] whose spectral transmittance is shown in Fig. IV.8 and IV.9.

2. Materials for Protective Glasses and Cowls

Materials, from which are prepared protective glass and cowls of infrared instruments, besides a high coefficient of transparency in the needed range of wave lengths, must satisfy the requirements of high durability, heat and moisture proof characteristics, and stability of properties in time, and must allow the manufacture of models of different configuration.

Therefore, considered in Section 1, the materials with the exception of glass, even if they can be applied as entrance windows of radiant flux receivers, as a rule, are unfit for protective glasses and cowls of infrared instruments.

Recently wide research has been conducted, which makes it possible to obtain new artificial materials combining good transparency in a wide range of wave lengths of the infrared region of the spectrum with good operational qualities.

Characteristics of such materials are given in Table IV.2 [4] and Fig. IV.10.

The glass "Servofrax", developed in the United States, is used for the manufacture of lenses and objects having minimum spherical aberration in a wave range of 2-5 μ. In order to decrease losses on reflection, surface of lenses is cleared [9].

Silver chloride in the form of rolled sheets [16] and articles of it are widely used where nonhygroscopicity and insolubility in water are required. The coefficient of transparency of silver chloride up to 18 μ is 80%. Increase of transparency may be attained by brightening surface; indeed, this introduces additional absorption bands caused by absorption of the film of polystyrene [17]. A deficiency of silver

Table IV.2. Basic Properties of Certain Materials Applied During the Manufacture of Cowls of Infrared Instruments

Material	λ_o μ	n_D	Solubility in water τ, g/100 cm^3	Properties
Glass	3	1.5-1.9	0	Homogeneous. Colorless. Easily cut, ground and polished. Nontoxic. Dimensions are unlimited. Value low.
Glass "Servo-frax" Al_2S_3 [9]	12	2.59	0	Homogeneous red glass. Nontoxic. Softened at +195 C. Is dissolved in alkalis. Dimension is limited by structural considerations. Can be applied for all types of optical systems.
AgCl	23	2.07	0	Colorless cubic crystals. Isotropic. Will not crack. Soft. Are subject to fluidity at low temperatures. Darken in sunlight. Cause corrosion of metals. Are dissolved in NH_4OH, $Na_2S_2O_3$ KCN. Are prepared in dimension up to 100 mm. Value high.
Fused Quartz Glass SiO_2	4	1.43	0	Isotropic. Has good technical and thermal properties. Is dissolved in HF. Dimension is limited only by optical homogeneity. Value average.
Sapphire Al_2O_3 [10]	5.5	1.77	0	Artificial hexahedral crystals. Will not crack; scratch with difficulty. Mechanical durability excellent. Thermal properties good. Maximum dimensions up to 125 mm. Value high.
Periclase MgO [8]	10	—	0	Artificial isotropic mineral. Mechanically very sturdy. With passage of time its surface dims due to formation of $Mg(OH)_2$. Value average.
Silicon [12,13,14]	20	3.5	0	Cubic crystals of grayish-steel color. High melting point. Are dissolved in HF and HNO_3. Are prepared in dimension up to 40 mm. Value high.
Germanium [14,15]	40	—	0	Crystals of grayish-steel color with dark blue nuance. Are well processed. Mechanically stable. In the region of 1.5-15 μ transparency is not less than 40%. Value high.
KRS-5 TaBr+TaJ	38	2.63	0.02	Red cubic crystals. Will not crack, easily scratch, are difficult to polish. High coefficient of expansion. Are toxic. Are dissolved in HNO_3 and in aqua regia. Are prepared in dimension up to 125 mm. Value high.
KRS-6 TlBr+TlCl	—	—	—	Optical properties better than for KRS-5. Toxic. Value very high.

chloride is the fact that it is impossible to apply in daylight. To prevent blackening of silver chloride its surface is covered by antimony or selenium, which leads to a certain increase in reflection of radiant flux due to the larger value of refractive index for antimony and selenium than for silver chloride.

Artificial sapphire finds application for cowls of rocket missiles with infrared homing devices [10]. At present production of nose cones with diameter of 140-175 mm has become familiar. Synthetic sapphire passes 90% of the radiation with wave lengths up to 4 μ and 50% on 6 μ wave. In hardness artificial sapphire stands next to diamond and preserves it up to a temperature of 1,800°C (Fig. IV.11).

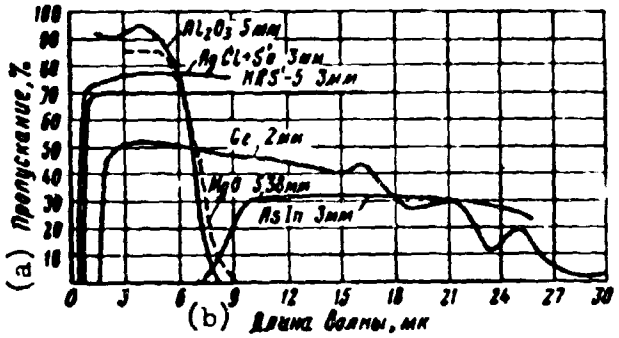

Fig. IV.10. Transmission of certain materials for cowls of infrared systems.
KEY: (a) Transmission, %; (b) Wave length, μ .

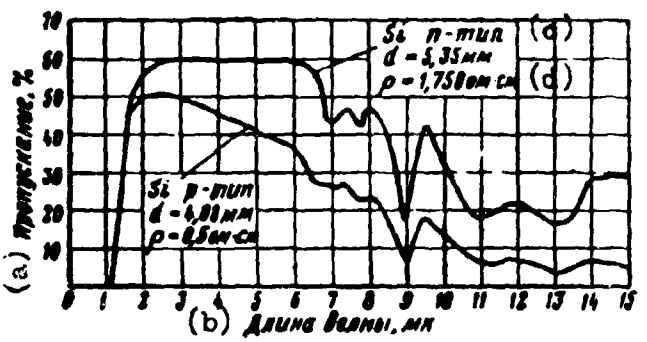

Fig. IV.11. Transmission of silicon.
KEY: (a) Transmission, %; (b) Wave length, μ ; (c) Type; (d) ohm.cm.

Germanium and silicon have become serious competitors to quartz, sapphire, and silver chloride as optical materials for infrared instruments, in spite of the comparatively high cost of obtaining them. These elements very similar in optical respects, possess good transparency in a wide range of the spectrum, allow the clearing of their surfaces and have good thermal and mechanical properties [12, 13, 14, 15].

Along with crystal materials glass like materials have come into wide use.

Tellurite black glass [16], containing from 20 to 81.5% TeO_2, and as impurities - CaO, MnO_2 and V_2O_5, passes, in a wave range of 0.8-5.0 μ , up to 70% of radiation energy. Having similar properties are: Tellurite glass TeO_2 - PbO-ZnF_2 [17],

lead-lanthanum germanium glass type G-135, calcium-aluminum - silicate glass type C-1458, and, equivalent to them, germanate glass C-1434 [18] (Fig. IV.12).

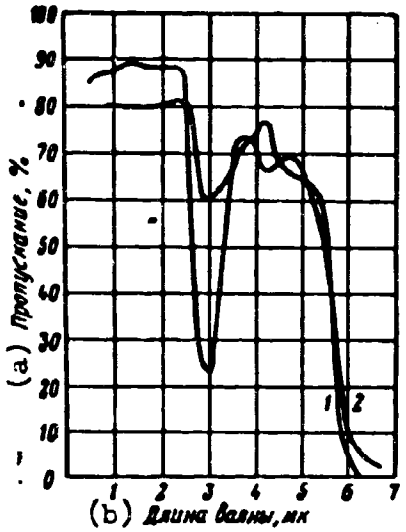

Fig. IV.12. Transmission of glass: 1--G-135, thickness 2mm; 2--C-1434, thickness 2 mm.
KEY: (a) Transmission, %; (b) Wave length, μ .

Analogous curves of transmission have glass like materials on a base of calcium aluminate [19], which in a wave range of 2-5 μ have a coefficient of transparency up to 90% and a refractive index for a 4.26 μ wave of 1.592 — 1.753.

Glass-like materials with a wider range of spectral transmissivity have been created on a base of selenium, arsenic and sulfur [17, 20].

Sulfur-arsenic glasses (Fig. IV.13) are transparent up to 14 μ and in a case of 20% sulfur content they will pass up to 50% of the radiant flux (curve 1, a), and with 60% sulfur content the coefficient of transparency of radiant flux is increased to 65% (curve 1,b). Glass-like selenium (curve 2) has an almost uniform transparency in a wave range of 1-21 μ , equal to 60-65%.

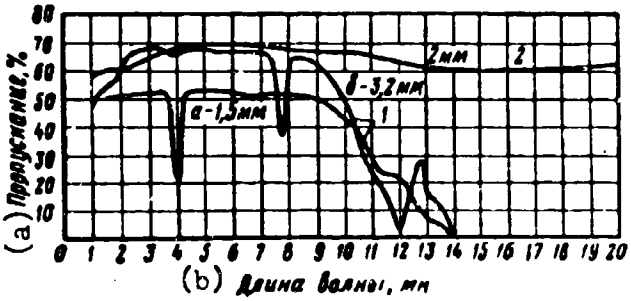

Fig. IV.13. Transmission of glass of sulfur-arsenic 1 and selenium 2.
KEY: (a) Transmission, %; (b) Wave length, μ .

The most successful was glass from pentaselenide and pentasulfide of arsenic, whose spectral curves of transmission are shown in Fig. IV.14.

Trisulfide of arsenic, obtained Freric, constitutes a glass-like substance of a dark red color. At normal temperature coefficient of expansion is $26 \cdot 10^{-6}$, point of softening +195°C, solubility in water at normal temperature $5 \cdot 10^{-5}$ g/100 cm^3, density 3.2 g/cm^3. Transmissivity in the 1-12 μ region is 70%. The glass is hard but easily yields to grindir .

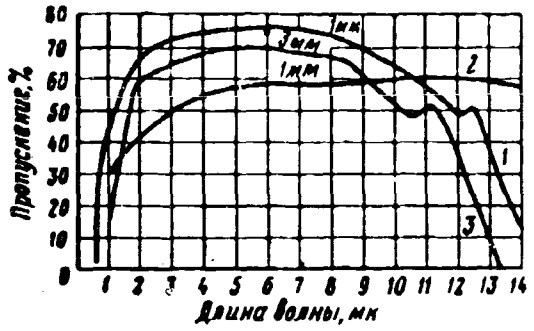

Fig. IV.4. Transmission of pentasulfide (1), pentaselenide (2), and trisulfide (3) of arsenic. KEY: (a) Transmission, %; (b) Wave length, μ :

Pentaselenide and pentasulfide glass, black in appearance with a brilliant surface, is insoluble in water at normal temperature (at 100°C their solubility constitutes 0.0017 g/100 cm^3), and has a density of the order of 4.4 g/cm^3 and a softening point of 200°C. In a wave range of 0.6-13 μ transparency of the glass constitutes 60-65%.

3. Reflecting Coverings

In instruments of infrared technology reflecting optical systems are frequently applied. Their basic advantage, as compared to lens optics, is the absence of chromatic aberration, which allows us to use the same objective in a very wide spectral range. Furthermore, the value of mirror objectives is lower than the value of lens.

To mirrors are presented two basic requirements: high reflectivity in the needed spectral range and good quality of image. The first is attained by corresponding selection of reflecting covering; the second - by the quality of manufacture of the sublayer (glass or metallic) of a definite form: paraboloid, hyperboloid, ellipsoid, part of a sphere or, finally, a plane. The sublayer material most widely used is glass, which processes well and allows us to obtain reflecting surfaces of high quality.

The external surface of mirrors is covered by a dense layer of well reflecting infrared rays of metal by means of its evaporation in a vacuum, since reflectance of coverings precipitated in a vacuum is always higher than for the polished surface of metal.

In the infrared region of the spectrum high reflectance is possessed by silver,

gold, copper, rhodium, and aluminum (Fig. IV.15). For wave lengths, more than 4 μ, reflectivity of these coverings may be defined by the formula

$$\rho = 1 - 0{,}365\sqrt{\frac{r}{\lambda}}, \qquad \text{(IV.1)}$$

where r is the specific resistance of metal, ohm/mm^2/m;

λ is wave length, μ.

Silver in the infrared region of the spectrum has a reflectivity of 99%, however, only in the freshly prepared layer. With passage of time the layer darkens, and reflectance strongly drops. Moreover, because of comparatively bad cohesion with glass, the physical durability of the layer is insignificant.

Alloy of aluminum and magnesium (69% Al + 31% Mg) is more stable than silver, but reflectivity in the infrared part of the spectrum attains 92%.

Gold and platinum have the same reflectivity in the infrared part of the spectrum, as silver, and in their chemical and physical stability do not differ except in rhodium coverings. A layer of gold is very convenient if it is necessary to lower reflection of visible radiation.

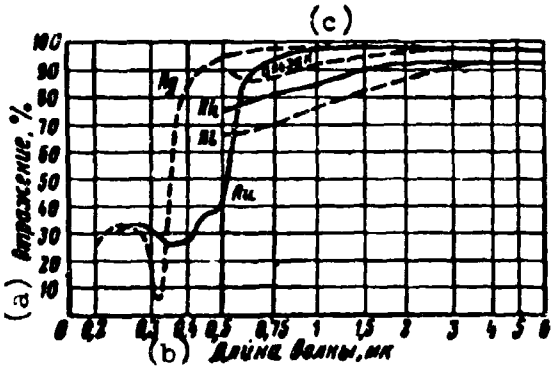

Fig. IV.15. Spectral reflectivity of certain coverings.
KEY: (a) Reflection, %; (b) Wave length, μ; (c) Alzak.

Aluminum has high reflectivity in all the optical part of the spectrum of electromagnetic oscillations - from vacuum ultraviolet to the far infrared region. Possessing good cohesion with glass and protective oxide film, the reflecting aluminum layer has good mechanical durability (covering can be washed by water with soap) and does not dim in air. The thickness of the protective oxide film attains 100 Å. To increase its durability a spray of a thin film of SiO is applied, which, even under conditions of heating up to 450°C for 40 hours and the effect of a 10% solution of NaOH for an hour, ensures preservation of reflectance of the layer.

Frequently it is desirable to use the reflective element as a filter for cutting out an unnecessary section of wave lengths or isolation of a desirable band of radiation. With this goal, in recent years there have been developed different combinations of selective reflecting films [21].

In the simplest form, such reflective filters consist of opaque, well-reflecting metal (for instance, aluminum), dielectric lining and a semitransparent layer of metal. Maximum reflection is for those wave lengths, for which the thickness of the lining is equal to an even number of quarters of wave lengths; minimum - for those wave lengths, for which thickness of lining is equal to an odd number of quarters of wave lengths. Reflectivity for maximum is equal to the reflectivity of opaque metal, but reflection for minimum may be brought to zero by means of corresponding selection of thickness of semitransparent metallic film (Fig. IV.16).

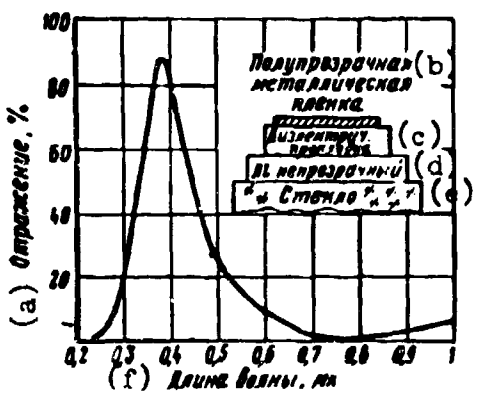

Fig. IV.16. Construction and spectral reflectivity of selectively reflecting filter. KEY: (a) Reflection, %; (b) Semitransparent metallic film; (c) Dielectric lining; (d) Opaque aluminum; (e) Glass; (f) Wave length, μ.

Filters of such type are prepared for all the optical region of electromagnetic oscillations and micro-waves. It was determined that, applying several film pairs, it is possible to prepare very narrow-band reflecting filter.

Very frequently it is necessary to cut out the visible and ultraviolet part of the spectrum for the purpose of decreasing the effect of scattered light in the instrument. With this goal, two film combinations of such "dark" mirrors were developed (Fig. IV.17).

In first type aluminum is covered by germanium film and SiO, where each of the films has a thickness approximately a quarter of the wave length. Germanium is used because of its good absorption in the visible part of the spectrum and good transmission in the infrared.

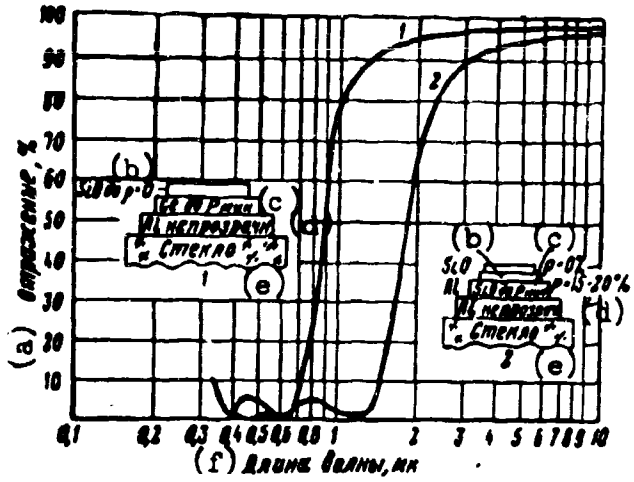

Fig. IV.17. Construction and spectral reflectivity of "dark" mirrors.
KEY: (a) Reflection, %; (b) Up to; (c) Minutes; (d) Opaque; (e) Glass; (f) Wave length, μ .

In the sec d type two coverings of SiO are used (divided by semitransparent aluminum film applied on an opaque layer of aluminum.

II. Optical Systems

4. Assignment and Classification

Optical systems are designed for reception (transmission) and redistribution of radiant flux with the purpose of its more effective use.

They can be a component part of a source of radiation energy. In this case optical systems serve either for concentration or radiant flux in a small solid angle to obtain great luminuous intensity in a definite direction, or for obtaining a definite form of rays of radiant flux.

If optical systems are applied jointly with a receiver (indicator) of radiation energy, then they are designed for focusing radiant flux incident on the optical system and the direction of it to the sensitive element of the receiver. Thanks to this, irradiance of the sensitive element can significantly exceed irradiance of the surface of the optical system.

There are three groups of optical systems:

a) lens or dioptric, in which radiant flux is redistributed as a result of passage of it through re racting media,

b) reflective or catoptric, in which radiant flux is redistributed in space as a result of reflection from one or several mirrors of different form,

c) mixed, combining lens and reflective systems.

These three groups of optical systems have found wide application in instruments of infrared technology.

Quality of optical systems in infrared instruments in many respects is determined by their resolving power, which in many cases should be very high. Thus, in visible and near-wave infrared regions of the spectrum where as sensitive elements are used the eye, a photographic plate or an image converter, having a resolving power sometimes less than 10 μ, from optical systems there is required a resolving power not less than 40-50 lines per 1 mm. Starting from 2 μ and above the resolving power of contemporary sensitive elements constitutes a magnitude of the order of 100 μ and more, which somewhat lowers the requirement for resolving power of optics. This circumstance makes it possible to apply, in certain types of infrared instruments, simpler optical systems.

Resolving power of the ideal optical system is limited by the diffraction pattern around the image of the observed point. Diameter of the image of a point source, in this case, may be determined from relationship

$$\frac{d}{\lambda}=1{,}22\frac{f}{D}, \qquad \text{(IV.2)}$$

where d is the diameter of the central maximum of point image in the same units as λ.

f is focal length of objective, effective for a given λ,

D is diameter of inlet.

This expression shows that with increase in λ and f, resolving power of optical systems worsens.

In real optical systems, resolving power additionally worsens due to distortions inherent in them (aberrations).

5. Lens Optical Systems

Any lens optical constitutes a definite combination of lenses, therefore, basic operational principles of such systems can be explained by the example of the work of a single lens. The lens is that component made out of some kind of transparent material, limited by one or two spherical surfaces whose centers are disposed on one line called the main optical axis of the lens (Fig. IV.18a).

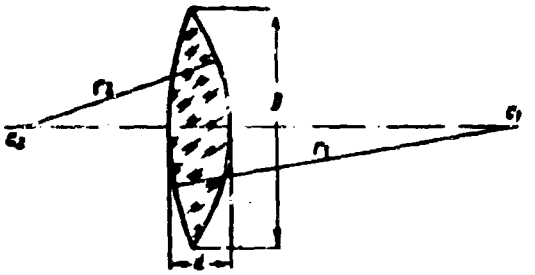

Fig. IV.18a. Parameters of a lens.

For description of geometric forms and properties of a lens it is sufficient to know the radii of curvature of surfaces r_1 and r_2, axial thickness d, diameter D and index (refractive index of material n_1 from which lens is prepared.

In the case of collecting systems (objectives) the basic problem of optics is obtaining an image of luminescent points or extended objects.

An image of luminescent points, obtained with the help of lenses, differs from real sources by the fact that although from the real source radiant flux spreads to all sides and may be revealed from all sides, from its image, obtained with the help of a lens, radiant flux spreads in a limited solid angle ω. The magnitude of this solid angle is determined by the relative opening of the lens. Thus, if one decreases the diameter of the lens by the diaphragm, then the solid angle will be narrowed and, within limits, an image will be observed only in one definite direction (Fig. IV.18b).

In the considered example source of radiation S is on the main optical axis of the lens. Its image S' is obtained also on the main optical axis at a point called conjugate. If one moves the source of radiation from the lens to such a distance that it is possible to consider the rays falling on the lens parallel, then the image will be at a point called main focus F.

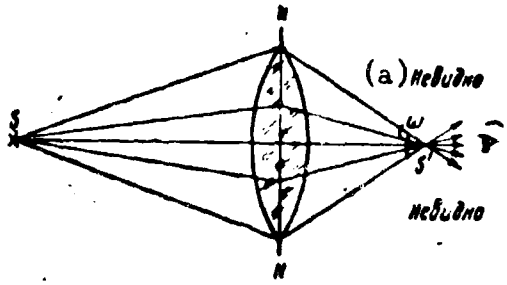

Fig. IV.18b. Observation of an image of a luminescent point through a lens.
KEY: (a) Unseen.

The distance from the main plane of lens HH to the main focus is called main focal length f'. Main focal length f' depends on magnitude and direction of radii of curvature, refraction index of material and thickness of lens

$$f' = \frac{nr_1r_2}{(n-1)[n(r_2-r_1)+(n-1)d]}. \quad \text{(IV.3)}$$

In diagrams of objectives there are usually indicated magnitudes f' and v' (summit focal length). This allows us to find the main back focus F' and, deferring to the left of it, the main focal length f', to obtain the positions of the main plane H'H' (Fig. IV.19).

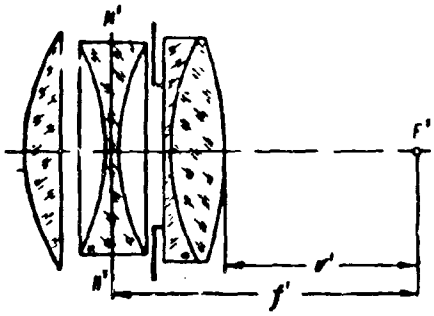

Fig. IV.19. Definition of the main plane of objective.

Introduction of the idea of main plane H'H' allows us to replace the actual refraction of the ray on all surfaces of the lenses of the objective by a fictitious one, and thereby carry out more simply, a geometric construction of the image.

Illuminance of the image created by the objective is proportional to the candle-power, i.e., the illuminance of the image is increased with an increase of diameter and a decrease of focal length of objective

$$E = c\left(\frac{D}{f}\right)^2. \quad \text{(IV.4)}$$

In this connection one should consider the question concerning brightness of the image of the observed object obtained with help of the objective. Here two cases are characteristic: observation of an extended object and observation of a point source of radiation (Fig. IV.20).

In the first case at distance l from the objective with an area of inlet S there is a body with surface σ. The image of this body with area σ_1 is constructed by objective at distance l_1:

$$\frac{\sigma}{l^2} = \frac{\sigma_1}{l_1^2}. \qquad \text{(IV.5)}$$

Radiant flux, directed from the body to the objective may be defined by formula

$$\Phi = B\sigma\omega,$$

where B is brightness of surface σ;

$\omega = \frac{S}{l^2}$ is solid angle, in which flux Φ, spreads, consequently,

$$\Phi = \frac{B\sigma S}{l^2}. \qquad \text{(IV.6)}$$

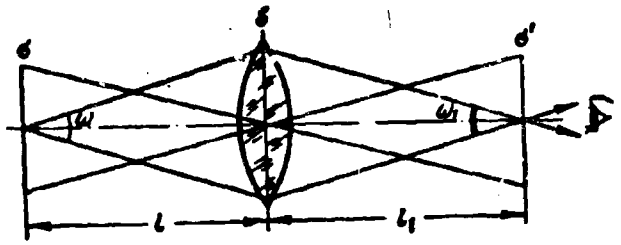

Fig. IV.20. To calculate brightness of image.

Emerging from the objective, radiant flux will decrease its magnitude due to losses in the objective

$$\Phi_1 = \tau\Phi.$$

This flux creates an observable image by area σ_1 and brightness B_1,

$$\Phi_1 = \frac{B_1\sigma_1 S}{l_1^2} = \frac{\tau B\sigma S}{l^2},$$

whence

$$B_1 = \tau B. \qquad \text{(IV.7)}$$

Consequently, brightness of the image built by the objective is always less than the brightness of the observed object ($\tau < 1$).

Illuminance of the image created in this case by the objective may be calculated by the formula

$$E = \frac{\Phi_1}{\sigma_1} = \frac{B_1 S}{l_1^2} = \frac{\tau B S}{l_1^2}. \qquad \text{(IV.8)}$$

If one considers, with optical instruments, point sources of radiation, then one can obtain also amplification of brightness of the image. However, in this case a decisive role is played by a characteristic of the work of the eye during observation of extended and point objects.

During observation of a point source all of its image falls on one light sensitive element of the retina of the eye regardless of whether it was considered by the naked eye or through an optical instrument. During observation of a source by the naked eye the luminous flux falling on an element of the retina is proportional to the area of the pupil of the eye. If, however, a source is observed in an optical instrument, then on the eye falls a luminous flux proportional to the area of the objective. Thanks to this the brightness of the image increases proportionally to the ratios of the squares of the diameters of the objective and the pupil of the eye. And since the brightness of background, as an extended object, remains constant, contrast of image simultaneously increases.

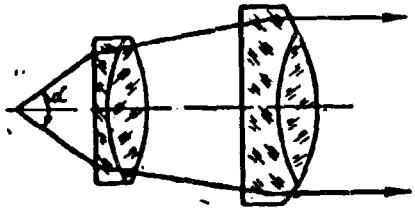

Fig. IV.21. Aperture of an optical system.

Very frequently optical systems are characterized, along with the idea "relative opening" or "candle-power," by the idea "aperture of optical system" (Fig. IV.21).

Angular and numerical apertures differ. Under angular aperture we understand maximum angle α between extreme effective rays of a conical light ray passing into the optical system. Numerical aperture is $n \sin \frac{\alpha}{2}$, where n is the refraction index of a medium in which the object is observed. With the help of the aperture one can determine the quantity of effective radiant flux and resolving power of the optical system. Thus, the brightness of the image is proportional to the square of the numerical aperture, and the resolving power is proportional to the angular aperture.

In instruments intended for visual observation in infrared rays, along with objectives, ocular systems are also used. In its simplest form the eyepiece is a magnifying glass (magnifier) allowing the eye to observe an object under an increased angle (Fig. IV.22).

The magnifier is placed before the eye, and the considered object - at a distance equal to, or somewhat smaller than the focal length of the magnifier. In this case there is obtained an imaginary straight line and an increased image of the observable object.

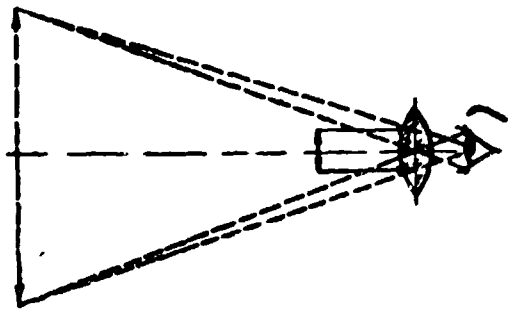

Fig. IV.22. Construction of an image by a magnifier.

The magnifying power of the ocular system is characterized by the ratio of the tangent of the angle at which the object is seen through the magnifier to the tangent of the angle at which the object is seen without the magnifier from a distance for best eye sight, 250 mm:

$$\Gamma_{ok} = \frac{\tan \omega_1}{\tan \omega}. \qquad \text{(IV.9)}*$$

If the object is in the focal plane of the eyepiece, then from every point of the object from the eyepiece emerges a parallel pencil of rays which leads by eye to the point, and on the retina is obtained a sharp image of the observed object. This case is the most frequently encountered in practice, since the eye of the observer is in a state of rest and consequently, does not cause fatigue. In this case the magnifying power of the eyepiece may be determined from relationship

$$\Gamma_{ok} = \frac{250}{f'}. \qquad \text{(IV.10)}$$

From formula (IV.10) it is clear that the magnification of the ocular system can be very large if one decreases its focal length. However, the practical limit of the magnifying power of the eyepiece is determined by the minimum permissible focal length from the point of view of observation convenience. Therefore, in optical instruments, including infrared instruments, eyepieces with a magnification of more than 15-20 times do not find application. Total magnification of such instruments is determined by the ratio of the focal length of the objective to the

*The Russian subscript "OK" indicates "ocular".--Ed.

focal length of the eyepiece, but in a case of the presence of an intermediate element (for instance, an image converter) also by its magnification.

$$\Gamma = \frac{f_{об}}{f_{ок}} \Gamma_{э.он}, \qquad \text{(IV.11)}^*$$

where $\Gamma_{э.он}$ is the electronic optical magnification of the converter.

The useful range of focal lengths of ocular systems, applied with a given objective, is limited, on the one hand, by weakening of light distributed on too magnified an image (lower limit), and on the other - by the magnitude of the output pupil (upper limit).

The diameter of the pupil of a man can change from 2 to 8 mm. Since the purpose of the eyepiece is to gather all the light from the observed object and to direct its parallel beam to the eye, it is necessary that all the light enter the eye opening. This is especially important for instruments working in conditions of low illuminance. Therefore, in eyepieces, as a rule, we try to get an image picked up near the eye to a circle in diameter less than 8 mm.

6. Reflective Optical Systems

Reflective optical systems [spherical or parabolic concave (convex) mirrors] find application as optics of irradiated systems of instruments of night vision, in heat direction finding instruments, and in homing devices for focusing radiant flux from a target to a sensitive element and in other devices where it is not necessary to obtain simultaneously all the image of the field of survey (Fig. IV.23).

A real reflector has two surfaces - the face and the back. The facing surface is turned toward the source of radiation or the sensitive element. It determines the aperture of the reflector (a circle limited by the edges of a mirror) or its light opening. The distance from the shear plane of the reflector to its summit is called depth (H). The point at which the rays gather, which fall on the

*The Russian subscript "об " indicates "object."--Ed.

reflector of the optical axis in parallel is called the focus of reflector F, and the distance from summit O to focus is focal length f.

Angle of scope ω of the reflector is called a solid angle with summit in focus, resting on the light opening. Its value may be expressed through plane angle $\varphi_{макс}$ * in the form of relationship

$$\omega = 2\pi(1 - \cos\varphi_{макс}). \quad (IV.12)$$

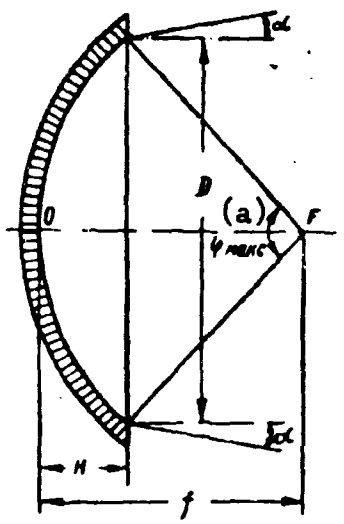

Fig. IV.23. Basic parameters of a reflector.
KEY: (a) Maximum.

Depending upon construction (Fig. IV.24) reflectors are subdivided into small ($\varphi_{макс} < 180°$), deep ($\varphi_{макс} \geq 180°$), and with a blind spot. The latter have an opening in the central part, against which something is attached which shields this part.

Since the source of radiation or the sensitive element has finite dimensions, reflectors have a certain angle of divergence (2α), the magnitude of which is determined by the ratio of dimensions of the radiator (sensitive element) to the focal length of the reflector. In certain cases angle 2α is assumed to be the instantaneous field of sight of the optical system.

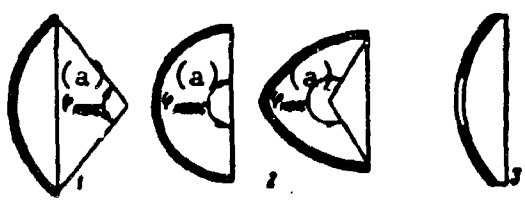

Fig. IV.24. Types of reflectors.
1—small; 2—deep; 3—with blind spot.
KEY: (a) Maximum.

Because of the presence of an angle of divergence in reflectors of irradiated devices the axial luminous intensity remains constant only from a certain distance L_o, called the distance of beam shaping. Starting from this distance,

*The Russian subscript "makc" indicates "maximum."—Ed.

which exceeds by tens and hundreds of times the focal length, it is possible to apply the inverse square law, determining irradiance at distance L:

$$E = \frac{J}{L^2} \cdot \tau. \qquad (IV.13)$$

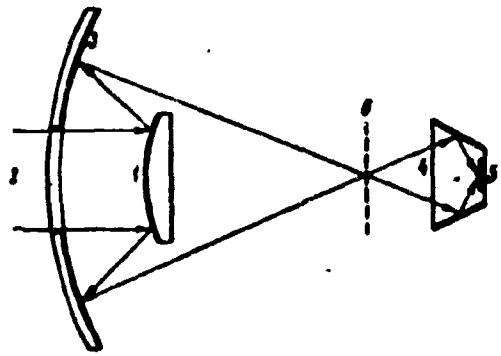

Fig. IV.25a. Diagram of the optics of an infrared homing device "Krebs".

At present in infrared instruments both glass and metallic reflectors find application.

As an example of the application of glass reflectors in heat direction finding systems, in Fig. IV.25a there is given a diagram of the optics of an infrared homing device "Krebs" (Germany), intended for guiding fire ships to ships of an enemy.

The optical system consists of convex mirror 1 with a diameter of 35 mm, on which radiant flux falls from target 2 through blind opening of concave mirror 3 with a diameter of 250 mm and with focal length 55 mm. Reflected from mirrors the radiant flux proceeds to mirror condenser ("light trap") 4 and from there to receiver 5. In the focal plane of mirror 3 there is screen disk 6, allowing determination of direction to target - "to the right - to the left". Field of sight of optical system is 45°, however on its edges sensitivity sharply drops which permits, virtually, the use of only the central part of the field, i.e., 20°.

In Fig. IV.25b is shown a diagram of a two-mirror objective, in which the blind opening serves for transmission of flux to receiver.

Along with the glass reflectors in infrared instruments, metallic also find wide application. The latter are simpler in manufacture, cheaper, and have less weight as compared to glass.

Coarse metallic reflectors, obtained by electroplating or electrochemical method, are used in irradiated installations and any kind of signaled devices. Accurate metallic reflectors for mirror objectives and heat direction finding instruments are obtained by electrolytic method.

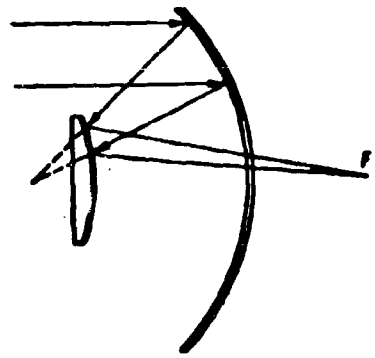

Fig. IV.25b. Diagram of mirror objective.

7. Combined Optical Systems

Mirror and mirror-lens objectives, coming into use relatively recently, allow us significantly to decrease dimensions of optics (length) with great focal length and to avoid chromatic distortions connected with the passage of radiant flux through the great thickness of glass.

In spite of the fact that construction of mirror objectives was known as early as Newton, the obstacle to their manufacture for a long time was the difficulty of manufacturing undimming mirrors. Only after adjustment of the technology of manufacturing aluminized mirrors did it become possible to prepare mirror-lens systems with high reflectivities (Fig. IV.26).

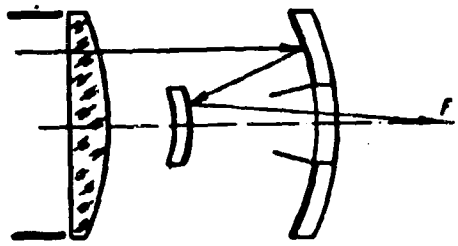

Fig. IV.26. Diagram of a mirror-lens objective.

From examining the optical diagram of a mirror-lens objective the distinctive peculiarity of such system is conspicuous that the presence of an annular form of entrance pupil decreases its area. Due to this, the area of the entrance pupil of mirror and mirror-lens objectives is less than a lens of the same diameter.

In Fig. IV.27 is given the diagram of the objective of a German homing device, the "Vasserfal" ("Waterfall"), consisting of concave positive mirror 1 with a diameter of 250 mm and a focal length of 450 mm, convex negative mirror 2, co recting

lens near focus 3 for correction of aberration comae, screen 4, condenser 5 and photocell 6. Field of sight of optical system $2\beta = 6°$.

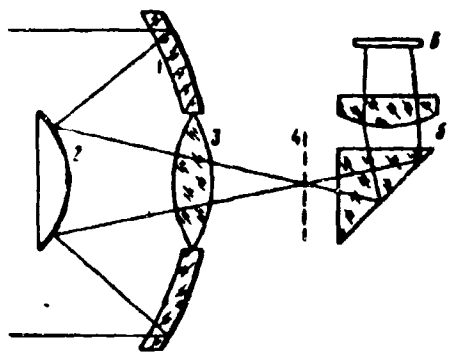

Fig. IV.27. Diagram of mirror-lens objective of thermal head "Vasserfal".

In certain constructions of mirror-lens objectives, on a lens serving for the protection of the concave mirror from dust, sweating, and mechanical damages, is placed also the correction of spherical aberration, comae, and astigmatism. Furthermore, on this lens is glued a second - negative, reflecting surface. Such objectives have obtained the name of meniscus. There can also be established simultaneously two lenses - for entrance to the objective and after output of the beam from the blind opening (near focus). In Fig. IV.28 is given a diagram of a meniscus objective with two correcting lens systems and two reflecting mirrors. A blind for the concave mirror is introduced in order to protect the image from rays which can penetrate into the bypass of the negative mirror.

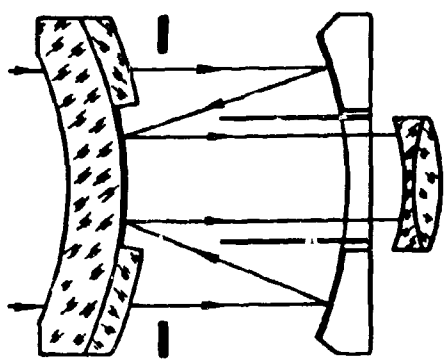

Fig. IV.28. Meniscus objective of D. D. Maksutov (f = 260 mm, A = 1, 5, 6).

At present sufficiently simple diagrams can be made of mirror-lens systems for infrared homing devices (Fig. IV.29), working jointly with cowls and having a sufficient field of sight and good resolving power.

These diagrams include primary concave mirror 1, secondary mirror with external or internal reflecting layer 2, cowl 3, and correcting lenses 4. The cowl in these diagrams plays an active role, lowering the spherical aberration of the optical system.

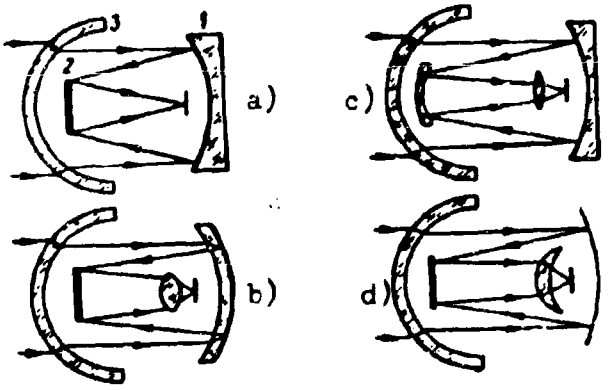

Fig. IV.29. Diagram of contemporary mirror-lens objectives for infrared homing devices.

The best of these diagrams d , does not have spherical and chromatic aberrations and ensures the size of the circle of confusion ~ 2 mrdn when angles of incidence of radiant flux are 6°, and near 2.5 mrdn when angles of incidence are 12°. Such a quality of obtained images makes the diagram promising for infrared homing devices and heat-direction finding instruments with a large field of sight.

For systems with a small field of sight diagram c is very convenient, which, when the cowl is made from fused quartz and the secondary mirror-lens and correcting lens from trisulfide of arsenic, allows us to obtain a circle of confusion near 1 mrdn for beams at an angle of 2° and less than 4 mrdn for beams at an angle of 4°.

However, in this diagram chromatic aberration increases the image of the circle of confusion all over the field of sight to 0.5 mrdn.

8. Losses of Radiation Energy in Optical Systems

During passage of radiant flux through optical systems its weakening occurs due to:

absorption by materials of the systems,

reflection from surfaces of lenses and other optical parts, and

scattering of radiant flux in the thickness of the material.

Absorption of radiant flux even in the most transparent optical glass is caused by the presence in them of impurities of oxide of iron and chromium, proceeding into the glass during cooking. It is characterized by a coefficient of absorption on the way, equal to 1 cm. For the visible part of the spectrum, depending upon the sort of glass, the coefficient of absorption varies within limits of 0.01-0.03,

dropping in the near-wave infrared region of the spectrum. Therefore, with thickness of glass m cm, transmissivity of the optical system only due to absorption of radiation energy may be determined from relationship

$$\tau_a = (1-a)^m. \qquad \text{(IV.14)}$$

Losses on reflection of radiant flux take place both in lens and in mirror elements of optical systems. These losses depend on the refractive index of the medium in which radiant flux spreads and the angle of its incidence to the boundary of the two media.

In a case of reflection of radiant flux from interface "air-glass" or "glass-air" with angles of incidence up to 45-50° to the normal, reflectivity may be calculated by the formula

$$\rho = \left(\frac{n-1}{n+1}\right)^2. \qquad \text{(IV.15)}$$

where n is the refractive index of the glass from which the lens is prepared.

In Table IV.3 are given values of refractive indices of certain optical media for various wave lengths.

Table IV.3. Refractive Indices of Certain Optical Media

Material	Refractive Index n		
	$\lambda = 0.68\ \mu$	$\lambda = 2.2\ \mu$	$\lambda = 4.3\ \mu$
Air	1.000292	—	—
Organic Glass	1.49	—	—
Canadian Balsam	1.54	—	—
Optical Glass	1.5-1.92	1.5-1.7	—
Fused Quartz	1.43	1.43	1.37
Arsenic Trisulfide	—	2.38	2.35
Sapphire	1.77	1.73	1.68
Lithium Fluoride	1.39	1.38	1.34
KRS-6	2.63	2.2	2.19
Germanium	4.13	4.08	4.02
Calcium Bromide	1.55	1.54	1.53
Silver Chloride	2.071	2.01	2.00

For the most wide-spread material for objectives of infrared instruments of the near region of the spectrum (glass) the refractive index oscillates within limits of 1.5-1.92; therefore, in accordance with formula (IV.15) reflectivity from one interface between glass and air can be assumed equal to 0.04-0.06.

In case of presence n of reflecting surfaces, transmissivity of objective (or any optical unit) during calculation of onl. losses on reflection may be calculated by the formula

$$\tau_\rho = (1-\rho)^n. \qquad \text{(IV.16)}$$

Taking into account losses on absorption and reflection transmission of an optical system can be calculated by the formula

$$\tau_{o.c} = \tau_\rho \tau_\alpha = (1-\rho)^n (1-\alpha)^m. \qquad \text{(IV.17)}*$$

Losses of radiant flux in the thickness of the medium from which the optical system is made are caused also by its scattering due to presence in the medium of some kind of heterogeneities: bubbles, knots, small stones, and so forth. These losses, as a rule, are increased in the process of operating the instruments during careless treatment which leads to the appearance of scratches, spots, and deposits on the surfaces of optical parts, to their sweating, being strewn with small particles of mud and metallic shaving, ungluing of glued surfaces, etc.

Losses of radiation energy can be essentially narrowed down to two methods: reduction of the quantity of reflecting surfaces and brightening of the optics.

In the first case a decrease in losses is attained due to gluing separate parts of the optical system by Canadian balsam or balsamine, having a refraction index close to glass.

When gluing of optical parts is not allowed, brightening of optics is applied. Under the brightening of optical parts we understand decrease of reflectivity of radiation energy from operating surfaces of optical components by creating on them films with a refraction index close to the refraction index of the material from

*The Russian subscript "o.c." indicates "optical system."—Ed.

which the optical part is made. This film, while decreasing the loss of radiant energy, increases the actual candle-power of the optical system, decreases the magnitude of illumination, and renders anti-halo action.

In Fig. IV.30 is shown the effect of the brightening layer on the transmission of a germanium filter.

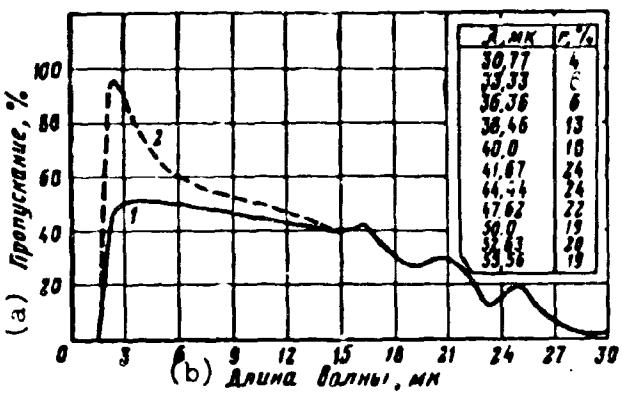

Fig. IV.30. Transmission of germanium filter before (1) and after (2) applying the brightening film.
KEY: (a) Transmission, %; (b) Wave length, μ .

Applying brightening films to optical parts may be carried out by either chemical or physical means. In the first case the film will be formed due to change of structure of the ultrafine surface layer of the optical component when under the effect of chemical compounds (for glass, for instance, siliceous acid). In the second case on the surface of the brightened part by evaporation is deposited film from another transparent substance (for glass - fluorides of magnesium or calcium).

Literature

1. Catalog of colored glass. Oborongiz, 1951.
2. "Advances of physical sciences", 1941, Vol. XXV, Issue I.
3. JOSA, 1948, Vol. 38, p. 775.
4. A. Lokk. Missile control. State Technical Press, 1957.
5. "Advances of physical sciences", 1950, Vol. 41, Issue 2.
6. JOSA, 1947, Vol. 37, p. 451.
7. Instruments and Automation, 1957, Vol. 30, No. 12.
8. Electronics, 1957, 10 Aug., Vol. 30, No. 8A.
9. M. A. Anpo. Infrared radiations. State Power Engineering Publishing

House, 1957.

10. Jet Propulsion, 1957, May, Vol. 27, No. 5.

11. Western Aviation, 1957, Vol. 35, No. 5.

12. JOSA, 1957, Mar., No. 3.

13. JOSA, 1955, Jun., No. 6.

14. JOSA, 1947, Vol. 37, p. 337.

15. JOSA. 1947, Vol. 37, p. 113.

16. J. Soc. Class Techol., 1954, Vol. 38, No. 183.

17. Rev. Optique, 1954, Vol. 33, No. 10.

18. Amer. Ceram. Soc. Bull., 1955, Vol. 34, No. 9.

19. JOSA, 1957, Vol. 47, No. 6.

20. JOSA, 1953, Dec., No. 12.

21. JOSA, 1955, Vol. 43, No. 11.

CHAPTER V

RECEIVERS OF RADIATION ENERGY

1. Classification of Receivers of Radiation Energy

In the optical region of the spectrum of electromagnetic oscillations there are four basic methods of registering the energy of radiation, visual, photographic, photoelectric, and radiometric. However, although the last three methods find wide application in laboratory practice, in infrared instruments for military purposes, as a rule, the photoelectric method of registering radiation is applied.

Table V.1. Classification of Receivers of Radiation Energy

Nonselective receivers	Selective receivers
Thermoelements	Photocells with photoemission
Bolometers	Photocells with photoconductive effect (photoresistance)
Pneumatic indicator	Photocells with photovoltaic effect
Atmograph	Photocells with lateral photoeffect
Radiometer	Photocells with photomagnetic effect
Optical-acoustic receiver	

The photoelectric method of registering radiation, with which there occurs direct energy transfer of quanta of radiation to electrons of a photosensitive substance, is characterized by very high sensitivity and little time lag. However,

peculiar to it, in distinction from the radiometric method, is an irregularity of sensitivity with respect to spectrum within a comparatively narrow wavelength range (Fig. V.1).

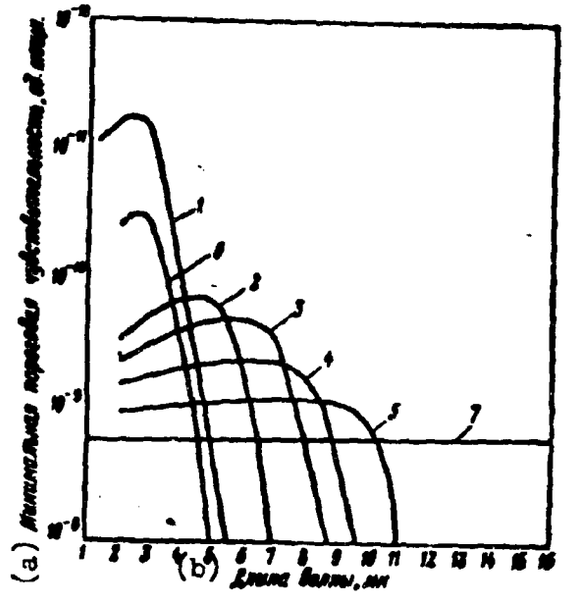

Fig. V.1. Relative sensitivity of indicators of infrared radiation.
1—PbS cooled (193°K); 2—PbTe cooled (90°K); 3—PbSe cooled (90°K); 4—InSb cooled (90°K); 5—Ce cooled (90°K), alloyed with Au; 6—PbS uncooled (293°K); 7—Thermoindicator.
KEY: (a) Minimum threshold sensitivity, units of power; (b) Wave length, μ.

Table V.1 presents a more detailed classification of receivers of radiation, and the subsequent paragraphs consider in detail only photoelectric receivers, as the most wide-spread, and in some measure superconducting bolometers. With the work and characteristics of contemporary thermoelements and bolometric diagrams it is possible to become acquainted with corresponding courses of physics and spectroscopy.

2. Nonselective Receivers of Radiation Energy

Based on the principle of action of nonselective receivers of radiation, for which the transformation of radiation energy into thermal must occur, a series of specific requirements is presented to them.

1. Receiving surface should have high absorbing ability. Usually this is attained by "blackening" of receiving surface.

2. Time lag of the receiver depends on build-up rate of its temperature. Consequently, it should have minute dimensions and small thermal losses because of thermal conduction and radiation. This demanded the development of structures of thermal receivers with the application of deep cooling and vacuum, and also the selection of semiconductors and dielectrics as receiving surfaces.

In military instruments of infrared technology thermal receivers, due to their insufficient sensitivity and high time lag, do not find, at present, wide application. In Table V.2 are given data of certain contemporary thermal receivers which are used in research laboratories.

Table V.2. Basic Characteristics of Contemporary Thermal Receivers

Type	Area of Receiving Surface, cm^2	Temperature, °K	Time Constant, sec	Threshold of Sensitivity, w/cm^2
Thermoelement of Fast....	$1.5 \cdot 10^{-2}$	300	$8 \cdot 10^{-3}$	$1.3 \cdot 10^{-7}$
Thermoelement Metallic...	$5 \cdot 10^{-3}$	300	$3.6 \cdot 10^{-2}$	10^{-8}
Thermoelement of Kozyrev.	$2.4 \cdot 10^{-2}$	300	—	$2.3 \cdot 10^{-9}$
Metallic Bolometer of Brockman.....	$5.3 \cdot 10^{-2}$	300	$50 \cdot 10^{-4}$	$9 \cdot 10^{-6}$
Semiconductor Bolometer of Moon.....	$0.5 \cdot 10^{-2}$	300	$50 \cdot 10^{-4}$	$5 \cdot 10^{-10}$
Dielectric Bolometers of Clays.....	$0.5 \cdot 10^{-2}$	300	0.1	$100 \cdot 10^{-10}$

It is natural that for registration of fast-flowing processes the above considered receivers of radiation cannot be used.

From the point of view of military application, of known interest are superconducting bolometers, possessing high sensitivity in a wide range of infrared spectrum and a comparatively small time lag.

The phenomenon of superconductivity of certain materials was discovered long ago and consists of the fact that near absolute zero (t = 273.15°C) resistance of certain materials drops practically to zero with a change of temperature several thousand fractions of a degree as compared to the initial critical temperature.

Consequently, such materials, in conditions of superconductivity, will possess very large temperature resistance coefficients, which is one of the necessary conditions for obtaining highly sensitive bolometers. Heat capacity of materials

in conditions of superconductivity becomes extraordinarily small, which is the second condition for obtaining highly sensitive bolometers. Furthermore, at very low temperatures fluctuations of voltage on clamps of the sensitive element sharply decrease, approaching zero. This allows significant amplification of useful signal, usually limited by its own circuit noises, and, consequently, improvement of the sensitivity threshold of the receiver.

In spite of the evident promise of such bolometers, for a long time we did not manage to obtain any useful, operational instrument. This is explained by the fact that for an overwhelming majority of materials the phenomenon of superconductivity sets in at very low temperatures (lead 4°K, tantalum 3.22-3.23°K), which it is possible to ensure only by using liquid helium as a cooling agent.

The discovery of the phenomenon of superconductivity for nitride of niobium and columbium nitride at higher temperatures, obtained during the application of liquid hydrogen, allowed the creation, on their basis, of useful superconducting bolometers and the studying of their basic properties (Fig. V.2).

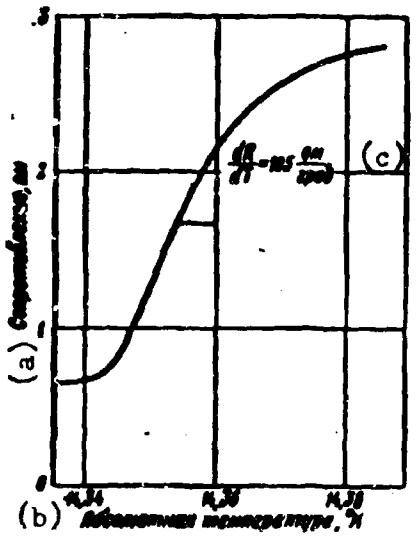

Fig. V.2. Change of resistance of a superconducting bolometer of columbium nitride.
KEY: (a) Resistance, ohm; (b) Absolute temperature, °K; (c) Degree.

For columbium nitride the transition from normal state to superconductivity sets in between 14.34 and 14.38°K. In this range of temperatures on a linear section of the curve the change rate of resistance constitutes a magnitude of 105 ohm/degree. To obtain such temperatures is significantly simpler, since the application of liquid hydrogen is sufficient. The laboratory of John Hopkins University in Baltimore, where a superconducting bolometer was made from columbium nitride, developed also a

portable installation weighing 24 kg for obtaining liquid hydrogen from the usual gasiform with a productivity ensuring filling of a thermostat during 2 hours (Fig. V.3).

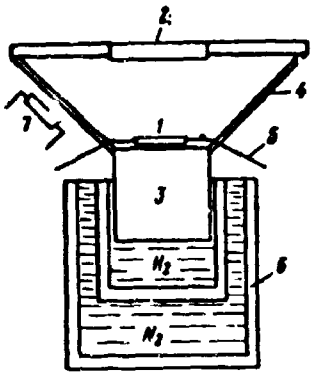

Fig. V.3. Construction of superconducting bolometer.

A bolometer consists of tape 1 of columbium nitride 6 μ thick, 0.25 mm wide, and 5 mm long, glued with the help of bakelite varnish on the face of a massive copper cylinder, 3, 1 cm in diameter and surrounded, for mechanical protection and protection from outside radiation, by copper hemisphere 4. The cylinder is dipped in thermostat 6, consisting of several dewar vessels, filled with liquid nitrogen and hydrogen. The sensitive element is in a vacuum at a temperature of 14°K. In order to bring the temperature to the most favorable (14.36°K), in direct proximity to the mass of copper surrounding the bolometer is located a 500 ohm resistor 7, through which a 10 ma current is conducted.

Required temperature and efficiency of bolometer remain constant for 4 hours after charging.

Fluctuating noises of voltage on clamps of the bolometric resistor are equal to approximately 0.5×10^{-6} microvolt, i.e., correspond to a signal with an average energy of 10^{-5} erg, however, applying narrow-band amplifier, it is possible to improve threshold of sensitivity to $2 \cdot 10^{-6}$ erg, or $2 \cdot 10^{-13}$ w·sec.

Since construction of a bolometer ensures fast heat removal caused by absorption of radiation energy due to thermal conductivity and fast return to a state of equilibrium after ceasing of action of radiant flux on sensitive element, then the time lag of such a bolometer is insignificant. In Fig. V.4 is given the growth curve of the signal depending upon the time of irradiation of the bolometer by a radiant flux modulated with a frequency of 13 cps. As can be seen from the curve,

the signal attains maximum value during the time of 0.3 millisecond. Consequently, the time constant of a superconducting bolometer may be estimated as 0.0003-0.001 sec.

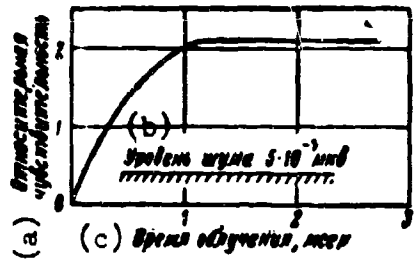

Fig. V.4. Growth of signal of superconducting bolometer, depending upon time of its irradiation.
KEY: (a) Relative sensitivity; (b) Noise level $5 \cdot 10^{-7}$ microvolt; (c) Exposure time, millisecond.

At present a large quantity of bolometric diagrams are known, founded on the phenomenon of superconductivity and used, so far, for spectroscopic targets. Introduction of bolometric diagrams in applied technology of infrared rays, including military, so far prevents the difficulty of obtaining necessary cooling.

However, such a method of registration of thermal radiation is long-term, since few receivers reveal a flux of radiation energy of 10^{-10} w with a sufficiently small time lag in a wide spectral range of sensitivity.

Table V.3. Basic Characteristics of Superconducting Bolometers

Author	Dimension mm^2	Resistance, ohm	Time Constant, Sec	Threshold of Sensitivity, w	Type of Filler
Andrews....	1.25	5	$5 \cdot 10^{-4}$	$5 \cdot 10^{-10}$	Vacuum
Milton.....	0.8	—	10^{-4}	$10 \cdot 10^{-10}$	Vacuum
Nelson.....	0.8	—	$18 \cdot 10^{-4}$	$3.5 \cdot 10^{-10}$	Vacuum

3. Receivers with External Photoeffect (Photoemission)

The region of photoelectric phenomena includes the appearance of electromotive force under the effect of radiant flux (photovoltaic effect), the change of resistance of substance during its irradiation (photoconductivity), and the emission of electrons from the surface of bodies under the effect of incident radiant flux (photoemission).

In usual conditions, in any metal there is nearly 10^{23} free electrons in 1 cm^3. All of them carry a definite energy supply and freely shift in all possible directions inside the mass of metal. However, their energy is still insufficient to allow them to leave the matter. For that, as is known from quantum theory, it is necessary to impart additional energy to the electrons.

Additional energy, in particular, can be energy of infrared radiation, which, being absorbed by matter, is partially expended on heating it, and also partially on giving the electron additional kinetic energy and pulling it out of the substance. Thus, in the case of photoemission there occurs a transformation of radiation energy into energy of flying electrons, i.e., into electromagnetic energy (if initial velocity of electrons is $v \neq 0$).

An electron can abandon a substance (metal) only when radiation energy is absorbed by the substance and it suffices to surmount the binding forces between the electron and the surface of a body, and also imparts a certain speed v to the electron

$$h\nu = e\varphi + \frac{mv^2}{2}. \qquad (V.1)$$

The first member of equation (V.1) indicates the magnitude of minimum necessary energy which must be given to an electron in metal in order to pull it beyond the limits of a substance with zero speed. This energy has obtained the name of "work function", the magnitude of such energy is constant for pure metals, oscillating on the average from 1 to 5 ev (see Table V.4).

In this case all the energy of a photon is expended on surmounting the potential barrier, and expression (V.1) can be written in the form

$$h\nu_0 = e\varphi_0, \qquad (V.2)$$

where ν_0 is threshold frequency of electromagnetic radiation, at which electrons depart from the surface of metal with zero speed.

Threshold frequency ν_0 corresponds to wave length λ_0, called long-wave or "red" boundary of photoeffect:

$$\lambda_0 = \frac{1.236}{\varphi_0}, \qquad (V.3)$$

where λ_0 is in microns, and φ_0 is in electronvolts.

Table V.4. Work Function of Certain Elements

Element	φ, Electron-volt	Element	φ, Electron-volt
Lithium	2.49	Cadmium	4.1
Silicon	4.2	Antimony	4.14
Calcium	2.26	Tellurium	4.76
Nickel	5.24	Cesium	1.9
Germanium	4.5	Tungsten	4.5
Selenium	4.4	Platinum	5.36
Silver	4.79	Bismuth	4.25

The "work function" can be decreased and, consequently, the long-wave boundary of sensitivity of photoemission increased by "contamination" of metal, i.e., by means of the adsorption on the surface of metal of atoms or ions of a substance with a smaller "work function". In this case on the surface of metal are formed dipole layers with positive charges turned outward decreasing the magnitude of the potential barrier. Therefore, all sensitive layers with photoemission, which are sensitive to visible and infrared radiation, consist of several components.

Photoemission sets in practically instantly after the beginning of irradiation of the surface of the photocell (time lag does not exceed $3 \cdot 10^{-9}$ sec).

From the point of view of practical application in instruments of infrared technology, we will be subsequently interested in the following characteristics of photoemission.

1. Integral sensitivity—the ratio of photocurrent in the circuit of the receiver to the power of the radiant flux incident on receiver. Integral sensitivity is expressed in microamperes per watt or in the case of visible light - in

microamperes per lumen. For counting it one of the following relationships is frequently used:

$$S = \frac{I_\Phi l^2}{q J_\Omega} = \frac{I_\Phi}{\mathcal{E} q} = \frac{I_\Phi}{\Phi}, \qquad (V.4)$$

where I_Φ is maximum value of photocurrent,

Φ is incident radiant flux,

$\mathcal{E}$ is irradiance of receiver, w/cm^2,

q working area of receiver, cm^2,

l is distance from a source of radiation with a known temperature to receiver, cm,

J_Ω angular density of radiation, w/sterad.

Frequently integral sensitivity of a receiver is determined by the quantum yield of its photosensitive layer, under which we understand the quantity of electrons departing from a photosensitive layer under the effect of one quantum of incident radiant flux. Quantum yield of a substance capable of photoemission is determined by the totality of its physical properties. In an ideal case, every photon falling on the surface of a photosensitive layer can liberate one electron, i.e., the theoretical limit of photoelectronic emission is quantum yield equal to unity. However, such an output never is attained.

Part of the energy of incident radiant flux cannot turn into energy of moving electrons, since it either will be reflected from the surface of the photosensitive layer or will pass through it without encountering an electron on its way. But even with full absorption of photons by a substance, the probability of output of electrons from it is small, since certain photons, while not liberating an electron completely, will change it into an excited state, and other photons, although they will create free electrons, the latter will not emerge from the substance due to the loss of obtained energy as a result of nonelastic collisions with other electrons or due to transfer to its lattice. Therefore, in the best case the quantum yield of photoemission layers does not exceed 10-20%.

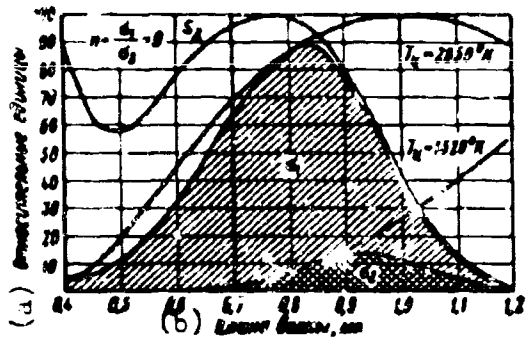

Fig. V.5. Effectiveness of oxygen-cesium photosensitive layer to radiation with different temperature.
KEY: (a) Relative units; (b) Wave length, μ .

2. Spectral sensitivity is the dependency of sensitivity of receiver on wave length of incident monochromatic radiant flux. It, in the end, determines the effectiveness of the application of infrared instruments during their joint work with sources of radiation energy.

In Fig. V.5 as an example is determined the effectiveness of a receiver with cesium oxide sensitive layer to radiation of an electrical incandescent lamp with different color temperature of the filament of incandescence.

3. The threshold of sensitivity (threshold flux) is the minimum magnitude of radiant flux in watts or in lux for visible light, which may be still revealed by receiving device.

The threshold of sensitivity of the receiver is determined by the level of noises in the circuit of the receiver. It is determined basically by leakage current and dark current, appearing as a result of auto- and thermionic emission.

In instruments of infrared technology photoemission is used in image converters and photoelectronic multipliers, and also in night transmitting television tubes of heightened sensitivity. In these instruments, as photocathodes, are used cesium oxide, cesium antimonide, bismuth silver cesium photosensitive layers, and also, developed recently, multi-alkali photocathodes. Spectral characteristics of sensitivity of these photocathodes are shown in Fig. V.6.

The properties of the first three photosensitive layers are considered sufficiently in literature [1, 2, 3]. Multi-alkali photocathodes have been developed relatively recently [4, 5], however, in a whole series of properties they

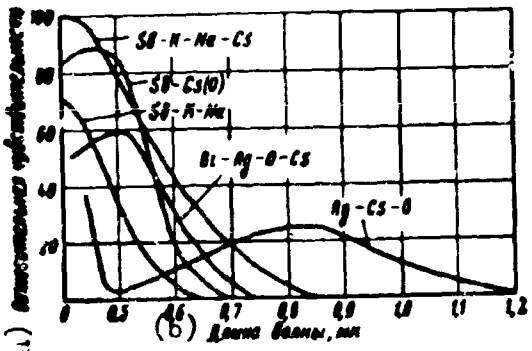

Fig. V.6. Spectral sensitivity of certain photocathodes.
KEY: (a) Relative sensitivity; (b) Wave length, μ.

are of interest as sensitive elements in instruments of night vission. These properties, in the first place, are the high integral sensitivity of the photocathode and the very small dark currents, allowing high amplification of image brightness without cooling of the photocathode.

Table V.5. Basic Characteristics of Photocathodes with Photoemission

Photocathode	Wave length of maximum sensitivity, μ	Red Boundary $\lambda_{0.01}$ μ	Quantum yield for the visible section of the spectrum	Integral Sensitivity, Microampere/lu
Ag–O–Cs	0.85	1.4	0.005	50
Sb–Cs	0.45	0.65	0.1	25
Sb–Cs (0)	0.48	0.70	0.2	90
Bi–Ag–O–Cs	0.48	0.75	0.1	90
Sb–K–Na	0.4	0.62	0.1	60
Sb–K–Na–Cs	0.4	0.82	0.2	200

4. Receivers with Internal Photoeffect (Photoresistance)

A photoresistor (FS) is a semiconductor instrument which changes internal resistance under the effect of radiation energy.

In distinction from metals where atoms of crystal lattices lose the external valence electrons, in a semiconductor at low temperatures the majority of electrons are connected with atoms of the lattice. However, this bond is not durable. While participating in thermal motion, atoms are rocked about and lose their valence electrons. Therefore, during heating in a semiconductor the quantity is increased

of electrons able to carry current, which is equivalent to a decrease of its electrical resistance. This is the first distinction of a semiconductor from metal, for which increase of resistance is characteristic with an increase of its temperature.

Another peculiarity of a semiconductor is the fact that in it carriers of current are not only liberated electrons, but also the atoms left without external valance electrons, which obtain, due to this, positive charge (ions).

In order to grasp this phenomenon, we will turn to Fig. V.7. Under the effect of applied potential difference to the semiconductor a photoelectron, having left the outer shell of an outer atom, starts to move to the positive electrode. In the atom which lost the electron, on the outer shell there remains a free place - a "hole". However, it remains empty only an insignificant time (10^{-3}-10^{-7} sec). Under the effect of the electrical field, to it immediately passes an electron from a neighboring atom. This electron, not obtaining full freedom, passes to another atom while trying to move to the positive electrode. Again the liberated place is occupied by an electron from an atom more distant from the positive electrode, etc. Thus, as electrons move toward the positive electrode, "holes" move toward the negative. This is a somewhat simplified physical picture of the appearance of an electrical current in a semiconductor during its heating.

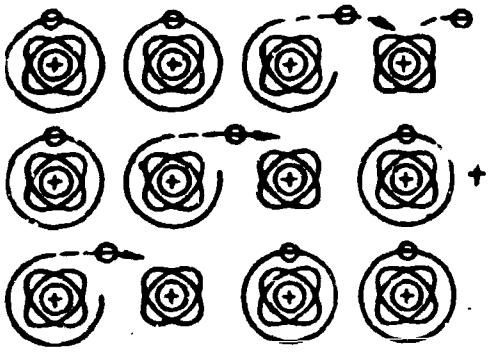

Fig. V.7. Formation and displacement of "holes" in a semiconductor.

Motion of the bound electrons from atom to atom in a direction toward the positive electrode creates a significant addition to the current through the semiconductor. "Holes" shifting toward the negative electrode also create an addition to the electrical current, transferring a positive charge, equal in absolute value to the charge of the electron.

Equality of electrons and "holes" can take place only in a case of an absolutely intrinsic semiconductor. The presence of even an insignificant quantity of impurities creates in a semiconductor either a surplus of electrons (n-type conductivity) or a surplus "of holes" (p-type conductivity). Since absolutely intrinsic semiconductors in nature virtually do not occur, in practice we usually deal with photoresistors having either electron (n) or hole (p) conductivity. Works of recent years have established that the presence of impurities in a semiconductor very strongly increases (sometimes tens of millions of times) its specific electrical conductivity. In this also lies one of the distinctions of a semiconductor from metal, for which electrical conductivity drops with an increase of impurities.

Introduction of impurities in a semiconductor allows decreased width of forbidden band ΔE. Let us remember that under the width of the forbidden band, expressed in electronvolts we understand the minimum magnitude of energy which must be imparted to an electron so that it may pass from a bound state to a free state (in the conduction band). Width of the forbidden band, as also the work function in the case of external photoeffect, determines the long-wave boundary of sensitivity of the semiconductor photoresistance.

Table V.6. Semiconductors Possessing Photoconductivity in the Infrared Region of the Spectrum at t = 20°C (according to Frederick and Blant)

Compound	ΔE Electronvolt	λ_0 μ	Compound	ΔE Electronvolt	λ_0 μ
PbS	0.4	3.1	Mg_2Sn	0.22	5.6
PbTe	0.34	3.7	Bi_2S_3	1.25	0.98
PbSe	0.25	5	Ag_2S	0.9	1.38
InSb	0.16	7.8	MoS_2	0.6	2.1
InAs	0.3	4.1	HgTe	0.4	3.1
GaSb	0.65	1.9	ZnSb	0.55	2.25
Mg_3Sb_2	0.8	1.55	Cd_3As_2	0.6	2.1

In Table V.6 are presented values of width of forbidden band and long-wave boundary of sensitivity of certain semiconductor compounds possessing photoconductivity in the infrared region of the spectrum.

Subsequently will be considered only some of the photoresistors shown in the table since others present now only a theoretical interest for understanding the phenomena occurring in semiconductors.

It is necessary beforehand to stipulate that in published materials various authors introduce different values of width of forbidden band and long-wave boundary of sensitivity. This is possible to explain both by the degree and character of contamination of the investigated samples and the accuracy and method of the actual experiment. Furthermore, in the majority of works it is assumed, as in the given table, to characterize the long-wave boundary of sensitivity as that wave length where sensitivity constitutes 50% of the maximum value. However, certain authors hold the boundary to a sensitivity 10% of maximum. To facilitate comparison of different works we will subsequently keep to the definition of the red boundary of sensitivity as taken in Table V.6.

Historically, photoresistors from compounds of lead: lead sulfide, lead telluride, and lead selenide first found application in instruments of infrared technology as receivers.

These compounds are semiconductors with electrical conductivity of both electron and hole types and with mobility of current carrier 1-50 $cm^2 \cdot sec \cdot v$ for polycrystalline layers, obtained by evaporation. In single crystals mobility of the current carrier is significantly higher and constitutes at room temperature (290°K) a magnitude of the following order:

	PbS	PbTe	PbSe	
Mobility of electrons	640	2,100	1,400	$cm^2/sec \cdot v$
Mobility of holes	800	840	1,400	$cm^2/sec \cdot v$

At low temperatures mobility of the current carrier sharply increases and attains for PbS at 77°K $10^4 cm^2/sec \cdot v$ and at 20°K $10^5 cm^2/sec \cdot v$. This ensures increase in sensitivity of photoresistors during their cooling. Differing from thermal indicators, photoresistors have a clearly expressed maximum of sensitivity and little time lag.

In spite of the fact that in nature we encounter pure crystals of PbS - Galena, PbTe - Altaite and PbSe - clostalite, in instruments of infrared technology are applied artificial photosensitive layers of these compounds.

Recently there have been developed two methods of obtaining photosensitive layers - chemical and physical.

In the first case, the film of the photosensitive layer is precipitated from solution in the presence of an oxidizer. These layers can remain open in the air after covering by protective varnish.

In the second case the sensitive layer is obtained by evaporation in vacuum with subsequent preheating in atmosphere with small pressure of oxygen or direct evaporation in atmosphere with low pressure of oxygen.

Photosensitive layers (thickness nearly 1 μ) of photoresistors, obtained by evaporation, form a porous structure consisting of accumulations of small crystals from 0.1 to 1 μ in dimension. Resistance of obtained layers of PbS and PbSe at room temperature is of the order of 0.5-2 Mohm. During cooling of layers their resistance sharply increases, attaining for PbTe and PbSe values of many megohm (for instance, for PbTe up to 30-50 Mohm).

With the cooling of photosensitive layers of compounds of lead is connected one more of their properties: with increase of depth of cooling the maximum of spectral sensitivity and the long-wave boundary are displaced in the direction of longer waves with a simultaneous increase in time lag of indicators (Fig. V8a - c).

From the given curves plotted in semilogarithmic scale, it is possible to note that with large wave lengths photoresistor sensitivity quickly decreases.

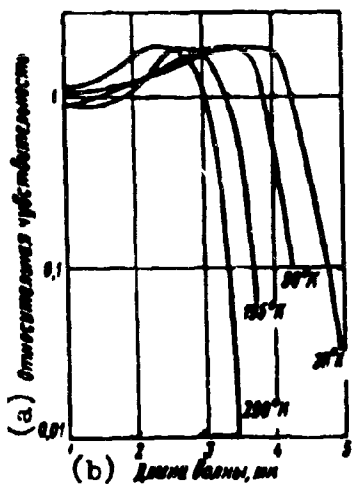

Fig. V.8a. Change of spectral sensitivity of PbS during cooling.
KEY: (a) Relative sensitivity; (b) Wave length, μ .

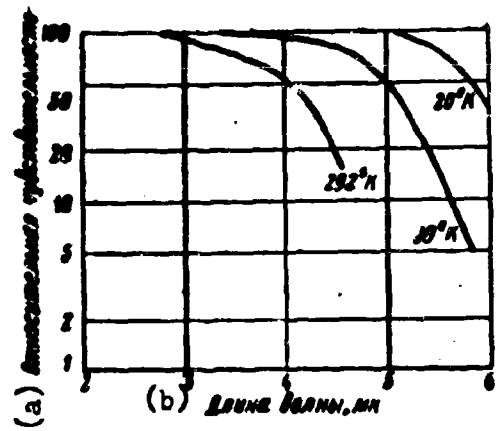

Fig. V.8b. Change of spectral sensitivity of PbTe during cooling.
KEY: (a) Relative sensitivity; (b) Wave length, μ .

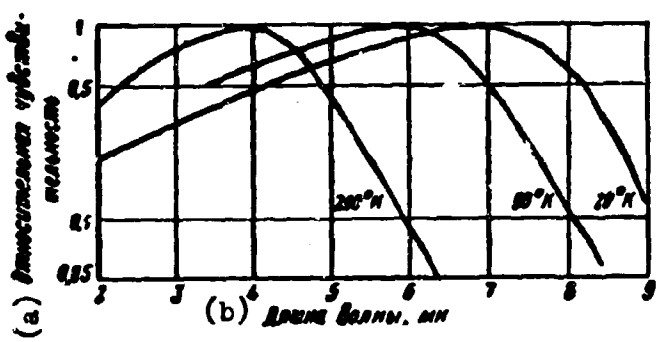

Fig. V.8c. Change of spectral sensitivity of PbSe during cooling.
KEY: (a) Relative sensitivity; (b) Wave length, μ .

Mohs [6], offering to consider the red boundary of sensitivity as that wave length (λ_0 , 5) where it is equal to 50% of maximum value, gives the following values of it at various temperatures

Photoresistor	Temperature, °K			
	295	195	90	20
PbS	2.9 μ	3.3 μ	3.8 μ	4.1 μ
PbTe	3.9 μ	—	5.1 μ	5.9 μ
PbSe	5.0 μ	—	7.1 μ	8.2 μ

Smith [24], publishing a great survey on photoresistors on the basis of compounds of lead, introduces analogous data and, at the same time, values of red boundary during a sensitivity equal to 1% of maximum value:

Photoresistor	Temperature, °K		
	295	90	20
PbS	3.5 μ	4.5 μ	—
PbTe	—	5.75 μ	—
PbSe	7 μ	9.3 μ	10.2 μ

The integral sensitivity of photoresistors from compounds of lead also strongly changes with temperature. Thus, for PbTe at room temperature it turns out to be immeasurably small. As a rule, integral sensitivity of compounds of lead grows with lowering of temperature to temperature of liquid air, after which it remains practically constant [7]. Lead sulfide photoresistors (in distinction from lead telluride and lead selenide) can work even at room temperatures, i.e., without cooling; however, their sensitivity in this case noticeable decreases. It was determined that at room temperature photoresistor sensitivity changes approximately 5% with a change of temperature by 1°C.

Limiting sensitivity of PbS is no less than 100 times higher than sensitivity of contemporary thermoelements. Minimum energy which can still be detected by a PbS photoresistor near the maximum of its sensitivity with a 1 cps passband has a magnitude of the order of 10^{-12} w. Smith [24] introduces a calculation of the sensitivity of uncooled PbS to radiation with a temperature of 200°C in a 1 cps passband, which turned out to be equal, in this case, to $\Phi_n^* = 10^{-10}$ w. Cooling by solid carbon dioxide increases sensitivity and allows the recording of radiation with $\lambda = 2.2$ μ with a power of $4 \cdot 10^{-12}$ w/cps. Measurements were made with a modulation frequency of radiant flux of 800 cps.

*The Russian subscript "п" indicates passband.—Ed.

Photoresistors from PbTe during deep cooling have a limiting sensitivity also in 100 and more times better than contemporary thermoelements [8]. Consequently, it is possible to expect that minimum quantity of monochromatic radiation at maximum sensitivity of PbTe will constitute 10^{-12}-10^{-11} w with a 1 cps passband.

A photoresistor from PbSe at the temperature of liquid air has an integral sensitivity somewhat less than the best PbTe but exceeds by 6-10 times the sensitivity of the best contemporary thermoindicators, i.e., it should be equal to $3 \cdot 10^{-11}$ w. In distinction from PbTe, PbSe has noticeable sensitivity at room temperature.

Mohs [6] introduces calculated data of the sensitivity threshold of photoresistors from PbS and PbTe, presented in Table V.7.

Table V.7. Calculated Data of Limiting Sensitivity of Photoresistors from PbS and PbTe

Type of Photoresistor	T, °K	q, mm^2	λ radiation, μ	Φ_n, w
PbS	273	1	—	$5 \cdot 10^{-14}$
PbS	90	1	—	$0.8 \cdot 10^{-14}$
PbS	293	10	2.2	$2 \cdot 10^{-11}$
PbS	90	10	2.2	$4 \cdot 10^{-12}$
PbTe	90	1	4	$5 \cdot 10^{-13}$

The given table shows that when registering radiation with a wave length near 4 μ, to which lead sulfide photoresistors become little sensitive, the advantages of photoresistors from lead telluride sharply increase.

These advantages are graphically shown in Table V.8, where data are presented on the effectiveness of the use of radiation of an ideal black body heated to different temperatures by lead sulfide, lead selenide, and lead telluride layers. Fig. V.9 also illustrates the dependency of the sensitivity threshold of lead sulfide photoresistors on the temperature of the ideal black body.

sensitivity of indium antimonide is very small for its wide use in instruments of infrared technology.

Cooling of indium antimonide displaces the maximum of sensitivity and long-wave boundary $\lambda_{0,5}$ in the direction of shorter waves with speed $1.7 \cdot 10^{-4}$ ev/degree, which it is possible to trace on curves in Fig. V.11.

Various authors give different magnitudes of long-wave boundary of sensitivity of indium antimonide, however, a majority of them estimate the threshold of sensitivity for radiation with wave length 4 μ and with cooling of photosensitive layer to 90-77°K as a magnitude of the order of 10^{-11}–$5 \cdot 10^{-12}$ w/cm^2. It is necessary to assume that divergence in appraisal of long-wave boundary of sensitivity of single crystals of indium antimonide depends on cleanness of materials and the method of its determination. Since research of properties of photoconductivity was carried out with comparatively pure single crystals of indium antimonide obtained in laboratory conditions, in industrial scales, where obtaining of very pure samples is hampered, photoresistors from indium antimonide can have parameters differing from those shown in Table V.10. This in some measure explains parameters of industrial photoresistors of indium antimonide (Table V.11) published in the press of the United States [9].

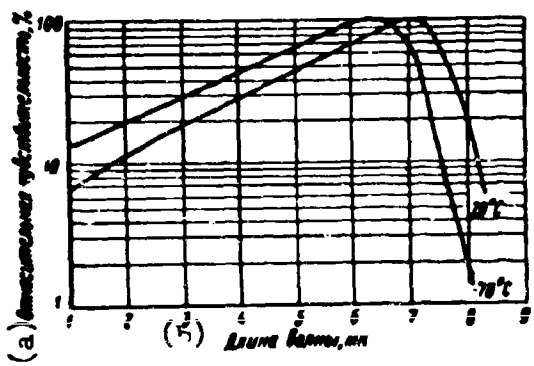

Fig. V.11. Spectral sensitivity of InSb at various temperatures. KEY: (a) Relative sensitivity, %; (b) Wave length, μ.

Of great interest, along with indium antimonide is germanium, which also allows us to carry out different methods of registering infrared radiation.

Pure germanium is a gray substance, similar to metal and having metallic brightness. From a smooth surface is reflected nearly 50% of visible light. In infrared region of the spectrum

Table V.8. Effectiveness of Different Types of Photoresistors to Radiation of an Ideal Black Body (AChT)

t_{ACHT} °C	Effectiveness, %		
	PbS, 293°K	PbTe, 90°K	PbSe, 90°K
300	3.5	25	48
150	0.26	8	26
50	0.01	2	11
20	0.004	1	7
0	0.001	0.6	5

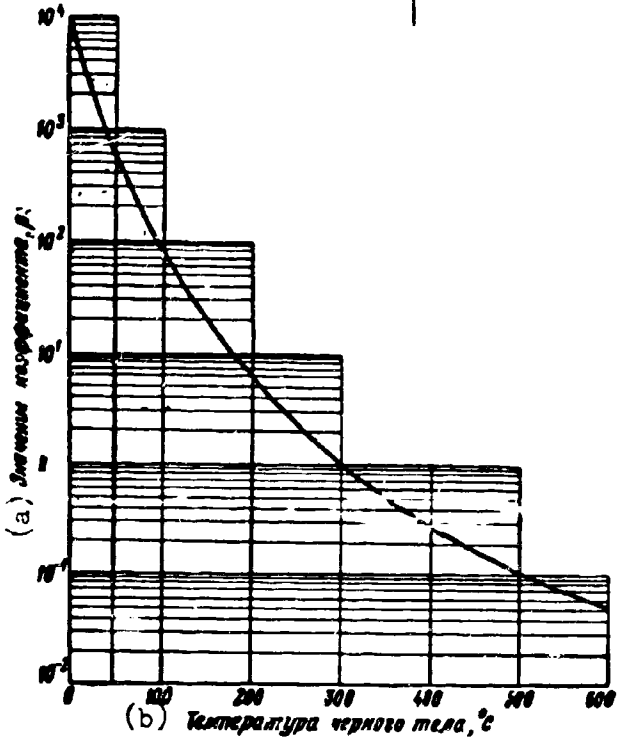

Fig. V.9. Change of the integral sensitivity of PbS with change in temperature of the black body.
KEY: (a) Values of coefficient; (b) Temperature of black body.

In the latter case calculation was carried out by the formulas;

$$\left.\begin{aligned} \Phi_{\text{эф}} &= \beta(\Phi_{\text{э}})_{300^\circ\text{C}}, \\ \beta &= \frac{\left[\int_0^\infty r_\lambda S_\lambda d\lambda\right]_{300^\circ\text{C}}}{\left[\int_0^\infty r_\lambda S_\lambda d\lambda\right]_{t^\circ\text{C}}}; \end{aligned}\right\} \quad \text{(V.5)}$$

where

r_λ is spectral density of radiation of an ideal black body with a temperature of 300°C and t°C.

S_λ is spectral sensitivity of photoresistor.

When registering modulated radiant flux the time lag of the photoresistor is large, which is assumed to be characterized either by the frequency-response curve (i.e., dependency of output signal removed from the photoresistor, on modulation frequency of incident radiant flux), or the time constant of the photoresistor, characterizing the time during which the signal receives a value, equal to 50, 63, and 90% of its maximum value.

Above it has already been noted that the constant of the photoresistor is significantly lower than for thermal receivers of radiation energy. Thus, the time constant of PbS, having a temperature of 293°K, oscillates from 10^{-4} to 10^{-5} sec, and for PbTe and PbSe is less than 10^{-5} sec.

Depending uopn the method of obtaining the photosensitive layers, time constant $\tau_{0.5}$ can take, for PbS photoresistors, a value from 1-2 to several hundred microseconds with a physical method and from several hundreds of microseconds to 1 millisecond with a chemical method of obtaining the layer.

For these photoresistors there exists a sharp dependency of magnitude of time constant on temperature. When cooling by solid carbon dioxide or liquid air the time constant can attain the value of 10^{-2} sec. Above 200°K the time constant fast decreases with increase of temperature (in the first approximation by exponential law).

Significantly less are inertial photoresistors of PbTe and PbSe. Thus, the time constant of PbTe equal to 5 microseconds, and for PbSe 0.5-1.5 microsecond, not decreasing essentially down to deep cooling. This makes it possible to carry out with their help the registration of radiant flux, modulated with a frequency to 20 kilocycle, without noticeable decrease of output signal.

Photoresistors from compounds of lead have found wide application in instruments of infrared technology as sensitive elements of systems of fire control, homing guidance systems of rockets, and their noncontact exploding, and in recommaisance apparatus. They have more than doubled their sensitivity since the Second World War. Based on published material photoresistors produced commercially in the USA have the parameters shown in Table V.9.

Table V.9. Parameters of Film Photoresistors for Instruments of Infrared Technology

Type of Photoresistor	λ_{μ} maximum,	T, °K	q, cm^2	$\mathcal{E}_{n}$ w/cm^2	τ, μ sec
PbS	2.2	290	0.25	$2 \cdot 10^{-10}$	40
PbTe	4	90	0.04	$2 \cdot 10^{-10}$	10
PbSe	4	77	—	10^{-9}	10

Despite advances in the creation of photoresistors of high-sensitivity and quick response on the basis of lead compounds, beginning approximately in 1952 particular attention was given to the study of semiconductor compounds formed from elements of the II, III, and V groups of the periodic system and also germanium. Interest toward it was caused by the fact that, in distinction from compounds of lead, the technology for obtaining such photoresistors is simpler, and they successfully compete with lead compounds in relation to the long-wave boundary of sensitivity, time lag, and magnitude of proper noises.

Of these compounds as indicators of infrared radiation, the most widely used is antimonous indium (indium antimonide) InSb, possessing photoconductivity in film samples and single crystals, photovoltaic effect, photomagnetic, and lateral effect. A characteristic peculiarity of indium antimonide when using it as an indicator of infrared rays is its very little proper noise (to 10^{-8} v), which allows us during corresponding selection of amplifying diagram to ensure registration of very small radiant fluxes.

Time constant for InSb at room temperature and at deep cooling is very small (to 10^{-7} sec). It was established experimentally that during cooling of InSb by liquid air, the time after which output signal attains 63% of its maximum magnitude constitutes approximately 0.8 microseconds. At room temperature time constant of photoconductivity could not be measured.

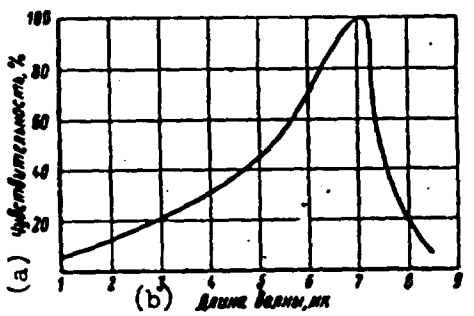

Fig. V.10. Spectral sensitivity of InSb at t = 20°C.
KEY: (a) Sensitivity; (b) Wave length, .

Spectral spread of sensitivity of photoresistors of InSb at room temperature (Fig. V.10) shows that it has the biggest red boundary of sensitivity of all the known uncooled photoresistors $\lambda_{0,5}$ = 7.5--7.75 μ, which corresponds to width of forbidden band 0.16 ev. However, according to research, in these conditions integral

reflectivity decreases. Resistance of pure germanium is 47 ohm·cm, width of forbidden band at 0°K is 0.75 ev. Germanium is very stable chemically.

Table V.10. Basic Parameters of Photoresistors of InSb According to [10]

T, °K	$R_{external}$, kilohm	Φ_n, watts	$\lambda_{maximum}$, μ	$\lambda_{0.5}$, μ	Sensitivity, v/w
90	2.08	$2.6 \cdot 10^{-11}$	5.6	5.85	1300
195	1.8	$7 \cdot 10^{-11}$	5.6	6	400
249	0.49	$4 \cdot 10^{-10}$	6.2	6.85	30
292	0.12	$7 \cdot 10^{-10}$	6.7	7.2	1

As an indicator of infrared rays germanium may be used as a photoresistor, photodiode, and as an element changing its dielectric constant during its irradiation by infrared radiation.

Table V.11. Parameters of Industrial Photoresistors of InSb, Released in the United States in 1958

Type of Photo-resistors	$\lambda_{maximum}$, μ	T, °K	q, cm^2	τ μ sec	Sensitivity to Radiation with $\lambda = 4\ \mu$, w/cm^2
InSb	4	90	0.014	1	$3.6 \cdot 10^{-9}$
InSb	4	77	0.001	1	$1 \cdot 10^{-8}$

As a photoresistor pure germanium may be used only at a temperature of liquid nitrogen, since at higher temperatures it has very large dark currents. For the purpose of increasing the photoconductivity of germanium and expanding the boundaries of spectral sensitivity it is artificially alloyed by the introduction of atoms of gold, antimony, and zinc. The most widely used as a photoresistor is germanium alloyed with gold. Solubility of gold in germanium constitutes approximately 10^{15} atoms per 1 cm^3. On the basis of germanium of the electron and hole type, alloyed

with gold, highly sensitive photoresistors were created sensitive in a region up to 10 μ with its cooling by liquid nitrogen.

In Table V.12 are given data of industrial samples of germanium photoresistor alloyed with gold. In the same place are given computed values of sensitivity.

Table V.12. Basic Parameters of Industrial Samples of Germanium Photoresistors Alloyed with Gold [9]

Type of Photo-resistor	$\lambda_{maximum}$, μ	T, °K	q, cm^2	τ μ sec	Threshold of Sensitivity to Radiation $\lambda = 4\ \mu$, w/cm^2
p	4	77	0.04	1	$1 \cdot 10^{-9}$
p	4	77	0.12	0.1	$4.4 \cdot 10^{-10}$*
n	4	90	0.16	20	$1.6 \cdot 10^{-10}$
n	4	90	0.16	20	$3.8 \cdot 10^{-13}$*

NOTE. Computed values of sensitivities are marked by sign *.

In literature there is also reported the development of a large quantity of germanium photoresistors for the detection of comparatively low-temperature target According to literature [11] Westinghouse has developed germanium p-type photoresistors alloyed with gold for work in the region of 1-10 μ with its cooling by liquid nitrogen. The photoresistors have a threshold of sensitivity (equivalent power of noise) $5 \cdot 10^{-11}$ w at 78°K and $1.6 \cdot 10^{-11}$ w at 60°K. Time constant is less than 0.2 microseconds. It is indicated that PbSe in these conditions has comparab sensitivity in a wave range of 2-5 μ with a time constant of 30 microseconds.

Spectral sensitivity of germanium photoresistors is shown in Fig. V.12.

Concerning germanium photoresistors alloyed by zinc and working at a temperatu of liquid helium of type 536-1ZIP, it is reported that their sensitivity spreads to 40 μ with a time constant of 0.01 microseconds [12]. Photosensitive layer has dimensions 2 X 2 mm. Threshold of sensitivity to radiation of a black body with T = 500°K is characterized by equivalent power of noises $4 \cdot 10^{-9}$ w with a 1 cps

passband and a modulation frequency of radiant flux of 800 cps.

It is indicated also [13] that on a base of germanium photoresistor alloyed by antimony and working at a temperature of liquid helium they managed to create a laboratory installation for registering radiations in a wave range of 55--100 μ during time constant 10^{-5} sec.

In conclusion one should note one more property of germanium photoresistors, which allowed the construction of a highly sensitive radiotechnical device for registering energy of infrared radiation [14, 15]. This device (Fig. V.13) is a crystal of germanium alloyed with gold, excited at normal temperature by a field of super-high frequency.

The crystal of germanium is placed inside a cavity resonator with sharp adjustment. When infrared radiation hits it, there occurs a change of the complex dielectric constant of germanium and a detuning of the resonator.

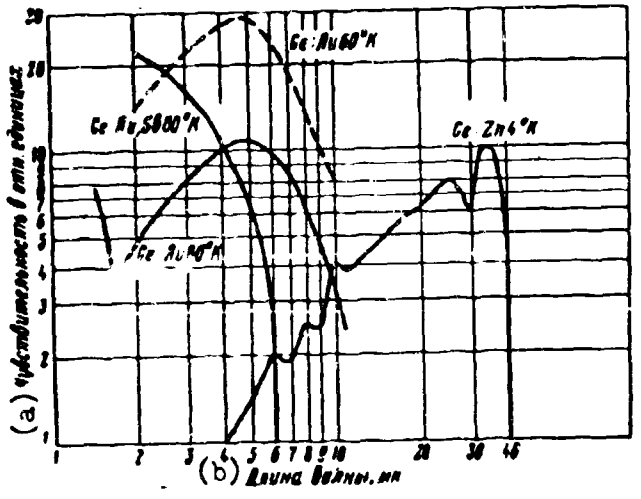

Fig. V.12. Spectral sensitivity of germanium photoresistor alloyed by different alloys.
KEY: (a) Sensitivity in relative units; (b) Wave length, μ .

An indicator constitutes a waveguide tee, one of the arms of which is loaded by two identical resonators and germanium crystals suspended inside them. The second arm serves for a supply of shf energy from the power supply. The signals reflected from the resonators are added in the third output arm with a phase difference of 180°. If reflected signals have identical amplitude, then on output there is no signal. If, however, one of the crystals is irradiated by infrared rays, then equality of amplitudes and phase relationship will be disturbed and on output there will appear a noticeable signal.

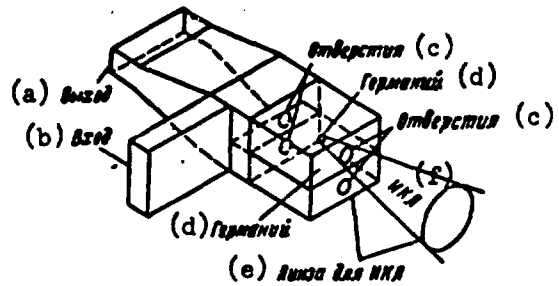

Fig. V.13. Diagram of a germanium indicator of infrared rays in waveguide.
KEY: (a) Output; (b) Input; (c) Holes; (d) Germanium; (e) Lens for infrared rays; (f) Infrared rays.

5. Receivers with Photovoltaic Effect (Rectifying Receivers)

Transformation of radiation energy to electrical with the help of photosensitive layers can be carried out, using rectifying, or, as it is sometimes called, photovoltaic effect. In essence it consists of the fact that at contact of semiconductor and metal there will be formed a thin intermediate layer with one-sided conductivity (barrier layer). During irradiation of such a receiver by radiant flux the current carrier can shift in only one direction; for instance, from semiconductor to metal, creating between them potential difference and current in the external circuit.

Rectifying receivers, as compared to photoemission layers, possess significant integral sensitivity which is possible to see from Table V.13.

However, rectifying receivers have not found wide application in instruments of infrared technology because of high time lag, nonlinearity of light characteristic with increase of load and comparatively small operating wave range 0.5-1.4 μ.

In postwar years, becoming widely applied, have been new photoelectric radiation receivers - photodiodes (FD), phototriodes (FT), whose principle of action is similar to the barrier-layer effect.

Table V.13. Integral Sensitivity of Receivers to a Source with Temperature T_u = 2850°K

Receiver	S, microampere/lumen
With photoemission	150-200
Silver sulfide rectifying	3,000-8,700
Thallium sulfide rectifying	to 11000

Photodiodes, as compared to earlier developed rectifying receivers, profitably differ both in their spectral and integral sensitivity and in their small time lag, high efficiency, and stability of parameters in time.

At present, the most widely used are germanium photodiodes of three types - with point contact, with n-p junction and multipliers (phototriodes) with n-p-n junction, whose diagram of arrangement is shown in Fig. V.14.

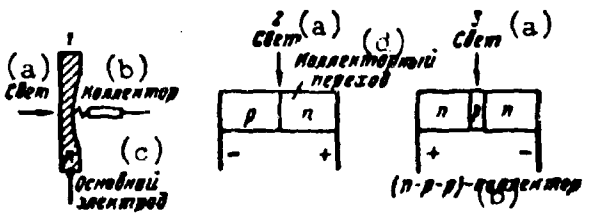

Fig. V.14. Diagram of arrangement of germanium photodiodes 1, 2 and phototriode-multiplier 3.
KEY: (a) Light; (b) Collector; (c) Basic electrode; (d) Collector junction.

These photodiodes can be included in circuits for registering radiant flux in two conditions, consecutively with, as a source of direct current, voltage from several volts to 80-100 v (photodiode conditions) and without a source of current (rectifying method). In the first case there is attained a significantly large sensitivity of receiver.

A point photodiode constitutes a lamina of a single crystal of germanium with electron conductivity (n-type) with deepening on the internal side. In this place to the germanium is connected a collector - a metallic electrode from resiling tungsten wire. During irradiation of external surface of the germanium plate, on the point of the collector will be formed a region nearly 1 mm in diameter with

p-type conductivity, in which is created a junction of type n-p, determining a junction in the barrier layer. Sign of displacement in this case corresponds to the barrier direction, i.e., from the semiconductor to the metal.

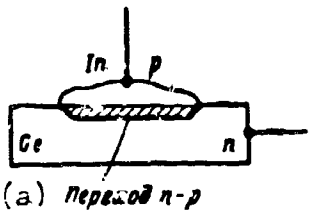

(a) переход n-p

Fig. V.15. Point photodiode with drop of indium. KEY: (a) An n-p junction.

In construction, point photodiodes are made in the form of a cylindrical cartridge 5-6 mm in diameter and 10-12 mm in length. Plate of germanium with point contact is strengthened with heat- and moisture-resistant resins for one of the face sides of the cartridge, which is the receiving side of the photodiode. On the other side of the cartridge emerges the collector lead.

Recently becoming wi ely used have been point-contact photodiodes, for which, instead of a tungsten collector, a drop (welded with it) of a single crystal of another substance with p-type conductivity, for instance indium contacts n-type germanium. Construction of such a photodiode is shown in Fig. V.15. In this case, due to heightened mobility and concentration of holes, for indium there is created a more effective intermediate layer with an n-p junction, which allows, significantly, an increase in the sensitivity of point photodiodes.

Germanium plane photodiodes with n-p and n-p-n junctions are prepared from rectangular plates of a single crystal of germanium with various signs of conductivity. Dimension of plates are of the order of 1 X 1 X 3.5 mm. In a photodiode with n-p-n junctions, both junctions are disposed at a distance near 0.05 mm.

With n-p junctions the sign of displacement corresponds to the reverse direction (an element with n-type conductivity is positive).

With n-p-n junctions, to one of the junctions moves voltage in the barrier reverse direction, to the other - small voltage in a straight direction.

Sensitivity of all three types of photodiodes depends on the place the radiant flux hits the surface of germanium.

The biggest effectiveness is attained when radiant flux hits within limits of several tenths of a millimeter from the junction. Germanium photodiodes have small dimensions. Thus, for the considered French photodiode, for which length of plane junction constitutes 2.6 mm the "effective area" will be equal to 1.05 mm^2.

Dark current at room temperature (+20°C) for germanium photodiodes in photodiode conditions constitutes a magnitude within limits of 3-10 microampere, being increased with a 1°C increase of temperature by 2-3% for point contact photodiodes and by 10% for plane.

Spectral sensitivity of germanium photodiode spreads up to 1.8-2 μ at maximum near 1.5 μ (Fig. V.16).

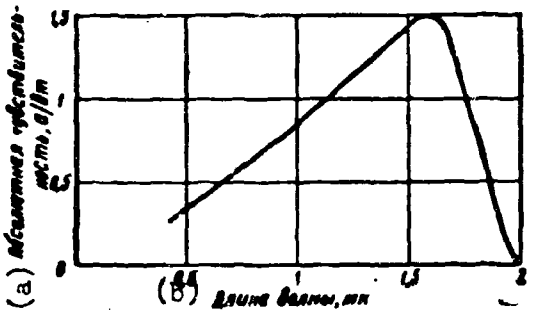

Fig. V.16. Spectral sensitivity of a germanium photodiode.
KEY: (a) Absolute sensitivity, amp/w; (b) Wave length, μ.

Such distribution of sensitivity will agree well with works of Shive [17] and Moss [18], measuring quantum yield of a germanium photodiode with a n-p junction.

In distinction from old rectifying receivers, germanium photodiodes possess very insignificant time lag. In Fig. V.17 is given the frequency-response curve of the French photodiode, from which it is clear that up to 10^4 cps the photodiode is virtually without time lag, and only at a frequency of 75 kilocycles the value of sensitivity decreases to half, as compared to conditions of constant irradiation.

Volt-ampere characteristics of germanium photodiodes depend on their type. Thus, for a point-contact photodiode rectilinearity of volt-ampere characteristics, with an increase in intensity of irradiation, is disturbed. In distinction from point-contact plane photodiodes have volt-ampere characteristics with good linearity at small magnitude of saturation voltage (1.5-4.5 c), and their parallelism is determined by proportionality of current and magnitude of radiant flux.

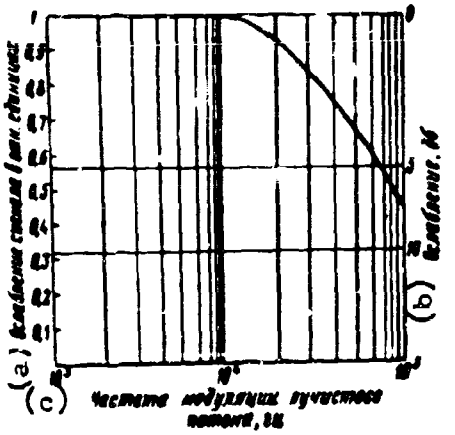

Fig. V.17. Frequency-response curve of a germanium photodiode. KEY: (a) Weakening of signal in relative units; (b) Weakening, db; (c) Frequency of modulation of radiant flux, cps.

Shive [17] presents the following basic parameters of germanium photodiodes (Table V.14).

On the basis of new semiconductor compounds boundaries of sensitivity of contemporary photodiodes were expanded. At present photodiodes are developed on a base of InSb and InAs. In Fig. V.18 are given spectral characteristics of sensitivity of these photodiodes. Possessing high sensitivity in a wider wavelength range with small time lag, these photodiodes, however, require for their work cooling to a temperature of 75-77 K.

Table V.14. Magnitude of Basic Parameters of Germanium Photodiodes

Type	Current	Temperature Coefficient of Dark Current, %	Resistance, ohm	Sensitivity, amp/lu
Point-contact	1-2 ma	2-3	20,000	0.1
n-p	1-10 μa	10	10^7	0.03
n-p-n	20-40 μa	10	10^5	3-10

In the press there have been published certain parameters of a photodiode from indium antimonide (calculated and experimental), on the basis of which Table V.15 is composed. In the table values of the threshold of sensitivity of a photodiode are given for radiation with wave length 4 μ.

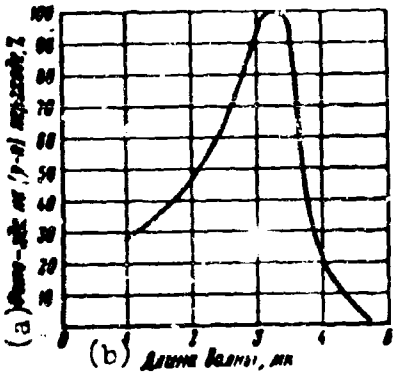

Fig. V.18a. Spectral sensitivity of a photodiode from InSb.
KEY: (a) Photo-emf on (p-n) junction, %; (b) Wave length, .

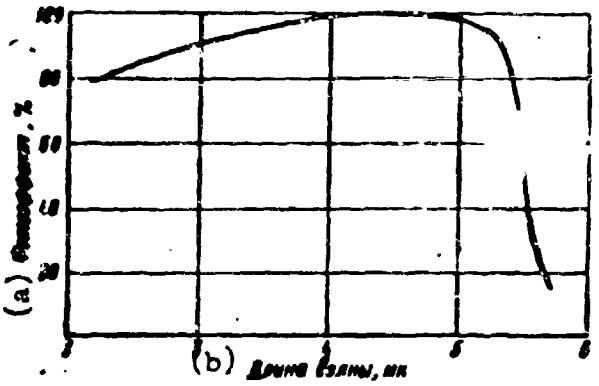

Fig. V.18b. Spectral sensitivity c photodiode from InAs.
KEY: (a) Photoeffect, %; (b) Wave length, μ .

Table V.15. Parameters of a Photodiode from Antimonous Indium [9]

$\lambda_{maximum}$, μ	Temperature of Photosensitive Layer, °K	Area of Photosensitive Layer, cm^2	Time Constant, Microsecond	Threshold of Sensitivity, w/cm^2
4	77	0.01	2	$1.1 \cdot 10^{-8}$
4	77	0.01	2	$1.1 \cdot 10^{-9}$*

NOTE. Computed values of sensitivities are marked by sign *.

6. Receivers with Lateral Photoeffect

As was noted in Section 5, during illumination of a semiconductor junction of germanium photodiode n-p between two sides of this junction there appears photo-electromotive force. Further research of photoelectric effect in germanium photodiodes brought to detection the so-called lateral photoeffect during nonuniform illumination of the site of the receiver [20, 21].

Essence of lateral photoeffect consists in the appearance of additional photo-electromotive force, parallel to the junction, and in the addition of it to the photo-electromotive force appearing between the two sides of the junction if the

radiant flux gets on the sensitive site not symmetrically to the axis of the photocell. The diagram of such interaction is shown in Fig. V.19. If one irradiates a germanium photodiode by a light spot (in dimensions smaller than the dimensions of the sensitive surface) symmetrically to its axis, then voltmeter V_1 will show the presence of voltage between p-n junction of the photodiode. If one were to now displace the light spot to any side relative to a central point (axis of the receiver). Then voltmeter V_2 connected to any two points lying on the surface of the germanium layer will show voltage between these points. The lowest potential is at point of incidence of light and is increased when moved from center to edges of receiver.

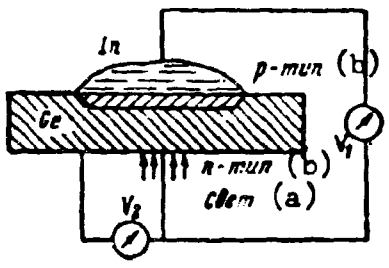

Fig. V.19. Diagram of the formation of lateral (longitudinal) photoeffect for a photodiode.
KEY: (a) Light; (b) Type.

For use of only lateral photoeffect a receiver (germanium plate with fused drop of indium) is supplied with two base contacts for removal of lateral photo-electromotive force, which are located symmetrically relative to the center of the sensitive surface. Necessity in contact with indium drop falls off since longitudinal photo-electromotive force in this case is not measured, and indium, so to speak, can be left electrically floating.

With such construction of a photodiode the sign of lateral photo-electromotive force will change from positive to negative value depending upon position of light spot on the surface with respect to axis of symmetry of photocell. Consequently, point source of light, image of which is projected through objective on the receiver, will create a signal which will change depending upon the angle between direction to source of light and axis of symmetry of the "receiver - objective" system, i.e., the receiver can measure direction to source of light by null method, possessing high accuracy. During change of direction to source of light, polarity of signal changes also.

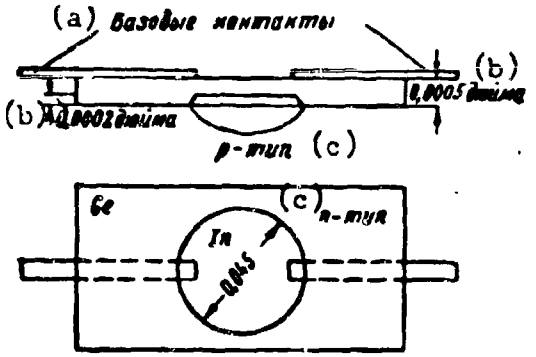

Fig. V.20a. Construction of a photodiode with lateral photoeffect.
KEY: (a) Base contacts; (b) Inches; (c) Type.

In literature is described the following construction of a photocell with lateral photoeffect (Fig. V.20a).

A germanium plate 0.0127 cm thick (0.005 inch) and 0.635 cm^2 (0.25 square inch) in area had specific resistance 1-2 ohm/cm. An indium drop 0.114 cm in diameter (0.045 inch) was fused to germanium 0.005 cm deep (0.002 inch) and had 0.001 ohm/cm specific resistance of junction. Two base contacts were disposed symmetrically.

If a ray of light drops in the center of the sensitive surface above the indium point, then on the contacts are established two equal in magnitude voltages so that the voltage between the base contacts will be equal to zero (Fig. V.20b).

If light point shifts from center, then total output voltage may be calculated by the formula

$$U_{вых} = \frac{\rho}{q}\frac{Ix_1}{2l}(-x_1) + \frac{\rho}{q}\frac{I(2l-x_1)}{2l}(2l-x_1) = 2\frac{\rho}{q}I(l-x_1), \quad (V.6)^*$$

where ρ is resistance,

q is area of sensitive element,

$2l$ is distance between base contacts,

x_1 is current coordinate of light spot.

When light point is in position A, total base voltage, which is the difference in voltage between light point and left and right ends of receiver, will attain its maximum value (for the shown receiver $U_{вых}$ = 1.5 millivolt). When light point moves in the direction of position C, output voltage will start to decrease, will pass through zero, and polarity will change, attaining maximum value at point C.

*Russian subscript "Bblx" indicates "output".—Ed.

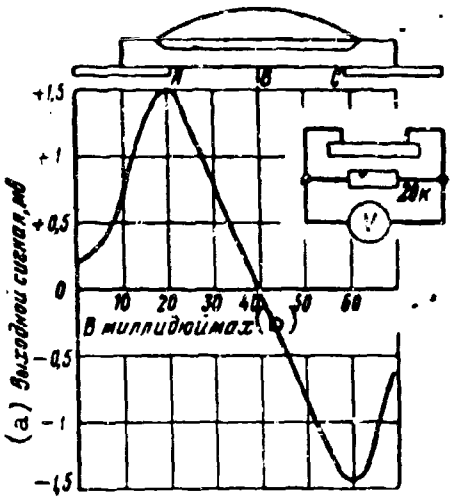

Fig. V.20b. Dependency of photoelectromotive force on position of light spot on sensitive surface. KEY: (a) Output signal, millivolt; (b) In milli-inches.

Resultant curve of change of output voltage in the operating sections will be rectilinear. On boundaries of the operating section of the receiver, in direct proximity to base contacts, the curve has a sharp drop due to loss of sensitivity on boundaries of fusing of the indium drop.

With the help of such a receiver can be obtained two coordinates, if one were to introduce a second pair of base contacts, perpendicularly to the first. In such an element deflection of a light ray from the center will be determined by a pair of intercontact voltage, whose amplitude and sign simply determine the position of the light spot on the surface and, consequently, the direction to source of radiant flux.

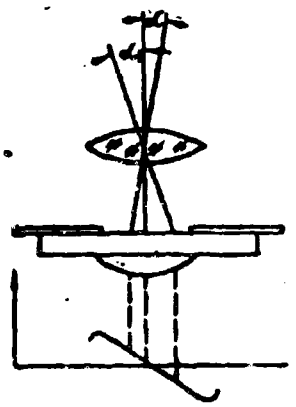

Fig. V.20c. Diagram of determination of direction to source of radiation.

Consequently, with the help of the shown receivers it is possible to determine direction to source of radiation, i.e., actually to carry out direction finding of radiation sources. Actually, if radiant flux is focused by the optical system in the central part of the receiver (Fig. V.20c), then on its output voltage will be equal to zero. If, however, luminous flux is focused to the right or to the left of the axis of symmetry of the photocell, then on its output will appear voltage. Magnitude and sign of voltage allows us to judge the distance of the spot to the right or to the left of the axis of symmetry. Turning the device to the

corresponding side until output voltage disappears, one can determine direction to source of radiation.

In literature it is indicated that the accuracy of determining direction to source of radiation by this null method attains 0.1 angular second, since error of combination of the light spot with the axis of symmetry of the receiver does not exceed 100 Å. If, however, we use a receiver with two pairs of base contacts, then it is possible to determine direction to source of radiation with such accuracy immediately in two coordinates - in azimuth and in elevation.

Deficiency of such a method of determining direction to target is its large time lag since it is necessary to turn the receiver until output voltage disappears. Therefore, this method does not allow direction finding of briefly effective sources of radiation, for instance the flash from a shot of a cannon. Duration of a flash constitutes a period of the order of several milliseconds and, naturally, to turn a receiver for such an interval of time is impossible.

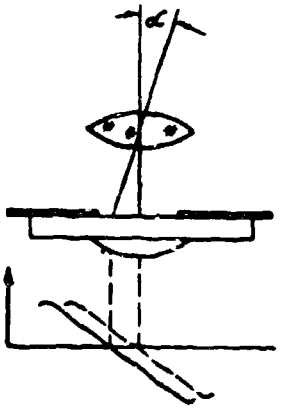

Fig. V.20d. Imitation of the turn of a device by displacement of the axis of the characteristic.

However, lateral photoeffect allows the imitation of a turn of receiver by displacement of axis of the characteristic (Fig. V.20d) or, as we say, application of the electron shift.

Such a shift of characteristic is possible to carry out, passing to base electrodes bias voltage of corresponding sign.

Influence of bias voltage applied between base contacts from external batteries may be determined from relationship

$$\left.\begin{aligned} U_0 &= 2\frac{\rho}{q} I (l + cU_0 - x_1), \\ c &= \frac{R_n}{R_n + R_6}\frac{q_n}{2\rho l}. \end{aligned}\right\} \qquad (V.7)$$

where $U_б$ is voltage of bias battery,

$R_б$ is internal resistance of battery,

$R_п$ is resistance of receiver.

Expression (V.7) gives dependency of the change of characteristic along the axis of abscissas depending upon the change of voltage of battery $U_б$.

The curve is displaced to one side during displacement current of one sign and to the other - during displacement current of the other sign, which is clear from Fig. V.20e.

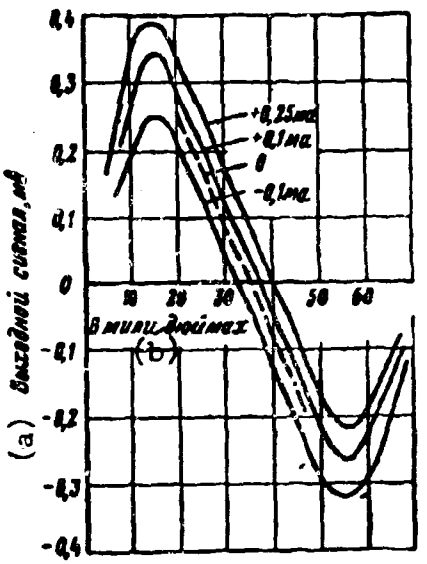

Fig. V.20e. Change of characteristic during change of bias voltage. KEY: (a) Output signal, millivolt; (b) In milli-inches.

Besides mechanical modulation of radiant flux, with the given receiver it is possible to carry out electron modulation of output signal by application of alternating bias voltage to the junction contact by the diagram in Fig. V.21.

Changing the magnitude of forward current through the junction between the drop of indium and the two base contacts, it is possible to decrease sensitivity of receiver approximately to 10% its initial magnitude, which is equivalent to the modulation of the signal. This decrease of sensitivity is explained by potential drop in the base region due to forward current which junction of current carrier from drop of indium to germanium due to the action of radiant flux. In other words, with an increase of current through junction the slope of characteristics decreases.

An electron interrupter (EP) may be made in the form of an electron key (type of multivibrator), alternately connecting and disconnecting plus of the battery from the drop of indium.

It is necessary to note that during the given method of modulating radiant flux, simultaneously interrupted also are leakage currents and fluctuating noises of the semiconductor and consequently, they cannot be separated during subsequent amplification.

Linearity of the operating section of receiver response is sustained with precision $\pm$ 1%, and the steepness of it depends on the distance between base contacts. The less the distance between base contacts, the bigger the slope of the characteristic.

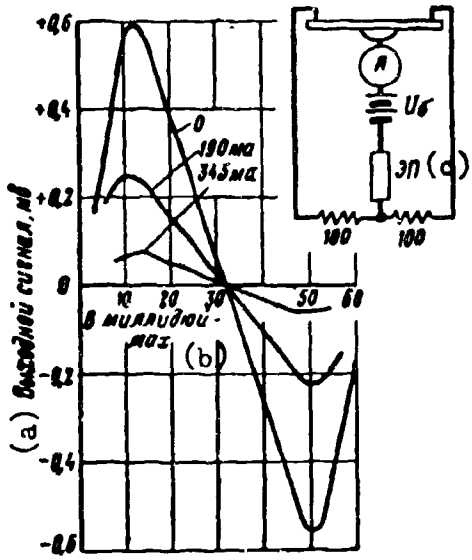

Fig. V.21. Electronic modulation. KEY: (a) Output signal, millivolt; (b) In milli-inches; (c) Electron interrupter.

During optimum selection of spot diameter we manage to obtain a 45% steepness of characteristic per 0.0254 mm (1 milli-inch).

Conducted research of a model of receiver with characteristic having a maximum of 1.5 mv and 43% steepness per 0.0254 mm (change of magnitude of voltage from maximum value to 43% during displacement of light spot 0.025 mm from center), showed the possibility of registering voltage of 10 microvolt during change of position of spot along the operating surface of the receiver on 100 Å. In case of application of an objective with focal length 25.4 mm (1 inch) angular accuracy is equal to 0.1 angular second (accuracy, which may be ensured by eye, constitutes 0.5-1 angular minute, but for good optical range finders 10-15 angular seconds [22]).

The device made it possible to reveal a source of monochromatic radiation with λ = 6000 Å, power Φ = 10 w at ambient temperature T = 300°K from distance L = 1000 m. Magnitude of current of noises during an amplifier passband of Δf = 1 cps at room

temperature constituted a magnitude of the order of 10^{-11} amp, and the signal-to-noise ratio during the experiment was 20 db. In the device was used an objective with aperture $A_0 = 10$ cm^2 and transmicsivity $\tau_0 = 0.8$.

Fig. V.22. General form of receiver with lateral photoeffect and device for determining direction to source of radiation.

Receiver with interbase resistance R = 100 ohm had a reflectivity from the sensitive surface of 0.37.

Under these conditions sensitivity of device may be estimated to be a magnitude of the order of 200 microampere/lu.

At present a report has appeared about the manufacture, on the basis of a receiver with lateral photoeffect, of instruments for determining direction to source of radiation, appraisal of position of missiles, their stabilization and, as an exact optical indicator of precession of gyroscopes and accelerometers [23].

General form of one such instrument is shown in Fig. V.22. The instrument has the following characteristics:

maximum output voltage, developed by receiver during load is 20,000 ohm, 42 $\frac{v}{inch \cdot w}$;

linear sensitivity 0.32 $\frac{v}{inch \cdot w}$;

angular sensitivity 16 $\frac{v}{inch \cdot w}$ with focal length of objective 254 mm (10 inches);

minimum energy content causing signal 1 v, 0.015 w (with a source with T_a = = 2600°K);

time constant 5 microseconds;

internal resistance 3000 ohm.

7. Receivers with Photomagnetic Effect

In 1934 Noskov and Kikoin revealed that if the plate of a semiconductor is placed in magnetic field B (Fig. V.23) and irradiated by radiant flux perpendicular to the direction of the force lines of the field, then in the plate will appear potential difference directed perpendicular to the field and radiant flux.

Later this phenomenon, called photomagnetic effect, was investigated in detail [24, 25, 26] in germanium, silicon, lead sulfide, indium antimonide, indium arsenide, and magnesium stanide. The most reassuring results were obtained recently on sufficiently pure samples of indium antimonide.

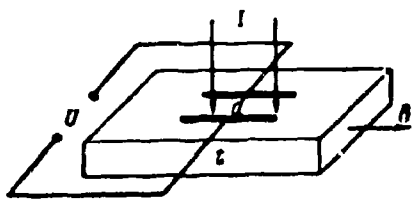

Fig. V.23. Diagram of photomagnetic effect.

If one were to irradiate one of the surfaces of a rectangular sample of the above-indicated compounds, in their surface layer would be formed "electron - hole" pairs, which then would start to spread inside the sample and, under the action of the transverse magnetic field, to deviate in opposite directions. As a result of this, on the sample will be formed potential difference perpendicular to the magnetic field and direction of the radiant flux. Voltage between two linear electrons located on the sample d cm from each other, can be calculated by the formula

$$U = IdBs \cdot 10^{-8} \text{ v}, \qquad (V.8)$$

where s is speed of surface recombination of current carrier, cm/sec;

I is intensity of radiant flux;

B is magnetic field strength, oersted. $\frac{\text{quantum}}{\text{sec} \cdot \text{cm}^2}$

(In the case of germanium with s = 10,000 cm/sec at d = 0.1 cm, B = 10,000 oersted, and intensity I = 1 $\frac{\text{quantum}}{\text{sec} \cdot \text{cm}^2}$ U = 0.1 v).

Research of indium antimonide as an indicator of infrared rays has shown that photomagnetic electromotive force exceeds the magnitude of the signal due to photoconductivity. The relation of these signals, in the case of indium antimonide possessing proper conductivity in accordance with the theory offered by Mohs, may be determined from relationship

$$\frac{e_{\Phi м}}{e_{\Phi п}} = 0{,}32 \frac{Bd}{u} \sqrt{\frac{\mu}{\tau}}, \qquad (V.9)^*$$

where u is voltage applied to the sample during measurement of photoconductivity;

μ is mobility of charge carriers, $cm^2/v \cdot sec$;

τ is lifetime of carrier, sec.

Short circuit current i_{k3} during change of magnetic field strength changes according to the law

$$i_{K3} = \frac{kB}{1 + cB^2}, \qquad (V.10)$$

which fully agrees with experimental data (Fig. V.24); however, photomagnetic electromotive force with a change of magnetic field strength does not follow this law since resistance of the sample increases with an increase of magnetic field. As the research of D. N. Nasledov and Yu. S. Smetannikovaya [27] has shown, the dependency of photomagnetic electromotive force in a single crystal of n-type InSb with a concentration of donors $2 \cdot 10^{13}$–$2 \cdot 10^{14}$ cm from magnetic field strength in the range of 300–20,000 oersted is almost linear.

In literature there is presented no data about spectral sensitivity of the indicator, although it is noted [6] that results of spectral measurements of photomagnetic effect in pure sample of InSb, InAs and Mg_2Sn allow us to consider them useful for receiving radiation in the comparatively distant infrared region of the spectrum. Furthermore, a rough estimate of spectral sensitivity of the photomagnetic effect in indium antimonide is reported [24]. The reaction was measured of indium antimonide to the radiation of an ideal black body heated to 300°C, with

*Russian subscript "$\Phi_м$" indicates "photomagnetic"; "$\Phi п$" indicates "photoconductivity".--Ed.

a quartz plate 3 mm thick as a filter and without it. During location of the quartz plate before the tested sample photomagnetic electromotive force decreased 5 times. This allowed the authors to consider that photomagnetic effect in indium antimonide is caused basically by radiation with a wave length higher than 4 μ.

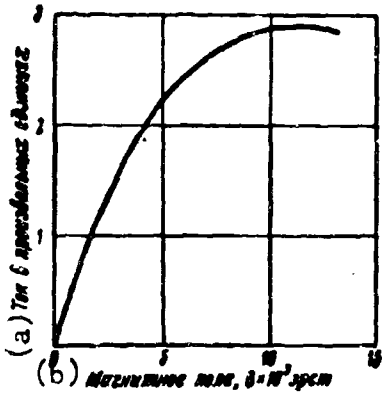

Fig. V.24. Change of short-circuit with change of magnetic field in InSb.
KEY: (a) Current in arbitrary units; (b) Magnetic field, B X 10^3 oersted.

In literature [28] a photomagnetic receiver is described on the basis of a single crystal of InSb, working at room temperature and possessing spectral sensitivity to 7.5 μ. Its threshold of sensitivity to radiation with a wave length of 6.6 μ is equal to $6.7 \cdot 10^{-10}$ w with dimension of receiving site 0.71 mm^2 and passband of amplifier Δf = 1 cps. In the same place it is indicated that the time constant of the receiver, measured on drop of signal "e" times, is less than 1 microsecond.

Table V.16. Calculating and Experimental Characteristics of InSb Receiver with Photomagnetic Effect [9]

Characteristics	Material	λ_{μ} maximum, μ	Current of Detector	Area cm^2	Threshold of Sensitivity w/cm^2	τ μ sec
Calculating	InSb	4	300	0.3	$1 \cdot 10^{-9}$	1
Experimental	InSb	4	300	0.16	$2.5 \cdot 10^{-8}$	1

The considered method of detection of infrared radiation profitably differs from application of photoresistors by its insignificant noises, limiting the threshold of sensitivity. Therefore, the application of photomagnetic effect in InSb requires the use of amplifiers with very little set noise. Otherwise gain from application

of highly sensitive method of registering infrared radiation in a wide range of the spectrum may be significantly lowered due to impairment of threshold sensitivity of all the system on the whole.

8. Cooling of Photosensitive Layers

As already was noted, the majority of receivers of radiation require cooling. Cooling of photosensitive layers allows increase of their integral sensitivity, expansion of spectral range of sensitivity in the direction of longer waves, and decrease of internal noises, limiting the threshold of sensitivity of infrared instruments.

Cooling of a photosensitive element may be attained when it is placed in a Dewar vessel, filled with corresponding refrigerant, ensuring temperature of cooling, shown in Table V.17.

Table V.17. Obtaining of Low Temperatures

Refrigerant and its State	Obtainable Temperature	
	°K	°C
Melting of ice	273.16	0
Volatilization of solid carbon dioxide	194.7	-78.46
Boiling of liquid air	88-85	-185 to -183
Boiling of liquid oxygen	90.2	-183
Boiling of liquid nitrogen	77.4	-195.8
Boiling of liquid neon	23	-250.16
Boiling of liquid hydrogen	20.5	-252.66
Boiling of liquid helium	4.22	-268.94

The methods shown in the table have found wide application in laboratory conditions and can be used for cooling of laboratory samples of receivers, since here, in the end, only economic considerations and required consumption of cooler

play a role. Such cooling is attained by locating photosensitive element in a cryostat.

As an example in Fig. V.25 is given a diagram of cooling of a highly sensitive germanium photoresistor, alloyed by zinc (536-1ZIP, Perkin-Elmer). Cooling of photoresistor is carried out by liquid helium, filling the internal volume of the cryostat. Around the internal vessel is placed a second external vessel, filled by liquid nitrogen for the purpose of slowing the evaporation of the liquid helium. The actual photoresistor is placed in vacuum on the internal wall of the first vessel. External wall of bottom of vessel (window) is prepared from KRS-5.

The photoresistor is cooled to temperature 4°K and has the following parameters:

dimensions of cryostat - length 45 cm, diameter 15 cm;

dimensions of photosensitive layer - from 2 X 2 mm to 20 X 20 mm;

spectral sensitivity - 2-40 μ ;

time lag - 0.01 microsecond.

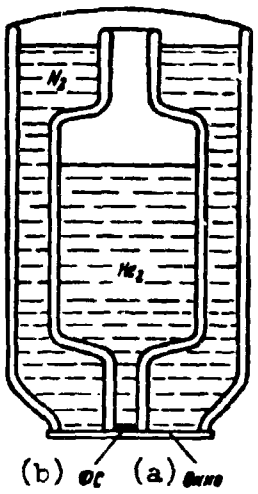

Fig. V.25. Cryostat for cooling photoresistor. KEY: (a) Window; (b) Photoresistor.

Indicator is released in series by the firm Perkin-Elmer and is designed for the detection of comparatively low-temperature radiation [12].

In the case of development of cooling systems of photosensitive layers for infrared instruments with a military assignment, besides the economic factor, of paramount value is reliability of operation, weight, dimensions, time of preservation of refrigerant, and the possibility of application in any place and in any time.

In order to judge those difficulties which must be faced when developing such systems, we will consider the peculiarities of their work:

a) system of cooling can be established in the infrared homing device of rockets, on satellites, piggyback plane equipment, in carried instruments, etc. Consequently, they have to be small-size and have small weight with insignificant consumption of external energy;

b) time of action of cooler can change from several minutes to several days without milking;

c) systems of cooling should unfailingly work at any height, at any temperature and in any position which they may take in space together with the object;

d) systems of cooling should ensure maximum reliability and especially preservation of gas in pure state, and also mechanical durability of material working under very low temperatures.

Considering all the above-stated, it is considered [29] that among the many technical problems facing the industry releasing instruments of infrared technology for military and civil assignment, one of the first in the list of the most difficult is the problem of cooling infrared indicators.

For cooling photosensitive layers in infrared instruments four basic types of systems can find application:

cryostat systems;

systems operating by adiabatic expansion of the operating substance;

systems of direct cooling by liquified gas (heat exchangers), and

thermoelectric systems.

A common condition for the first three systems is the necessity of using closed systems to guarantee the greatest cleanness of refrigerant and prolonged work without milking. Furthermore, in space conditions open systems are unfit in principle.

A simplified block-diagram of a refrigerating installation, working on a closed cycle, is shown in Fig. V.26.

From reserve bottle 1, where there is saved a reserve of liquid coolant or gas, the refrigerant proceeds through measuring hopper 2 into compressor 3 and from there under pressure - along coil 4 to nozzle 5, located in direct proximity to cooled photosensitive layer 7. The photosensitive layer is placed in the vacuum of closed insulated cryostat 6. Liquid coolant is evaporated and is expanded in the nozzle, cooling internal volume of cryostat. Then cooling gas by tube 8 enters compressor, where again it is compressed, and then under pressure enters nozzle, where, repeatedly being expanded, it cools the internal volume of the cryostat. Thus, from cycle to cycle there occurs gradually a cooling of photosensitive layer. At the needed moment the measuring hopper can supply the installation with an additional portion of liquified gas. For the purpose of increase efficiency of installation, gas under pressure is transported along coil, reeled on tube 8, which allows its preliminary cooling.

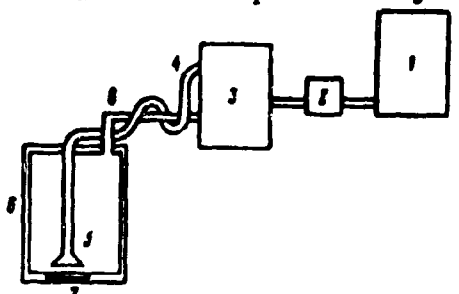

Fig. V.26. Block-diagram of a refrigerating installation working on closed cycle.

Sometimes coil is reeled on tube proceeding from reserve bottle to measuring hopper and having temperature of liquified gas.

Cryostats in construction and principle of action can be broken down into three groups.

a) cryostats in which cooling is attained by application of compressed gas;

b) cryostats in which cooling of photosensitive layer is attained by washing its sublayer with liquified gas, with gradual augmentation of liquid coolant as it is expended;

c) cryostats with application of compressor in a closed system.

The operating principle of the first group of cryostat systems (Fig. V.27) can be comprehended by the diagram of a cooler working on the principle of expansion of preliminarily compressed gas (nitrogen or helium).

Compressed gas under pressure of 180 atm proceeds from reservoir A through capillary and filter B and solenoid valve C to dilator D, where it is expanded and liquified. Supply of gas is regulated with the help of a transducer, for which resistance is changed with decrease in level of liquid coolant affecting solenoid valve (measuring hopper).

By analogous diagram is carried out a cooler of the firm of Linde, shown in Fig. V.28.

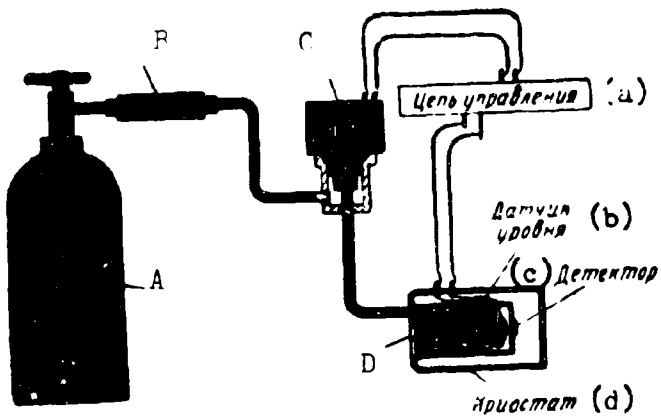

Fig. V.27. Diagram of cooler working on the principle of adiabatic expansion of gas. KEY: (a) Control circuit; (b) Transducer level; (c) Detector; (d) Cryostat.

In this system as a work substance compressed helium is used, which enters cooled cavity (cylinder 0.8 cm in diameter and length 5 cm) under pressure of 20 atm. Being expanded in cryostat near photosensitive layer, helium allows us to obtain temperature to -210 to -213°C. Weight of device is 220 g. Its application, as is shown in literature, will allow decrease in weight of aircraft infrared equipment to 4 kilogram.

A characteristic peculiarity of the given construction is the fact that in it is applied only one mobile part - a plastic piston in the cryostat.

Cryostats with direct transfer of liquid coolant (Fig. V.29) consist of a special vessel for storage of liquified gas under pressure, a capillary, on the end of which is a cooled indicator of infrared radiation, and a preheater. Heating of liquid (nitrogen) with the help of a spiral causes expansion of liquid and rise by capillary to cooled indicator.

It is indicated that such systems are the most promising for aircraft equipment. In filled state, the weight of the system constitutes nearly 4 kg, and it ensures continuous cooling of eight indicators to a temperature of -195°C for 6 hours.

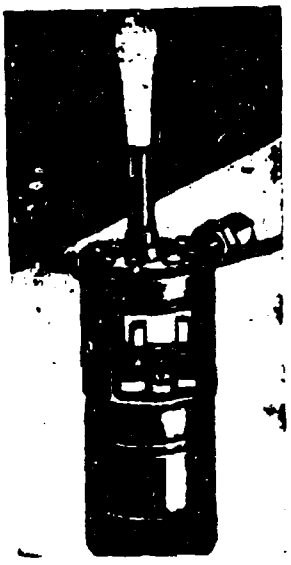

Fig. V.28. General form of cooler with adiabatic expansion of gas.

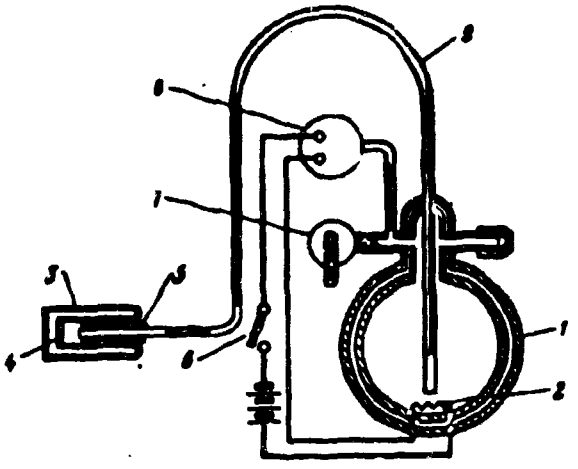

Fig. V.29. Diagram of a cooler with direct transfer of liquid. 1--reservoir with nitrogen; 2--heater; 3--bottle; 4--detector; 5--to atmosphere; 6--manual switch; 7--differential value; 8--pneumatic switch; 9--pipeline.

The advantage of such a system, as compared to a system founded on adiabatic expansion of compressed gas, is the absence of a necessity to have instruments for adjustment of temperature changes in cooled cavities, since evaporation of liquid occurs at a fully definite temperature, and also the absence of any moving parts at low temperatures. Furthermore, in this case these systems ensure a high degree of cleanness of cooler, since all soiling impurities are frozen out.

However, systems with direct transfer of liquid are absolutely unfit for work in space conditions of high rarefaction of air. As a deficiency, one should note (this pertains also to systems with adiabatic expansion of gas) their low economy and great consumption of cooling substance.

A variety of cryostat systems of the second group are Dewar vessels for cooling lead sulfide of photoresistors with the help of solid carbon dioxide or freon (Fig. V.30).

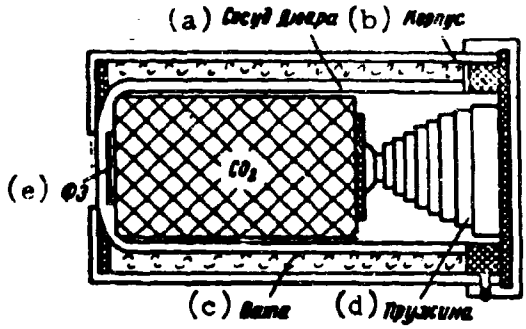

Fig. V.30. Construction of cryostat for cooling PbS by solid carbon dioxide.
KEY: (a) Dewar vessel; (b) Body; (c) Cotton; (d) Spring; (e) Photoresistor.

Inside a Dewar vessel is placed a briquette of solid carbon dioxide, which, as a result of volatilization cools the photoresistor, being in contact with the briquette through the glass bottom of the vessel, to a temperature of -78°C. In order to ensure constant contact of briquette and photoresistor, briquette is held to bottom of vessel by special spring, secured on cover of cryostat.

In connection with noted deficiencies of open cooling systems, at present a basic trend in the creation of cooling systems is the development of cooling methods with the help of closed cryostat systems with liquid nitrogen or helium. Cooling of photosensitive layer is carried out either by expanded gas or by spraying method - condensation of gas on a cooled surface.

In the first case liquid is provided in an insulated bottle under low pressure and proceeds through capillary to photoresistor, where, being evaporated, it cools it. Exhaust gas is repeatedly compressed with the help of a compressor and proceeds on a closed curve again to cryostat.

In the second case, near sublayer of cooled photosensitive layer are created conditions corresponding to "dew point" for a given gas. The gas, being condensed on sublayer of indicator, cools it, but then later on its evaporation again is compressed by compressor and enters cooled cavity. As gas is expended, its augmentation occurs from reserve bottle [30].

In Fig. V.31 is shown a system of the firm of Linde, for which photosensitive layer is mounted directly on sprinkler. In this system liquid washes back side of photosensitive layer both during work and during non-working time. Consequently, photosensitive layer is always cold and, being in vacuum, is always ready for work. It is indicated that the installation weighs to 3.4 kg and can ensure cooling

to 8 photosensitive layers during 6 hours after 24 hours of preparation.

Considered systems of cooling require for their work a reserve of cooling substance. This is not always convenient and can lead to the fact that at a needed moment a reserve of liquid coolant will not be at hand. Furthermore, the presence of a bottle with liquid coolant, although of limited volume, and a compressor installation makes these systems comparatively bulky.

Therefore, efforts of industry now are already directed toward creation of new, in principle, methods of cooling photosensitive layers.

One such way, if deep cooling is not required, is the use of thermoelectric generators. As early as 1834 the French scientist Peltier revealed that if one were to pass current through a thermojunction in a direction reverse to thermoelectric current, appearing during heating of the thermojunction, then the latter will lower its temperature (Peltier effect). Thus, passing current from antimony to bismuth, Peltier cooled a junction 45°C with respect to ambient temperature.

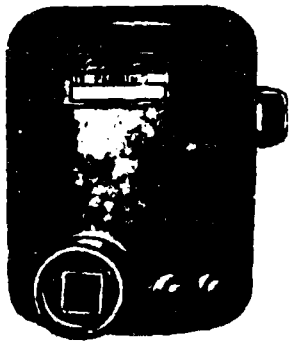

Fig. V.31. Installation of Linde with sprinkler in contact with photosensitive layer.

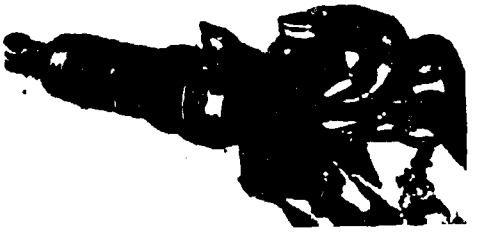

Fig. V.32. Thermoelectric refrigerator of Westinghouse.

The Peltier effect quite noticeably appears on the junction of two semiconductors. Therefore, only recently, after much achievement in the region of semiconductor physics, has it become possible to apply, in practice, the Sang effect.

At present, an intense search is in progress of materials possessing low thermal conductivity, high electrical conductivity, and thermo-emf.

Simultaneously, construction of thermoelectric refrigerators is being developed for cooling lead sulfide photoresistors (Fig. V.32).

Thermoelectric refrigerators are ultimately reliable in work, do not have mobile parts, possess little weight, and can be constructed with photosensitive layer. Their consumed power is very small 2-2.5 w. Thus, the thermorefrigerator shown in Fig. V.32 consumes 20 amp current at a voltage of 0.1 v, ensuring temperature drop of 50°C at ambient temperature +25°C.

Increase of temperature drop by approximately 50% may be attained by application of two-stage cooling. As reported in the press, at present two-stage thermoelectric refrigerators have been developed, allowing a drop up to 79°C.

It is indicated that thermoelectric refrigerators have three peculiarities as compared to other systems, namely:

operation of refrigerators is not subject to the influence of vacuum and the surrounding situation;

efficiency of refrigerators is improved with growth of temperature of ambient air;

energy for work of refrigerators may be taken from any outside source.

Literature

1. M. A. Margolin, N. P. Rumyantsev. Bases of infrared technology. Voyenizdat, 1957.

2. Luk'yanov. Photocells.

3. P. Gerlikh. Photocells, State Technical Press, 1948.

4. IRE Trans. on Nuclear Science 1956, Nov., No. 4.

5. "Lighting technology", 1959, No. 4.

6. Proc. of the IRE, 1955, Vol. 43, No. 12.

7. Adv. Phys., 1953, Vol. 2, p. 321.

8. Science, 1953, Jan., p. 115.

9. Proceedings National Electronics Conf., 1958, No. 13.

10. J. Scient. Instruments, 1957, Sep., Vol. 34, No. 9.

11. Aviation Week, 1959, 4, May.

12. Aviation Week, 1959, 13, Apr.

13. J. Scient. Instruments, 1959, Vol. 36, No. 4.

14. Electronics, 1959, Vol. 32, No. 1.

15. Electronics, 1959, Vol. 32, No. 5.

16. Electronique, 1956, No. 110.

17. JOSA, 1953, Vol. 43, p. 239.

18. Physica, 1954, Vol. 20, p. 989.

19. Nachrichtentechnik, 1955, Vol. 5, No. 10.

20. Proc. IRE, 1957, Vol. 45, No. 4.

21. Electronics, 1957, 7 Mar.

22. Optical-Instruments, Chemical Publishing Co. Inc., Brooklyn, 1945, No. 4.

23. Aviation Week, 1959, 21 Sep.

24. "New semiconductor materials". Collection edited by B. C. Kolomiyts. Publishing House of Foreign Literature, 1958.

25. W. Danlap. Introduction to physics of semiconductors. Publishing House of Foreign Literature, 1959.

26. Proc. Phys. Soc., 1953, Vol. 66, Sec. B, p. 993.

27. "Solid state physics", 1959, Jan., No. 4.

28. J. Appl. Phys., 1959, Vol. 30, No. 5.

29. Missiles and Rockets, 1959, 9 Nov.

30. Missiles and Rockets, 1959, May, No. 21.

C H A P T E R VI

IMAGE CONVERTERS

Under image converter we understand an electrovacuum device which allows conversion of an optical image of one spectral composition to another by means of constructing an intermediate electron image. The aim of such a conversion can be either the transfer of an image from one spectral region to another or the amplification of image brightness, both simultaneously. The most widely used image converters at present are electron-optical (EOP).

1. Converters with External Photoeffect

Historically, the first image converters (1934) were the simplest two-electrode converters of the "Holst Cup" type (Fig. VI.1).

Two-electrode converters are made in the form of a flat capacitor placed in a glass shell, in which vacuum is created of an order of 10^{-4}-10^{-5} mm Hg so that photoelectrons can move without collison with molecules of air. On the front wall of the shell from the internal side is applied a very thin transparent layer of silver which is one of the two electrodes of the converter. On it, as on the sublayer, is deposited by evaporation in vacuum a semitransparent photosensitive layer (cesium oxide or cesium antimonide).

On opposite wall of shell also on silver transparent sublayer is deposited a layer of luminophor (willemite or zinc sulfide). Between the cathode and the

screen is applied high tension (to 12,000 v), creating inside the converter a plane-parallel electrostatic field with intensity

$$E = \frac{U}{d}, \qquad \text{(VI.1)}$$

where d is distance between photocathode and screen, cm.

Infrared rays reflected from the observed object are projected with the help of the objective on the photocathode, creating on it an inverted and decreased image, not visible to the eye, with a distribution of "bright" and "dark" places on the photocathode, corresponding to the distribution of radiation intensities of separate sections of the observed object. In "brighter" places of the image electrons will burst from the photocathode in a larger quantity than from the "darker" places. Pulled from the photocathode, the electrons (photoelectrons), getting into a plane-parallel electrostatic field, will move with uniform acceleration to the screen.

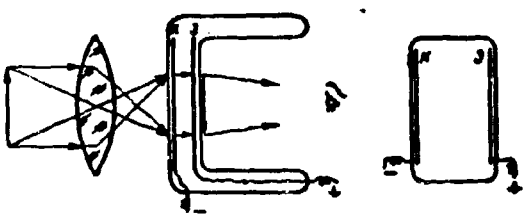

Fig. VI.1. Diagram of the simplest converter.

Density of photoelectron current appearing in the converter from different sections of the photocathode will be proportional to the intensity of their irradiation. Due to this the electron image will correspond to the optical image on the photocathode. Photoelectrons of the electron image, obtaining, during their motion toward the screen, kinetic energy eU ev, bombard the screen and cause its glow. Intensity of glow of separate points of the screen is proportional to the power of the photoelectron current. This allows us to observe on the screen of the converter a one-color image of the object observed in the infrared rays with a distribution of brightness tones corresponding to the distribution of radiation intensities (proper and reflected) of separate points of the object.

Quality of the image of the object observed in a two-electrode converter of this type remains low due to imperfection of the electron-optical system of the

"flat capacitor" type. During plane-parallel transfer, electrons, based on the cause of their various initial velocities v_0, move in the field not in parallel with each other, but along parabolas with a summit at the point of emission. This does not allow them to gather on screen at a point, conjugate with a corresponding point on the photocathode. Therefore, any point on the cathode will be depicted on the screen in the form of a circle of confusion, which determines resolving power of the electron-optical converter.

Possibilities of increasing resolving power of a two-electrode electron-optical converter are limited by the following factors:

1. During a field strength for a photocathode of the order of 10 kv/cm, field emission starts from the photocathode, sharply lowering contrast of image.

2. A decrease of distance between the photocathode and the screen leads to an increase of reverse gating of the photocathode by radiation of the screen, leading to a decrease of resolving power of the converter and imposition on the image of a general parasitic background.

3. Increase of operating voltage or decrease of distance between electrodes is limited also by the onset of disruption between them and as a result of this - breakdown of the instrument.

4. With small distance between screen and photocathode technological difficulties appear in obtaining a photocathode uniform in area during its sensitization by vapors of cesium.

These limitations do not allow us to obtain converters with high resolving power. Thus, in the best samples of two-electrode converters there can be obtained a circle of confusion in diameter D = 0.1 mm, i.e., in this case resolving power constitutes a magnitude of the order of 10 lines/mm.

To improve image quality in the simplest converters combined electrostatic and magnetic focusing of photoelectrons was offered (Fig. VI.2).

The photocathode and screen in such a converter are separated by a large distance (sometimes up to 7 cm), and the accelerating voltage is lowered to 500 c. Focusing of electrons is carried out by long magnetic lens.

There can be practically obtained, with such a method of focusing electrons, resolving power of converters 20-30 lines/mm (with distance between electrodes d = 7 cm, U = 500 v).

In spite of their simplicity, two-electrode converters during the Second World War were replaced by more advanced multi-electrode converters, including electorstatic electron optics. Three- or multi-electrode converters, in spite of the fact that their manufacture is more complicated than the two-electrode type, have a number of advantages over the latter, which promoted their wide application, especially in instruments of military infrared technology.

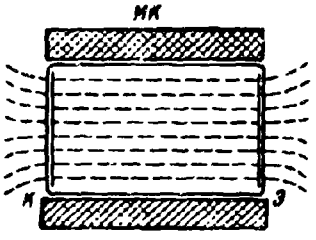

Fig. VI.2. Two-electrode converter with magnetic focusing.

Such advantages are:

1. Improvement of shielding of photocathode from gating by radiation of screen with the help of diaphragms. This allows the use of cathodeluminophors with great brightness of glow and high accelerating voltages, at which screen efficiency sharply increases.

2. Application of several electrodes allows gradually increasing intensity of electrostatic field from photocathode to screen. This makes it possible to apply very high accelerating voltages without danger of appearance of field emission from photosensitive layer.

3. Multi-electrode converters allow us to obtain an image not only in a 1 to 1 scale, but also with increase and decrease. The latter has a very important value for amplification of image brightness, since with decrease of image density of current grows as well as brightness of glow of screen.

4. Application of focusing systems increases resolving power of converter as compared to parallel translation of electrons.

For the case of electrostatic focusing diameter of the circle of confusion can be calculated by the formula (VI.2), and during combined - by (VI.3),

$$D=2d\frac{\Gamma_0}{2\Gamma_0+1}\frac{v_0}{U}, \qquad \text{(VI.2)}$$

$$D=d\frac{\Gamma_0}{2\Gamma_0+1}\frac{v_0}{U}, \qquad \text{(VI.3)}$$

where v_0 is initial speed of photoelectron,

U is difference of potential between anode and photocathode,

d is distance between electrodes,

Γ_0 is electron-optical magnification of converter.

5. With multi-electrode construction of a converter, between the photocathode and the basic focusing electrode is placed a number of intermediate electrodes, to which from the potentiometer moves voltage. Such construction allows a change of relative distribution of potentials between electrodes and to carry out thereby electron focusing of image on converter screen.

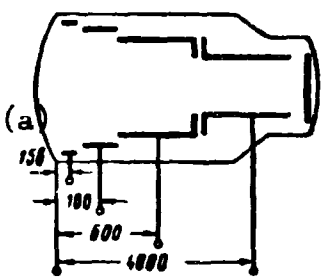

Fig. VI.3. Diagram of a 1-P-25 converter.
KEY: (a) Volt.

A typical representative of such converters is the 1-P-25 converter, developed during the Second World War in the United States (Fig. VI.3).

6. For multi-electrode converters in the presence of an aperture diaphragm (Fig. VI.4) there is the possibility of changing magnifying power. For that, to the diaphragm should pass variable potential U_3, changing from U_1 to U_2. Total magnifying power of such a converter (at $U_3 = 0$) is equal to $l_2:2l_1$. However, if one were to pass potential $U_3 = U_2$ to the diaphragm, then magnification will be less, and at $U_3 = U_1$ it will be more than the shown ratio.

7. Transition to multi-electrode converters also improved the quality of the image due to weakening of distortion with application of a spherical photocathode. Radius of the sphere is chosen in such a manner that its center is in the region of the plane of division of the basic focusing electrodes. The effect of using a spherical photocathode is shown in Fig. VI.5.

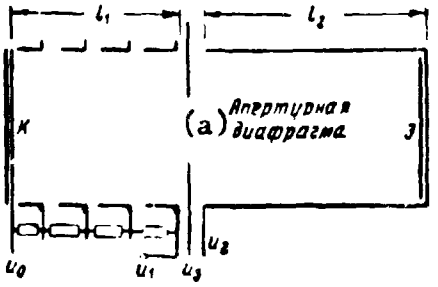

Fig. VI.4. Diagram of a converter allowing change of electron-optical magnification.
KEY: (a) Aperture diaphragm.

The considered advantages of multi-electrode image converters led to the fact that toward the end of the Second World War converters with plane-parallel electrostatic field were completely replaced.

Of the multi-electrode converters in foreign countries the most widely used were converters of the firm AEG (Germany), the 1-P-25 (United States) and the firm Muellard (England).

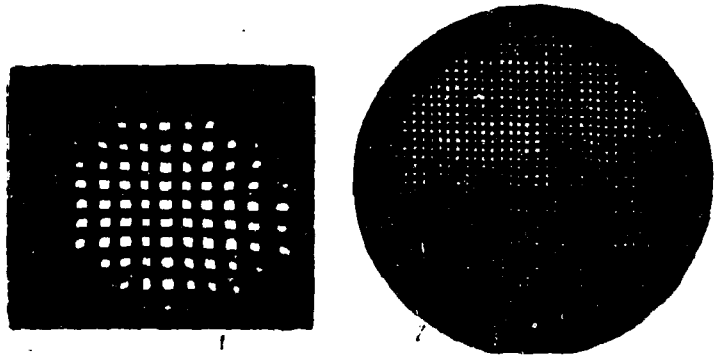

Fig. VI.5. Quality of image during application of flat 1 and convex 2 photocathodes.

AEG released its converters during the Second World War in two versions - with screen diameters of 50 and 30 mm (Fig. VI.6). The electron lens of the converter is formed by a cylindrical glass with a hole in the bottom, to which moves a 5 kv potential relative to the photocathode, and a frustum of a cone electrically united with the screen to which moves an 18 kv potential. Converter is 160 mm long and 80 mm in diameter. The photocathode is cesium oxide with a "red" boundary of

sensitivity $\lambda_0 = 1.3\ \mu$.

In the converter is applied aluminization of the internal surface of the screen from zinc sulfide-selenide. Covering of the screen by a thin dense film of aluminum allows us to increase screen efficiency and to weaken gating of photocathode, which allows improvement of image contrast and also increased clearness of image.

Fig. VI.6. A converter of the firm AEG (Germany).

Increase in overall efficiency of the screen occurs in this case due to reflection of luminous flux of the screen in the direction of the observer from the internal surface of aluminum film, as from a mirror. This leads to significant weakening of luminous flux of screen in the direction of the photocathode.

Increase of image clearness is attained due to the good electrical conductivity of aluminum film, ensuring fast runoff of the space charge eroding electron image near screen.

The converter of the firm AEG, when using candle-power optics, allows amplification of image brightness, having the following basic characteristics:

sensitivity of photocathode is 30-25 microampere/flux;

electron-optical magnification is 0.65;

resolving power in center of field of sight, attributed to screen, is 40 lines/mm.

Converter 1-P-25, 110 mm long and 40 mm in diameter (Fig. VI.7) uses multielectrode electron lens, on whose electrodes is given voltage of 15, 100, 600, and 4000 v.

The photocathode is cesium oxide with "red" boundary of sensitivity $\lambda_0 = 1.3\ \mu$; the screen is willemite, whose spectral composition of radiation well agrees with spectral sensitivity of the eye. The conversion factor of image brightness lies

within 0.5-0.4, i.e., the converter cannot be applied as amplifier of brightness with comparatively high basic parameters.

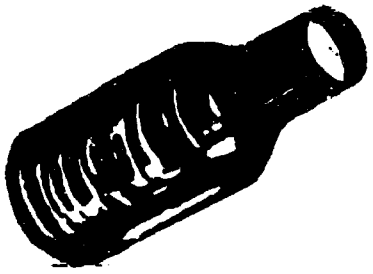

Fig. VI.7. Converter 1-P-25 (The United States).

Basic Parameters of American Converters

Designation of Parameter	Unit of Measurement	Value	
		1-P-25	6914
Length	mm	115	68
Diameter	"	42	43
Operating Voltage	v	4000	16000
Intermediate Focusing Voltage	"	3	None
Magnification	X	0.5	0.8
Average field-of-sight resolving power	lines/mm	8	28
Conversion Factor		0.4	30
Sensitivity of Photocathode	mka/lu	20-30	30-40

In 1959 in the United States there began to be released a converter of the type 6914 [13], whose basic parameters, as compared to parameters of converter 1-P-25, are given in the table. As can be seen from the comparison, the given converter allows, essentially, the increase of image brightness due to the high conversion factor.

Muellard released a series of image converters of the brand ME (Fig. VI.8).

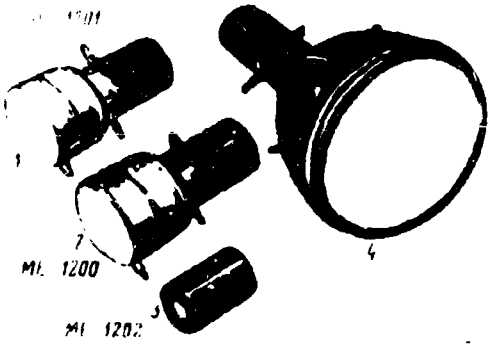

Fig. VI.8. Converters of the Muellard firm (England).

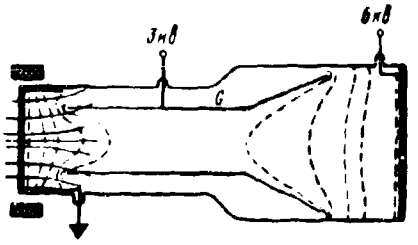

Fig. VI.9. Diagram of an ME-1201.

A characteristic peculiarity of these three-electrode converters is their ability to use either electrostatic or combined focusing of electron beams, and also to work with constantly applied accelerating voltage and in pulse conditions.

A diagram of an ME-1201 converter is shown in Fig. VI.9. The converter has a cesium oxide photocathode and a screen of zinc sulfide covered with aluminum semitransparent film. Dimensions of the converter: length 235 mm, diameter of photocathode 30 mm, diameter of screen 115 mm.

In the converter is carried out variable electron-optical magnification from 1 to 4 at uniform resolving power on a 20 line/mm screen. (at $\Gamma_э = 1$) by the application of combined focusing of electron beams.

2. Basic Characteristics of Electron-Optical Converters

Image converters are applied mainly in instruments of visual or photographic observation of objects. Effectiveness of their application in each concrete case may be estimated with the help of the following basic characteristics.

1. Spectral sensitivity of photocathode $S(\lambda)$ determines region of spectrum, in which observation is produced. At present in image converters cesium antimonide or multi-alkali (for observation in ultraviolet and visible regions of spectrum) and cesium oxide (for observation in visible and infrared regions of spectrum) photocathodes are used.

2. Integral sensitivity of photocathodes S determines general sensitivity of instrument of observation. It is characterized by the ratio of photocurrent in a converter to the radiant flux getting on the photocathode (microampere/lm).

3. Brightness of image is $B_э$. If it is considered that the glow of the screen will obey the law of Lambert, then the brightness of converter screen may be determined from relationship

$$B_э = \varkappa S_к \mathcal{E}_к U \Gamma_э^{-2} \cdot 10^{-6}, \qquad \text{(VI.4)}$$

where $\varkappa$ is luminous efficiency of screen in external hemisphere, which is a function of the energy of exciting electrons, cp/w;

$\mathcal{E}_к$ is irradiance of photocathode, w/cm^2;

U is accelerating voltage, v;

$\Gamma_э$ is electron-optical magnification.

Consequently, other things being equal, image brightness on screen is proportional to luminous efficiency of cathodeluminophor and accelerating voltage applied to converter.

4. Spectral distribution of image brightness b_λ characterizes the degree of coordination of radiation of screen with spectral sensitivity of receiver perceiving the image (eye, photographic emulsion). Knowledge of this parameter of the converter is necessary, since it can render a strong influence on effectiveness of application of the instrument on the whole. It can appear that with achievement of even great brightness of radiation of screen, but sharply differing from spectral sensitivity of receiver, efficiency of the instrument on the whole will be very low.

5. Conversion factor η is the ratio of the flux of energy of radiation of the converter screen to the external hemisphere to the flux of radiant energy falling on the photocathode:

$$\eta = \frac{\Phi_э}{\Phi_к} = \varkappa S_к U \cdot 10^{-6}. \qquad \text{(VI.5)}$$

As can be seen from expression (VI.5), at sufficiently large voltages luminous efficiency of screen and sensitivity of photocathode conversion factor can become

larger than unity. In this is one of the possibilities of amplification of brightness of image with the help of image converters.

6. Brightness of background of screen is B_Φ.

In the absence of irradiation of photocathode of converter, the screen of the latter has some brightness caused by the presence of dark current from the photocathode as a result of thermo-emission,

$$B_\Phi = \pi I_T U \cdot 10^{-4} \Gamma_e^{-2}, \qquad \text{(VI.6)}$$

where I_T is density of dark current of converter.

Density of dark current from a cesium oxide photocathode attains values of 10^{-12}-10^{-11} amp/cm^2, and from a cesium antimonide photocathode attains 10^{-15}-10^{-16} amp/cm^2.

Since on a background with brightness B_Φ is produced observation of image of an object with brightness B_o, then contrast of image is lowered and may be approximately determined from relationship $(B_o > B_\Phi)$

$$k = \frac{B_o - B_\Phi}{B_o}. \qquad \text{(VI.7)}$$

Therefore, for the purpose of decreasing brightness of background by lowering density of thermo-emission current, it is necessary, in a number of cases, to cool photocathode (especially cesium oxide).

7. Electron-optical magnification Γ_e promotes increase in sensitivity of converter (at $\Gamma_e < 1$). This is connected with the fact that increase of image brightness is proportional to decrease of its area. In spite of the fact that such a decreased image must be considered in an eyepiece with small focal length and great aperture, which causes additional losses of light, the advantage consists in that it manages to gather to the eye a larger part of the light radiated by the screen within limits of the rear hemisphere.

8. Resolving power N of the converter determines that minimum angle, at which two separate points are distinguished separately.

From formulas (VI.2) and (VI.3) it is clear that with correct selection of parameters of the converter the resolving power, due to elements of electron optics,

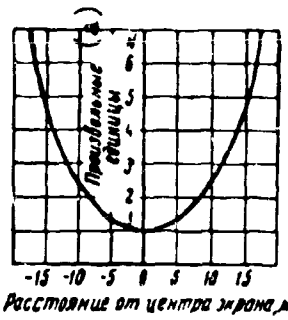

Fig. VI.10. Change of resolving power on screen of converter. KEY: (a) Arbitrary units; (b) Distance from center of screen, mm.

will be sufficiently high for axial beams of electrons. Practically, however, such resolving power all over the field of sight is not attained because of the scattering of radiant flux on the granular structure of the photocathode and luminophor, and also the off-axis aberrations. The latter causes sharp impairment of resolving power of converter in field of sight.

3. Amplification of Brightness of Image

In preceding divisions were considered photoemission image converters, intended, basically, for observation of objects in reflected infrared rays. Meanwhile, in a number of cases, image converters are used for observation of objects with small levels of illuminance, i.e., in conditions of natural night illuminance. In this case image converters are used as amplifiers of brightness.

With the help of purely optical instruments, in principle, it is possible to increase brightness of image, as compared to brightness of observed object.

In electron-optical instruments this is possible to do by electron amplification, i.e., supply of energy to converter from without.

It is possible to show [2] that the amplification factor of image brightness on the screen of the observation instrument, relative to brightness of the object, will be equal to

$$\frac{B_1}{\mathscr{B}} = \frac{\pi A^2}{4\Gamma_0^2} = \frac{\pi A^2 S U_k^2 \cdot 10^{-8}}{4\Gamma_0^2}, \qquad \text{(VI.8)}$$

where $A = \sqrt{\tau_{об}}\frac{D_{об}}{f_{об}}$ is physical candle-power of objective;

$\mathscr{B}$ is brightness of object;

B_1 is brightness of image of object on converter screen.

Consequently, amplification of image brightness may be attained by a decrease in scale of image ($\Gamma_0 < 1$), an increase of candle-power of objective A, integral

sensitivity of photocathode φ, accelerating voltage U, and luminous efficiency of the screen in the direction of observer ξ.

If luminous efficiency of screen is expressed in light engineering units (lu/w, cp/w), then in the case of using not the eye for registration of radiant flux from the screen, but some other kind of receiver, the brightness of screen may be calculated from relationship

$$B_1' = \beta B_1,$$

where

$$\beta = \frac{\int S_{np(\lambda)} B_1(\lambda)\, d\lambda}{\int V(\lambda)\, B_1(\lambda)\, d\lambda}; \qquad \text{(VI.9)}$$

$V(\lambda)$ is relative luminosity of eye;

$S_{np(\lambda)}$ is spectral sensitivity of receiver;

$B_1(\lambda)$ is spectral brightness of screen.

Mandel' [3, 4] calculates increase in brightness of image with the help of a image converter with a cesium antimonide photocathode and a screen from zinc sulfide, activated by silver. For the case of visual observation increase of image brightness attains magnitude 32, and with coordination of spectral composition of radiation of screen with sensitivity of panchromatic photomaterial it is 90.

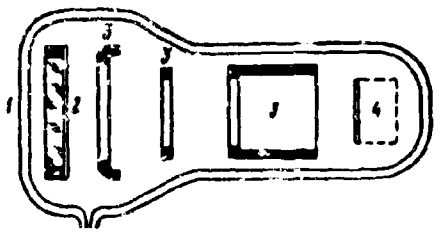

Fig. VI.11. Diagram of electron-optical instrument for photographing weak stars.

In technology unilocular converters have found practical application, for which amplification of brightness is attained by coordination of spectral characteristics of radiation and sensitivity of photocathode, and also by increase of screen brightness with increase of accelerating voltage [5].

For photographing weak stars, in France was developed an electron-optical attachment to a telescope, allowing photography by means of the direct influence of the electron image on photographic emulsion (Fig. VI.11).

The attachment consists of dismountable glass vessel 1, from which continuously air is pumped. Inside the bottle are placed photocathode 2, system of electrodes 3, and cassette with photographic plates 4. With the help of the objective of the telescope an image of weak stars is projected on the photocathode. Under the effect of accelerating voltage of 40,000 v photoelectrons are focused on the emulsion of the photographic plate, causing its blackening in places corresponding to the position of weak stars in the field of sight of the telescope. Amplification factor of density of blackening of emulsion during application of such an attachment is equal to 100.

From the shown example it is clear that to obtain comparatively small amplification factors of brightness in unilocular converters it is necessary to apply bulky arrangements and to apply series of measures with respect to coordination of radiation with the receiving part of the tube. Therefore, such converters could find application only in laboratory conditions.

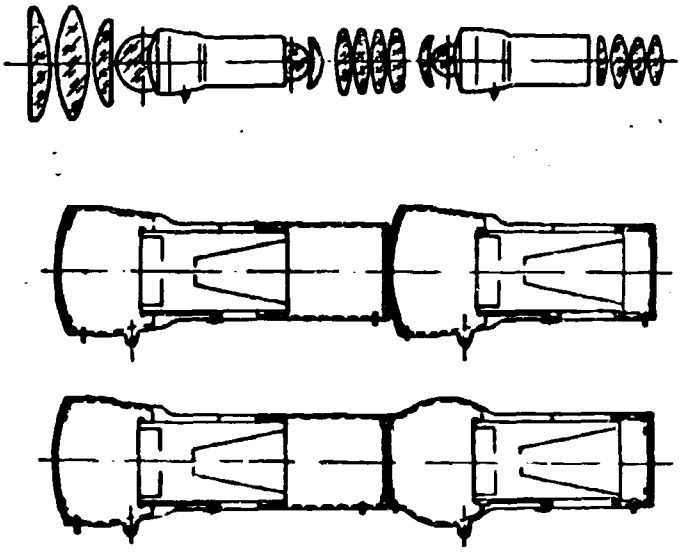

Fig. VI.12. Diagrams of construction of dual chamber converters with one amplifier stage of brightness.

Wider application of brightness amplifiers became possible after the development of methods of consecutive connection of two, three, and more image converters [6]. Diagrams of such a connection of two converters into one instrument, called a cascade converter, are shown in Fig. VI.12.

During consecutive connection of two image converters (one-stage electron-optical converter) by means of intermediate optics brightness amplification may be estimated by formula

$$\frac{B_2}{B} = \frac{A_1^2 \eta_k}{4} \frac{\sin^2 \frac{\theta_1}{2} \eta_k \tau_{1-2}}{r_{21}^2 r_{12}^2 r_{1-2}^2}, \qquad \text{(VI.10)}$$

where θ_1 is aperture angle on the part of the first screen.

In work [6] it is indicated that in the case of connection of two AEG image converters with the help of intermediate optics it is possible to obtain an amplification factor of brightness, equal to 115. During application of optical contact between screen of first converter with photocathode of second, the amplification factor of brightness attains values of 1460.

For the purpose of obtaining large amplification factors of image brightness in such two- and three-chamber converters (one and two stage electron-optical converters) the entrance photocathode and the output screen are made based on requirements presented by the source of radiation and recording instrument, but the intermediate photocathodes and screens are made from cesium antimonide and the luminophor of dark blue-azure glow, to which the cesium antimonide photocathode is most sensitive.

When using a cesium oxide entrance photocathode, there is observed a noticeable dark current due to thermo-emission. This dark current is strengthened in subsequent cascades and creates a bright background on the output screen.

Therefore, during application of cascade converters with a cesium oxide entrance photocathode, it is necessary to cool photocathode to temperature of the order of -40 to -50°C, in order to decrease dark current.

Cascade image converters are considered in literature as one of the possible ways of creating equipment for night vision during natural night illuminance of the earth's surface. At present they have found application as the preliminary amplifier stage of image brightness of night television intelligence instruments, considered in Chapter VIII.

4. Electron-Optical Converters with a Cathode from a Photoresistor

Image converters with a photoemission cathode allow the detection of objects by intrinsic emission if the temperature of their surface is higher than 250-300°C. For detection of objects having a temperature lower than 250°C, it is necessary to apply photoresistance. Therefore, naturally, research has been conducted for the purpose of examining the possibility of creating image converters with a photoresistor as a cathode. The principle of action of such a converters differs from the principle of action of photoemission converters.

Radiated by preheated cathode 1 (Fig. VI.13) a beam of electrons 2 drops on surface of photoresistor 3, to which moves small positive (with respect to cathode) potential. An electron beam creates current through photosensitive layer, causing lowering of potential on its surface and reflection, due to this, of part of the electrons 5 in the direction of luminescent screen 6. If one now projects on photoresistor the image of object 4 observed in infrared rays, then transverse resistance of separate points of the photosensitive layer will be changed in accordance with intensity of radiant flux falling on these points. Change of resistance will cause change of current through photoresistor and of potential at every point of its surface, which in turn will change also the quantity of electrons reflected from corresponding points in the direction of the screen. Since the quantity of reflected electrons from the photoresistor depends on the intensity of incident radiant flux, the intensity of radiation of screen will be proportional to radiant flux. Consequently, there appears the possibility of constructing an image of the observed object with the help of a photoresistor if one were to focus on the screen the reflected electron beam.

Photoresistors for such converters, besides high integral sensitivity, are required to have very high specific resistance in a transverse direction (of the order of 10^9 ohm·cm), necessary for obtaining sufficient potential difference between irradiated and unirradiated points and also for preventing "spreading" of charge along reflecting surface [7].

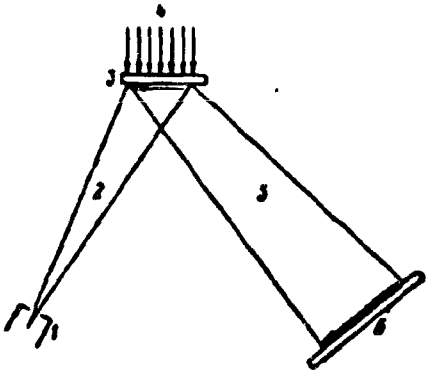

Fig. VI.13. Principle of action of an image converter with a photoresistor.

Separation of incident and reflected electron beams can be produced both with help of magnetic and electrostatic fields [8, 9].

A converter with magnetic separation of incident and reflected beams of electrons (Fig. VI.14) consists of a cylindrical bottle with four branches located in one plane. In branch I is placed electron gun 5. In branch II with plane-parallel window 3, transparent in the infrared region of the spectrum, are placed photoresistor 4 and two cylindrical electrodes 9 creating retarding field for incident electrons 7 and accelerating field for reflected electrons 8. In branch III is placed luminescent screen 6, from which object is observed.

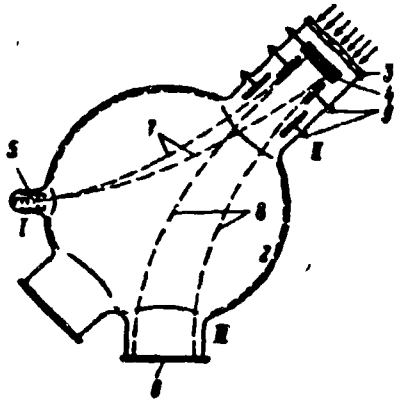

Fig. VI.14. Converter with magnetic separation of electron beams.

Internal surface of bottle is covered by Aquadag 2 (water solution of graphite) and is under potential 4 kv. On the bottle is put a solenoid, creating a uniform magnetic field, perpendicular to the plane of motion of electrons. An electron ray by expanded beam emerges from the electron gun, gets in the magnetic field inside the bottle and deviates it in the direction of the photocathode. Here electrons are retarded in a field of cylindrical anodes and are reflected from the photoresistor. On the reverse path of electrons cylindrical anodes execute the role of the accelerating system, and the magnetic field deflects electrons in another direction in the direction of the screen (the sign of vector of velocity of electrons changes).

Converters with an electrostatic field for separations of incident and reflected beams of electrons were developed in Germany (Fig. VI.15a) and in the United States by RCA (Fig. VI.15b).

The converter (Fig. VI.15a) consists of photocathode 1, made from bismuth selenate, luminescent screen 2, reflective mirror 3, electron gun 4, system of electrodes 5, and ocular system 6. Narrow beam of electrons 7 passes through hole in reflective mirror and luminescent screen. Getting in the system of electrodes, the electron beam is expanded, and electrons delay their speed. Reflected from the photocathode, electrons 8 are accelerated by this system of electrodes and are focused on the screen. Getting on the screen, the electron beam causes its glow, observed in the ocular system by means of a reflective mirror. The photocathode applied in the converter had a sensitivity to 2 μ with maximum of spectral sensitivity near 1 μ . Specific resistance of photosensitive layer (10^6 ohm·cm) turned out to be very low, which did not make it possible to obtain an image of good quality. Therefore, the converter did not emerge from the stage of laboratory research.

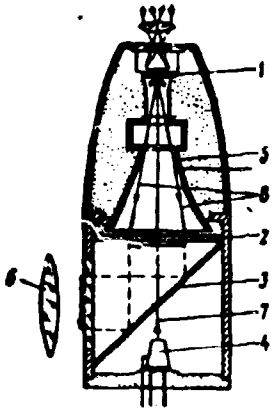

Fig. VI.15a. Converter with electrostatic separation of electron beams (Germany).

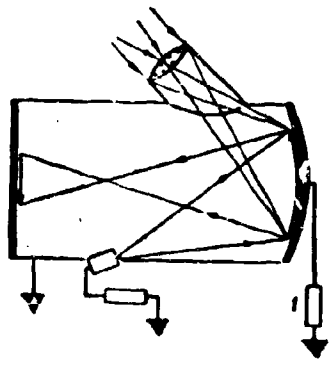

Fig. VI.15b. RCA converter with electrostatic separation of electron beams (The United States).

The RCA converter (Fig. VI.15b), in principle, consists of the same elements as the German, although it is constructed differently. An electrostatic field is created with the help of bias battery 1 creating potential difference between photocathode and screen of the order of 5–6 kv.

In spite of the imperfection of the above considered converters with photoresistors, certain models possessed sensitivity of 0.1 lux, i.e., make it possible to distinguish on the image a difference in illuminance of separate sections of an object of 0.1 lux for radiation in the visible part of the spectrum with true temperature of 2700°K. The converters allowed observations of objects whose surface temperature was lower than 200°C. Resolving power of the converters in the best samples did not exceed 20 lines/mm.

5. Power Supply of Electron-Optical Converters

Contemporary image converters are fed from special high-voltage power units. Depending upon assignment of electron-optical instrument, its place of installation, and operating conditions, high-voltage units can be both self-contained and connected to an external network of electrical current.

Independent of type, power units must be economical, light-weight, and small. Their power should be sufficient for normal operation of an image converter in the whole range of operational illuminance of the photocathode, with little dependence of output voltage on oscillations of primary voltage.

In connection with the small consumption of current in image converters, the power developed by a power unit may be very insignificant. Thus, if one were to consider only the operating photocurrent through a converter of the order of microamperes, then with voltage of 18 kv consumed power will constitute 0.1-0.2 w. However, because of power consumption by the voltage divider and absorbing resistors, because of losses on leakage in the glass and in cable joints, the power of the power unit must be increased to 0.5-1 w.

Thanks to small consumption of current in the converter, the voltage developed by a high-voltage unit is determined by its peak values, obtained during conversion, which significantly simplifies diagram of the unit.

At present, circuits on alternating current and circuits on direct current, both

self-contained and supplied from a network, are in use.

If, as a primary source of current, alternating current is used, the diagram of the high-voltage power unit is the simplest, since no vibrapack is in it. Such circuits are executed either on the principle of double transformation of current (Fig. VI.16a) or on a voltage-multiplying circuit (Fig. VI.16b).

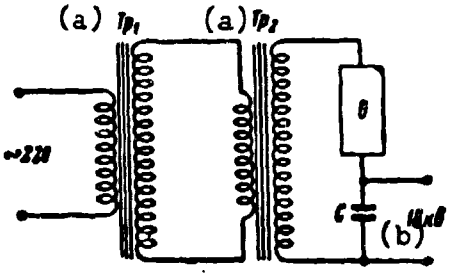

Fig. VI.16a) Alternating current unit with double transformation of voltage.
KEY: (a) Transformer; (b) kv.

With double-transformation of alternating current (Fig. VI.16a) to the entrance of primary transformer moves alternating voltage of commercial or heightened frequency. To the output winding of the secondary transformer is connected a rectifier and capacitor, from the plates of which move 18 kv of direct current. The power consumed by the power unit from the primary network, constitutes 15-30 va. The deficiency of such a circuit are the large leakages of current both in the actual transformer and in the rectifying device. With the aim of decreasing them, all the circuit must be placed in oil or potted.

The circuit of a high-voltage unit on alternating current with subsequent doubling of voltage profitably differs from the preceding both in dimensions and weight and in consumed power from the circuit of the primary source of current.

For instance, in one of the designs of a high-voltage unit the circuit consists of high-voltage step-up transformer (Fig. VI.16b) with primary winding n_1 = 300 turns, to input of which moves, through regulating resistance R_1, voltage 115 v, 400 cps. Secondary winding has n_2 = 19,000 turns, which ensures the obtaining, on output of the winding, of a 7-10 kv voltage. In parallel, the secondary winding is connected to the circuit of doubling and rectifying of voltage accumulated on directly heated kenotrons CBK-1 ($Л_1$ and $Л_2$) and high-voltage capacitors (C_1 and C_2). In distinction from filament-supply kenotrones, in directly heated ones the cathode is

activated by cesium, which ensures a small work function, but the anode has a large work function. This ensures passage of current in one direction (cathode - anode) when supplying it by alternating current.

In the first half-period, when the anode of kenotron $Л_1$ turns out to be under positive voltage with respect to cathode, the voltage of the transformer charges, through $Л_1$, capacitor C_1. In the second half-period $Л_1$ cuts off, and the voltage on the winding of the transformer is added with the voltage on C_1, becoming almost equal to the doubled peak value. In this half-period kenotron $Л_2$ is triggered, charging capacitor C_2 to double peak value of the voltage on the winding of the transformer. From capacitor C_2 voltage through resistor R_3 moves to image converter. Resistor R_3 limits the current removed from the unit to 15-20 microampere.

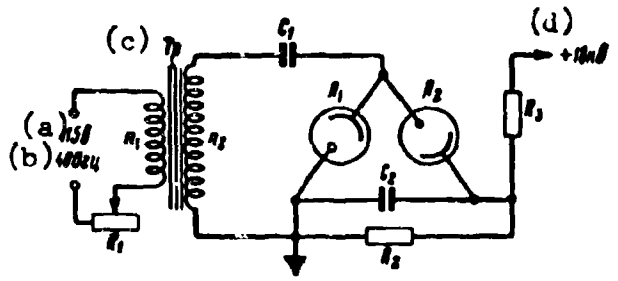

Fig. VI.16b. Alternating current unit with doubling of voltage. KEY: (a) v; (b) cps; (c) Transformer; (d) kv.

Resistor R_2, connected in parallel to C_2, promotes fast discharge of capacitor C_2 after the turning off of the supply unit.

A high-voltage power unit arranged on such a diagram, consuming from the power network no more than 10 va, develops a voltage within 15-20 kv with a 1 microampere load current.

Self-contained units of direct current, in distinction from alternating current units, use basically low capacity sources of primary voltage (dry batteries and storage batteries of small capacity) and require application of special conversion of direct current into alternating for subsequent transformation and rectifying. Therefore, questions of the economical use of the energy of the primary source here have a decisive value.

The most economic is a power unit on direct current with application of vibrapack and doubling of voltage (VI.17).

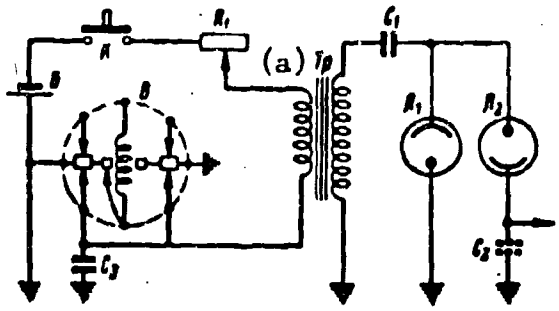

Fig. VI.17. Self-contained power unit with vibrapack.
KEY: (a) Transformer

Efficiency of vibrapacks does not exceed 50-70%. If, however, we consider additional losses in the transformer and in the rectifier, then on the whole the efficiency even of comparatively economical units will be no higher than 50%.

In this connection converters of voltage without vibrators, developed on the basis of semiconductor triodes, present definite interest. Distinctive peculiarities of such converters are their high efficiency and small dimensions.

The principle of work of semiconductor converters of voltage can be comprehended by the circuit in Fig. VI.18.

Triode $ПП_1$ is connected to the primary winding of the transf mer on a circuit with the grounded emitter. It plays the role of a key, turning on and turning off the voltage of the battery to the path of the primary winding of the transformer, which moves through the collector - emitter circuit of the triode. Since resistance of the collector - emitter circuit is insignificant, practically all the voltage $E_б$ moves to winding of transformer I. Current in winding I starts to grow, inducing in windings II and III alternating voltage, proportional to the speed of change of current in winding I. As current speed grows its change decreases, which leads to a decrease of voltage in windings II and III. Decrease of voltage U_3 causes decrease of current of base of triode, which in turn decreases current of collector, etc. As a result cutoff of triode $ПП_1$ will occur. While triode is closed, voltages $U_к$ and U_3 drop to zero and change their sign, causing thereby the appearance of base currer and collector current. There occurs cutoff of triode and again the whole work cycle of the converter is repeated.

The efficiency of semiconductor converters reaches 80-90%.

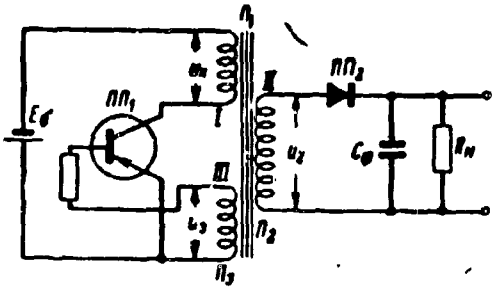

Fig. VI.18. Supply unit on semiconductors.

The above considered circuit of high-voltage supply units include, as an obligatory element, a primary source of current, which makes them often bulky or requires an outside source of current.

Recently, more and more frequently, there have appeared reports about the development of high-voltage atomic batteries to supply certain circuits of electronic equipment and, in particular, image converters [10, 11, 12].

For the creation of such sources of electrical energy it is possible to use both radiation of charged particles and uncharged (γ-radiation and neutrons).

Basic sources of charged particles, having obtained industrial application, are strontium-90, yttrium-90, mixtures of them, and also tritium and promethium-147. For obtaining uncharged particles we can use, mainly, cobalt-60, whose quantum energy of γ-radiation is equal to 1.33 Mev and half-life is 5.3 years.

Transformation of radiation into electrical energy is possible to carry out by the self-charged capacitor method.

A self-charged capacitor consists of a central electrode with a radioactive isotope, possessing β-radiation (emitter), and an external one gathering departing electrons (collector).

With a sufficiently large time of accumulation of electrical charge such batteries make it possible to obtain very high voltage. Thus, by available data [10], an emission battery with sufficiently great load capacity allows us to obtain a voltage of 360,000 v during power of 0.2 milliwatt.

Batteries of the "self-charged capacitor" type with β-radioactive isotopes possesses rigidity of construction, absence of corrosion of parts, small weight, high operational reliability, stability against short circuits, linearity of

charging characteristic, and a very long period of service (25 years). Furthermore, they will be able to sustain extreme high pressures of temperature and acceleration.

Literature

1. "Technology of television", 1955, No. 10 (16).
2. Z. angew. Math. und Phys., 1958, 25 Sep., Bd. IXa, No. 3.
3. Sci. News, 1956, No. 40.
4. J. Scient. Instruments, 1955, Oct., Vol. 32, No. 10.
5. Radio Electronics, 1955, May, No. 5.
6. Annalen der Physik, 1954, Vol. 14, No. 1-2.
7. "Advances of electrovacuum technology". Collection of articles. State Power Engineering Publishing House, 1956.
8. Z. angew. Phys., 1948. Bd. 1, No. 2.
9. Elektron in Wissenschaft und Technik, 1949, Apr., H. 4, S. 141.
10. Engineering, 1955, 180, No. 4678.
11. Electronics and Communications, 1957, Vol. 5, No. 2.
12. Electronics Industr. and Tele-Tech, 1957, Vol. 16, No. 7.
13. Proc. IRE, 1959, 47, No. 9.

P A R T II

APPLICATION OF INSTRUMENTS OF INFRARED TECHNOLOGY IN MILITARY MATTERS

C H A P T E R VII

SUPPORT OF COMBAT ACTIONS

1. Driving Transport and Firing at Night with the Help of Instruments of Infrared Technology.

In modern combat, night operations have acquired a considerable role and value. It is natural that to guarantee concealment of night actions, corresponding technical means are considered. One such means is infrared technology, which, in the opinion of many foreign military specialists, will ensure concealment and surprise action for their troops. Thus, F. O. Mikshe in the book "Atomic Weapons and the Army" indicates an ever increasing value of infrared technology methods in conducting night operations. Already at present with the help of instruments of infrared technology the following problems are solved. Driving transport at night and combat technology, night firing of small arms, detection of military objects on the field of battle by their thermal radiation (tanks, cannon, ships, and so forth), signalling and communication between separate subdivisions and objects, designating moving columns, monitoring movement, and observing actions of enemy [1].

Infrared instruments for driving machines at night (Fig. VII.1) consist of an electron-optical observation instrument, a searchlight (irradiator) covered by an infrared filter, and a power unit for the observation instrument.

In construction instruments of observation are subdivided into direct-flow (monocular or binocular type) and periscopic (Fig. VII.2). Instruments of observation are established firmly on machines or are braced on helmet of driver.

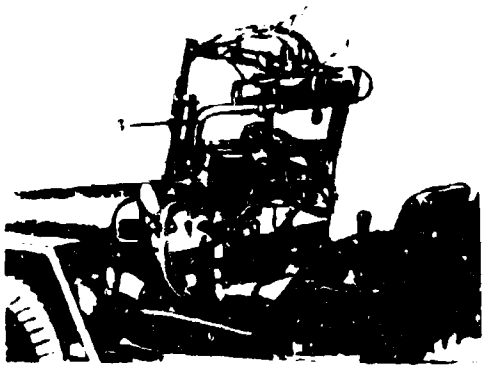

Fig. VII.1a. Swedish instrument of night driving on an automobile of the "Jeep" type: 1—electron-optical instrument of observation; 2—power supply; 3—bracket for bracing instrument.

Fig. VII.1b. American instrument of driving.

Infrared headlights, irradiating the site ahead of machines,can be self-contained and arranged in parallel with the usual illuminating headlights, as this is done on the American medium tank M-48 (Fig. VII.3),or, when indispensable, before the diffuser of the illuminating headlights infrared filters are established. As a rule, for the purpose of limiting propagation of radiant flux of headlights into upper hemisphere and in other cases special limiting visors and diaphragms are applied.

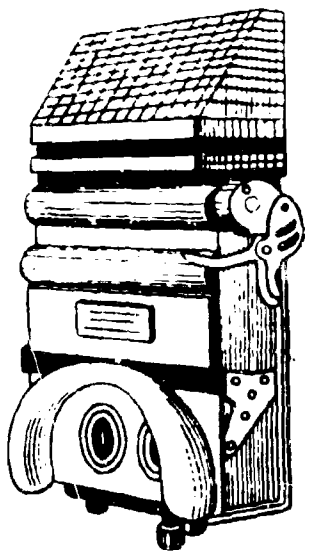

Fig. VII.2. Tank periscopic instrument M-41.

For improvement of conditions of camouflage when driving columns of machines, in the foreign press it is recommended to equip instruments with a head, one or two intermediate, and a locking machine. In this case, to guarantee safety of motion it is recommended to establish on the machines special light-signs, observable by the driver of the machine behind, and also at necessary places on the roads to establish special infrared signal lights and indicators.

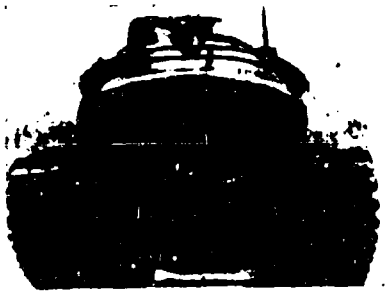

Fig. VII.3. Location of infrared headlights on an M-48 tank.

Since visual range and angle of visibility of site in an instrument of observation are limited, then, naturally, limited also is the speed of the machines. By report of the American press, speed of armored carriers at night should be no less than 10 km/hr [2], however, one of the recent instruments for driving machines, the T-6A, which passed its test in 1958 and was taken into use by the Army of the United States, ensures, supposedly, a speed at night equal to the speed by day on dirt roads.

Character of the image of site, observed by day 1 and at night 2 in an electron-optical instrument, is shown in Fig. VII.4.

Along with instruments for driving machines at night, in the ground troops of a number of countries infrared electron-optical sights for carbines, rifles, machine guns, and cannons have found application.

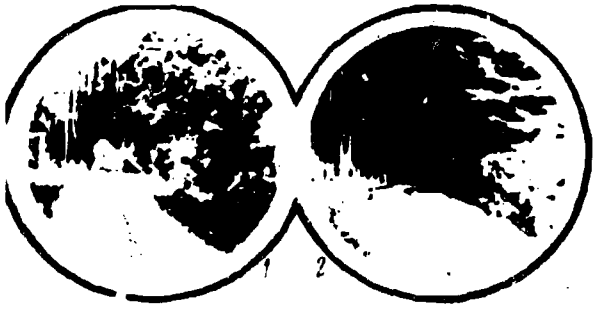

Fig. VII.4. Section of a road observed in an instrument for driving machines, by day 1 and at at night 2.

Such a sight is the M-2 sight (United States) for a carbine. This sight consists of an infrared searchlight with a 25 w tube, an electron-optical instrument of observation with a 1-P-25 converter and a power unit transportable by a soldier in a shoulder bag. Distance of aiming is 100 m.

In 1954 in the United States, taken into service was an infrared sight, the "Supersniperscope", for the "Garand M-1" rifle [3] (Fig. VII.5), consisting of the same main centers (searchlight and electron-optical instrument) as the M-2, but possessing aiming distance of 250-270 m. Increase of aiming distance was attained

thanks to application of a more highly sensitive converter with accelerating voltage of 20,000 v and a 30 w searchlight. Weight of the sight outfit without storage battery is 12 kilograms.

In distinction from the M-2 searchlight (1), the sight of the "Supersniperscope" is located above the rifle, and not under the carbine, and has a common bracket with the instrument of observation (2). The latter circumstance allows fast change of day version of rifle into night version, and back again.

In foreign literature the following tactical application of rifles with infrared sights is recommended: soldiers having such rifles act in pairs - one produces bias lighting of site, and the other, being at some distance from the first, during this time conducts fire on target.

Fig. VII.5. "Supersniperscope" on the "Garand M-1" rifle.

Infrared sights for machine guns (Fig. VII.6) and cannons are analogous in construction to rifle sights, however, they have longer aiming distance due to the application of more powerful searchlights and sources of supply. Thus, the sight for the hand machine gun "Chatelraux" (France), weighing 8 kg (without power source), allows aiming from distances up to 400 m. In it the searchlight and high-voltage power unit are assembled on the receiver near the instrument of observation. The storage battery for power supply of searchlight and instrument of observation has comparatively great weight and is transported by one of the soldiers of the machine gun crew.

To apply machine guns with infrared sights, just as with rifles, it is considered expedient to use pairs, placing them on flanks of subdivisions. Sometimes to the sight outfit is given a powerful outlying searchlight. With the aim of camouflage it is recommended to carry the searchlight aside from the shooting machine gun.

It is possible to judge the effectiveness of application of infrared sights for small arms by the operation to capture the island of Okinawa. In this operation the Japanese army lost 30% of its men, killed only because US marines used carbines with the M-2 night sight.

In the American M-60 tank are used the following instruments: a searchlight giving infrared and visible light, two-channel optical and electron-optical periscopic sights, a monocular range finder and a closed television system. These instruments allow a tank to fight at any time of the twenty-four hours.

Fig. VII.6a. French light-weight machine gun "Chatelraux" with infrared sight.

Fig. VII.6b. Heavy machine-gun with infrared sight.

For "illumination" of the field of battle, on the tank is fixed a combined searchlight developed by "General Electric", replacing the earlier applied 18-inch searchlight. The searchlight has a xenon incandescent lamp and is fixed on the armored cover above the gun. For inclusion of infrared irradiation between tube and reflector a small infrared filter is introduced.

The tank commander and the gunner have two-channel periscopic sights which allow them to conduct observation in infrared and visible beams. They observe in the optical channel with 8 X magnification with the left eye, but in the electron-optical channel with the same magnification - with the right.

A monocular range finder, working on the principle of range finders of small-size cameras (a combination of two images of the target), allows them, without special difficulties, to determine distance in a range of 500-4400 m.

Application in the tank of closed television equipment increases the capability

of armored troops when carrying out combat actions at night. The equipment consists of a transmitting television chamber, two receivers, and auxiliary units. A distinctive peculiarity of the equipment is the fact that it can work in two conditions: in conditions of the usual television equipment and with the use of the principle of memorisation of signal. The first conditions are intended for work by day; the second - in conditions of natural night illuminance when the site is not examined even by optical instruments.

It is indicated that such a system essentially supplements the infrared sight and is absolutely passive.

The essential deficiency of the considered sights is the presence of the special infrared searchlight for bias lighting of the target. Its radiation is the revealing factor, and the enemy, armed by an infrared instrument, can not only reveal, but destroy the searchlight by rifle, machine gun, or cannon fire.

Therefore, in the period of the Second World War attempts were undertaken to create passive infrared sights, using for their work thermal radiation of targets.

One of the first sights was the antiaircraft electron-optical sight "Orel" (Germany), revealing a B-29 because of the thermal radiation of its motors from a distance of nearly 30 km.

Attempts were made to install electron-optical sights on aircraft for detection of and aiming at air targets. Thus, in 1942 in the English Air Force there appeared night fighters with electron-optical sights fixed firmly in the cabin of the aircraft. Initially they were designed for detection of their own aircraft, marked by infrared headlights. However, later the instrument was used as a collimator to facilitate aiming.

At the same time in Germany there was developed and fixed on certain fighters an electron-optical sight, the "Schpanner-IIA," with a motionless laying mark. This sight (Fig. VII.7) had candle-power optics with a large inlet ($A = 1 : 0.8$, $f = 90$ mm) and differed by its large dimensions. As a sensitive element in the sight was applied

a converter of the firm AEG. With a 30° field of sight, the sight allowed detection of a B-29 from distances of 8-10 km.

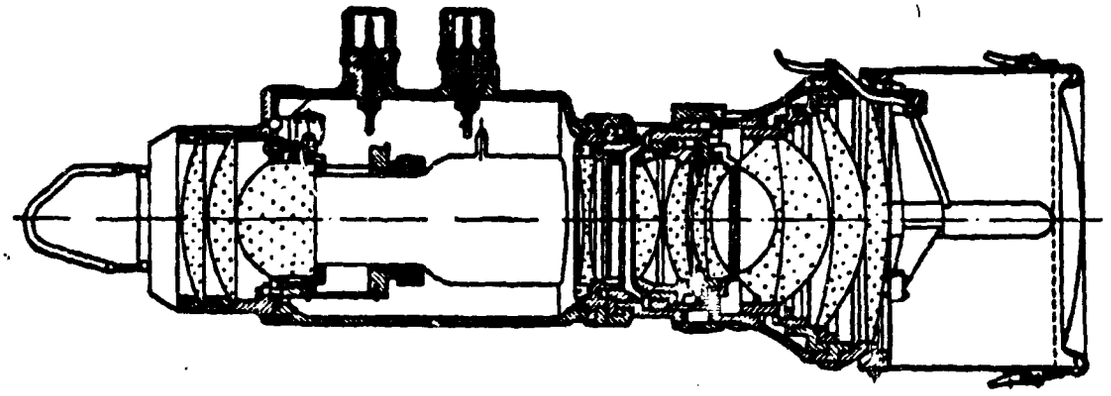

Fig. VII.7. German electron-optical sight, the "Schpanner-IIA.:

2. Infrared Range Finders

Infrared passive systems of detection and aiming do not allow measuring directly the distance to target. It is necessary to apply radiotechnical or optical means to determine distance to target.

Therefore, efforts of many specialists of infrared technology were directed to the creation of range finders, working in the infrared region of the spectrum. The creation of such range finders would allow them to make the operation of systems of detection and aiming more flexible and noiseproof, and also would significantly increase concealment of their work.

In principle of action, infrared range finders are identical with optical working in the visible region of the spectrum and can be divided into electrooptical, base, and axial.

Optical range finders, working in the visible region of the spectrum, have found wide use in artillery, in geodesic, and engineering works; infrared range finders, due to a number of specific requirements presented to them, until now have not been widespread. Nevertheless, the principle of construction of such range finders may be comprehended from analysis of existing systems.

Range finders belonging to the active type are based on measurement of time of propagation of radiant flux along a route, equal to a doubled magnitude of the measured distance.

If speed of propagation of radiant energy is known in a given medium (a.., $v=\frac{c}{n}$, then the measured distance may be obtained from simple relationship

$$D=v\frac{t}{2}+k. \qquad \text{(VII.1)}$$

where k is the correction constant of the range finder.

Characteristic for this form of range finders is the necessity of irradiating target with electromagnetic energy differing in some manner from radiation of the surrounding background. This requires presence of special modulation of radiant flux, i.e., change of characteristics of radiant flux in time. As a rule, such a change of characteristics is based on amplitude modulation, which may be carried out by different devices: a mechanical modulator, by pulse radiation, or by application of electrooptical Kerr effect or piezoelectric effect.

In the case of application of pulse tubes for radiation of radiant flux, electrooptical range finders, by analogy with radar technology, have obtained the name of "light locators."

Range finders of the base type pertain to passive systems, since their work is the registration of radiant flux radiated by the actual target.

Base range finders can be divided into internal and external base. In the first case the base, with receiving heads located on the edges, is on the object from which distance is measured, in the second case distance is measured with respect to a base (on whose edges there are sources of radiation energy) located on the object to which distance is measured. As can be seen, in the second case capabilities of a range finder are limited, since it is required beforehand to know dimensions of base.

However, in any case it is required to measure parallactic angle Δ (Fig. VII.8), included between two lines of sight of end-points of the base.

Distance to object in this case may be calculated from simple ratio

$$D = \frac{B}{\Delta} \mu, \qquad \text{(VII.2)}$$

where B is the base, m;

Δ is the parallactic angle, rdn.

Work of axial range finders is based on the fact that every point of space at distance L from objective of range finder corresponds fully to a fixed point in the picture plane at distance L', where its image will be the sharpest. Measuring distance L', one can determine also distance to observed object from ratio

$$\frac{L'}{f} = \frac{1}{\frac{L}{f} - 1}, \qquad \text{(VII.3)}$$

where f is focal length of objective.

Axial method of measurement of distance has not found propagation in military technology, since displacement of picture plane during measurement of large distances is insignificant and, consequently, accuracy of measurement of distances will be low. More or less acceptable accuracy with this method may be attained during measurement of distances smaller than (100-200)f.

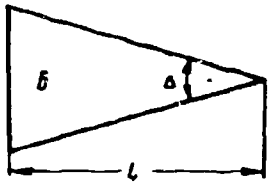

Fig. VII.8. Parallactic angle during base range finding.

Nevertheless, during the Second World War, in Germany there was developed an axial range finder for an electron-optical antiaircraft sight, the "Orel" (Igel). In this sight, focusing of target image (luminescent point from branch pipes of aircraft) was produced by shifting one of the lenses of the projecting objective. This allowed them to determine (approximately) the slant range to target, with respect to angle of sight - and the height of its flight, necessary for conducting sighted antiaircraft fire.

Let us consider more specifically the work of the most promising types of range finders - electrooptical and base.

[illegible] range finder, although it was applied for other purposes.

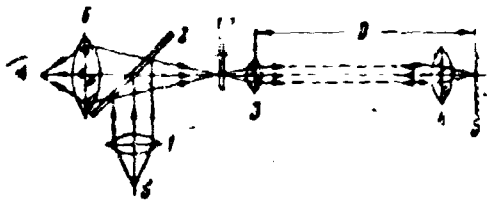

Fig. VII.9. Diagram of the experiment of Fizo.

Light from source S (Fig. VII.9) is designed with the help of objective 1 and semitransparent mirror 2 in plane of rotation of a toothed modulating disk 7 with quantity of teeth n and revolving with a speed of N rps. With the help of output lens 3 radiant flux from the source is directed by parallel beam to mirror surface 5, ahead of which focusing objective 4 has been located. The focusing objective was established at one focal length from the mirror, in connection with which radiant flux reflected from the mirror again was collected by objective and headed in the opposite direction by parallel beam and was observed through eyepiece 6. During certain turns of the toothed disk luminescent image of source of light in reflected beams disappears. At this instant the distance to mirror may be determined from relationship

$$D = \frac{c}{4Nn}, \qquad \text{(VII.4)}$$

where c is speed of light ($c \approx 3 \cdot 10^{10}$ cm/sec).

From the operating principle of Fizo's device, it follows that an electro-optical range finder (Fig. VII.9) should include the following basic units: a source of radiation energy, a modulating device, an optical system sending modulated radiant flux in the needed direction, a receiver of reflected radiant flux, a device for measurement of propagation time of signal, and a surface reflecting the optical signal in the opposite direction.

During development of an electrooptical range finder for any assignment two basic requirements are presented to it: guarantee of necessary range and needed measurement accuracy of this distance.

[illegible] range [illegible] electrooptical range finders in the first place, is caused by scattering and absorption of radiation energy in the atmosphere and on the reflecting surface of the target, whose size can vary in wide limits and cannot be considered beforehand when designing the range finder. Therefore, the source strength of the radiant energy must be taken with known supply. In this respect it is more profitable to use infrared beams, since they better pass through the atmosphere and have higher reflectivity from the majority of metallic surfaces. Furthermore, their application to a lesser degree uncovers the work of the range finder.

Guarantee of needed accuracy in measurement of distance to target may be carried out by selection of corresponding characteristic of radiant flux modulation and by the application of special devices for measuring very small time intervals (of the order of microseconds).

From the view point of forming an optical signal radiation energy may be characterized by frequency, phase of oscillations, and their magnitude (amplitude). Up to now amplitude modulation has had practical application in range finders for forming signal.

For the purpose of changing intensity of radiant flux in range finders there are applied/ mechanical modulators, pulse tubes, electrooptical Kerr effect, piezoelectric effect and the phenomena of diffraction and interference of radiant flux. All of them have found sufficiently wide application, especially in geodesic electrooptical range finders.

Accuracy of distance measurement, as this follows from modified expression (VII.4) $c = 4DNn$, is proportional to the frequency of modulation of radiant flux (Nn). Furthermore, in practice it is established that operational accuracy of a range finder is increased as the law of modulation approaches harmonic.

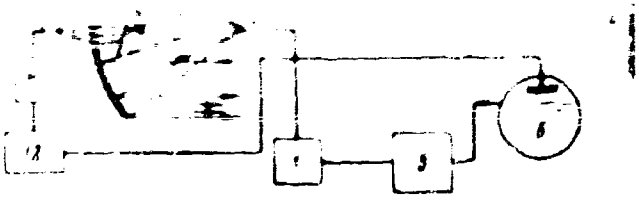

Fig. VII.10. Block-diagram of pulse electrooptical range finder.

[illegible] law of modulation with a very high frequency (up to $30 \cdot 10^6$ [illegible]).

In range finders for military assignment, where very high accuracy of distance measurement is not required, pulse modulation is applied. Application of pulse tubes has one important advantage, as compared to sources of constant radiation, and that is namely; with small average power consumed by tube from power source, the pulse energy may be very great.

We will consider the work of such a pulse electrooptical range finder, for example, an American range finder, developed in the United States in 1948. The range finder (Fig. VII.10) was designed for measurement of distances up to 4550 m. As a source of radiant flux, a pulse tube served, creating pulses of light 1 [illegible] in duration at a pulse recurrence frequency of 20 imp/sec.

Pulse tube 2, placed in the focus of parabolic mirror 3, is lit by source of supply 1. At flash of tube simultaneously sweep generator 5 is started, creating on electron-beam tube 6 a horizontal sweep trace.

Reflected from target 4, the ray with the help of parabolic reflector and flat mirror 7 heads through diaphragm 8 and objective 9 to photocathode of enlarger 10. After preliminary amplification 11 the appearing current pulse heads to the amplifier of vertical deflection of the ray of the electron-beam tube. As a result on the horizontal sweep trace will appear a vertical mark of reflected pulse of radiant flux.

Since the beginning of the sweep coincides with the moment of light pulsing, then the distance from the beginning of the sweep to the vertical pulse will be proportional to the time of passage of signal or doubled distance to target.

the beginning of sweep.

The considered diagram of a pulse range finder allowed measurement of distance with 1.82 m precision both at night and by day; however, in the latter case accuracy was worse.

Electrooptical range finders, in spite of the possibility of obtaining, with their help, high accuracy of distance measurement, due to their active principle of operation, reveal their own work as do radar range finders. The work of electro-optical range finders, to a significant degree, depends on the time of day and the state of the atmosphere. The low reflectivity of surfaces of the majority of military objects also requires application of very powerful sources of radiation for covering large distances.

In this respect more profitable are passive base range finders, if it is not necessary to obtain very high accuracy during measurement of distances.

In stations of fire control of greatest interest are internal base range finders, since their base enters in the structural dimensions and is always exactly known. Such range finders have to include: a receiving head with sensitivity in the range of wave lengths of the radiation of the target, a summing calculating unit, and a distance indicator. Receiving heads, located on the edges of the base, are the most responsible elements of the diagram, since their accuracy in determining angular coordinates gives, in the end, accuracy in determining distance to target,

$$\frac{dD}{D} = \frac{d\Delta}{\Delta}. \qquad \text{(VII.5)}$$

This is especially important, if one considers that the magnitudes of the parallactic angle, subjected to measurement, are minute (Table VII.1).

Base, m	Distance, km						
	1	2	3	5	7	10	15
1	206	103	68	42	21	14	10
2	412	206	137	82	41	27	20
4	824	412	275	164	82	55	41
10	2060	1030	687	412	206	135	103

Small values of measured parallactic angle, not exceeding several minutes in magnitude, lead to the fact that base range finders have to be extraordinarily exact goniometrical instruments, protected from external influences; shaking, shocks, changes of temperature. They also have to have a very high rigidity of base. Therefore, besides the named basic elements, base range finders have to include additionally a whole series of devices compensating for these external influences.

If the problem of compensating for errors due to external influences for stationary base range finders (ground and ship) is solved at the expense of complicating the design or increasing weight and dimensions, then for range finders of aircraft stations of fire control, where dimensions and weight play sometimes a decisive value, solution of it is very complicated. In literature there is no information about development of infrared range finders for aircraft interception stations. Inasmuch as the accuracy of work of optical range finders, in the first place, depends on the accuracy of measurement of minute parallactic angles, very useful for these targets can be receivers with lateral photoeffect, considered in Chapter V. High accuracy of measurement of angular target position data, reaching to hundredths of angular seconds, allows, with this method, measurement of small parallactic angles during the use of short bases. This significantly will increase rigidity of the system and, consequently, will lower the requirement for compensating diagrams, which, in turn, will simplify the range finder.

[illegible] therefore, range finders can be instruments of small accuracy.

An example of the application of such range devices is the simplest collimator gunsight with a range grid expressed in thousandth fractions of distance.

The gunner, by the silhouette of the target, determines its dimensions and by the quantity of scale divisions packed in the dimensions of the target, determines the distance to it by the formula

$$D = \frac{B}{n} 1000 \text{ м}. \qquad \text{(VII.6)}$$

Such a method is very simple in use and is graphic, but contains large errors due to the absence of exact data about the actual dimensions of the measured base and the inaccurate measurement of the angle, especially at large distances. Therefore, accuracy of measurement of distance to target constitutes a magnitude of the order of 15% and more.

A type of external-base range finder may be a device for determining distance between two of one's own objects, marked sources of infrared rays, delivered to a known distance.

The principle of work of such a range device is based on wedge-type compensation of shift of image, well-known in optics (Fig. VII.11).

If on an objective drops a parallel beam of light, then in its focal plane is obtained an image of the source (point A). If, however, now we place before the objective an optical wedge, then it will cause slope of beam to angle $\delta = (n-1)\alpha$, as a consequence of which the image of source will shift and will correspond to the position of point B in the focal plane. With this, distance is

$$AB = a = f\delta = f(n-1)\alpha. \qquad \text{(VII.7)}$$

where f is focal length of objective.

If the wedge is in the form of a thin truncated cylinder, then during its rotation around optical axis, displacement, having horizontal and vertical components,

opposite directions. In this case image of source point A, during rotation of wedges, will shift in the horizontal plane, where the magnitude of this displacement will be proportional to the angle of rotation of wedges (φ).

This property of the revolving wedge may be used for compensation of parallactic angle in an external-base range finder.

The principle of construction of such a range finder may be comprehended from Fig. VII.12.

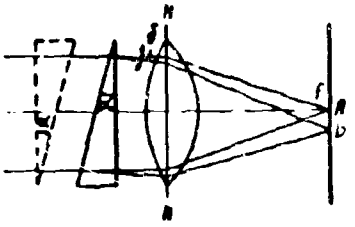

Fig. VII.11. Principle of action of wedge-type compensator.

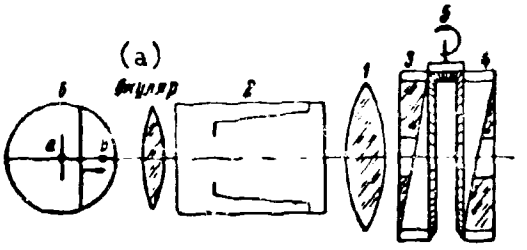

Fig. VII.12. Diagram of the arrangement of a wedge-type range finder. KEY: (a) Eyepiece.

From the external side of objective 1 of electron-optical instrument 2 there are established two identical wedges 3-4, connected by conical transmission 5. With the help of this transmission their rotation to opposite sides is carried out. The wedges have, in the center, a hole, through which radiant flux from one of the infrared sources limiting the external base proceeds to objective 1 and then to the photocathode of the image converter 2.

Image of source a on the screen of converter 6 is combined with the center of cross lines, which is the mark of the optical axis of the instrument. Image of another source b is projected on the photocathode by means of two wedges. If the wedges are located strictly in opposition, then they form a plane-parallel plate, and the distance between the two images exactly corresponds to the magnitude of the parallactic angle at which the external base is visible to the instrument.

photocathode of the converter by the objective through the holes in the wedges. This position on the screen of the converter may be marked by a vertical filament, with which there is produced a combination of image of the second source.

The angle of rotation of wedges φ and, consequently, of the handle, on which can be drawn divisions, is used for calibration of instrument with respect to distance,

$$D = \frac{\delta}{2\theta\,(\cos\varphi_0 - \cos\varphi)}, \qquad \text{(VII.8)}$$

where φ_0 is initial adjusting angle of wedges.

As can be seen, such a method of measuring distance is very simple and does not require special skills, however, in it also is inherent error from the possible change in dimension of base. Therefore, it may be used where high accuracy of distance measurement is not required.

3. Protective Interlocks

For the purpose of increasing reliability of protection of certain objects important in a military relation, interlock of passages and certain sections of the site, when visual observation for any reason is hampered, an automatic photoelectronic emergency signal (APhES) is used.

In its principle of action APhES equipment may be passive and active.

In the first case, the object, intersecting the interlock line, is revealed by special equipment at the moment it appears in the field of sight of the receiving device, either by thermal radiation of the object or by contrast between the object and the background. Such a form of interlock found application even during the years of the First World War. An example can be the blocking of the entrance to the Harbor of Ostende with the help of the simplest thermal direction finder, recording the entrance into the harbor of ships by the radiation of their stacks.

In the case of an active principle of operation, the guarded object is embraced along a perimeter by a continuous ring of infrared rays, the intersecting of which, in any place, causes an alarm signal. Such a system, consequently, should consist of sources of infrared rays, receiving devices with amplifiers of photocurrents, and a system of relay including the necessary indicator instrument.

Source of radiation usually is an electrical incandescent lamp placed in the focus of an optical system, forming a radiant flux with a very small angle of divergence. The lamp is covered by an infrared filter, but in order to exclude the effect of background radiation and to simplify amplification of photocurrent in the receiving device, radiant flux on the output of the radiator is modulated.

Emitter (VII.13) consists of a stand, a tube, and a modulator. For exact alignment of ray in the direction to the receiving device the stand has two pairs (stop and micrometric) of screws for coarse and exact aiming [13].

In the tube are placed the prism lens and the infrared filter. Focusing of radiant flux is carried out by displacement of lamp relative to prism-lens. The incandescent lamp, 12 v X 15 w, is supplied by lowered voltage 11 v for the purpose of increasing reliability in work. Modulation of radiant flux is carried out by a disk with 12 holes, revolving with a speed of 3000 rpm.

The receiving device (VII.14) constitutes a high-sensitivity photorelay, consisting of a photocell and a three-vacuum-tube amplifier of alternating current, tuned to a frequency of 600 cps with an amplification factor of the order of 10^6. Proceeding through inlet, the radiant flux is focused by lens on the photocell, exciting in it photocurrent. For the purpose of decreasing fatigue of photocell by daylight the entrance window is simultaneously an infrared filter.

Intensive current joins the coil of the output relay, which locks the contacts of the winding of the power supply of the intermediate relay on the shield of signal reception.

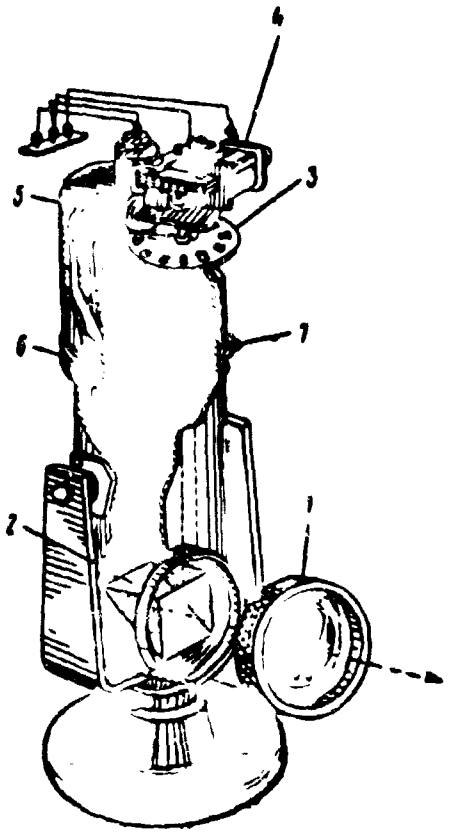

Fig. VII.13. APhES Emitter IKO-6:
1--light filter; 2--prism-lens; 3--disk of modulator; 4--electrical motor of modulator, 12 v, 3,000 rpm; 5--lamp, 12 v, 15 w; 6--moving ring of focusing; 7--stop screw of moving ring.

Upon intersection of the ray by an opaque object the photocurrent ceases, disconnecting the output relay, which, in turn, disconnects the intermediate relay. This causes appearance of the alarm signal and luminescence of a corresponding section on the lamp register. Characteristic for this design is the fact that the winding of the intermediate relay is always under current. Therefore, luminescence of the corresponding zone on the lamp register occurs both in the case of disturbance of zone and upon the appearance of a fault in any circuit of the design.

If it is necessary to determine direction of penetration of forbidden zone, then there are established two parallel lines of infrared rays. In this case the order of luminescence of light lines of the register testifies to the direction of penetration of zone.

When blocking penetrations or protecting military objects of great value is well considered and carried out camouflage of equipment. With this goal it is made small-size and very reliable in work, in order not to require checks and repair for a prolonged time.

An example of such equipment, intended for blocking penetrations through a boundary, strategic crossings, roads, bridges, mine barriers, airports and air bases, and storehouses of ammunition and materiel is the infrared barrier equipment, L -80, developed by the VVT firm (France) [4].

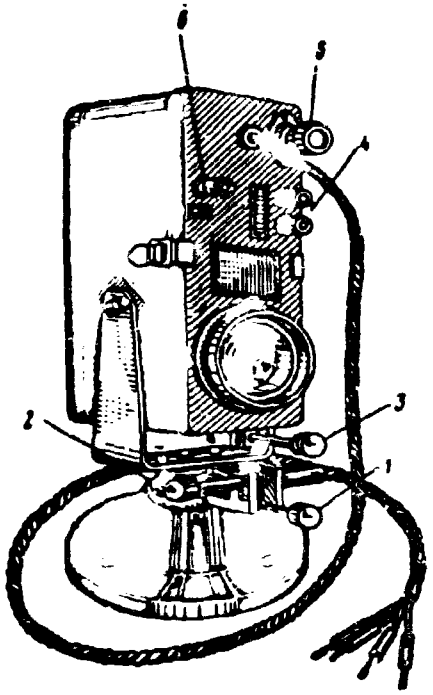

Fig. VII 14. APrES Receiver: 1—stop screw of horizontal aiming; 2—micrometric screw of horizontal aiming; 3—screw of elevation; 4—terminal of connection of control milliammeter; 5—safety device; 6—terminal of grounding.

The L-80 equipment consists of an emitter of infrared rays, modulated with a frequency of 50 cps, and a receiving head with amplifier and signal apparatus.

A source of radiation (lamp 2.5 v X X 0.3 amp), covered by an infrared filter, is disposed in focus of a lens 80 mm in diameter. Modulation of radiant flux is carried out by electrical method, by means of supplying to the lamp one half-period of alternating voltage with a frequency of 50 cps. Such a form of modulation of radiant flux ensures full noiselessness of work, which is necessary in order to guarantee concealment of the application of optical blocking.

Entrance window of the receiving device is a lens 80 mm in diameter, in the focus of which is disposed a photocell. Photocurrent moves to entrance of two-tube amplifier of alternating current, tuned to a frequency of 50 cps.

The range of the "emitter-receiver" system, with a reserve for guarantee of reliability of work in bad weather conditions, constitutes 500 m.

In a case of disturbance of guarded space the receiving device passes a command to the signal instrument, on which a red alarm light lights and a bell starts to ring. To stop the alarm signal and a repeated starting of the circuit, there is a special switch.

The supplying of power to the equipment is carried out through step-down transformers from a power network of 110, 125, 220, and 250 v. Total consumption of energy is 20 w.

4. Communication in Outer Space

In the conditions of the terrestrial atmosphere communications on infrared rays has limited application and significantly yields in range to radio communications. With increase in height the effectiveness of using optical means of communication continuously grows. Outside the terrestrial atmosphere infrared means of communication not only do not yield to radio, but have a practically unlimited range.

Successes, attained in the region of mastering outer space, again set the problem of communicating on infrared rays as a subject of theoretical and experimental research.

Interest toward such a form of communication is not accidental, since this communication has a series of advantages, as compared to radio communications.

1. The spectrum of infrared radiation is sufficient for distribution of many millions of communication channels.

2. Communication on infrared rays in outer space allows the use of solar radiation or heat given off inside the spaceship as a source of energy of carrier frequency.

3. The necessity for special transmitters drops, only modulators of radiation energy are required.

4. A sharp decrease in wave length of radiated energy allows the use of small-size optical systems with very high directivity of radiation (it is assumed possible to obtain rays with an angle of the order of 10^{-5} rad).

5. With increase in directivity of radiation, at a given diameter of optical systems the power of the transmitter decreases reciprocally to the square of the wave length.

Theoretical calculations show that for communication between Earth and Mars, with the application of coherent radiation of a quantum-mechanical generator of optical range and a sensitive element with an equivalent power of noises 10^{-17} w/cps

(w·sec) at a 1 m aperture of optics and a transmission speed of 10^6 binary elements per second, average power of 100 w is necessary.

However, during development of communication systems on infrared rays it is necessary to meet at present a series of problematic questions. The main ones are:

a) Creation of coherent optical generators and amplifiers and, in particular, quantum-mechanical;

b) Development of systems of exact tracking to guarantee strict mutual directivity of transmitting and receiving devices;

c) Development of the technology of manufacturing inexpensive optical systems with very rigid requirements with respect to allowances in their manufacture.

A complicated problem is also the direct test of models of equipment in outer space. Namely, therefore, the question of application of infrared rays for communication in space, as yet has not emerged from the framework of theoretical research, although it is considered very promising. Questions of the adjustment of certain elements and general block-diagrams of equipment for communicating on infrared rays are an exception.

It is known, for instance, that the Farrand Optical Co. Inc. works on the creation of incoherent sources of radiation. Thus, developed by this firm, a spark source of light with a 11 mm diameter gives a brightness of $40 \cdot 10^9$ cp/cm^2 (more brightness than the Sun) and may be used in systems of communication with pulse modulation. This firm suggests the use of continuous radiation of a source of infrared rays as a carrier frequency, modulated by sinusoidal oscillations with lower frequency.

In Table VII.2 are presented certain optimum properties of sources of radiations, which can be used for optical communication, and in Table VII.3 — optimum properties of sensitive elements, intended for these purposes.

Table VII.2. Optimum Properties of Sources of Radiation for Purposes of Optical Communication [5, 6, 7].

Source of Radiation	Radiation intensity, w/stered		Power, w		Bandwidth, cps	
	In pulse	Average	Input	Output	Total	Modulation
Carbon arc	10^7	10^7	$3 \cdot 10^3$	$1.5 \cdot 10^3$	10^{15}	10^8
Other forms of discharge	$3 \cdot 10^8$	10^4	—	1	10^{15}	10^8
Reflected sunlight	10^7	10^7	—	10^3	$5 \cdot 10^{14}$	10^8
Mercury arc of high pressure	10^9	10^7	10^3	$5 \cdot 10^2$	10^{15}	10^8
Quantum-mechanical generator of optical range	$5 \cdot 10^{16}$	$5 \cdot 10^{11}$	10^3	10^2	10^{12}	10^9

Table VII.3. Optimum Properties of Receivers [5, 6, 7].

Sensitive element	Equivalent Power of Noise, w/cps	Bandwidth of Carrier, cps	Bandwidth of Modulation, cps
Thermal	10^{-11}	10^{15}	—
Photoresistor	10^{-13}	10^{15}	—
Human eye	10^{-16}	$3 \cdot 10^{14}$	10
Photocell with quantum-mechanical amplifier	10^{-17}	10^{15}	10^9
Enlarger	10^{-17}	10^{15}	10^8
Detector of shf	$2 \cdot 10^{-23}$	10^9	10^9
Quantum-mechanical amplifier of optical range	10^{-13}	10^8	10^8

A block-diagram of one of the systems of communication on infrared rays, SOCOM, developed by the firm Electro-Optical Systems [5, 6, 7] is shown in Fig. VII.15.

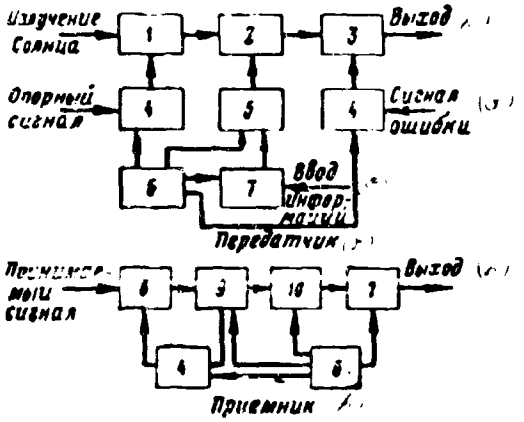

Fig. VII.15. Block-diagram of a receiver and a transmitter of the SOCOM system.
1—collecting antenna; 2—optical modulator; 3—transmitting antenna; 4—servomechanism; 5—submodulator; 6—source of supply; 7—information processing unit; 8—receiving antenna; 9—detector of carrier; 10—detector of subcarrier frequency.
KEY: (a) Solar radiation; (b) Output; (c) Support signal; (d) Error signal; (e) Input of information; (f) Transmitter; (g) Received signal, (h) Receiver.

In the SOCOM system for transmission of information an optical range of solar radiation is used as carrier frequency.

The transmitting and receiving antennas constitute a system of mirrors with variable orientation, allowing collection of solar energy at any angle.

In the transmitter solar radiation accumulates and is formed into a narrow beam, which then is passed through the modulator. A modulating signal is created after passage of information through the data processing unit and submodulator. After modulation the coded signal proceeds to the transmitting mirror for transmission to surrounding space.

Tracing the sun is done by a special watching device, sensitive in range of wave lengths 0.5–1.1 μ.

Transmitted radiation is picked up by receiving antenna, in the focus of which is disposed a sensitive element. After passage of corresponding processing, signal proceeds to output device for reproduction.

On the statement of the firm, the transmitter, weighing 13–18 kg, consumes power of 10–15 w. It is expected that during transmission of signals to a distance of 10^6–10^7 km with mirrors 1 m^2 in area and passband of 10 cps, the signal-to-noise ratio is equal to 10 db. This ratio can be increased as much as 10 times by cooling of the photosensitive element.

5. Prevention of Midair Collisions of Aircraft

During flights at great heights with cloudless sky or above overcast, a phenomenon occurs, known as "myopia of vacuum" [8]. In this case a pilot with normal sight suddenly becomes nearsighted, and his eyes will focus at a distance of no more than two meters.

If one considers that observation conditions of air targets at great heights are hampered by the dark background of the firmament and very little scattering of sunlight, then the importance is understood of solving the problem of early detection of encountered aircraft for prevention of collisons. Furthermore, on contemporary aircraft, and especially on jets, the pilot is forced to expend more than half of the time on observation of instruments on the instrument panel in the cabin and cannot, therefore, allot much time to surveying the space outside the cabin.

These peculiarities of the work of the pilot in high-altitude and high-speed machines demanded the creation of special equipment for the prevention of midair collisions.

According to information available in literature [9, 10, 11] such equipment should consist of both an indicator of approach of another aircraft and of a complex automatic system for preventing collisions of aircraft.

The indicator is designed to warn pilot about presence in the air of another aircraft. Its indications must be easily read, since for the pilot they are the only warning of possible danger, after which the pilot concentrates his attention in the direction which the instrument indicates and, after being convinced of his threatened position, starts a corresponding maneuver. In connection with this the indicator of approach is most useful during good weather.

A system of preventing midair collisions should reveal approaching aircraft, average obtained data, determine if both aircraft are on threatening courses, reject

information about nondangerous aircraft and indicate to pilot the correct maneuver. The system should continuously analyze danger created by every approaching aircraft and not require the attention of the pilot until there is a necessity to maneuver.

Free-space range of approaching aircraft at a height of 3,000 m with a 90% probability of detection was fixed for low-speed aircraft (speeds of flight up to 550 km/hr) at 3.2 km and for high-speed (speeds of flight over 550 km/hr) at 13 km.

This distance should be ensured in a zone $\pm$ 240 m in height relative to the height of flight of the protected aircraft, since the minimum difference in flight altitudes of separate aircraft is taken as 300 m.

By 1957 there were developed and published abroad two basic designs of indicators of approach. These systems use the principle of registering infrared radiation of approaching aircraft or registering modulation of infrared background of the atmosphere either by the propellers of the aircraft or by the turbulence of gas flux behind the jet nozzle exit.

The first design, which gives the pilot only the course angle to the approaching aircraft consists of a receiver of radiation in an azimuthal plane, two receivers of radiation in upper and lower hemispheres, an indicator on the instrument panel, and a power supply unit with a data converter.

Fig. VII.16. Survey zones of equipment.
KEY: (a) Miles; (b) Feet.

Receivers of radiation are established on the fuselage of the aircraft to ensure obtaining the antenna radiation pattern shown in Fig. VII.16.

The azimuthal receiver of radiation consists of a revolving mirror inclined at a 45° angle, and an optical system in whose focus is disposed an uncooled lead sulfide photoresistor. The projecting part of the azimuthal receiver is placed in a hemispheric dome 9.2 cm in diameter. Search for aircraft is carried out by a 15° band at a 360° angle with a speed of 30 rpm.

Minimum range of the azimuthal receiver depends on the type of approaching aircraft, its foreshortening, and the state of atmosphere, and attains 3.2-6.4 km.

Receivers of the upper and lower hemispheres consist of uncooled lead sulfide photoresistors, mosaic type, covered by a dome lens.

All three receivers are united through the data converter with a switch indicator 75 mm in diameter. On the glass of the indicator is drawn a silhouette of the aircraft. A pointer is attached to a revolving disk, whose front side is broken down into four quadrants for signalling the pilot that the approaching aircraft is in one of the following positions relative to his aircraft: on the right, on the left, above, or below. Behind the disk is placed five tubes, one of which (in the center) is connected with the azimuthal receiver, and the other four with the corresponding hemispheric receivers.

When infrared radiation from the approaching aircraft hits the azimuthal receiver the pointer of the indicator instrument will turn synchronously with the turn of the mirror and will indicate its course angle, and the central tube will start to blink with a frequency of 1-2 cps. If the nearing aircraft is in the dangerous 240-meter zone in height, then the tube lights, illuminating the corresponding quadrant of the instrument, which allows the pilot graphically to determine where the approaching aircraft is: on the right or on the left, above or beneath his aircraft.

There are two other varieties of similar design.

One of them anticipates installation on aircraft of special infrared emitters of circular action, which allow an increased range and noise immunity of the indicator of approach but anticipates installation of additional equipment.

In the second modification, in the tail part of the aircraft is established a controlled television camera. After the pilot obtains warning of the presence of another aircraft in the rear hemisphere, he can turn on the television camera, direct it in the direction of the nearing aircraft, and observe on the screen of an electron-beam tube the air situation created.

Experimental check of this design showed that a four-engine aircraft is r - vealed from distances at which it had not been seen in an optical instrument with fourfold magnification.

In one of the designs of the indicator of approach uncooled lead sulfide photoresistors are established in the nose and afterbodies and on wing cantilevers from above and from below, which allows examination of upper and lower hemispheres around the aircraft (Fig. VII.17).

Each receiver constitutes a set of three rings on a common dome-shaped base, on which is placed along the circumference 36 photoresistors each. The receiver is covered by a plastic dome 20 cm in diameter, which passes infrared radiation well in a wave range 0.9-8 μ. This material (chemically stable, light, and durable) sustains heating well up to a temperature of 300°C.

The number of elements in the ring determines the accuracy of the design in the azimuthal plane, since every element has a limited field of sight - not more than 10°. Number of rings in each receiver determines the resolving power with respect to elevation.

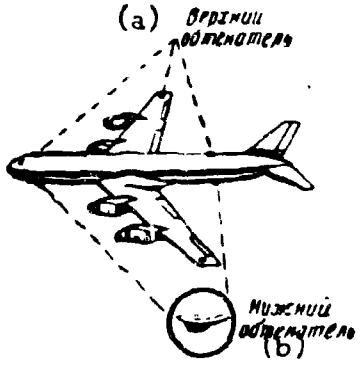

Fig. VII.17. Installation of radiation receivers on aircraft. KEY: (a) Upper dome; (b) Lower dome.

The range of the indicator of approach in the horizontal plane is equal to 16 km, and in the vertical it makes it possible to determine entry of approaching aircraft into the 240-meter zone from above or from beneath aircraft.

The entire set of equipment, which includes receivers of infrared radiation, amplifier, commutator, sweep generator, computer and indicator, weighs 13.5 kilograms.

Successive examination of space in the azimuthal plane is carried out by series connection of the photoresistor to the computer and the indicator instrument.

Distance to revealed aircraft is determined by the method of triangulation by the known base between the two receivers and by the angles of sighting of aircraft from each receiver.

Sensitivity of the equipment is determined by noise level when switching on photoresistors, by the commutator equal to 10 microvolts, and by the losses in optics. Errors in distance measurement, caused by deformation of wings in flight, change of pitch angle and yaw of aircraft, reach 4% for small aircraft and 10% for large.

6. Navigation

With the help of infrared instruments it is possible, by simple means, to carry out reliably the guiding of objects on the sea and in the air along given routes.

Most simply resolved is the question of navigation by double infrared beacons (maintaining place in formation, leading ships through mine fields and harbor channels). For that it is practically necessary to have on ships electron-optical instruments of observation and, fixed in corresponding places, signal infrared sources. For laying a course on the high sea it is sufficient to have optical or photoelectric sextants with manual or autotracking of stars.

In conditions of high-altitude and high-speed aviation the problem of dead reckoning at present has become the most urgent. Methods of air navigation applied earlier in conditions of high-speed and high-altitude flight lead to large errors. Methods of radio navigation also do not ensure high accuracy of air navigation. Therefore, considerable attention is allotted methods of astronavigation, allowing us comparatively exactly to carry out flights of piloted and pilotless aircraft. This problem becomes most urgent in connection with growth of flight altitudes,

since at great heights celestial bodies are practically the only real reference points. In this case manual tracking of stars are insufficient. Application of automatic devices is necessary tracking celestial bodies and continuously giving out coordinates of stars with minimum expenditure of time.

One of such automatic devices is the astrocompass, the MD-1 [12].

From the fundamental diagram of this instrument (Fig. VII.18) it is clear that the basic elements of a photoelectric automatic astrocompass are: sensitive element 4, perceiving radiation of celestial body, gyro-stabilized platform 7 for stabilization of sensitive element in the plane of the true horizon; device for isolating signal from star; generator of error signal 9, 10; and servomotors for influence on gyro-stabilized platform 8, 12.

As sensitive elements we can use: photocell, enlarger, and iconoscope, which are placed in the focus of objective 2. Between the sensitive element and objective is placed modulator 3.

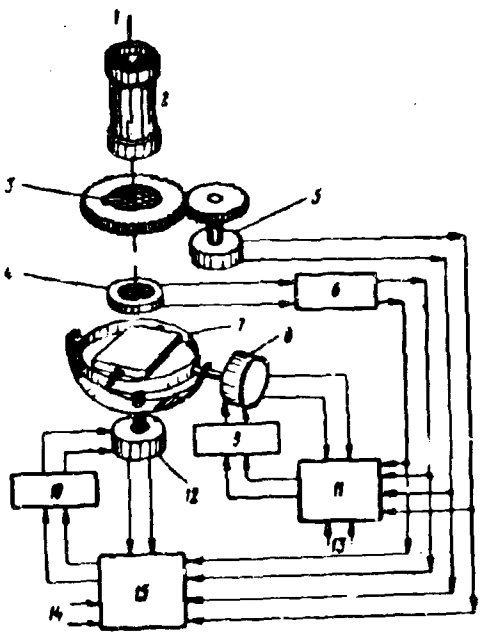

Fig. VII.18. Kinematic diagram of astrocompass MD-1.

The optical elements must meet very high requirements since it is important to obtain a good image in the whole range of waves (from blue to infrared) radiated by the stars. Also necessary is a two-objective system to guarantee a wide survey region (wide-angle objective) and high accuracy of tracking stars (long-focal objective with possibly a narrow field of sight).

For stabilization of the position of the photoelectric transducer and the modulator relative to the true horizon (true vertical) they are established on the gyro-stabilized platform.

The sensitive element produces a signal when the celestial body is in the field of sight of the receiving head. This signal allows us to obtain necessary data for determining direction to star and magnitude of error with respect to data proceeding from the computer.

Modulators, executing simultaneously the role of coordinator, can be mechanical, optical, or electronic devices.

Mechanical modulator (a disk with grooves) is applied in systems with an enlarger or single photoresistor. Speed of disk rotation is synchronized by signals proceeding from generator of support signals 5 revolving with the help of the same motor. Comparison of signals of photoelectric transducer 6 and support allows us to obtain data relative to the instantaneous position of a star. Appearing as a result of comparison, error voltage 9, 10 affects directly the gyro-stabilizing device until radiation from the star gets into the center of the field of sight of the photosensitive system. At this instant feedback signal leads to zero position the generators of error signal 11, 15 with respect to azimuth and elevation. The magnitude of the voltage of the feedback signal is proportional to the relative bearing of the star and may be easily converted into a signal proportional to the error between measured and true position of the star.

With the optical method of modulation several photoresistors are applied, which are located around the center of the field of sight.

If data from a tracking device coincide with data of computer 13, 14, radiant flux from the star gets into the center of the field of sight and the error signal is not produced. At the appearance of error, radiant flux gets on one of the photoresistors, as a result of which error signal appears, which then is compared with computer data and affects the gyrostabiliser.

The great merit of the optical modulator is the absence of mobile parts; the direction of error is determined by which the photoresistors gets radiant flux.

A type of optical method is the electron modulator, applied with the iconoscope, a mosaic of which is divided into four sectors, and for determination of direction to star magnetic yokes are used.

Literature

1. Army Quarterly, 1953, Jul.
2. Military Review, 1956, Nov.
3. J. Franclin Inst., 1954, Nov.
4. Prospectus f. VVT (France) on I-80 equipment.
5. Missiles and Rockets, 1960, 6 Jun., No. 23.
6. Electronic Design, 1960, 8 Jun., No. 12.
7. Aviation Week, 1960, 2 May, No. 18.
8. Whiteside T. The problem of vision in flight at high altitude. London, 1957.
9. Trans. IRE, 1957, Jun., Vol. ANE-4, No. 2.
10. Electronics, 1957, Jul., Vol. 30, No. 7.
11. Aviation Week, 1957, 13 May.
12. J. Institute of Navigation, 1958, Vol. 6, No. 1.
13. Instruction in the use of the AFOS installation with launch equipment, 1956. Ministry of instrument-making and methods of automation of the USSR, 1956.

C H A P T E R VIII

INTELLIGENCE WITH THE HELP OF INFRARED RAYS

For the purpose of increasing the interval of time necessary for intelligence, increasing its quality, operational nature and continuity considerable attention is allotted to the improvement of instruments and methods of intelligence with the help of infrared rays.

There are developed instruments of night vision, television systems of heightened sensitivity, aerial cameras for photographing either on special infrachromatic film or by means of converting an invisible image to visible with subsequent photographing on the usual photographic film, instruments for making a thermal map of the site, and passive radar.

In spite of the fact that the effectiveness of these instruments, to a great [illegible], depends on meteorological conditions, interest toward it continuously increases, since these instruments allow us:

to obtain an image of observed objects at night because of their temperature contrast with the surrounding background;

to obtain an image of remote objects through air haze, when application of visible rays for these targets becomes little effective or even impossible;

to reveal objects, masked from detection in the visible and radar regions of the electromagnetic spectrum.

1. Photographing on Infrachromatic Films

Silver halide photographic emulsions are sensitive to blue-violet rays. In order to make them sensitive to other rays of longer wave length, it is necessary to introduce into the emulsion certain dyes, i.e., to produce optical sensitization of photographic material.

In the infrared region of the spectrum, for these purposes, we use dyes created on the basis of cyanogen: cryptocyanine, neocyanine, and others. Colored by these dyes, emulsions are called infrachromatic and differ in the wave lengths of infrared radiation to which they are sensitive. At present, infrachromatic materials with a "red" boundary of sensitivity to 1.36 μ find application.

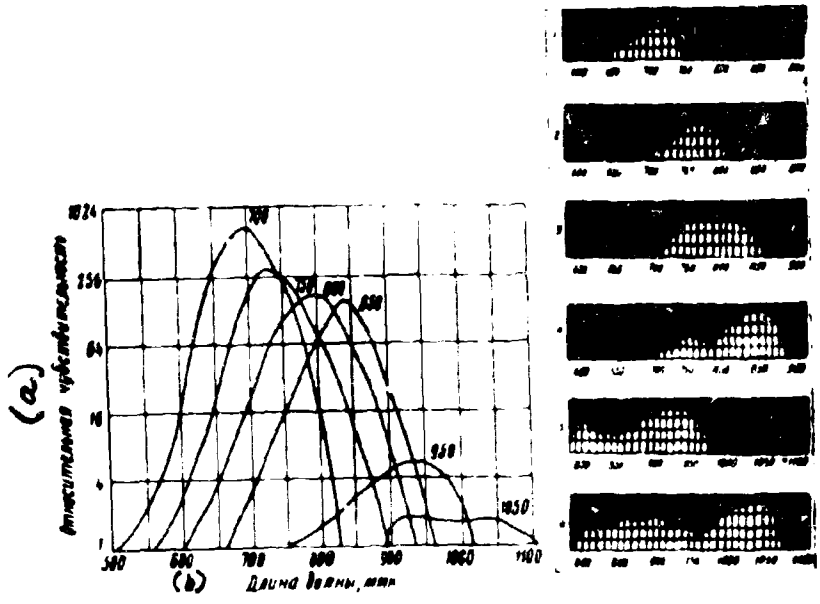

Fig. VIII.1. Spectral sensitivity of infrachromatic films "Agfa".
KEY: (a) Relative sensitivity; (b) Wave length, mμ.

In examining curves of spectral sensitivity of infrachromatic emulsions (Fig. VIII.1 and VIII.2), there can be made one conclusion, very important for practice, that with increase in maximum wave length of sensitization there occurs a constant and sharp drop of integral sensitivity of photomaterial in the infrared region of the spectrum. This drop of sensitivity is possible to characterize graphically by

the curve in Fig. VIII.3.

With growth in maximum wave length of sensitization, the guarantee period for preservation of the film also decreases. This is caused by the fact that during storage of infrachromatic material there occurs a fast drop in its light sensitivity with a simultaneous growth of veil. The greater the sensitivity decrease, the longer the wave length of sensitization.

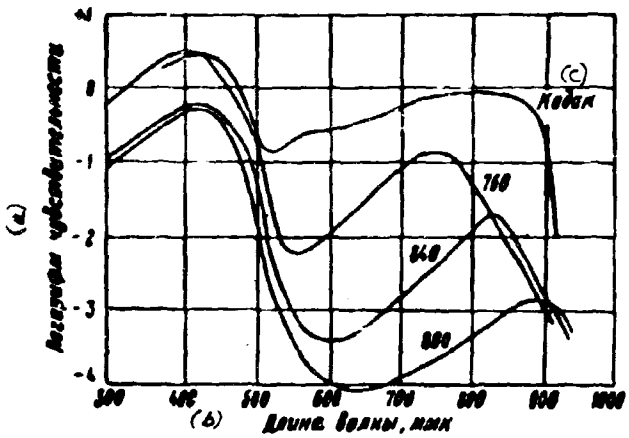

Fig. VIII.2. Spectral sensitivity of native infrachromatic films "Infra" and aerial film of "Eastman-Kodak" (The United States).
KEY: (a) Logarithm of sensitivity; (b) Wave length, mμ; (c) Kodak.

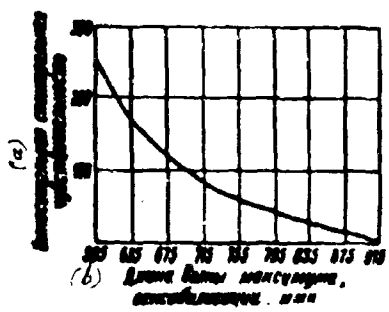

Fig. VIII.3. Drop in sensitivity of infrachromatic materials with change in wave length of maximum sensitization.
KEY: (a) Relative spectral sensitivity; (b) Wave length of maximum, sensitization mμ.

Partial increase in stability of infrachromatic materials may be attained by storage of them in hermetic packing in refrigerators.

The above-considered peculiarities of infrachromatic materials (drop of integral sensitivity and impairment of stability of infrachromatic materials sensitized in a region of the spectrum of longer wave lengths) predetermine application in practice of the more sensitive emulsions sensitized to radiation in a wave range of 0.76–0.85 μ.

Infrachromatic materials with a boundary of sensitivity of a longer wave length, as a rule, are applied only in scientific surveys, where large exposures are allowed, and the preparation of emulsion is produced directly before its application. There is another obstacle to wide application of photographic emulsions sensitized to infrared rays of a longer wave length: radiation of bodies heated to room temperature, will

noticeably affect an emulsion sensitized to λ = 2 μ, causing its fogging. It is natural that work with such materials will be strongly hampered, if not quite impossible.

Fig. VIII.4. American camera for photographing in infrared rays.

For photographing in infrared rays, in 1955-1957 special photographic cameras [1, 2] were created with long-focal objectives. Thus, for photographing in ground conditions in the United States, a camera was developed with an objective having a focal length of 254 cm and relative hole 1:12.5 (Fig. VIII.4). Dimensions of frame are 12.7 X 17.8 cm. Shutter has 10 speeds of operations with minimum exposure 1/200 sec. The camera is designed for photographing objects at distances up to 50 km and makes it possible to decipher on a photograph a single motor vehicle photographed from a distance of 10 km.

An even longer focus objective (17 m) was applied in a German camera during the Second World War, with the help of which was produced photographing of the English sea coast across the English Channel from a distance of 33 km in conditions of strong haze.

Fig. VIII.5. Mountain view, taken from a distance of 60 km in infrared A and light B rays.

With the help of similar cameras it becomes possible to produce a survey of remote objects, hidden by air haze from observation in visible rays (Fig. VIII.5),

to carry out a survey of aerolandscapes, whose light-transmission will differ from light-transmission during photographing in visible rays (Fig. VIII.6). Furthermore, it is possible to determine the presence of targets and their character, to watch for changes in camouflage of the enemy, in the system of organization of defense and fire, to facilitate target designation and orientation of our own artillery, and also to improve camouflage of our own troops.

Certain authors [3, 4] note that with the help of infrachromatic materials it is possible to obtain photographs with more contrastive isolation of objects on the site than during photographing on panchromatic materials, because of different light-transmission of dark and light places. Furthermore, as a merit of infrared aerial photography is the possibility of photographing sites through breaks in overcast, since in this case the effect of concealment of objects by cloud shadow sharply decreases as compared to photographing on panchromatic film.

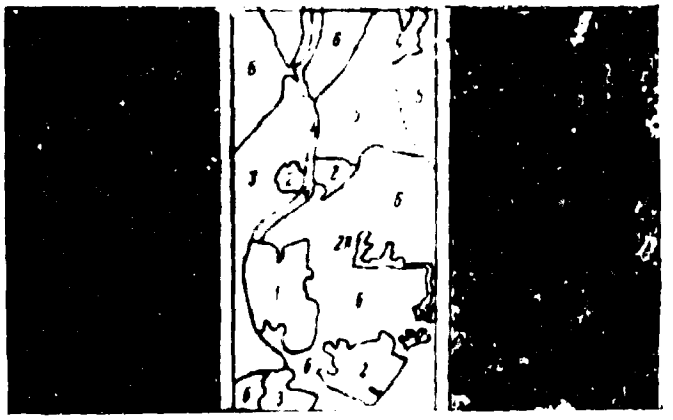

Fig. VIII.6. Aerolandscape of forest in yellow-red (on the left) and infrared (on the right) rays:
1—pine (old trees); 2—pine (young trees); 3—pine and leafy trees; 4—teuga; 5—teuga and leafy trees; 6—leafy trees.

The process of light-transmission of the image of observed objects is noticeably affected by spectral composition of light reflected by the object, spectral sensitivity of the receiving device, and spectral attenuation factor of radiant flux in atmosphere. Other conditions of observation being equal (the same object, identical transparency of atmosphere, the same distance to observed object and the same source of its illumination), the light-transmission of the image will depend on actinism of radiant flux A_λ, reflected by the object,

$$A_\lambda = S_\lambda \cdot A_\lambda, \qquad \text{(VIII.1)}$$

where S_λ is spectral sensitivity of receiving device;

r_λ is spectral density of reflected radiation;

τ_λ is spectral transmissivity of atmosphere.

In Fig. VIII.7 are given curves of spectral sensitivity of the eye 1 and of a cesium oxide photocathode 2, spectral distribution of energy of sunlight 3 taking into account transparency of atmosphere. As a result of multiplication of corresponding ordinates of curves we will obtain curves of actinism of radiant flux for the eye and a cesium oxide photocathode depending upon the wave length of optical radiation (without calculation of selectivity of reflection of object).

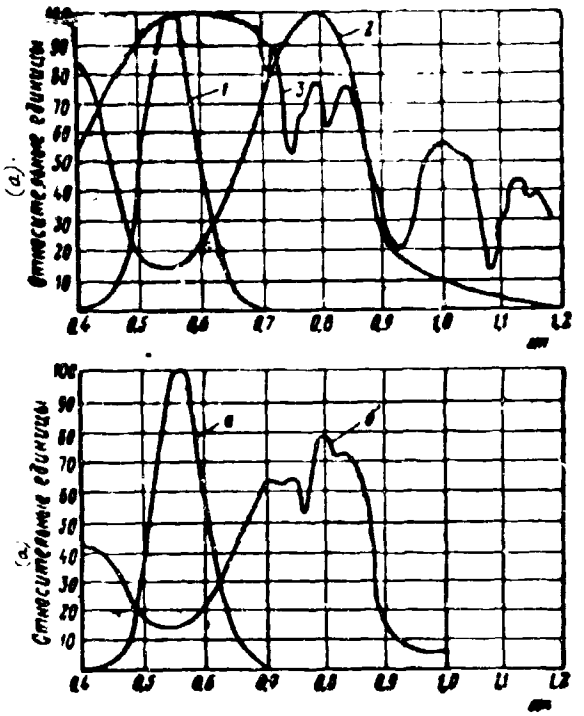

Fig. VIII.7. Distortion of light-transmission of image during observation in different sections of the spectrum.
KEY: (a) Relative units.

From comparison of curves a and b in Fig. VIII.7 it follows that for the eye, radiation with wave length in the range of 0.54–0.58μ will be reflected the brightest and for a cesium oxide photocathode (curve b) maximum brightness for reflected radiations will correspond to a wave length of 0.78–0.86 μ. It is possible to show that a similar character of distribution of image brightness will be obtained also when using infrachromatic photographic material.

The effect of distortion of light-transmission during photographing on infrachromatic materials during simultaneous photographing of effect of air haze (veil on photographic material) may be used with success to increase the effectiveness of aerial photoreconnaissance by day and facilitate deciphering of obtained photographs.

Fig. VIII.8. Image of a shooting battery, obtained by the method of combined photograph on infrachromatic film.

The low sensitivity of infrachromatic materials, which is their deficiency, may be used with success to determine the exact position of hostile searchlight installations and artillery batteries. For that, at night, when the shutter is open cameras photograph, for instance, flashes from shots of cannons. The weak night light does not affect infrachromatic film, and on it is obtained only a latent image from the flashes. By day, during constant position of cameras, they photograph the site. As a result there is obtained a photograph (Fig. VIII.8), on the background of whose site is clearly determined the direction to artillery positions [5].

Carrying out similar photographs from 2-3 positions and knowing azimuthal angles of camera installations, one can determine even the position of the actual batteries.

2. Photographing with the Help of Electron-Optical Converters

As already was noted in 1, application of infrachromatic emulsions encounters difficulties: their very low integral sensitivity and bad stability in time. In order to avoid this, it is necessary preliminarily to convert the invisible infrared image to visible and to photograph the latter on the usual, comparatively stable, and highly sensitive photographic emulsions. Conversion of an invisible infrared image to visible may be carried out with help of an image converter, recording evaporimeter, and phosphorescent materials sensitive to infrared rays.

The fundamental plan of photographing in infrared rays with the application of an image converter is shown in Fig. VIII.9.

Radiant flux 1, reflected from photographed object, passing through infrared filter 2, is focused with the help of objective 3 on photocathode of image converter

4. The visible image obtained on its screen, with the help of optical system 5, is transfered to photographic film 6.

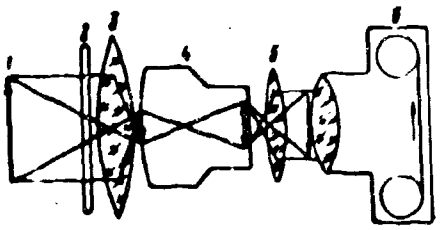

Fig. VIII.9. Fundamental diagram of camera with image converter.

All the system, including the projecting objective, the image converter, and the system of transferring the visible image to the photographic emulsion, has obtained the name of electron-optical objective.

Inclusion of an image converter as an intermediate element worsens a number of parameters of the optical system of the camera and, therefore, it is necessary to take special measures for their removal or partial compensation. This, in the first place, pertains to resolving power and to the requirement for geometric similarity of the image to the photographed object.

The requirement for geometric similarity in the case of an electron-optical objective is not fulfilled. This is connected with the fact that for converters, especially with a flat photocathode, there is, as a rule, distortion, i.e., inconstancy of linear magnification of sections as the distance increases from the center to the edges. For its removal special correction of the projecting and photographic objectives is necessary for the purpose of obtaining in them distortion of the reverse sign.

Resolving power of electron-optical objectives, as a rule, is less than for the usual objectives, because of low reso ing power of the image converter. Therefore, it is necessary to increase artificially the resolving power of converters and to design objectives with more uniform resolving power with respect to field of sight.

Most effective are the following ys of increasing resolving power of converters:

a. application of combined focusing of electrons by the electrostatic and magnetic fields. By this method the firm of Muellard (England) managed to develop the MF-1201 image converter for photographing in infrared rays with a resolving power all over the field of sight, equal to 20 lines/mm [6];

b. significant increase of focusing voltage on electrodes of the converter. During constantly applied voltage to electrodes, breakdown between cathode and other electrodes is prevented. Furthermore, during large supply voltage the appearance of fatigue of luminophor and breakdown of the converter on the whole is possible.

All this it is possible to avoid, if instead of constantly applied voltage there are passed to electrodes pulses of high tension. As shown by investigation [7], during supply to electrodes of square pulses of voltage 1-10 microseconds in duration breakdown potential can be increased 5-7 times, since in this case pulse duration is comparable with time necessary for development of breakdown. Transition to pulse feed of converters permits an increase in gradient of field for photocathode from 4.5 to 30 kv/cm and, consequently, a significant increase in resolving power of converter. Furthermore, with such feed it is possible to increase also the brightness of the image on the screen without danger of its burning out or irreversible fatigue.

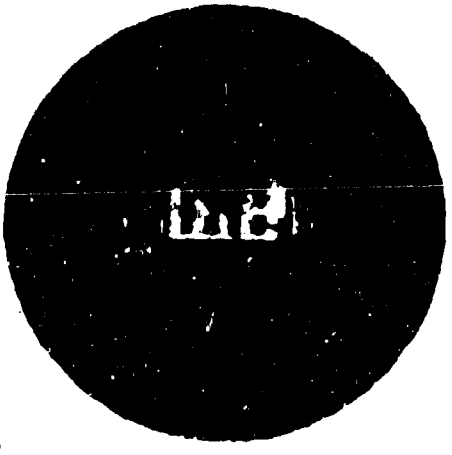

Fig. VIII.10. Image of landscape, obtained with the help of an electron-optical camera.

In the electron-optical objective, due to application of converter allowing amplification of brightness of image, it is possible to increase candle-power significantly as compared to the usual lens objective. This allows us to obtain in the focal plane (on film) sufficient illuminance for photographing with a small exposure time.

Indirectly, candle-power of an electron-optical objective can be increased by corresponding selection of spectral radiation of luminophor of converter screen and spectral sensitivity of photographic film.

The essential advantage of this method of photographing is the possibility of its application during low levels of illuminance, when the usual and infrachromatic photomaterials become ineffective, and, furthermore, this method allows application of ordinary highly sensitive and stable photomaterials.

As an illustration, in Fig. VIII.10 is a photograph taker in the pretwilight hours with the help of an image converter.

3. Evaporation Recording

The above-considered methods of photographing in infrared rays allow photographing either by reflected radiation or by intrinsic, if the temperature of the surface of the object is higher than 250-300°C. This is connected with the fact that the considered methods use comparatively short-wave infrared radiation with wave length not more than 1.2 μ.

In the method of evaporation recording, suggested by the German physicist Tscherny, long-wave radiation of bodies having low surface temperatures is used.

The essence of the method of evaporation recording consists of the following (Fig. VIII.11).

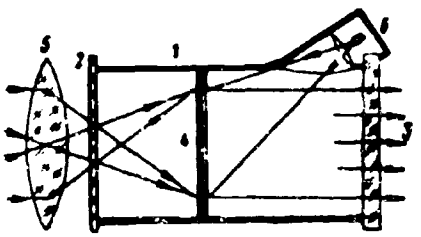

Fig. VIII.11. Fundamental diagram of evaporation recording.

In vessel 1 with entrance window 2, transparent for infrared rays, and output window 3, thin mica film 4 is established. The side of the film, turned to objective 5, is covered by platinum black or soot for best absorption of infrared ray. From the opposite side of the film there is precipitated by evaporation a film of some kind of viscous liquid (for instance, camphor oil). Thickness of the layer of oil is selected so that, because of

interference of light, minimum reflection of radiant flux from outside source of light 6 would be ensured.

If on the blackened surface of the film the image of the photographed object is projected, then in places where the intensity of infrared rays is greater, the film will be heated, which will lead to partial evaporation and spreading of oil to places which are colder. Interference of reflected rays from source 6 will not completely extinguish visible rays, and on the film will appear an interference image corresponding to the distribution of temperatures on the surface of the object. This is possible to observe either visually or to photograph through output window of the evaporograph.

For the purpose of removing the effect of external temperature on the volatility of the condensed layer of oil a mica film is placed in vacuum, but the body of the receiving part of the instrument is made from good thermo-insulational material.

Since conversion of radiant energy into heat, utilized in this method, is the least profitable method of detecting radiation energy, then it is impossible to expect from it great sensitivity, just as resolving power. Furthermore, for the heating of the film and the evaporation of the layer of liquid certain time is required, as a consequence of which such instruments possess noticeable time-lag: in order to photograph another object it is necessary to wait a definite time for the condensation of a new layer of camphor oil on the film.

In spite of noted deficiencies inherent in this method, such instruments find application in military technology since they allow us, in principle, to solve the question of vision in darkness because of the intrinsic emission of targets.

As an example we will consider the night vision equipment "Eva," developed by Baird Associates (The United States) in 1956 and taken into service by the Air Force in 1957 [8, 9, 10].

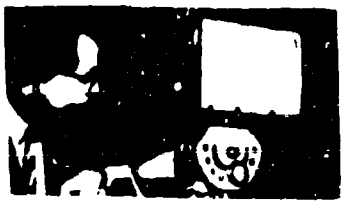

Fig. VIII.12a. General form of the "Eva" instrument.

The "Eva" instrument (Fig. VIII.12a) makes it possible, in full darkness, to distinguish the outline of an object with a surface temperature differing from the temperature of the surrounding background and to identify it by the nonuniform distribution of temperatures of its separate points. Sensitivity of the instrument is 0.1°C. It can record a change in temperature of bodies in a range from several units to several thousand degrees.

The instrument (Fig. VIII.12b) consists of five main centers, long-focal mirror objective I, vacuum chamber II, optical tube for observation III, camera IV, and illuminator V.

The objective ($2\beta = 5°$; A = 1:2.5; f = 20 cm) includes two mirrors - spherical 1 and refracting 2, are a lattice neutral filter 3 for the weakening of radiant flux from powerful sources of radiation, and a flap on the entrance of objective 4 for covering access of radiant flux while restoring instrument for repeated observation.

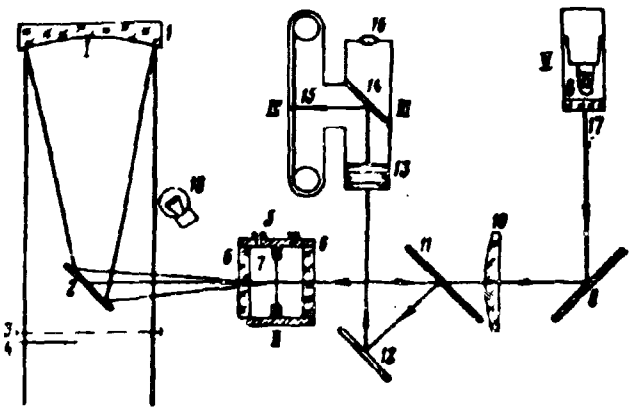

Fig. VIII.12b. Optical diagram of the "Eva".

Sensitive element 7, located in focus of mirror 1, constitutes a thin film from nitrocellulose, covered from one side by platinum black and from the other by a film of camphor oil. The film is pl ced in hermetic vessel 5, from which, periodically, is pumped air. Entrance window 6 is prepared from crystal of rock salt, covered by film of vinyl varnish. The ... wall of the chamber is prepared from glass passing only visible light and cutting infrared radiation.

Optical sight III is designed for visual observation of interference picture and consists of long-focal objective 13 which is simultaneously the objective of small-size camera 15, semitransparent mirror 14 and eyepiece 16. Semitransparent mirror rejects 50% of the visible radiation to the photographic film and 50% passes in the direction of the observer.

Illuminator V consists of tungsten incandescent lamp 8, filter 17 cutting all infrared radiation of the tube, mirror-reflector 9, and condenser 10. On the path of the parallel beam of light, after the condenser, semitransparent plate 11 is disposed with a reflection coefficient of 50%. Light passing through this plate and the output window of the camera gets on the sensitive film. Being reflected from it, the light, by means of the semitransparent plate and mirror 12, is rejected to the objective of the telescope and camera.

Fig. VIII.13. Image of a motor vehicle, an aircraft, and a man, obtained with the help of the "Eva" in darkness.

After observation ceases, the flap of the objective is closed; tube 18 turns on, the radiation of which, by means of reflective mirror 2, gets on the blackened surface of the sensitive film, evenly heating it and erasing thereby the oil film.

Control for erasing of film and subsequent precipitation on it of oil is carried out visually through a telescope by change of color of the oil film in the reflected rays from yellow (oil is absent) to greenish-yellow (thickness of oil film corresponds to operational value).

In literature it is indicated that with the help of the "Eva" one can photograph in full darkness a man at a distance of 180 m and a building at a distance of 1,800 m (Fig. VIII.13).

The principle of transforming thermal energy into visible radiation which can be observed either visually or photographed is assumed also in the basis of work of

another semiconductor converter of a similar type, recently developed in England [11].

The operating principle of the instrument (Fig. VIII.14) is based on the use of the dependency of the absorption of light falling on a semiconductor on its temperature. If the film of a semiconductor is examined in monochromatic light passing through it, which has a wave length close to threshold, then the least change in temperature of separate sections of the film causes a corresponding change in their transparency.

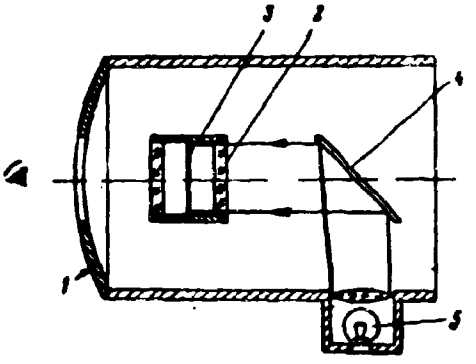

Fig. VIII.14. Semiconductor image converter:
1—parabolic mirror; 2—window from rock salt; 3—film of selenium and chromium; 4—mirror; 5—sodium tube.

Infrared rays being reflected from parabolic mirror 1 and passing inside vacuum chamber through the entrance window of rock salt 2, get on semiconductor sensitive film 3. The film consists of of chrome sublayer and a layer of amorphous selenium 1 μ thick turned in the direction of the mirror objective. A peculiarity of such film is the fact that it absorbs infrared rays well when they fall from the selenium side and absorbs them badly when they fall from the chromium side.

The image of the object, or more exact - the distribution of intensity of infrared radiation of different parts of the object, is examined in the light of the sodium tube.

Sensitivity of the instrument is limited by the ability of the eye or photographic film to distinguish the slightest contrasts. In the first sample it was comparatively low, since it made it possible to photograph objects whose surface temperatures differed by 15°C from the temperature of the surrounding background during an exposure time of 2 sec. Time lag of the instrument is 0.5 sec. Resolving power of the instrument, limited by quality of mirror, camera window, and film,

constitutes 4 lines/mm.

Vacuum in the chamber with sensitive film is supported with the help of a getter and constitutes 10^{-4} mm Hg.

4. Instruments of Intelligence in the Near-wave Part of the Infrared Spectrum

For detection of special sources of infrared radiation can be applied any instruments possessing sensitivity to near-wave infrared radiation (to 2 μ) - a metascope with phosphorus as a sensitive element, monocles or binoculars with image converters, and also special detectors with photoresistors or photodiodes. Since such instruments do not require high resolving power and great sensitivity, they can be made by simple construction, with small scales and dimensions.

In metascopes is used the phenomenon of "extinguishing" or "stimulating," by infrared rays, the phosphorescence of phosphorus, preliminarily excited by α-radiation or ultraviolet light.

An example of such instruments is the metascope UF/F (The United States), developed during the Second World War, and the metascope CMFT (France), developed in the postwar period. Free-space range for metascopes of sources of infrared radiation of average power constitutes several kilometers.

In spite of the small dimensions and the absence of special sources of supply for metascopes, the low resolving power limits their application, in consequence of which they have been replaced by more advanced instruments with image converters.

The above-considered instruments were designed for observation of infrared sources of radiation, the results of which have made it possible to obtain an idea about the location of the enemy, the character and directions of shipments, limiting points of the enemy, and, partially, about the character of infrared means applied by the enemy. However, significantly more valuable data can be obtained by reconnaissance if one carries out observation of the situation at a site and not

separate sources of infrared radiation. For these purposes there can be used only instruments with candle-power optics and with high-quality image converters with irradiation of the site by searchlights covered with infrared filters, or observation in conditions of natural illuminance.

At the end of the Second World War in the ground troops of the United States an instrument of close reconnaissance on infrared rays found application - the "snooperscope" (Fig. VIII.15).

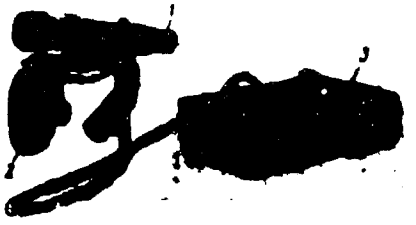

Fig. VIII.15. The "snooperscope" (The United States).

The "snooperscope" is an electron-optical instrument of observation 1, mounted jointly with small-size infrared searchlight 2. Power is supplied to instrument and searchlight from a special storage battery carried by the soldier in shoulder bag 3 or in a bag across the arm.

A searchlight 100 mm in diameter with a 30 w electrical incandescent lamp ensures axial luminous intensity of 7-10 thousand candles.

As an image converter in the observation instrument, at that time the 1-P-25 converter with supply voltage of 4000 v was widely used.

The radiant flux of the searchlight, reflected from objects on the site and hitting the objective of the observation instrument after conversion, creates on the screen of the instrument an image ahead of the horizontal site. Range of the instrument is 150 m.

In 1955 there appeared a report about the development of an instrument allowing observation at night at a distance up to 3600 m [13].

As an irradiating installation in it there is applied a 60-cm searchlight with a 1500 w X 9 v electrical incandescent lamp covered by an infrared filter with axial luminous intensity of 5 million candles.

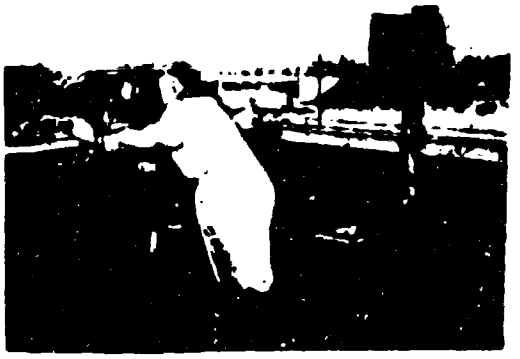

Fig. VIII.16. American instrument for observation in darkness.

The electron-optical instrument of observation with 6 X magnification is fed from a special high-voltage unit developing voltage of 20,000 v. The instrument of observation is synchronously connected with one or with several searchlights, which ensures the turn of the searchlights in the direction of observation (Fig. VIII.16).

Comparing characteristics of the two considered instruments of observations in infrared rays, it is possible to note that increase of visual range by 24 times led to an increase in power consumed by the searchlight, 50 times, and luminous intensity - 500 times. Therefore, a significant increase in the range of electron-optical instruments working in a set with irradiator installations should not be expected. These instruments will remain short range instruments for observation of a site directly adjoining the observer. Furthermore, such instruments, in principle, cannot ensure concealment of their use, since the enemy, armed with corresponding equipment, can always establish not only that a searchlight is operating, but also determine its position. In particular, with this goal in mind, there was created an instrument, the IRI-03 [14], to warn if soldiers were being irradiated by infrared rays (Fig. VIII.17).

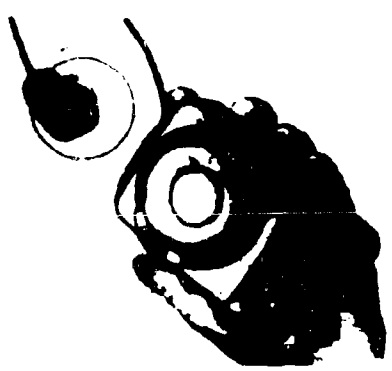

Fig. VIII.17. The IRI-03 instrument.

The IRI-03 consists of a photo-generator of beats of an audio-frequency and a dynamic telephone which ensures sonic signalling of irradiation.

The photogenerator of beats uses semiconductors and includes generator of constant frequency f_1, sweep generator f_2

with control photoresistor and mixer stage, producing frequency of beats f_s, to which the telephone reacts directly.

In the absence of irradiation of the photoresistor, frequencies of oscillations of the generators are equal to ($f_1 = f_2$). During irradiation of the photoresistor by infrared rays, frequency f_2 changes proportionally to the intensity of irradiation, as a result of which after the mixer there appears a difference frequency audible in the telephone.

Both generators, the mixer, and the power supply are mounted in a plastic body 11 X 6.5 X 2 cm, weighing 200 g, which may be suspended on a button of a uniform. A dynamic telephone with constant magnet is united with the instrument by a cable and may be secured near the soldier's ear.

Power is supplied to the instrument by miniature batteries on 1.5 and 22.5 v, designed for 50 hours of constant work.

The photoresistor is sensitive in a wave range of 0.6-2.3 μ, and its construction ensures an angle of sight of the instrument near 140°. By increasing the frequency of the difference tone one can determine the direction to the source of infrared radiation with a precision of $\pm$ 5°.

By the height of the produced tone, it is possible tentatively to judge also as to whether the soldier is in a dangerous zone or in a zone of preliminary warning. Thus, if the soldier is in a zone of preliminary warning (within limits of 1-3 fold range of the observation instrument) the indicator produces a tone of low frequency at 200-2000 cps. When in a dangerous zone (range of the instrument of observation) the frequency of the tone is increased to 2,000-10,000 cps (grows as it nears the instrument of observation).

The IRI-03 has indisputable advantage over metascopes since the eye and hands of a soldier always remain free and, furthermore, with the help of the instrument, one can estimate, qualitatively, the direction to the irradiator and the distance to it (effect of proximity of irradiator).

Metascopes and instruments of the "Snooperscope" type do not allow observation without preliminary bias lighting of targets. Naturally, the question appears about creating equipment allowing the observation of targets because of their irradiance by the night sky.

At night the basic sources creating on the surface of earth a definite level of illuminance are the moon, the stars, and space filled with billions of stars invisible to the eye, but sending to earth a significantly larger energy content of radiation than all the stars visible to the eye. In night sky radiation a noticeable role is played by radiation in the infrared part of the spectrum, expecially with a wave length of 1.03 μ. In the presence of overcast, irradiance of ground objects sharply decreases due to scattering and absorption of radiation energy in the thickness of the clouds.

Dependency of illuminance of ground cover after termination of astronomical twilight (Sun is beyond the horizon more than 18°) on state of the overcast for average latitudes is shown in Fig. VIII.18 [15].

The given curves show that during clear weather and full moon, when on the site it is possible more or less to be oriented, illuminance of terrestrial cover constitutes a magnitude of the order of tenth fractions of lux. In the absence of the moon, illuminance sharply drops, attaining values of the order of 10^{-3}—10^{-4} lux. With such conditions, not only from the air, but also on earth from comparatively close distances, one cannot detect objects visually.

A. A. Gershun [16] presents averaged numerical values of levels of natural night illuminance:

in full moon during clear sky 0.2 lux;

on moonless clear night 0.001-0.002 lux;

on moonless night during overcast of average density 0.0005-0.001 lux;

on moonless night during overcast 0.0002 lux.

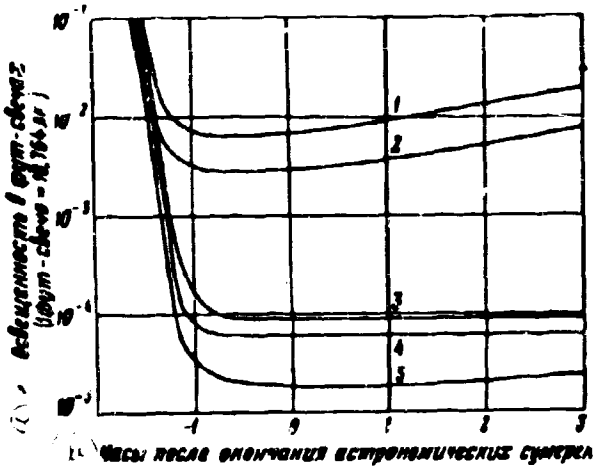

Fig. VIII.18. Night irradiance of earth's surface:
1—clear, full moon; 2—average overcast, full moon; 3—clear, no moon; 4—average overcast, no moon; 5—strong overcast, no moon.
KEY: (a) Illuminance in foot-candles (foot-candle = 10.764 lux); (b) Hours after termination of astronomical twilight.

Such illuminance of objects with coefficient of diffuse reflection $\rho = 0.4$ will create visible brightness within limits of $0.025 \cdot 10^{-4}$—$0.000025 \cdot 10^{-4}$ stilb (0.025–0.000025 nit).

It is established [17] that on a dark night the threshold of light signals for the eyes has the following values:

by spot, $B_п$* = (0.9–1) 10^{-4} nit;

by point, $E_п = 1 \cdot 10^{-7}$ lux.

The given values of threshold magnitudes are obtained when conducting special experiments and, therefore, can significantly differ during observation in real conditions, when physical and psycho-physiological factors, unaccounted for during the experiment, will have an effect. Depending upon this, the real threshold of brightness can differ from that given by 20–50 times to the larger side, i.e., $B_п \approx (2\text{–}5)\ 10^{-3}$ nit.

From the above-stated it follows that in real conditions, during visual observation of ground objects at night, their own brightness is insufficient for their detection; an exception will be observation in full moon during clear sky, if one considers that for identification of objects it is necessary to work, not at the threshold value of brightness, but at a significantly larger value.

In this connection it is necessary to note one more dependency, namely, the dependency of the resolving power of the eye on the brightness of observed objects (Table VIII.1).

*Russian subscript "п" indicates "threshold."—Ed.

Table VIII.1. Dependency of the Angle of Resolution of the Eye on Brightness of the Object.

Brightness, nit.	Angle of resolution, minutes	Brightness, nit.	Angle of resolution, minutes
$3.142 \cdot 10^{-4}$	50	1.57	2
$1.57 \cdot 10^{-3}$	30	3.142	1.5
$3.142 \cdot 10^{-3}$	17	15.7	1.2
$1.57 \cdot 10^{-2}$	11	31.42	0.9
$3.142 \cdot 10^{-2}$	9	314.2	0.8
0.157	4	1570	0.7
0.3142	3	3142	0.7

The resolving power of the eye, as also its ability to perceive threshold values of brightness or illuminance on the pupil, essentially depends on the conditions of observation and, therefore, can differ from experimental data by 5-10 times.

Thus, for execution of night reconnaissance it is necessary to increase brightness of image of observed objects with a simultaneous decrease of resolution angle.

Optical instruments cannot do this since (perceived by the eye) image brightness of an object observed in an optical instrument is always less than intrinsic brightness of the actual object, due to losses in optics, and may be calculated by the formula

$$B = B_0 \left(\frac{d}{d_0}\right)^2 \tau_{o.s}, \qquad \text{(VIII.2)}$$

where B_0 is brightness of the object;

d is eyepiece of the instrument;

d_0 is pupil of eye adapted to darkness ($d_0 \geq d$);

$\tau_{o.s}$ is optical transmission of the instrument ($\tau_{o.s} < 1$).

When applying electron-optical instruments for intelligence purposes, it becomes possible to increase brightness of image of observed objects at night so much that they will be easily deciphered by observer. As already was noted in Chapter VI, application of stage converters allows us significantly (100-1000 times) to strengthen brightness of image and to make possible observation of site at night, when objects are not examined by the eye. According to literature [18], multistage image converters allow us to obtain during optimum conditions an amplification factor with respect to brightness of $\eta = 10^5$. Such amplification of brightness gives the possibility of creating electron-optical instruments of intelligence during natural night illuminance 10^{-3}-10^{-4} lux.

5. Television Systems of Heightened Sensitivity

Instruments considered in Section 4 are instruments of direct observation of site and require presence of a special observer, who only after a certain time can transmit to command the subjective results of his observations. However, it is desirable to obtain information during all the time of observation directly at the command post.

With this goal, more and more being introduced are methods of television intelligence by day, in twilight, and night time.

Introduction of night television intelligence is connected with the necessity of creating special highly sensitive transmitting tubes, able to produce sufficient signal during small or very insignificant illuminance on photocathode.

Published data indicates that the present, usual television tubes can normally work during illuminance on the photocathode of the order of unity and tenth fractions of lux. In Table VIII.2, according to [20], values are given of necessary illuminance of objects $E_{об}$ and the optimum values of the relative hole of objectives A of contemporary transmitting tubes. In the same place are given computed values of illuminance of object and photocathode E_{Φ} when using an objective with relative hole A = 1:2.

Table VIII.2. Illuminance of Site, Necessary for Normal Work of Television Tubes.

Type of Tube	$E_{об}$. Lux	A	$E_{об}$. Lux A = 1:2	$E_{ф}$. Lux A = 1:2
Supericonoscope	3000	1:3.5	1000	25
Orthicon	1400	1:6.3	140	3.5
Image orthicon Li-17	100	1:4.5	20.8	0.5
Image orthicon Li-201	330	1:4.5	62.5	1.5
Vidicon	330	1:2	330	10

Illuminance $E_{ф}$ is calculated by the formula

$$E_{ф} = \frac{1}{4} \rho_{об} \tau_{об} \tau_{атм} A^2 E_{об}, \qquad \text{(VIII.3)}$$

where $E_{ф}$ is illuminance on photocathode;

$E_{об}$ is illuminance on object;

$\rho_{об}$ is reflectivity of surface of object;

$\tau_{об}$ is transmission of objective;

$\tau_{атм}$ is transmission of atmosphere.

As can be seen from the table, even such very sensitive tubes as image orthicons do not allow observation either at night or in twilight. Therefore, for the creation of night reconnaissance television systems it is necessary to increase sensitivity of the transmitting tubes.

Sensitivity of any transmitting television tube is limited by the noises appearing in the process of converting light into photocurrent, the noises of commutating electron beam, and the noises of the preamplifier. The last two sources of noises predominate. Consequently, it is most profitable to produce amplification of photocurrent until electron beam produces commutation of charge accumulated on the target.

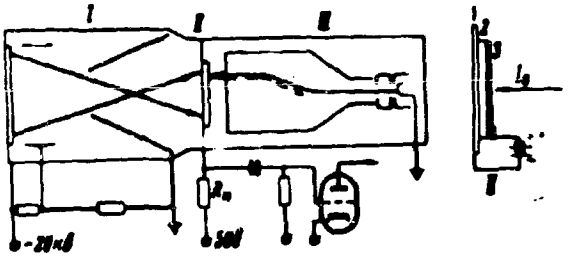

Fig. VIII.19. Diagram of the construction of an ibicon tube.

Such amplification of photocurrent may be performed by three methods:

by secondary electron amplification of photocurrent;

by induced conductivity;

by light amplification of the image on the principle of electron-optical conversion.

The last two methods have been used, which, judging by the available data in literature, brought reassuring results.

In Fig. VIII.19 is depicted a diagram of an ibicon tube using the phenomenon of induced conductivity.

With respect to signal formation an ibicon signal hardly differs from a vidicon, however, the addition of a section of transfer of electron image allows repeated increase of current, creating potential relief on target, and, consequently, sensitivity of tube.

In construction, an ibicon consists of three units: a section of transfer of electron image with photocathode and accelerating electrodes I, a target II in which is excited induced conductivity, and a section of communication with electron gun and system of electromagnets III. Intensive signal is removed directly from the target and moves to the input tube of the video amplifier.

If in the vidicon luminous flux is used directly for a change of resistance at separate points of the target, then in the ibicon it affects the photocathode, emitting, due to this, photoelectrons. Photoelectrons, getting in the accelerating field of the section of transfer, obtain high energy and strike against the semiconductor target. The target of the ibicon fulfills two functions - accumulation of charge and precommutation amplification of the photocurrent.

It is possible to present schematically the target of the ibicon II in the form of a thin plate of a semiconductor 2 (dielectric), confined between two conducting films 1 and 3, to which is applied voltage. The front (turned toward the photocathode) aluminum film 3, 0.2 μ thick, freely conducts photoelectrons accelerated by voltage of 20 kv and above to the layer of the semiconductor (dielectric), which causes the appearance of current I_ϕ (in the absence of photoelectrons there is practically no current in the semiconductor).

Appearance of a current of photoelectrons in the semiconductor evokes the appearance of induced current I. The ratio I/I_ϕ it is possible to consider as the amplification factor of the tube with respect to current, causing a corresponding light amplification of the image.

The ibicon tube (according to [23]) has a sensitivity 200 times better than the contemporary image orthicon. The tube makes it possible to obtain an image with a clearness of no less than 250 lines (operational surface of target 7 cm) during illuminance on the photocathode $3 \cdot 10^{-4}$ lux. The cesium oxide photocathode of the tube has a sensitivity of 40 microampere/lu and an accelerating voltage in the section of transfer of electron image equal to 30 kv, which ensures, at a given level of illuminance, a photocurrent of the order of 10^{-11} amp.

When using a cesium antimonide photocathode [24], the minimum level of illuminance of the photocathode is lowered to 10^{-5}—$5 \cdot 10^{-6}$ lux, which allows observation in the dark period of the twenty-four hours, on a clear moonless night.

Reassuring results were obtained also as a result of works with tubes of the image orthicon type. Adjustment of internal units of the image orthicon allowed increase in their sensitivity of 50-500 times. Thus, in the WL-7198 tube [25], intended for aircraft television equipment, only by increasing rigidity of internal construction could sensitivity and resolving power in conditions of vibrations and large accelerations be increased. This tube ensured the obtaining of an image with

clearness 250 lines during g-forces of [illegible], frequency of vibrations 50-500 cps, and illuminance of photocathode $3 \cdot 10^{-3}$ lux.

Moving grid from target 3-4 mm also promoted lifting of sensitivity of image orthicon due to the smaller influence of the potential of the grid on the potential relief of the target.

Recently there have been introduced new multi-alkali photocathodes with a sensitivity of 200 microampere/lu and above instead of 70-90 microampere/lu for bismuth silver. Such photocathodes will allow increase in sensitivity of image orthicons, increase in stability of their parameters, and longevity of operation [15].

However, there exists another very effective way of sharply increasing sensitivity of contemporary image orthicons, which solves the problem of intelligence at night with the help of television equipment. This way consists in the preliminary amplification of image brightness with the help of stage electron-optical amplifiers of brightness [15]. A diagram of such a tube with one amplifier stage of brightness is shown in Fig. VIII.20, and a general view - in Fig. VIII.21.

With the help of the objective, the image of the observed object is projected on the photocathode of the image converter, on whose screen is obtained an image amplified in brightness. In the case of one-stage amplification, the glow of the screen causes emission of electrons from the second photocathode, located on the other side of the film of the screen and starting the usual section of transfer of the image orthicon. During application of a two-stage amplifier, there occurs intermediate amplification of image brightness with the help of the first and second luminescent screens.

Sensitivity of such tubes depends on amplification of brightness in image converters. During coordination of spectral characteristics of radiation of screens and sensitivity of intermediate photocathodes, one stage ensures a current amplification of 10-20 times with an accelerating voltage of 10 kv; during two stages there can be obtained a 300-fold amplification.

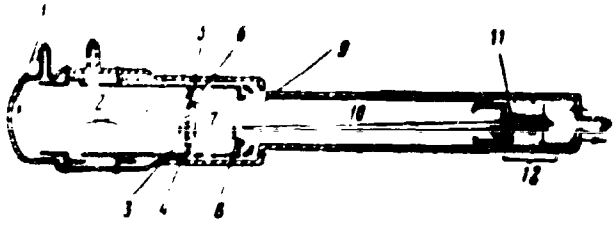

Fig. VIII.20 Diagram of image orthicon with one amplifier stage of brightness.
1—first photocathode; 2—forming of electron image; 3—aluminum film; 4—screen with phosphorus; 5—thin diaphragm from mica; 6—second photocathode; 7—secondary forming of electron image; 8—screen-trap; 9—thin glass target; 10—electron ray; 11—electron gun; 12—electron multiplier; 13—output of video signal.

Quantity of amplifier stages of brightness is limited by decrease in resolving power of instrument (especially along the edges of the field of sight), determined by aberrations of the electron-optical system and light scattering in films dividing the screens and intermediate photocathodes, and also granularity of screen. With optimum selection of thickness of film and granularity of screen resolution in the center of the field of sight can be obtained with one amplifier stage at 600–650 lines, but with two-stages - at 450 lines. A development type of such a tube, with a two-stage amplifier of brightness, made it possible to obtain an image with clearness not less than 100 lines during illuminance on photocathode of 10^{-6} lux.

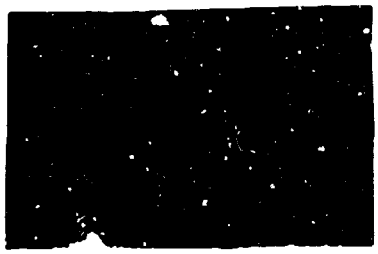

Fig. VIII.21. Image orthicon with one-stage amplification of brightness.

In Fig. VIII.22 is shown the dependency of the resolving power of studio image orthicon 1 and image orthicon with one amplifier stage 2 on the illuminance on the photocathode. In the same place there is given, theoretically calculated by Morton, curve 3 for an ideal instrument, in which there take place only fluctuations of photocurrent, and the sensitivity of which is limited not by noises of the electron beam, but by noises of the photocurrent.

The considered works in the region of creating highly sensitive transmitting television tubes allowed the development of equipment for carrying out recon naissance

on a moonless night (so-called "cat eye") [26, 27, 28], in which as a sensitive element is applied an image orthicon with one amplifier stage of brightness. It is noted that the sensitivity of the "cat eye" equipment is 1000 times higher than the sensitivity of the usual television cameras with image orthicon.

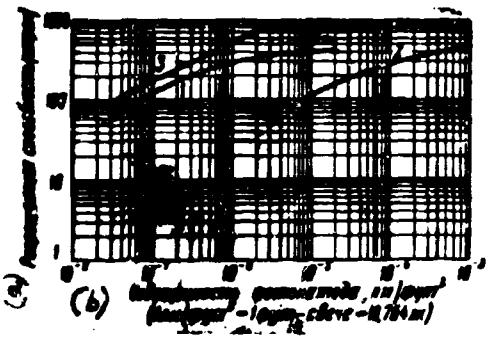

Fig. VIII.22. Dependency of resolving power of transmitting tubes on illuminance on the photocathode.
KEY: (a) Resolving power (lines); (b) Illuminance of photocathode, lu/foot (1 lu/foot^2 = 1 foot-candle = = 10.764 lux).

6. Instruments for Making a Thermal Map of a Site

As a rule, the methods of observation considered in preceding divisions use comparatively shortwave infrared radiation. An exception is the method of evaporation recording, in which for construction of an image practically all the radiation of the heated body participates.

During heat recording, on which is based the development of equipment for making thermal maps of sites, there is carried out the registration of all the spectrum of radiation, whose region is limited only by transparency of atmosphere and the optical elements of the recording instrument. However, application of long-wave radiation during heat recording is, at the same time, a deficiency of this method, since this radiation always accompanies the interferring scattered radiation of surrounding bodies, of the receiver itself, and so forth. Therefore, during heat recording, as during evaporation recordings, there will always be recorded a difference of temperatures (thermal contrast) between the observed object and the bodies surrounding it (background), and also between separate sections of the surface of the observed object.

Instruments for observation based on the heat recording method in general have to include: a receiver (thermoelement, bolometer, or other indicator) placed in the focus of the objective or spherical mirror with a small angle of sight, a turning device for an element-by-element examination of space, and a recording device for recording radiation intensity of each element of the examined space, and also a standard source of radiation for comparison of radiation intensity of the separate parts of landscape and a device compensating for radiation of the background.

As an example of such systems it is possible to present the photographic Beil telescope [29] and an instrument for thermal reconnaissance of a site [30].

The photographic Beil telescope is a system with an objective 30 cm in diameter, in whose focus is fixed a thermopile with a small time constant. The thermopile is connected in opposition to a compensating thermoelement having identical sensitivity but a large time lag. The resultant difference signal moves to the entrance of a highly sensitive galvanometer. Thus, the galvanometer reacts to a difference in the thermoelectric currents of the recording thermopile and the thermoelement irradiated by the total radiation of the landscape. The scanning of examined space is per line and is carried out by means of slow turn of telescope in a horisontal plane and a fast intermittent turn of it in a vertical plane around a horisontal axis. The turn of the mirror of the galvanometer at each given moment of time will be proportional to the surplus of temperature of the considered object above the average temperature of the background. A ray of light from the special source is reflected by the mirror of the galvanometer through a special triangular diaphragm to a photographic plate in such a way that its intensity, and, consequently, also the density of blackening of the photographic emulsion will be proportional to the angle of rotation of the mirror. The motion of the recording beam along the photographic plate is synchronized with the scanning system.

Time of exposure by the Beil instrument is rather long since all the considered picture is inspected by the turn of one sensitive element. Thus, if the time constant

of the recording thermopile is 0.1 sec, then it is possible to photograph only 10 points per second, and to obtain a full picture 10-35 minutes will be demanded, depending upon its dimensions. However, this time, in principle, can be reduced, increasing the quantity of receiving elements or preparing a mosaic of thermoelements.

In Fig. VIII.23 is a photograph of a water tower, taken due to its intrinsic emission from a distance of 1 km. Time of exposure was 10 minutes.

Fig. VIII.23. Thermal photograph of a water tower.

The instrument for photographing objects in the long-wave region of the infrared spectrum (Fig. VIII.24a) is, as in the first case, a device making it possible to obtain an image due to the difference in temperatures of separate elements of objects and the background. In distinction from the Beil telescope this instrument makes it possible to obtain a picture of the distribution of temperature along a surface by comparison of proceeding radiation with radiation of a standard black body.

The instrument (Fig. VIII.24b), with a total weight near 45 kg, consists of mirror-lens objective 1, in whose focal plane is placed a bolometer with amplifying diagram 2, turning mirror 3 synchronously connected with the system of recording 4 on photographic film 5, and a device regulating the intensity of recording beam 6 depending upon radiation energy hitting the bolometer.

In the focal plane of the mirror-lens objective is disposed a semiconductor bolometer, whose sensitive element is covered by a KRS-5 filter. The image of the observed object, by element, is projected on the objective with the help of the scanning mirror, located at an angle of 45° to the axis of the objective. Scanning of the image is carried out on a television principle - per line in a rectangular frame. Scanning time for the entire frame is determined by the sensitivity and time

lag of the bolometer, and also by the required degree of exposure of the parts and can be changed within 2-15 min with a bolometer time constant of 0.001 sec. The instantaneous field of sight of the "objective - sensitive element" system, which determines the resolving power of the instrument, is less than 30 angular minutes. The field of sight of the entire system is 10° vertically and 20° horizontally. The sensitivity of the instrument allows the recording of radiation of neighboring sections of the photographed object with a difference in temperature of 0.02°C. With such sensitivity the instrument can measure the surface temperature of the photographed object within limits of -170 — +300°C.

Fig. VIII.24a. General view of an instrument for photographing in the long-wave part of the infrared spectrum, the "Optitherm".

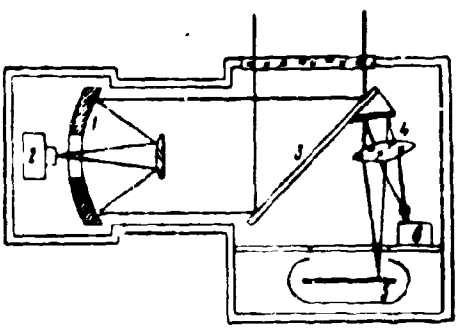

Fig. VIII.24b. Diagram of an instrument for photographing in the long-wave part of the spectrum, the "Optitherm".

Change of bolometer current after amplification is used for modulating the radiation of the neon tube of the glow discharge. Luminous flux of the glow discharge tube is scanned with respect to the usual photographic plate by the second mirror, synchronously connected with the scanning mirror. On the path of luminous flux propagation there is located a collimator lens, ensuring on the photographic plate a point image of the neon tube.

A bolometric receiver together with an objective, a modulating device, and a black body are placed in a massive housing to prevent changes in ambient temperature from affecting quality of image.

With the help of a special sector disk (modulator), rotatable by motor, the sensitive element of the bolometer is alternately subjected to irradiation from the

direction of the photographed object and the black body (Fig. VIII.24c). For that, opaque sectors of the modulator, not conducting direct radiation of an object to the bolometer, have on the rear side (turned to the bolometer) mirror surfaces. Radiation of a black body by means of a reflecting mirror inclined at an angle of 45° to the optical axes of the instrument, and of a black body at the moment when the entrance of the bolometer is covered by the sector modulator, gets on the bolometer.

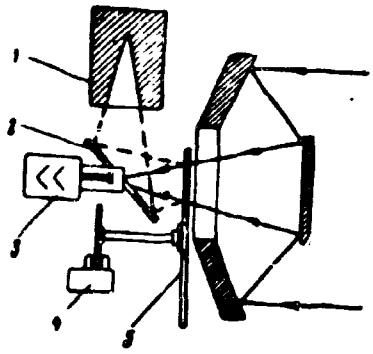

Fig. VIII.24c. Diagram of the head of the "Optitherm": 1--standard black body; 2--deflecting mirror; 3--bolometer with amplifier; 4--synchronizer; 5--modulator.

A second disk put on the same axis modulates radiation of a special tube, irradiating a phototriode intended for the oscillating of synchronizing signals. Comparison of phase relationships and amplitudes of signal from the bolometer at the moment of its irradiation by a black body (synchronizing signal) and by the photographed object gives the possibility of determining relationship of temperatures of the photographed object and the standard black body. In Fig. VIII.25 there is a photograph of a man, obtained with the held of the "Optitherm."

Fig. VIII.25. Image, obtained in full darkness with the help of the head of the "Optitherm."

Table VIII.3. Basic Data of the Radiometric Head of the "Optitherm".

Designation of parameter	Variety of bolometer		
	I	II	III
Dimension of receiver, mm	0.3 X 0.3	1.0 X 1.0	2.5 X 2.5
Instantaneous field of sight, degree	1 X 1	0.2 X 0.2	0.5 X 0.5
Time constant, sec	0.016	0.016	0.016
Sensitivity, w/cm^2	$2 \cdot 10^{-11}$	$6.7 \cdot 10^{-11}$	$1.7 \cdot 10^{-10}$
Equivalent temperature noises, °C	0.1	0.03	0.01

7. Observation from Space

Successful realisation of launchings of artificial earth satellites, capable of being in space near Earth for a long period of time, and successes in the region of radio electronics have made it possible to solve the problem of the observation (reconnaissance) of ground objects from space.

It is indicated that such reconnaissance in the case of launching a satellite on a polar orbit can be conducted for the purpose of obtaining information about military objects and for collection of data about forming of overcast of terrestrial atmosphere, which is necessary for exact weather forecast in any region of the globe.

In a published account in the United States of the Laboratory of Interplanetary Reconnaisance, "Basic Considerations About Conducting Reconnaissance from Satellites", [31, 32, 33] there are considered the physical capabilities and limitations of such equipment. From a large number of physical and structural questions the authors of the work separate three basic problems, knowledge of which is necessary for the creation of an actually effective means of intelligence. Among them are: peculiarities of radiation of the earth's surface, propagation of radiant flux long distances through atmosphere, and resolving power of equipment.

The earth as a source of radiant flux in space can be considered as a body, in the radiation of which are observed three components: reflected solar radiation, intrinsic low-temperature radiation, and radiation of artificial sources created by the activity of man.

The solar radiation reflected by earth's surface has a maximum spectral density of radiation in the visible part of the spectrum. It is determined both by irradiance of earth's surface and by its reflectance (albedo). In turn, irradiance of earth's surface depends on height of Sun, geographic latitude, time of the year and the day, and also on the state of the atmosphere.

Outside the atmosphere irradiance due to solar radiation constitutes 1.94 cal/cm^2·min, which in photometric units corresponds to illuminance of 13,600 foot-candles ($\frac{\text{lumen}}{\text{foot}^2}$) [1 foot-candle (1 $\frac{\text{lumen}}{\text{foot}^2}$) = 10.764 lux ($\approx$ 10.764 $\frac{\text{lumen}}{\text{m}^2}$)].

Due to losses in the atmosphere, illuminance of earth's surface at noon of a clear day can attain a maximum magnitude of 10,000 foot-candles, where 80% of the illuminance is caused by straight solar beams, and 20% is due to light scattered by the atmosphere. The value of average albedo of earth's surface and atmosphere oscillates within limits of 0.32-0.5ρ depending upon the state of the overcast, the variety of natural formations, the angle of incidence of radiant flux and its spectral composition. For a mean value of Earth's albedo is taken the magnitude 0.45.

Clouds, water, and snow reflect radiant flux very well. If reflection from clouds depends on their thickness and water content and preserves its constancy up to 3 μ, then green, having low reflection in the visible part of the spectrum, sharply increases its albedo in the infrared part of the spectrum. Reflectance of the smooth surface of water depends on height of Sun ($Z_\odot$) and during angles of incidence of radiant flux smaller than 40°, reflection is practically absent (at $Z_\odot$ = 43° ρ = 0.02, and at $Z_\odot$ = 85° ρ = 0.4).

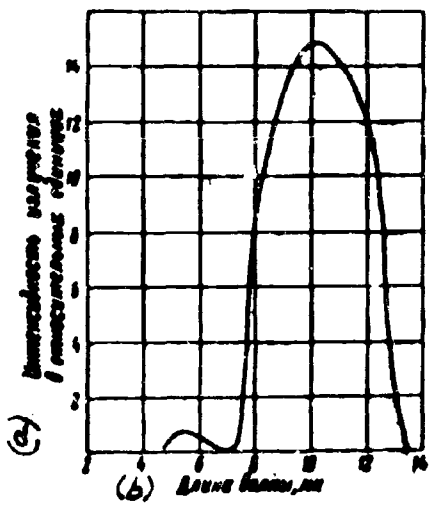

Fig. VIII.26. Radiation of Earth, going out beyond the limits of the atmosphere (by Fari).
KEY: (a) Intensity of radiation in relative units; (b) Wave length, μ.

Low-temperature radiation of Earth in space is the result of absorption of solar energy. It has a ontinuous spectrum in a wave range of 4-40 μ with maximum near 12 μ; however, due to selective absorption by atmosphere beyond its limits radiation goes out in a narrower spectral section (Fig. VIII.26). This radiation changes little during the twenty-four hour day and creates uniform background around Earth. In spite of the fact that the average temperature of Earth is equal to 287°K, the temperature of its effective radiation constitutes 252°K because of absorption of radiation energy by water vapor, carbon dioxide, and ozone.

The third component - radiation of artificial sources on Earth - differs from the first two both in its temperature and in its dimensions. They have surface temperatures significantly exceeding, sometimes, the temperature of earth's surface, different spectral composition of radiation, and, according to the character of their location, carry a local character which makes it possible to distinguish them on the background of low-temperature radiation of Earth.

During the observation, from very large distances, of separate sections of earth's surface, a serious problem is the lessening of their observable contrast because of the presence of a light halo around Earth and the scattering of radiant flux in the atmosphere.

Statistics shows [32] that absolute contrast of the overwhelming majority of ground objects is very small. Thus, in visible light in 95% of all cases contrast

constitutes 0.2, and in 90% of the cases - less than 0.1. During observation from large heights visible contrast decreases still more. In Fig. VIII.27 there is given the dependency of relative (observed) contrast on height of observation. From this dependency it is clear that already during observation from a height of ~ 3000 m the relative contrast of objects decreases 2-2.5 times.

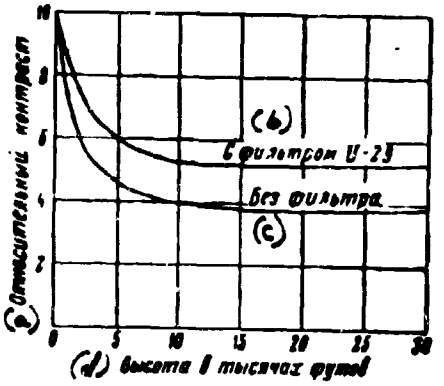

Fig. VIII.27. Lessening of observable contrast with height.
KEY: (a) Relative contrast; (b) With filter; (c) Without filter; (d) Height in thousand feet.

Further lowering of contrast of observable objects can lead to the fact that the magnitude of the signal given out by the system of image construction will decrease so much that it will become commensurable with the fluctuating noises of the reconnaissance equipment. At present it is considered that it is possible to detect objects of sufficiently large dimensions, if their contrast with the surrounding background exceeds 0.02.

Decrease of contrast between objects not only lowers the energy capabilities of reconnaissance equipment, but also worsens its resolving power.

Since weakening of the contrast of ground objects during observation from large heights is connected with the state of the atmosphere and, consequently, with the optical mass of the atmosphere, then one should expect improvement of conditions of observation during transition to a wave range of longer wave lengths, since with this equivalent optical mass of the atmosphere decreases and, as a result, the coefficient of brightness of air haze decreases.

In Fig. VIII.28 are given the dependencies of the optical mass of the atmosphere on wave length and of the coefficient of brightness of air haze on the magnitude of the optical mass of the atmosphere at different heights of Sun Z_θ. As can be seen

from these curves, the optical mass of the atmosphere decreases by three times during transition from observation in visible light to observation in the near-wave infrared region of the spectrum.

When accomplishing reconnaissance farther into the infrared region of the spectrum artificial heat-radiating objects will be observed on the background of low-temperature radiation of Earth. In this case selection of the range of wave lengths of the recording device is determined both by the transparency of the atmosphere and by the contrast of objects relative to the low-temperature background of Earth. For the majority of objects contrast with the surrounding background will grow in a wave range of 3-6.5 μ (Fig. VIII.29) due to their maximum radiation and the absence of radiation of Earth in this section of the spectrum. In a region of longer waves (6.5-12 μ) contrast again starts to decrease because of the sharp growth in the intrinsic emission of Earth.

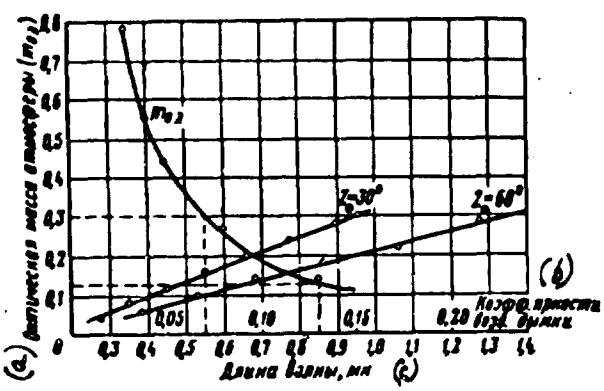

Fig. VIII.28. Dependencies of the optical mass of the atmosphere on wave length and of the coefficient of brightness of air haze on the optical mass (at different heights of Sun $Z_\odot$).

KEY: (a) Optical mass of the atmosphere ($m_{o\lambda}$); (b) Brightness coefficient of air haze; (c) Wave length, μ.

The necessity of registering, from large distances, comparatively small-size targets presents very hard requirements with respect to resolving power of reconnaissance systems established on artificial earth satellites and on other space craft. Therefore, for conducting reconnaissance of small-size objects it is considered expedient to set up as a basis a principle, similar to photographic, with transmission of data on radiotechnical communication lines [34]. Furthermore, it is indicated that at the contemporary state of technology the most probable conditions of reconnaissance from very

large heights are considered to be an illuminance of earth's surface of the order of ~86,000 lux, i.e., the conditions of "clear sun," since during illuminance of the order of ~43,000 lux brightness contrasts between ground objects scarcely makes it possible to distinguish their images. In this connection the most probable is the application of television methods with preliminary electron-optical amplification of light. An experiment of photographing by day, through the thickness of the atmosphere, the planet Jupiter and its satellites, with the help of the "cat eye" equipment, confirms this [35].

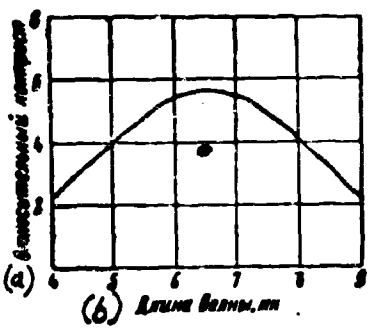

Fig. VIII.29. Relative contrast of ground formations during observation of them in different sections of the spectrum.
KEY: (a) Relative contrast; (b) Wave length, μ.

Since preliminary research, conducted at launches of the "Viking" rocket vehicle it possible to obtain, with a short-focused camera, photographs of earth's surface from a height of 258 km, on which it was possible to distinguish railroad junctions, runways and other details on a site, it was decided to assume a photographic principle as a basis of obtaining an image by the WS-117 system.

The "Samos" satellite was sent into a polar orbit with a maximum distance from Earth of 800 km. The area examined by equipment of the satellite constituted nearly 500 km^2.

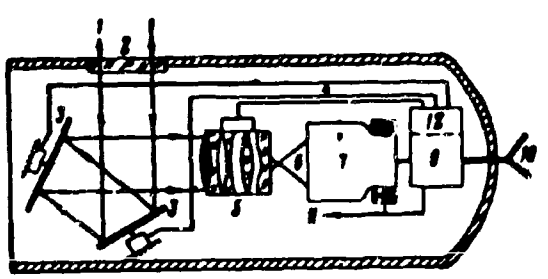

Fig. VIII.30. Block-diagram of the equipment of a reconnaissance earth satellite on the WS-117 project.

Reconnaissance equipment from artificial earth satellites in the United States began to be developed in 1956 [34]; in the beginning under the code "Big Brother", and then the project was appropriated the code WS-117.

In 1961 into orbit around Earth was launched a reconnaissance satellite "Samos," equipped with special combined reconnaissance equipment with transmission of data to Earth on a television channel.

In Fig. VIII.30 is shown an approximate skeleton diagram of the WS-117 reconnaissance system. The energy of radiation reflected from earth's surface 1, passing through entrance window of satellite 2, is projected on objective 5 with the help of two mirrors 3 stabilized in space. The objective has variable focal length for obtaining small-scale and large-scale image of photographed surface. As a sensitive element is applied a television transmitting tube of heightened sensitivity with one-stage amplifier of brightness 6. Subsequently, a video signal with the help of broad-band transmitter 9 and antenna 10 is transmitted to ground receiving stations, where visual or photographic registration of obtained images is carried out.

The problem of continuous orientation of the satellite in such a way that the optical system is always turned in the direction of the photographed surface of Earth and the constancy of the entrance angle of radiant flux to the objective is ensured was solved by application of a stabilizing device, developed in 1953. This device, consisting of two flat mirrors and an objective suspended on gimbal rings of stabilizing gyroscopes, allows the mutual displacement of three elements relative to one another on command from the ground stations. For this, there is receiver 12, giving out special signals, which control the stabilizing device and objective during change of scale of survey (circuit 4). Along this circuit move commands from the basic gyroscopic assembly which stabilizes the flight of the satellite. The power supply of equipment on circuit 11 is carried out from the general source of electric power for the satellite.

The second trend in the creation of reconnaissance systems, which at present has found practical application, consists of the development of infrared equipment with long-wave receivers for obtaining information about the forming of overcast above the surface of the globe.

In 1958 in the United States was launched the second artificial earth satellite in the "Vanguard" project, on which was fixed an infrared reconnaissance equipment, obtaining the name "atmospheric eye". The purpose of this equipment is to register and transmit to receiving stations the formation and density of overcast by different sections of the earth's surface, necessary for the composition of exact weather forecasts [38, 39].

In construction, the equipment consists of two telescopic systems with mirror optics fixed at an angle of 45° to one another on the external surface of the spherical artificial earth satellite, a system of recording obtained signals on magnetic tape, and a telemetric channel for transmission of data from the magnetic tape to Earth.

A parabolic mirror and an uncooled lead sulfide photoresistor are fixed in a cylinder 7.5 cm in diameter (Fig. VIII.31) of stainless steel 0.25 mm thick, whose external surface is gold-plated to decrease the influence of outside radiation.

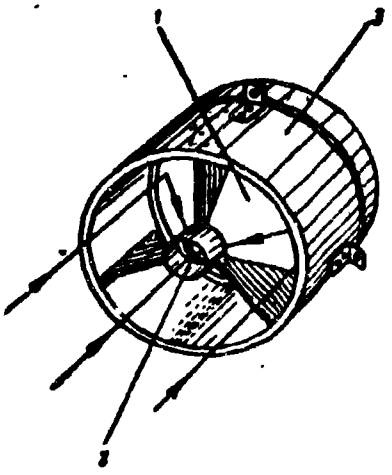

Fig. VIII.31. Receiving device for registration of overcast from earth satellites: 1--parabolic mirror; 2--receiver; 3--body.

Candle-power of the optical system, in order to guarantee fast scanning along the surface of the clouds, is very great - 1:0.7. The lead-sulfide photoresistor, being in the focus of the mirror, has an operational area equal to 1 mm^2. The operational surface of the photoresistor is covered by an infrared filter, cutting the visible radiation.

Power is supplied to the photoresistor from silicon solar batteries, mounted directly in the casing of the photoresistor. The weight of the receiving device is 100 g.

During flight of a satellite on a circular orbit at a height of 560 km the optical system of every receiver examines an area 11 X 11 km strictly under itself and 90 X 90 km on the edges of the disk of Earth. Speed of rotation of the satellite around its vertical axis constitutes 1 rps. The difference signal from the two photoresistors, modulated with a frequency of 290 cps, after amplification proceeds, for recording, to the magnetic tape, from which after a definite time it is read and transmitted by a telemetric communication line to a receiving point.

This equipment in such a form can scarcely find application for reconnaissance of small-size heat-radiating objects, since its resolving power is very low. However, there is no doubt that subsequently, with improvement of it, especially with improvement of resolving power, similar equipment on photoresistors may be used for detecting certain big objects, whose surface temperature differs from the temperature of the surrounding background.

Literature

1. Functionale Photography, 1955, Vol. 6, No. 5.
2. Army-Navy-Air Force J., 1957, Nov., Vol. 45, No. 11.
3. G. K. Brok. Physical bases of aerial photography. Geodezizdat, 1958.
4. A. Clark Photography by Infra-red, London, 1946.
5. "New military technology". Collection of articles. Voyenizdat, 1958.
6. IRE Trans. Telemetry and Remote Control, 1955, Vol. TRC-1, No. 2.
7. "Advances of physical sciences", 1956, Vol. IX, Issue 2.
8. Science, 1956, Vol. 123, No. 3193.
9. Discovery, 1956, May, Vol. 17, No. 5.
10. Instrum, and Automation, 1957, Feb., Vol. 30, No. 2.
11. Nature, 1958, Mar., Vol. 181, No. 4610.
12. Bur. Ships J., 1956, Vol. 4, No. 11.

13. Radio and Telev. News, 1955, Apr., 54, No. 4.

14. Translation No. 12318, BNT.

15. Proceedings National Electronics Conf., 1958, Vol. 13.

16. A. A. Gershun. Principle and methods of light camouflage. State Power Engineering Publishing House, 1948.

17. V. V. Meshkov. Illuminating installations. State Pow Engineering Publishing House, 1947.

18. "Reports of the Academy of Sciences of the USSR", 1956, Vol. III, No. 5.

19. Electronics, 1958, 26 Sep., Vol. 31, No. 39.

20. S. B. Gurevich. Physical processes in transmitting tubes. Fizmatgiz, 1958.

21. Phys. Rev., 1950, Vol. 79.

22. Proc. Phys. Soc., 1951, Vol. A36, p. 362.

23. National Convent Record IRE, 1957, pt. 3, p. 5.

24. Electronics, 1956, Nov., Vol. 29, No. 11.

25. Proc. IRE, 1957, Vol. 45, No. 4, p. 12A-13A.

26. J. of the Franklin Inst. 1957 Jun., Vol. 263, No. 6.

27. Army-Navy-Air Force J., 1955, 17 Dec.

28. Electronics, 1956, Mar., No. 3.

29. M. A. Ango. Infrared radiations. State Power Engineering Publishing House, 1957.

30. JOSA, 1959, Feb., Vol. 49, No. 2.

31. Aviation Week, 1959, 19 Jan.

32. Aviation Week, 1959, 26 Jan.

33. Aviation Week, 1959, 2 Feb.

34. American Aviation, 1956, 2 Jul.

35. Electronics, 1958, 15 Aug., Vol. 31, No. 33.

36. Aviation Daily, 1958, 19 Jun., Vol. 116, No. 35.

37. Aviation Week, 1957, 4 Oct., Vol. 67, No. 15.

38. Aviation Week, 1958, 18 Jul., Vol. 69, No. 7.

39. Missiles and Rockets, 1958, Jun., Vol. 3, No. 7.

CHAPTER IX

HEAT-DIRECTION FINDING SYSTEMS

1. The Operating Principle and the Arrangement of Heat-Direction Finders

Under heat-direction finder we understand an optical-electromechanical device intended for determination of angular coordinates of ground (naval) and air targets by their own thermal radiation.

Fig. IX.1. Fundamental diagram of the simplest heat-direction finder.

The fundamental diagram of such a device (Fig. IX.1) in the simplest case should include section 1 with sensitive element and amplifier, synchronizer 2, and indicator 3.

Thermal radiation of a target is perceived by the optical system and moves to the sensitive element, and the synchronizing device, on signals obtained from the amplifier of photocurrent, allows determination of its angular position relative to the optical axis of the receiving device. The position of the target can be visually observed in the form of a luminescent mark on the indicator instrument or fixed in the form of electrical signals proportional to its coordinates.

Heat-direction finding devices can be subdivided into two broad classes: scanning systems and scanning-follow-up or follow-up systems. The last ones have found wide application in homing guidance systems and will be considered in Chapter X.

Scanning heat-direction finders solve a narrower circle of problems and are designed for investigation, detection of target, and determination of direction to it. Scanning heat-direction finders find wide application for detection of heat-radiating targets, in fire control stations, and in equipment for thermal reconnaissance of a site.

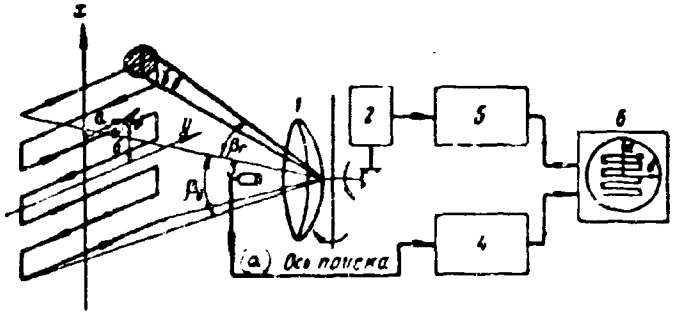

Fig. IX.2. Structural diagram of a scanning heat-direction finder. KEY: (a) Axis of scan.

The structural design of a scanning heat-direction finder (Fig. IX.2) in general should include the following basic elements: receiving optical device 1 picking up thermal radiation of a target and directing it to sensitive element, scanning system 2 which ensures scanning motion of receiving device on a given principle, sensitive element 3 converting thermal radiation from the target into an electrical signal, amplifier of photocurrents (voltage) 4, system of sweep and synchronization 5 ensuring creation of sweep on the screen of the indicator instrument which repeats the character of displacement of the optical axis of the receiving device during scanning of space, and indicator instrument 6 allowing visual estimation of target position relative to some axis.

A system of investigation or scanning is a necessary element in any heat-direction finder and, therefore, the selection of kinematics of motion of the receiving device, based on requirements for guaranteeing the best scanning conditions and the greatest probability and speed of target detection is an important problem.

The most widely applied, at present, method of examination of space is scanning by pencil beam or, as is sometimes called, scanning by [illegible] beam [1]. In this case the pencil beam, formed by a system "of an optically sensitive element" (angle γ in Fig. IX.2), on a given law of motion, examines space in a definite solid

angle - angle of sight ($\beta_в$, $\beta_г$). The period for which examination of this angle occurs is called the scanning period of the heat-direction finder.

Scanning of space by a needle-shaped beam allows:

determination of both angular coordinates of the target (ε, η on Fig. IX.2) simultaneously and ensures that they are single-valued;

increase in noise immunity of systems by lowering the influence of background during a narrow angle of sight;

increase in range of heat-direction finder, and

ensures rational modulation of thermal radiation proceeding from target.

From the point of view of tactical application any scanning heat-direction finder should ensure the most probable detection of target and have a small scanning period, but the indication of the target on the screen should ensure the possibility of determining position of target and its displacement in space.

Satisfaction of these requirements is determined in some measure by the law of displacement of a needle-shaped beam in space. In this case it is possible to separate two groups of scanning diagrams - with axial symmetry and plane. In the first case the examined region is limited by a conical surface (normal section is a circle), in the second - by a dihedral angle and two conical surfaces (normal section approaches rectangular or oval).

If angular displacement of the scanning beam in space is broken down into basic and movable, then depending upon the magnitude of the ratio of periods of basic and migratory motion, in each group it is possible to distinguish scanning of straight and reverse sequence and inconsistent scanning. Furthermore, each of these forms of scanning it is possible to subdivide into normal and alternate-line. The last ones are used to decrease scanning period, although with this the quantity of unexamined sections is increased.

In Fig. IX.3 are given forms of trajectories of beam with different kinematic diagrams for scanning.

... scanning ... and has the best dynamic characteristics, i.e., it a ... better compensation of inertial forces (especially scanning with reverse sequence).

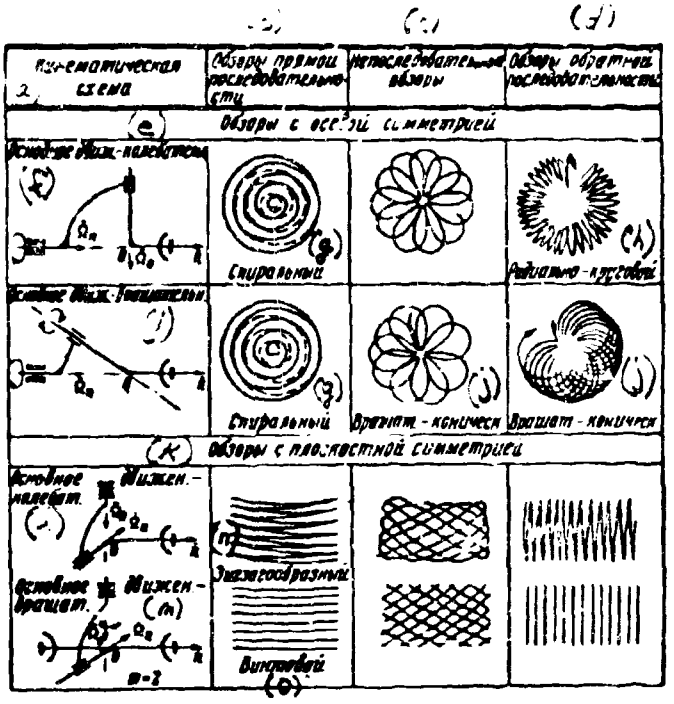

Fig. IX.3. Forms of beam trajectories during scanning.
KEY: (a) Kinematic diagram; (b) Straight sequence scanning; (c) Inconsistent scanning; (d) Reverse sequence scanning; (e) Scanning with axial symmetry; (f) Basic motion-oscillation; (g) Spiral; (h) Radial-circular; (i) Basic motion-rotation; (j) Rotation-conical; (k) Scanning with plane symmetry; (l) Basic motion-oscillation; (m) Basic motion-rotation; (n) Zigzag-shaped; (o) Helical.

In construction the scanning system can be carried out differently. In Fig. IX.4 are certain forms of scanning systems [2].

In the scanning system with exploring disk I the latter is disposed in the focal plane of the objective in direct proximity to the photosensitive layer. During its rotation, radiant flux hits the photosensitive layer through holes located on the spiral. Angle of sight with such a system is determined by the parameters of the objective and the dimensions of the photosensitive layer, which in this case should be sufficiently large, and the angular dimension of the needle-shaped beam (instantaneous angle of sight) - by the objective and diameter of the hole in the disk.

In mirror-lens systems II exploration motion is carried out by a flat mirror in two planes. As a result of such motion there occurs scanning of space by a pencil beam, whose angular dimension is determined by the parameters of optics and

dimension of the photosensitive layer. Angle of sight in this case is determined by the magnitude of angular displacement of the flat mirror.

Per line scanning III can be carried out by rotation of several objectives, located along a spiral on a cylindrical surface, in the center of which is disposed a photosensitive layer. Instantaneous angle of sight in this device is determined by arameters of objective and dimension of photosensitive layer, but the angle of sight of the system is determined by the angles of inclination of objectives relative to the cylindrical surface on which they are located.

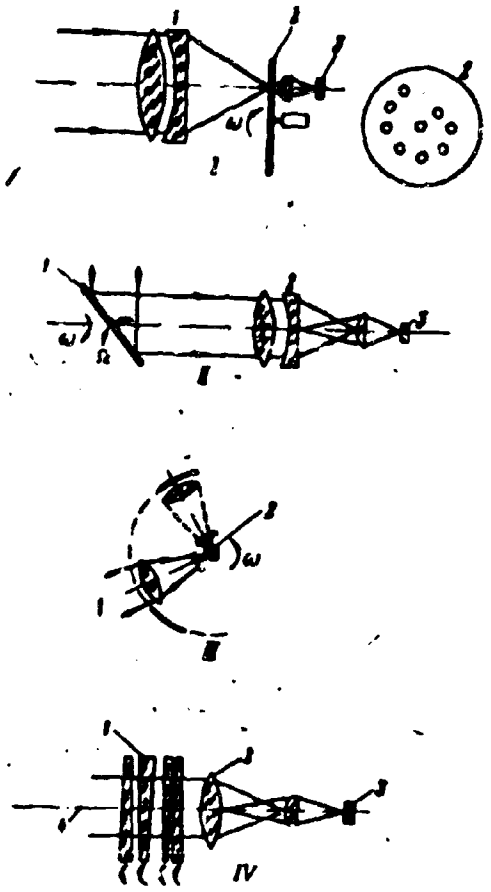

Fig. IX.4. Scanning optical systems: I--system with exploring disk: 1--receiving optics; 2--exploring disk; 3--receiver. II--system with flat receiving mirror: 1--scanning mirror; 2--objective; 3--receiver. III--system with revolving objectives; 1--receiving optics; 2--receiver. IV--system with revolving optical wedges: 1--revolving optical wedges; 2--objective; 3--receiver; 4--scanning axis.

A property of optical wedges is to deflect toward the base radiant flux passing through them. They also may be used for creating scanning motion. Such a system IV has two pairs of optical wedges, fixed before the objective and revolving, each pair in opposition. During their rotation effective refracting angle at summit changes and, due to this, deflection of the needle-shaped beam with respect to scanning angle is changed. Magnitude of scanning angle is determined by the material from which the wedges are made and the refracting angle at summit, but the angular dimension of the

[illegible] of heat is determined by the objective and dimension of the [illegible] sensitive layer.

Selection of the character of the scanning and its constructive fulfillment are determined by the purpose of the heat-direction finding [illegible], [illegible] fulfillment, and tactical-technical requirements. As an example of the work of an optical receiving device with scanning by a needle-shaped beam, we will consider the work of a receiving device of a heat-direction finding system for taking a thermal map of a site [2]. The given system is established on an aircraft and should ensure the reproduction, on the screen of an indicator instrument, of the thermal relief of the site above which the aircraft flies.

Aircraft at height H moves with groundspeed v. The scanning device of the equipment has a needle-shaped beam with angle of sight γ, composing a unit of angular minutes. The scanning field of the system will be formed by the rotation of a receiving optical element at angle 2β around an axis parallel to the longitudinal axis of the aircraft. Thus, during a turn of the receiving element at angle 2β there is carried out an examination of space in the form of a line. Depending upon the speed of flight of the aircraft and the speed of rotation of the receiving element the scanning lines traced on the site can be disposed either with omissions or overlapping. As the receiving scanning device in the considered equipment is applied a prism with n reflecting surfaces, revolving with speed r. Thus, after one turn of the prism on the site are traces n lines.

For the satisfactory work of equipment it is necessary to fulfill the following conditions:

a) to guarantee good resolving power angle γ should be very small, and scanning speed maximum. However, the latter is limited by the time constant of sensitive element τ;

b) time of displacement of image of site along sensitive element should not be less than $k\tau$ (k — positive number, characterizing reserve of time lag of sensitive

element. Number of resolvable elements in a unit of time will be determined by expression $2\pi r\gamma$, and, consequently, time of displacement of image on an angular magnitude corresponding to the angle of sight will be $\gamma/2\pi r$. Consequently, there is required fulfillment of inequality

$$k\tau \leqslant \frac{1}{2\pi r}. \qquad (IX.1)$$

The scanning device should work with such speed that there are no omissions on image of site. In the direction of flight the bandwidth of capture will be γH, and the width of capture for a unit of time γHnr. So that there are no omissions, there is required $\gamma Hnr \geqslant v$. From this relationship and from expression (IX.1) it follows that

$$r \geqslant \frac{1}{2\pi nk\tau} \text{ and } r \geqslant \frac{v}{Hn\gamma}. \qquad (IX.2)$$

Excluding r and γ from expressions (IX.2), we will obtain correspondingly:

$$\gamma \geqslant \sqrt{\frac{2\pi k}{n}\frac{v}{H}\tau}, \qquad (IX.3)$$

$$r \geqslant \sqrt{\frac{1}{2\pi kn}\frac{v}{H}\frac{1}{\tau}}. \qquad (IX.4)$$

Thus, the necessary instantaneous scanning angle of equipment for taking a thermal map of a site is determined by ratio $\frac{v}{H}$ and the time constant of the photosensitive element $k\tau$.

The value of magnitudes v and H, entering into expressions (IX.3) and (IX.4), are determined by the tactical application of the equipment, and $n = \frac{360}{2\beta}$.

For instance, for case H = 300 m, v = 300 m/sec, k = 2, n = 2, $\tau = 10^{-3}$ sec, we obtain $r = 360 \frac{\text{deg}}{\text{sec}}$, $\gamma \approx 0{,}5° \approx 10$ m·rdn.

Naturally, such an angle of sight cannot ensure good resolving power. For its improvement, with guarantee of site examination without omissions, it is necessary either to increase speed of scanning with a significant decrease in time constant of photosensitive layer or to apply mosaic photosensitive layers. In the latter case formulas (IX.3) and (IX.4) take the form

$$\gamma \geq \sqrt{\frac{1}{2\pi k n N}\cdot\frac{D}{H}\cdot\frac{1}{\tau}}. \qquad (IX.5)$$

$$\gamma \geq \sqrt{\frac{2\pi k}{nN}\cdot\frac{D}{H}\cdot\tau}. \qquad (IX.6)$$

where N - number of elements in mosaic.

Thus, if in the case of the preceding example we take $\tau = 10^{-6}$ sec, N = 9, then $\gamma = 3'$, which will allow us to have the equipment for taking a thermal map of a site with sufficiently high resolving power.

A somewhat different picture is observed during the use of similar equipment from great heights. Although during flight at 300 m altitude angular resolution at 1 mrdn gives a linear resolution of 30 cm, during flight at H = 30,000 m to obtain the same linear resolution there is required an angular resolution of 10^{-2} mrdn. Considering the expression for the limiting diffractional resolution of optical systems $\gamma = 1{,}22\,\frac{\lambda}{D}$, one can determine that even in this best case the diameter of entrance optics D during $\gamma = 10^{-2}$ mrdn and $\lambda = 10\,\mu$ should be equal to ~ 120 cm. Thus, the possibility of the application of equipment for taking a thermal map of a site from great heights can be affected by the technical limitations and, in the first place, the possibility of distribution of equipment on the aircraft.

When appraising the resolving power of heat-direction finding instruments for reconnaissance of a site, one should consider the inconstancy of linear resolution with respect to field of sight for such systems. It worsens as the optical axis of the scanning device deflects from vertical.

2. Prospects of Development of Heat-Direction Finding Systems

With the development of military technology heat-direction finding systems have obtained even greater development for all kinds of troops. Proceeding especially intensely is the work on the creation of semiautomatic and automatic infrared stations of detection and fire control.

In fire control stations requirements for devices which ensure the detection function (scanning) and aiming (tracking), are contradictory. An exploration device must ensure a high probability of target detection at great distances and at large scanning angles after a minimum scanning time. It must have high resolving power in order to reveal and determine the bearing of all targets in the field of sight.

The tracking device must have high angular accuracy and, as a rule, ensure determination of coordinates of one selected target.

Although in radar stations, as a rule, due to structural and size requirements both functions can be carried out in one device, for infrared systems sometimes it is more profitable to have scanning and follow-up system carried out separately.

In Table IX.1, there are presented, as an example, the basic requirements which must be satisfied by heat-direction finding fire control stations developed in the United States for the Air Force [3].

As follows from the given data, to the systems of detection are presented strict requirements with respect to distance and scanning angles.

In systems with a needle-shaped beam these requirements are contradictory; for instance, increase of scanning angle requires increase of area of sensitive element, but this leads to decrease of its sensitivity, which is equivalent to decrease of range, and also to increase of scanning time and impairment of resolving power.

Consequently, in systems with one sensitive element, whose area is small in order to guarantee necessary range, during scanning by a needle-shaped beam it is difficult to ensure the necessary magnitude of scanning field. Furthermore, scanning by a needle-shaped beam requires complicated kinematic diagram of the scanning system.

A way out of this situation is to change one sensitive element to a mosaic of a large number of small sensitive elements. In this case a system with a mosaic

consisting of N sensitive elements theoretically should be $\sqrt{N}$ times more sensitive than a system with one sensitive element similar in assignment, but with the same scanning field and the same speed of scanning motion.

Table IX.1

Designation of parameter	Unit of measurement	System of scanning	System of tracking
Basic assignment	--	Detection of all targets in the field of sight	Retention of one target in field of sight in the presence of several targets
Free-space range	km	20—100	10—20
Field of sight	deg	20—180	1—20
Angular resolving power	deg	1	0.05
Frequency of modulation (frequency of frames)	frames/sec	0.1--4	4—100
Output data	--	Position of target (two coordinates) Intensity of radiation Dimension of target Temperature of target	Position of target (two coordinates) Speed of change of position of target (two coordinates)

Transition to mosaic sensitive elements, naturally, is connected with the solution of a series of additional problems: the difficulty of manufacturing photosensitive layers with identical parameters, increase in the number of amplifiers or application of a commutating device for successive connection of elements of the mosaic to the general amplifier, lowering of noises etc.

At present there are known three types of systems with mosaic sensitive elements, for which,

a) every element of the mosaic has a separate amplifier;

b) all elements of the mosaic are successively connected to the general

amplifier;

c) the mosaic is replaced by a infrared vidicon.

Of greatest interest is the second group of systems [5], whose work may be clarified by Fig. IX.5.

The scanning angle of a heat-direction finder is determined by "objective - mosaic" system, with which system examination of the site within limits of the scanning angle is carried out by a motionless beam, formed by each separate element of the mosaic. Thermal radiation from the target, preliminarily modulated by a disk modulator, is focused by the optical system on one of the elements of the mosaic. Depending upon which of the elements of the mosaic gets the radiation energy of the target, from it is removed the signal, which until commutation is stored in the tuned oscillation circuit. With the help of a mechanical commutator, the rotor of which by turn visits all elements of the mosaic, the signal from the oscillation circuit moves to the entrance of the amplifier. After amplification the signal moves to the indicator instrument, whose sweep is synchronized with the rotation of the commutator. Therefore, the position of the mark on the screen of the indicator instrument will correspond to the position of the target relative to the optical axis of the receiving device.

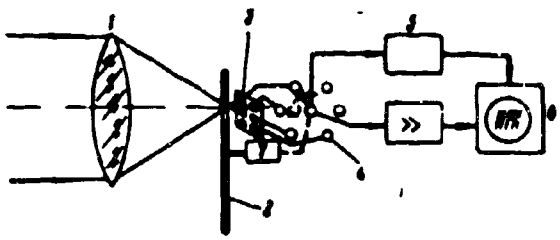

Fig. IX.5. Fundamental diagram of a system with a mosaic sensitive element and a general amplifier: 1—receiving optics; 2—modulation disk; 3—mosaic receiver with circuits; 4—commutator; 5—scan unit and synchronization; 6—indicator block; 7—motor.

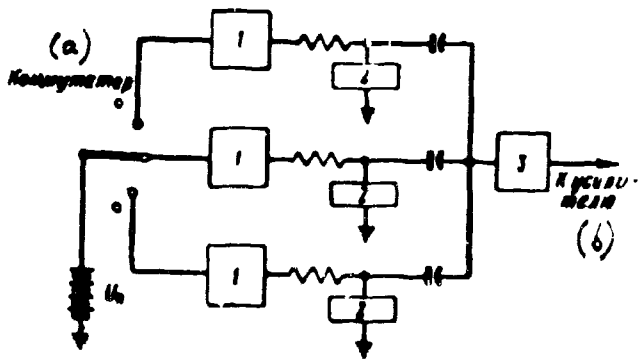

Fig. IX.6a. Diagram of commutation of supply voltage of separate elements of a mosaic. 1—narrow-band filter; 2—element of mosaic; 3—broad-band filter. KEY: (a) Commutator; (b) To amplifier.

As commutating diagrams may be applied a diagram of commutation of the supply voltage passed to separate elements of the mosaic (Fig. IX.6a), and a diagram of commutation of signals removed from the elements of the mosaic (Fig. IX.6b).

With commutation of supply voltage there appears one difficulty, connected with the fact that the duration of the transition process during supply of voltage to an element of the mosaic may be significantly more than duration of the signal from the target. To decrease the time of the transition process it is necessary to filter supply voltage with the help of multi-unit electrical filters. Consequently, with such a method of commutation, for every element of the mosaic it is necessary to provide compact multi-element electrical filters. A filter constitutes a ceramic plate with a printed circuit of an RC-circuit on its surface. On the surface of a 25 X 25 mm plate from barium titanate, is placed up to 10 sections of RC-filters with the capacitance of each element up to 0.01 microfarad [5].

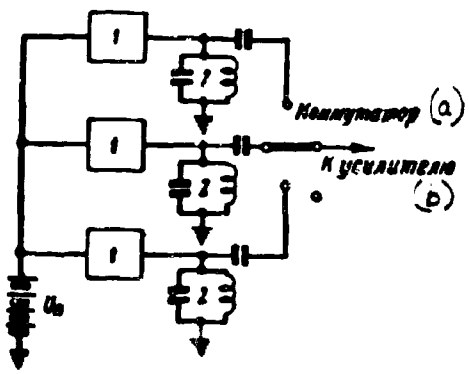

Fig. IX.6b. Diagram of commutation of useful signal removed from elements of mosaic:
1--element of mosaic; 2--resonance circuit.
KEY: (a) Commutator; (b) To amplifier.

In the second diagram of commutation, applied in the American heat-direction finder CODES, developed by the firm Avion, the output signal from each sensitive element of the mosaic, in turn, with the help of a mechanical commutator, moves to the entrance of the amplifier. To guarantee the successful work of such a system careful manufacture of circuits of commutation is necessary so that set noises of the commutating device do not exceed the useful signal removed from the element of the mosaic.

Further development of mosaic receivers, obviously, have to be electron tubes of the thermicon and vidicon type. Application of them will allow us to simplify

significantly the electronic circuit of scanning devices, to free them from troubles connected with commutation of weak currents. Furthermore, application of electronic sweeping will allow us to decrease significantly the scanning time of space and the effect of the background, and improve the resolving power of heat-direction finding systems. An example of such a system with electronic image scanning is the aircraft scanning instrument, the Filterscan, by "Philco" [6].

The basic element of a heat-direction finding system (Fig. IX.7) is an electron tube with high scanning speed without accumulation of signal. The conical part of the tube on one side is closed by a thin silico plate, and on the other - by a plate from material which is transparent in the required range of wave lengths. An electron gun is located in a branch at such an angle that the electron beam emitted by it irradiates the silicon plate.

An image of the target in infrared beams is focused by the receiving optics to the entrance window (silicon) of the electron tube. Radiation forming this image, after getting out of the tube, is focused with the help of mirror optics on the photosensitive element. As a sensitive element may be used any photoresistor, but in the considered model was applied indium antimonide with a threshold sensitivity of $1.3 \cdot 10^{-9}$ w to radiation with a temperature of 300°K and $1.5 \cdot 10^{-10}$ w to radiation with a temperature of 500°K.

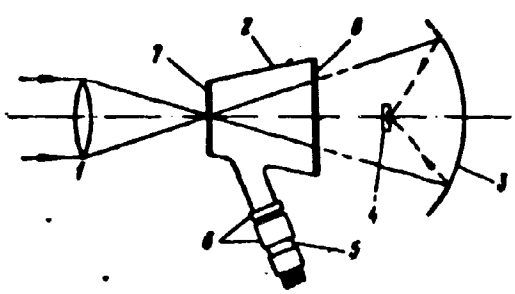

Fig. IX.7. Diagram of the Filterscan instrument: 1--first objective; 2--scanning tube; 3--second mirror objective; 4--indicator IK radiation; 5--electron gun; 6--focusing deflecting coil; 7--entrance window; 8--output window.

After turning on electron beam and focusing it on the internal surface of the entrance window of the electron tube, electrons accelerated by a voltage of 25 kv cause a local formation of free carriers in the semiconductor, which is equivalent to a change of conductivity

and, consequently, the coefficient of absorption at the place where the beam hits. The deflecting system forces the electron beam and the spot with high optical absorption created by it to shift along the surface of the silicon plate, thus carrying out image scanning (scanning by field of sight).

Since the energy content of radiation transmitted by flying spot in any moment of time is determined by the "brightness" of the section of infrared image covered by the spot, then the output signal from the photoresistor is also a function of time, the magnitude of which depends on distribution of "brightness" of infrared image on the entrance window of the tube. Thus, the sensitive element issues to the indicator instrument an output signal proportional to the change of radiation energy of consecutively examined elements of the field of sight. The sweeping of the indicator instrument is synchronized with the system of deflection of electron beam, which makes it possible to obtain on the screen of the instrument a thermal image of the scanning field.

The system is simple in design, light-weight and small and makes it possible to reveal objects with a temperature of 125°C with parameters which were applied in the model:

Area of absorbing spot.....$3.1 \cdot 10^{-4}$ cm^2

Area of screen..... 2.24 cm^2

Area of sensitive element..... 0.1 cm^2

Horizontal scan..... 1 kc

Vertical scan..... 30 cps

Relative hole of objective..... 1:3

Relative hole of mirror.....1:0.75

Pass band..... 30 kc

3. Construction of Heat-Direction Finding Systems

At present there have been developed abroad a significant quantity of types of

heat-direction finding equipment, intended for installation both on ground (naval) and air objects. While being identical in their principle of action, they differ in construction and tactical-technical data.

The biggest quantity of heat-direction finding systems is developed for the Air Force and intended for the detection of air and ground (naval) targets, intelligence, and navigation. Recently there began to be developed automatic heat-direction finding systems on pilotless jet aircraft and earth satellites for purposes of air intelligence and registration of rocket launches.

In 1944 in Germany there was developed and manufactured a night heat-direction finder "Kiel-4" (Fig. IX.8), consisting of receiving device 1, amplifier of photocurrents 2, indicator instrument 3, and control panel 4.

The receiving device of the heat-direction finder, established in the nose part of a fighter aircraft, included a revolving receiving mirror 250 mm in diameter, in the focal plane of which was placed a lead sulfide photoresistor, a unit for preliminary amplification of photocurrent, a mechanical rotation drive of the mirror, a mechanism for scanning target in the horizontal plane and potentiometers-transducers connected with the rotation drive of the mirror for synchronizing the sweep of the indicator instrument. The receiving device was covered by a glass cowl to give it a more streamlined aerodynamic form. The lead sulfide photoresistor was cooled to a temperature of - 78 °C by solid carbon dioxide.

Scanning of space at a solid angle of 20° was carried out by a needle-shaped beam approximately 1° in width. A simultaneous receiving device could accomplish scanning motion in a horizontal plane at an angle of 60°.

When radiation from the target hit the photoresistor, from it was removed a photocurrent pulse, which after amplification moved to the indicator block. Simultaneously from the sine potentiometers, connected with the rotation drive of the mirror, there was removed a voltage which passed to the deflecting electrodes

of the indicator electron-beam tube. This voltage created on the screen of the indicator tube a sweep repeating the character of displacement of the optical axis of the mirror in space.

When the heat-direction finder made a scanning motion in the horizontal plane, simultaneously, with the help of selsyn-transducers, there issued a voltage, proportional to the angular deflection of the axis of the heat-direction finder from the longitudinal axis of the aircraft, to the switch instrument. This allowed the pilot to judge where the target was - on the right or on the left of the axis of the aircraft.

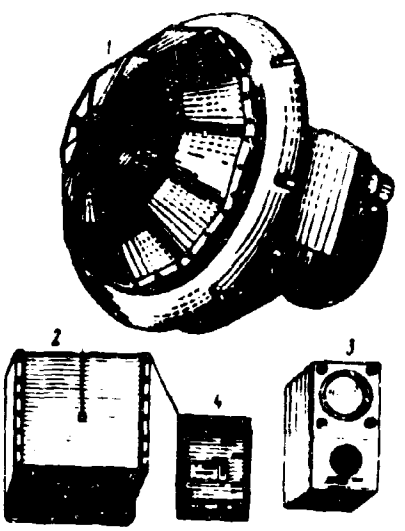

Fig. IX.8. The general form of the heat-direction finder set, the "Kiel-4".

Observing the position of the target mark on the indicator instrument and knowing its position relative to the longitudinal axis of the aircraft, the pilot could, by maneuvering his aircraft, combine the mark from the target with the center of the cross lines on the screen of the indicator instrument and approach the attacked aircraft until he could see it visually. After that the attack on the target was carried out visually.

The free-space range of the heat-direction finder "Kiel-4" for propeller-driven aircraft at medium altitudes constituted 8-10 km, and the direction to target was determined with a precision of $\pm$ 1°.

Further development of ideas embodied in the basis of the heat-direction finder "Kiel-4, the improvement of sweep and the automatic machine to guarantee tracking a revealed target led to the creation, in the postwar period, of semiautomatic and automatic heat-direction finding stations of aircraft fire control.

Thus, according to data available in literature [8], all F-100 type fighters in the United States are equipped with a fire control station on infrared beams (Fig. IX.9).

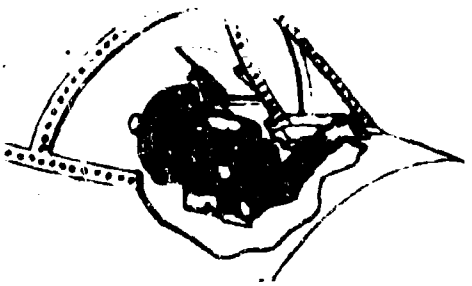

Fig. IX.9. Infrared sight AN/ASG-14 on the F-104.

The infrared sight, AN/ASG-14, for the F-104 "Starfighter" constitutes a monoblock construction, including an infrared system of detection, an electron amplifier and a projection system for visual indication of the target [9]. The projection system of the sight, after corresponding conversion and amplification, transmits an infrared image of the target to a reflective glass optical sight. A sensitive element (PbS) is placed outside the cabin before bullet-proof glass and is covered by a little entrance window, transparent in the region of sensitivity of the photoresistor.

The pilot observes on the reflective glass of the optical sight simultaneously a mark from the target and a sighting mark whose position in the field of sight is calculated by a computer of optical sight. This allows him to carry out an attack on the target at night just as if the target were visible directly to the eye.

In this sight, thanks to the large field of sight, there is no necessity for a special scanning device since on the reflective glass of the sight are observed simultaneously all targets in the field of sight of the receiving head. The pilot in this case executes the function of selection, distinguishing that target which it is necessary to attack.

In a more later infrared sighting station, the AN/AAR-21, developed by Hughes Aircraft Co., the scanning system and tracking are divided. As a sensitive element in the sighting station is applied a lead sulfide photoresistor, cooled to the

temperature of liquid nitrogen. In distinction from station AN/ASG-14 this station makes it possible to measure distance to target with the help of two tracking heads on infrared beams [10].

There are developed and combined optical-radar systems, for which the function of detecting the target and the preliminary tracking of it is done by passive infrared equipment, and after target is detected and a fighter starts toward it in a short time, automatically, a radiorange finer is switched on, with the help of which the coordinate of distance is introduced into the computer. Indication of radar and infrared images is produced on one screen as occurs on the Westinghouse interception station [11, 12, 13].

Application of similar combined systems with brief inclusion of a radiorange finder in the last stage of attack significantly decreases the possibility of premature detection of the attacking fighter by the enemy.

In 1957-1958 in the United States there was developed a scanning-tracking heat-direction finding system, CODES (Fig. IX.10a) [4, 14], in whose basis of operation was assumed the application of a mosaic of photoresistors with commutation of signals on alternating current and subsequent amplification in one amplifier.

Flat receiving mirror 1, [illegible] in azimuthal plane and connected with transducer of coordinates, carries out scan of target and directs radiant flux 2 to entrance of spherical optical system 3. The last, through correcting lenses 4, directs the obtained energy to the sensitive surface of mosaic 5.

The optical system includes also aperture diaphragm 6 and, located in it, an interference filter with a pass band of 1.8-2.7 μ and modulation lattice 7 with intervals between lines nearly 0.05 μ, applied on a curved surface 32 X 4 mm in dimension. With the help of the modulation lattice radiation from the target is modulated with a frequency of 40 cps. The aperture diaphragm, located in the plane of the center of the curvature of the spherical mirror, allows decrease of aberration

of the optical system due to the limitation on width of beams of radiation passing through.

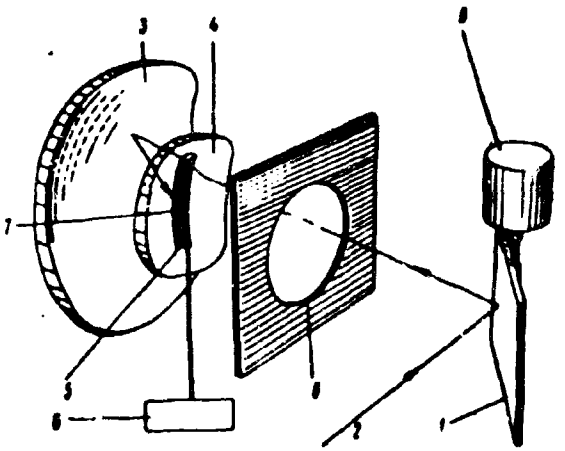

Fig. IX.10a) Diagram of optical system of CODES: 1—flat receiving mirror; 2—radiant flux; 3—focusing spherical mirror; 4—correcting lens; 5—mosaic; 6—aperture diaphragm; 7—modulation grid; 8—commutator; 9—hydromotor of scanning mirror.

A mosaic of photoresistors has a stretched form (32 X 2 mm), therefore, in order to ensure qualitative image of target on any of the elements of the mosaic, it is disposed in a meridional plane of the optical system. With this aim the mosaic is applied on a curved sublayer with radius of curvature equal to the radius of curvature of the focal plane of optics.

Angular dimension of an image of a pinpoint target on an element of the mosaic is equal to 1.2 mrdn, with good resolving power all over the field of sight. Instantaneous field of sight of the optical system constitutes 2.7° in azimuth and 40° in elevation. By this instantaneous angle the receiving device, due to rotation of the flat mirror, examines in space an angle 90° in azimuth and 40° in elevation. An angle of 40° is ensured due to the consecutive connection of elements of the mosaic to the entrance of the amplifier with the help of the commutator (Fig. IX.10b).

Output signals from elements of the mosaic are stored in separate oscillation circuits, tuned to a frequency of 40 cps. Such a resonance circuit executes a double function: it stores energy for a definite time determined by the frequency of commutation and separates the signal on a background of noises. The blocking capacitor C does not transmit the constant component to contacts of the commutator.

The mechanical commutator is prepared like the type applied in telemetric practice and has 60 lamellae. All thirty elements of the mosaic are connected to lamellae of the commutator in such a way as to obtain two cycles of commutation for one turn of the rotor of the commutator. Through the contacts of the commutator the signal from an element of the mosaic moves to the entrance of the amplifier, assembled on five semiconductor triodes.

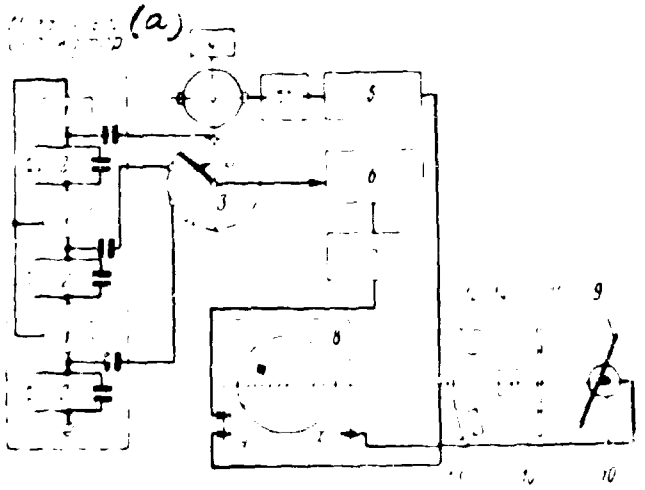

Fig. IX.10b. Block-diagram of the CODES system: 1--element of mosaic; 2--accumulator circuit; 3--commutator; 4--drive of commutator; 5--generator of sawtooth pulses; 6--amplifier; 7--detector and limiter; 8--indicator instrument; 9--scanning mirror; 10--transducer of coordinates; 11--aperture; 12--concave mirror; 13--correcting lens; 14--grid; 15--mosaic. KEY: (a) Mosaic indicator.

For guarantee of optimum sensitivity the pass band of the amplifier (Δf = 40 cps) is coordinated with length of signal from one element (0.023 sec).

After the amplifier signal is detected in the two-half-period detector and after limitation, it enters the indicator instrument.

The horizontal sweep of the indicator instrument is synchronized with the position of the receiving mirror with the help of the precision potentiometer which is the transducer of coordinates.

Vertical sweep in the indicator instrument is synchronized with the position of the rotor of the commutator by means of the generator of sawtooth voltage, giving out two pulses for one turn of the commutator. During the supply of these voltages to deflecting electrodes of the electron-beam tube of the indicator instrument the sweep repeats the sequence of scanning of space by the receiving device, and the position of the target mark on the screen relative to the center of the tube corresponds to the

position of the target in space relative to the optical axis of the instrument. The time of examining the scanning field is 1.5 sec.

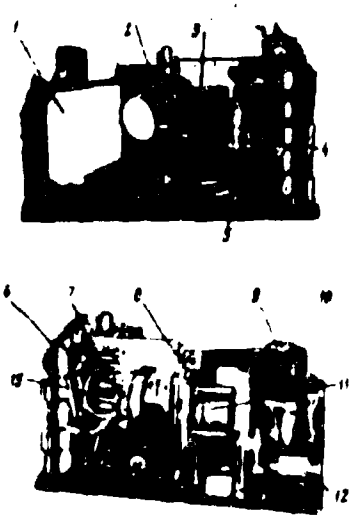

Fig. IX.11. General form of CODES equipment (without housing):
1--flat mirror; 2--filter; 3--modulating grid and elements of mosaic; 4--focusing lens; 5--correcting lens; 6--30 tuned circuits; 7--amplifier of signal; 8--generator of sawtooth voltages; 9--drive of mirror; 10--azimuthal potentiometer; 11--elevation pick-up; 12--drive of commutator; 13--commutator.

The general form of the heat-direction finder is shown in Fig. IX.11, and in Table IX.2 are given the basic parameters of the heat-direction finder.

On the basis of the CODES system in the United States there was developed a scanning system for the detection of artificial earth satellites by their thermal radiation [2]; the general form of the receiving device of this system is presented in Fig. IX.12.

The receiving head is established on a mobile platform with three degrees of freedom, which makes it possible to direct its scanning field to any part of the sky. In distinction from the earlier-considered CODES system, in this equipment the scanning motion is carried out by rotation of all the receiving head in an azimuthal plane within limits of the angles + 30 to +210°. The instantaneous field of sight, ensured by wide-angled optics and a mosaic consisting of 30 sensitive elements, is equal to 0.92 X 27°.5. Radiation of a satellite is modulated by a drum with slots with a frequency of 1000 cps. As sensitive elements of the mosaic are applied uncooled lead sulfide photoresistors. The signal of the elements of the mosaic, with the help of the commutator, moves to the oscillograph, on whose screen it is possible to observe a mark from the target and to watch its displacement.

Table IX.2. Basic Parameters of the CODES System

Designation of parameter	Unit of measurement	Magnitude
Scanning angle: in azimuth	deg	±45
in elevation	deg	40
Instantaneous angle of sight:		
in azimuth	deg	2.7
in elevation	deg	40
Time of sweep	sec	1.5
Diameter of entrance aperture	mm	43
Efficiency of optics	%	30
Relative aperture	—	F/1 (1:1)
Angular dimension of image from 90% energy	mrdn	1
Sensitive element	—	PbS
Dimension of element of mosaic	mm	1X2
Time constant	μ sec	200
Interval of sensitivity	μ	1.8—2.7
Integral sensitivity	w/cm^2	4.10^{-10}

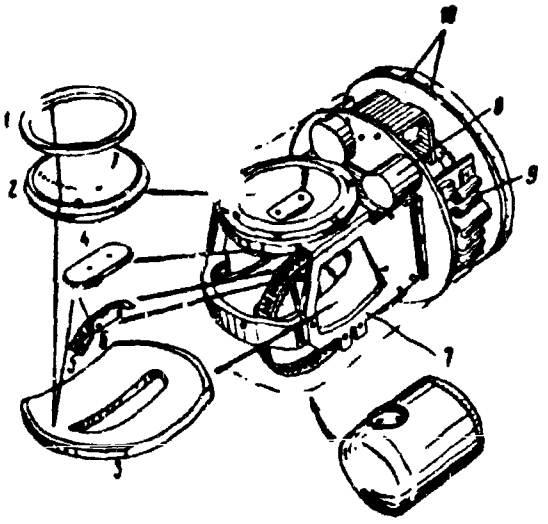

Fig. IX.12. Instrument for detection of artificial earth satellites: 1--inlet; 2--correcting lens; 3--spherical mirror; 4--secondary mirror; 5--modulation drum; 6--mosaic; 7--frame for bracing of optics; 8--motor of belt; 9--electron elements of the diagram; 10--scale of scanning angles.

MT-64-121
Infrared Technology in Military Science.
Moscow, 1963
Pages 285-292, 357-359

4. ON POSSIBILITY OF DETECTION OF BALLISTIC AND GUIDED ROCKETS

Progress in the area of development of tactical and strategic weapons, appearance of guided and ballistic rockets of medium and long range of operation in the arsenals of a number of countries demanded development of reliably working systems of distant detection of launching and entrance in atmosphere of rockets, with their subsequent destruction in the air far from the protected object. This problem, on which a great many people are working in a number of countries, and especially in the United States, is aggravated by the fact that equipment of rockets with nuclear warheads requires an absolute guarantee of their destruction at distances which are safe for protected object.

According to the estimate of foreign specialists, radius of defended hemisphere 2 (Fig. IX.13) around protected object 1 should be approximately 80 km. [25]. Here is considered range of operation of atomic charge with average trotyl equivalent, and distance which protects from injury people serving the object.

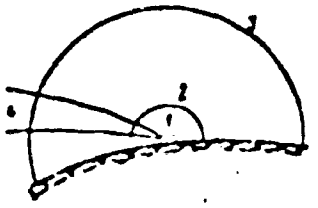

Fig. IX.13 Diagram of Defense from ICBM; 1--defended object; 2 -- hemisphere of defense; 3 -- zone of detection; 4 -- zone of possible appearance of ICBM.

To guarantee collision of antirocket rocket with ballistic rocket at the boundary of defended hemisphere, rocket should be detected ahead of time by some means

able to determine the coordinates of its trajectory and to calculate point of encounter. Minimum radius of detection of rocket is determined by its type, and also by the type by the type of antirocket rocket and system of guiding used for interception.

Contemporary radar systems detect and trac' intercontinental ballistic rocket (ICBM) at distances up to 800-1600 km [25]. However, they are subject to interference in the form of active countermeasures directly from rocket, interference from false targets, and influence of occasional interference from Aurora Borealis, reflections from the moon, etc.

In this connection there is great interest in work conducted abroad and, in the first place in the United States, on determination of possibility of detecting ICBM's using infrared equipment. These works are conducted in three main directions:

investigation of radiation of rockets and artificial Earth satellites;

investigation of possibilities of detecting ICBM's;

creation of systems of guiding antirocket rockets to ICBMS e tering .n dense layers of atmosphere.

Investigations of thermal radiation of ballistic rockets in the last stage of their trajectory [15] showed that nose cone of a rocket entering the atmosphere creates a shock-wave front behind which will be formed a high-temperature layer of air, intensely heating the body of the cone up to its melting (Fig. IX.14). In this layer air is ionized and radiates both in the visible and in the infrared region of the spectrum.

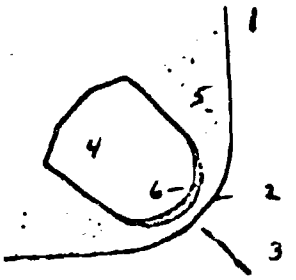

Fig. IX.14. Heating of Nose Cone of Rocket During its Entrance in Atmosphere: 1 -- shock-wave front; 2 -- stagnation point; 3 -- direction of flight; 4 -- nose cone; 5 -- high-temperature layer of ionized air; 6 -- plastic thermal insulation pad.

It is possible to judge the degree of heating of nose cone by reports of foreign press, from which it follows that

nose cone of Jupiter during its entrance in atmosphere was heated until white and rocket was seen visually for 24 sec., 1000 times brighter than the planet Jupiter, on background of which cone passed (Table IX.3).

Such high temperature are characteristic for the stagnation point; however, temperature of all body of cone can exceed magnitude of order 2000-2500°C. This allows not only to detect rockets by their thermal radiation, and also reliably to track them up to the moment of complete combustion or fall onto earth. Thus, during mentioned investigations of "Jupiter" rocket by the radiometric method it was possible to detect and to trace the trajectory of all three parts of rocket: nose cone, body of rocket and instrument section -- up to their fall in Atlantic ocean [17].

Table IX.3 Speed and Temperature of Typical Aircraft During Return to Earth [16]

(a) Объект	(b) Скорость, м/сек	(c) Температура, °C
(d) Ракета с дальностью 1 600 км	3 500	3 400
Ракета с дальностью 8 000 км	6 700	7 100
(e) Спутник с орбитой 480 км	7 600	8 600

KEY: (a) Object; (b) Velocity, m/sec., (c) Temperature, °C; (d) Rocket with range of; (e) Satellite with orbit.

Equally with investigation of thermal radiation of rockets, at present are conducted intense theoretical and experimental investigations of infrared radiation of spaceships and artificial earth satellites during their flight on orbits many hundreds of kilometers from surface of Earth [18]. Thus, series of trackings of flight of artificial earth satellites showed real possibility of their detection by day and at night by instruments of infrared technology. It was determined that radiation of artificial earth satellite significantly exceeds theoretically well-grounded radiation of body with temperature of 300°K and constitutes for the third of the Soviet artificial earth satellites, by measurements of Myron Block,

magnitude of the order of 1000 w. Although nature of radiation of artificial earth satellites is at present completely not determined, it is assumed that it is caused by the presence at these heights around the Earth of a zone of high-energy particles, and also by recombination on surfaces of satellite of electrons and ions which are at these heights. This hypothesis, in turn, makes it possible to assume possibility of detection of ICBM long before its entrance in dense layers of atmosphere during flight in cosmos at heights of the order of 500-1200 km..

The above investigations were carried out by specially developed experimental instruments -- radiometers and spectrometric installations. Structurally they were either portable, or were mounted on antennas of radar stations and artillery platforms in order to use their tracking systems.

Radiometer of firm Aerojet General type S8, weighing 9 kg, and with inlet diameter of 15 cm, was mounted either on a special tripod or on the gun-carriage of a naval cannon, as during launching of "Jupiter" rockets in May--June 1958. To decrease dimensions, long-focal mirror-lens optics with multiple reflection are used. Instrument S8 mounted on ships in the area of The Lesser Antilles made it possible to track trajectory of flight of rocket from launching to fall in ocean [19]. The same instrument was used by the firm to track the flight of the third Soviet artificial earth satellite.

Observation of the flight of The "Jupiter" rocket during its entry in to dense layers of atmosphere was carried out also using hand radiometer R-4K of the Boeing Engineering Co. [20]. The instrument, with field of vision of 4°, consists of radiometric head with replaceable sensing elements (PbS and germanium bolometer), and modulating disks to guarantee 24-hour operation and a circuit unit. Weight of instrument is 6 kilograms. Radiometric head is mounted on a rifle butt for convenient operation in the "hand" position; however it can be placed on any tracking mechanism for joint work in regime of tracking (Fig. IX.15). For initial guiding of radiometer onto rocket during its entry in atmosphere a telescopic sight is

mounted on body of head.

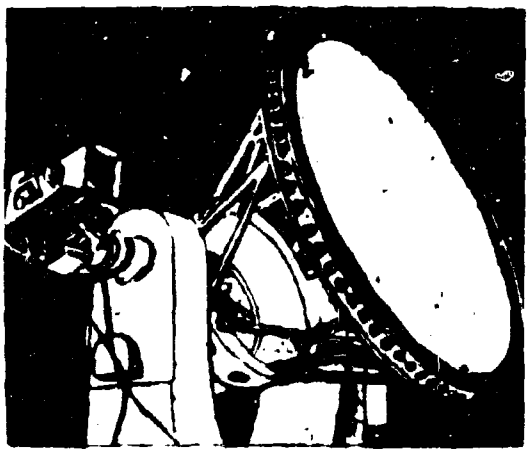

FIG. IX.15. Instrument of Increased Range, Combined with Radar Antenna.

Considerable attention also was allotted check of possibility of detection of rockets at moment of their launching and on active section of trajectory. Since infrared mechanisms possess high accuracy of measurement of angular coordinates, then obtaining of data about launching of rockets permit determination of launching coordinates calculation of trajectory of flight of rocket to moment of encounter with antirocket rocket.

Investigations in this direction were conducted both with the equipment considered above and also with special spectrometric infrared equipment.

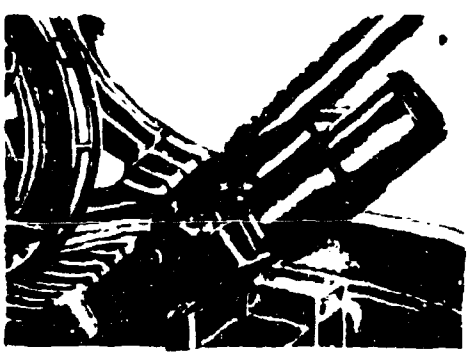

Fig. IX.16a "Rapid-Scan Spectrometric installation.

The Perkin-Elmer firm has for a long time conducted spectrometric investigations of radiation of rockets during launching and on active section of trajectory of their flight using a Rapid-Scan spectrometer mounted on a ROTI-MII optical follow-up tracking system [21] (Fig. IX.16a).

The main part of Rapid-Scan installation is infrared monochromator with fast scan, diagram of which is shown in Fig. IX.16b. Monochromator continuously records intensity of infrared radiation in 0.3 to 3.6 -μ strip. Frequency of scanning of mirror is regulated within limits of 2.5-180 cycles.

Observation of rocket launchings were carried out from a distance of 50 km. from rocket range. Simultaneously with recording of intensity of infrared spectrum photographing of flight of missile at long distances was carried out with an ROTI optical system. Received data were compared with spectrometric measurements to determine possibility of identification of rockets by their thermal radiation.

Installation of infrared instruments to detect ballistic rockets is assumed to be both on ground posts of detection, and also on patrol aircraft of distant warning service.

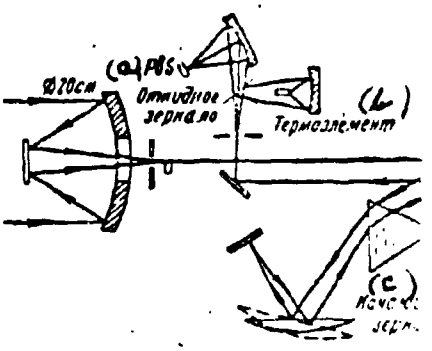

Fig. IX.16 b. Optical Diagram of Rapid-Scan Monochromator.
KEY: (a) Tipped mirror; (b) Thermoelement; (c) Rocking mirror.

Under the conditions of active electronic countermeasures from side of enemy, infrared systems can be an important source of obtaining information on distant approaches to protected object. However, organic deficiency inherent in such

systems (dependence of efficiency on state of atmosphere), lowers their tactical possibilities.

Problem of interception of controlled and ballistic rockets is not limited to timely detection and determination of trajectory of their flight. It is necessary to ensure guidance of antirocket rockets to them for the purpose of destruction at a considerable distance from protected object.

In this case, means of infrared technology can be very effective, especially in last phase of guiding of antirocket rocket.

In first phase, the approach of antirocket rocket to a ballistic rocket is assumed to be carried out by radio commands from earth. Tracking mechanisms must continuously introduce corrections in trajectory of antirocket rocket, considering information from stations tracking the ICBM. However, even in this case, is as shown in the press, error is very probable and as a result — miss of antirocket rocket. Miss can be caused by errors of tracking systems or its chance deviation from given trajectory due to external causes.

It is natural that in such conditions, probability of interception of ICBM becomes insignificant. Therefore, it is proposed to supply antirocket rocket with homing devices and, in particular, thermal devices. Thermal homing device on last stage of approach of antirocket rocket with ICBM locks on the latter, and subsequent approach to moment of encounter should occur by commands of homing guidance system.

High temperature of cone of ICBM and good transparency of atmosphere at altitudes of interception should ensure high effectiveness of thermal homing devices.

Literature

1. B. I. Polikarpov. Scanning by a needle-shaped beam. VVIA im. Professor Zhukovskiy, 1955.

2. Proc. IRE, 1959, Sep., Vol. 47, No. 9.

3. Space Aeronautics, 1959, [illegible], No. [illegible], N [illegible].

4. Electronics, 1959, Apr., No. 17.

5. Electronics, 1959, 32, No. 26, p. 38-41.

6. Proc. IRE, 1959, Dec., Vol. 47, No. 12.

7. "Foreign aviation technology," 1957, No. 12.

8. American Aviation, 1957, Dec., No. 30.

9. Aviation Daily, 1958, 9 Sep., Vol. 118, No. 6.

10. Aviation Week, 1959, 4 May, No. 18.

11. Missiles and Rockets, 1958, 22 Dec., Vol. 4, No. 25.

12. Signal, 1959, Feb., No. 6.

13. Aviation Week, 1959, 4 May, No. 18.

14. Missiles and Rockets, 1959, No. 16.

15. Interavia, 1959, No. 2.

16. "Questions of rocket technology", 1960. No. 4.

17. Electronics, 1959, Vol. 52, No. 6.

18. Missiles and Rockets, 1958, Vol. 3, No. 7.

19. Missiles and Rockets, 1958, 20 Oct., Vol. 4, No. 16.

20. Missiles and Rockets, 1958, 21 Jul., Vol. 4, No. 3.

21. Missiles and Rockets, 1960, 23 May. No. 21.

22. Missiles and Rockets, 1960, 14 Mar., No. 6.

23. Missiles and Rockets, 1957, Nov.

24. Electronics, 1954, Aug., No. 8.

25. M. N. Nikolaev. Missile against missile. Voyenizdat, 1960.

C H A I T E R X

THERMAL HEADS OF HOMING GUIDANCE SYSTEM

1. Principle of the Passive Homing Guidance System of Missiles

There exist several methods of controlling the flight of pilotless devices from the moment of their launching to target impact. One of the forms of such control is the method of [illegible] target.

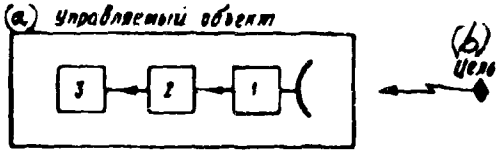

Fig. X.1. Fundamental diagram of homing guidance system.
KEY: (a) Controlled object; (b) Target.

In this case on the guided missile is established a special device, called coordinator of target, which determines the position of the target relative to the object of the homing guidance system and produces control signals during appearance of error between direction to target and given direction (axis of missile or coordinator, vector of speed of missile).

The fundamental diagram of a homing guidance system (Fig. X.1) usually includes three basic elements: coordinator of target 1, computer 2, and mechanism for controlling the flight of the missile 3.

A homing guidance system can be passive (Fig. X.2a) and also active (Fig. X.2b) or semiactive (Fig. X.2c).

With a passive homing guidance system, for obtaining the signal which controls the flight of the missile, energy is used, which is radiated by the actual target.

With an active homing guidance system, for obtaining the control signal energy is used, which is reflected from the target during its irradiation from the self-guided missile. Therefore, characteristic for this system is the presence on the missile of a special transmitter of energy radiated into surrounding space and a receiver tuned to this form of energy.

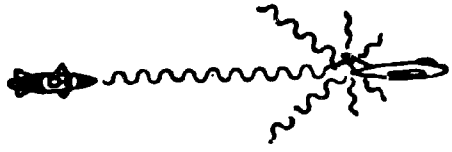

Fig. X.2a. Diagram of a passive homing guidance system.

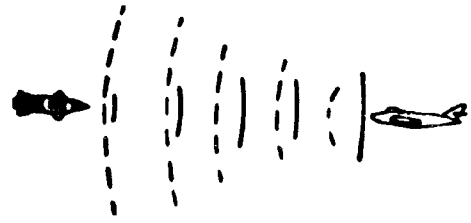

Fig. X.2b. Diagram of an active homing guidance system.

With a semiactive homing guidance system the target is irradiated by energy from a source fixed outside the missile, and after reflection from the target it is perceived by the receiver producing the control signal.

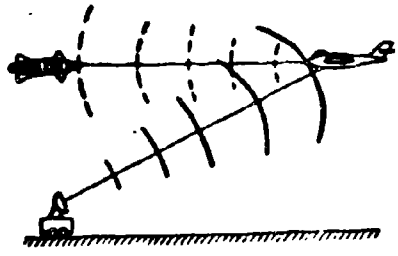

Fig. X.2c. Diagram of a semiactive homing guidance system.

Passive homing guidance systems require the least quantity of equipment on a guided missile, however, for their work the presence is necessary of a contrast of energy radiated by the target (sonic, light, thermal, radar), relative to the radiation of the surrounding background.

In recent years among systems of passive homing guidance the most widely used has been the thermal (infrared) homing device (TGS). The infrared homing device constitutes a closed follow-up system (Fig. X.3) and includes the following basic elements [1]: coordinator of target 1, producing an error signal as a result of the comparison of the entrance signal and the signal of the main feedback; amplifying element 2; executive element 3, producing a regulating influence applied to the object of adjustment 4, which [illegible] device [illegible] element of local feedback 6; and main feedback 7.

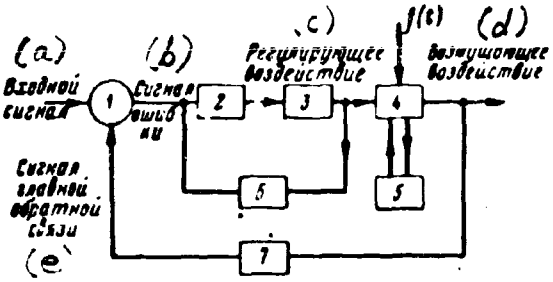

Fig. X.3. Block-diagram of an [illegible] homing device.
KEY: (a) Entrance signal; (b) Error signal; (c) Regulating influence; (d) Perturbing influence; (e) Signal of main feedback.

The coordinator of target is an optical-mechanical device perceiving thermal radiation of the target and determining its position relative to its own optical axis. In case of deflection of target from optical axis of the coordinator the latter produces an error signal. This signal, after amplification and conversion in other elements of the circuit, influences, through executive devices, the drive assembly of the head, which moves the receiving device in such a way as to remove the error signal, i.e., to combine the optical axis of the coordinator with the direction to target. In the process of tracking of the coordinator after the target electrical pulses, proportional to the angle of error or the angular velocity of the displacement of the receiving device, after necessary conversion, proceed to the mechanism of aircraft control.

In Fig. X.4 is given an example of the tactical use of a passive homing guidance system in "air - air" missiles supplied with an infrared homing device [2].

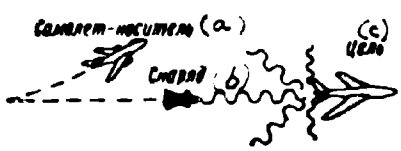

Fig. X.4. Attack on the target with the help of a missile with an infrared homing device.
KEY: (a) Carrier aircraft; (b) Missile; (c) Target.

After detection of an air target by a fighter with the help of any kind of airborne equipment and aiming at it, during which the infra-red homing device will lock on the target, a missile is released. Inasmuch as a passive system does not require radiation by an interceptor of any kind of energy, the fighter, immediately after launching the missile, is free and can pull out of the attack. Further guiding of the missile to the target is done by the infrared homing device.

This is one of the advantages of infrared passive homing guidance systems - the interceptor is in the zone of the enemy's defensive fire the minimum necessary time.

Of the other advantages of infrared homing guidance systems one should note: concealment of use due to the absence of the necessity of irradiating target, simplicity of equipment, reliability of its work, and comparatively low cost. Thus, for instance, the "Falcon" missile with a radar homing device is approximately 10 times more expensive than the "Sidewinder" missile with an infrared homing device. In the "Sidewinder" missile is applied only seven electron tubes, whereas in the "Falcon" several tens of them [3].

The simplicity of construction has a direct connection with its reliability. The absence of a transmitter and rather bulky antenna systems makes an infrared homing device compact, which has a special value for "air - air" missiles, the dimensions of which are very limited.

2. Thermal (Infrared) Homing Head (TGS)

Development of the first combat models of heat-seeking guidance systems was started in the period of the Second World War, when in Germany there was created a series of experimental models of heat-seeking guidance systems for different types of missiles, which, as a result of the crushing blows of the Soviet Army, did not find practical application. In the postwar period in Switzerland, France Italy, Sweden and, especially, in the United States and England these works were continued, and a series of missiles with infrared homing devices in recent years have been put in service.

Infrared homing devices may be broken down into two groups - tracking and indicator or wide-field.

In a tracking homing device, a block-diagram of which is shown in Fig. X.3, the control signal, through executive devices and main feedback, is used for removal

of error angle, and an electrical signal, proportional to the angle of rotation or angular velocity of displacement of the coordinator, is used for controlling the missile.

In indicator heads, having a wide angle of sight, the control signal is used directly to affect the missile control device, and error is removed immediately by means of simply turning the missile.

In tracking systems application of optics with a narrow angle of sight is possible, which allows an increase in the sensitivity and, consequently, the range of [illegible] homing devices. Furthermore, such systems turn out to be more noise-immune, since at small angles of sight the harmful influence of the background decreases. When using tracking heads it is possible to accompany the target within limits of significant angles, which makes it possible to expand the tactical possibilities of guiding missiles to target.

Application of narrow angle of sight in tracking heads has also its disadvantage; it is necessary either to have on board the carrier special equipment, ensuring detection and preliminary guiding of the coordinator to the target, or to construct the head in such a way as to ensure before launch or in flight the scanning motion of the receiving device, which complicates the equipment.

Indicator heads with wide angle of sight differ by simplicity of construction and make it possible to manage without preliminary guiding equipment, however, on the other hand, they are less noise - immune and have smaller range.

Both tracking and indicator infra-red homing devices can be divided into heads with relay principle of adjustment (on the principle "yes-no") and heads with proportional adjustment.

In heads working on the principle "yes-no", only the sign of the angle of error is worked out, and not its magnitude.

In heads with proportional adjustment the magnitude of the control signal is proportional to the angle of error.

Depending upon the principle of isolation of error signal [illegible] homing devices can be subdivided into heads with pulse, frequency, phase, and amplitude-phase methods of isolation of error signal.

These methods can be characterized by the following criteria:

pulse method, in which during the appearance of angle of error from the coordinator are removed separate electrical pulses, which, after their respective conversion, make it possible to estimate sign and magnitude of angle of error with the subsequent use of signal [illegible],

frequency method, in which different positions of the target with respect to axis of the coordinator correspond to signals of different frequency (Juno-1 "Linse",

phase method, when, depending upon the position of the target, from the coordinator are removed signals of different phase ("Emden-I"),

amplitude-phase method, with which, depending upon sign of angle of error and its magnitude, from the coordinator are removed signals different in phase and amplitude.

The thermal tracking homing device "Madrid", developed in Germany at the end of the Second World War, was intended for guiding antiaircraft missiles "Enzian" to air targets [4].

The [illegible] coordinator, "Madrid," (Fig. X.5) includes parabolic mirror 1, in the focus of which is placed cooled lead sulfide photoresistor 2. In direct proximity to the photoresistor is placed modulating disk 3 with one quadrant cut out (see Fig. X.6). Synchronously with the modulating disk revolves the rotor of the switch 4, ensuring four switchings for one turn.

When radiant flux from the target falls in the field of sight of the instrument the mirror creates, in the focal plane where the photoresistor is placed, an image of the target in the form of a circle of scattering. Besides from the photoresistor there will be removed pulses of photocurrent (voltage) with frequency

determined by the speed of rotation of the modulating disk. After amplifier 5, tuned to frequency of modulation, these signals move through the distributor of the commutator to windings 6 of relays P_r, P_R, affecting controls by position of coordinator.

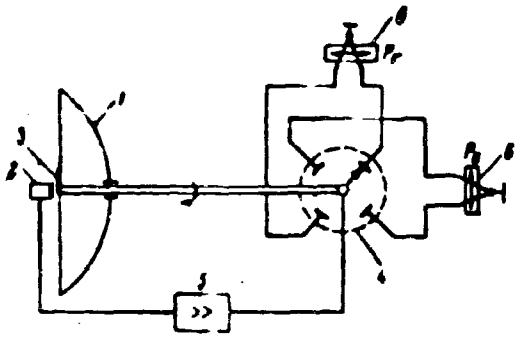

Fig. X.5. Diagram of the infrared homing device "Madrid".

If the image of the target is in the center of the field of sight (angle of error is equal to zero), then both windings of the relay are disconnected, since modulation of flux is absent, and the tracking system remains in the former position. Control signals actuating missile controls are zero; the missile controls occupy a neutral position.

During displacement of image from the center of the field of sight there appear modulated signals, proceeding through the commutator to windings of the relay. Depending upon what quadrant the image of the target is in, the signal will enter the corresponding winding of the relay so that the actuating mechanism turns the coordinator in the direction of a decrease in angle of error. The coordinator during the turn works the control signal which actuates the missile control in such a way that they turn the missile until its longitudinal axis combines with the direction to target.

In the "Enzian" missile to control the operation of the head there was applied an electro-pneumatic device, ensuring a speed of tracking target of 20 deg/sec during a tracking angle of $\pm$ 30°. Angle of sight of the optical system constituted $\pm$ 3°. Air necessary for operation was in a small steel cylinder. Weight of the "Madrid" head was equal to 5 kg, the number of electron tubes 3-4. Range with respect to aircraft constituted on the average 2-3 km.

Although the infrared homing device "Madrid" produced electrical signals of

error in the form of single pulses with a definite following frequency, in the homing device "Linse" signals of error differed in frequency, depending upon the position of the target relative to the optical axis of the coordinator.

The infrared homing device "Linse" with a 16-20° angle of sight, according to the earlier considered classification, belongs to the indicator type.

In distinction from the preceding head this instrument had two modulating disks (Fig. X.6), established in the focal plane of the optical system, behind which was placed the photoresistor [4, 5]. Every disk has two rows of slots each; the number of them in each row is different. During rotation of disks there are formed four covered fields with different frequencies of modulation. Depending upon which of the fields gets the image of the target, at the output of the amplifier of photocurrent will be formed a signal of a different frequency. When the image of target is projected at point A, there will be no signal from the photoresistor. From the output of the amplifier a mixture of various-frequency signals enters the electrical filters, each of which is tuned to one of the frequencies created by the modulating disks.

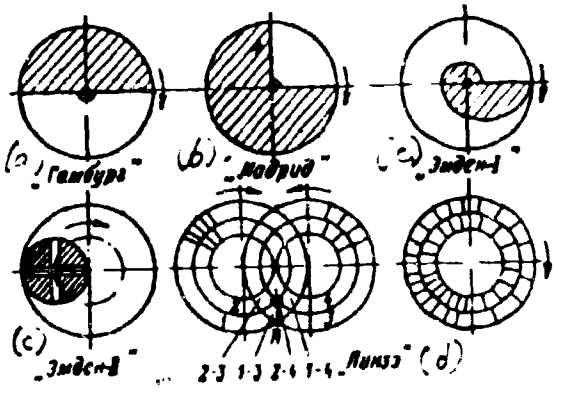

Fig. X.6. Modulating disks of coordinators of certain infrared homing devices.
KEY: (a) "Hamburg"; (b) "Madrid"; (c) "Emden"; (d) "Linse".

The work of the filters it is possible to trace in the example of the diagram of control signal emanation along one of the channels of control (for instance, vertical). Control for this channel is ensured with the help of two opposite fields (1-3, 2-4), formed by modulating disks.

The diagram (Fig. X.7) contains two filters tuned to frequencies of modulation by fields f_1 and f_2. Filters are connected to the anode circuit of the

last tube of the amplifier and have transformer coupling with rectifiers B_1 and B_2, assembled on bridge circuit.

If frequency of signal f_1 coincides with frequency of adjustment of filter Φ_1, then on clamps of secondary winding of transformer T_{P1} will appear alternating voltage, under the effect of which through resistor R_1 will flow rectified current i_1. On terminals a, b of relay P will appear voltage + u. The relay will operate; contacts K will close and voltage will pass to solenoid $З_1$. Core of solenoid with the help of rod T_1 is connected with missile control vane, which, deviating, creates control moment, correcting flight trajectory of missile until the optical axis of the coordinator coincides with direction to target. At the moment they combine the signal to output of coordinator will become zero; the relay will release contacts, disconnecting thereby the solenoid, and the control vane will stand in a neutral position.

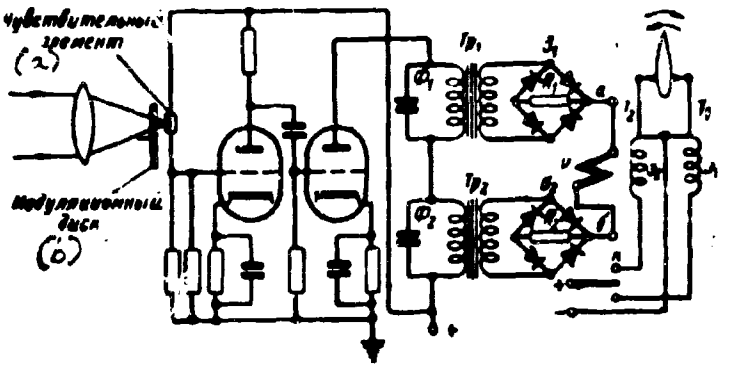

Fig. X.7. Fundamental diagram of emanation of control signal along vertical channel in a head of the "Linse" type.
KEY: (a) Sensitive element; (b) Modulation disk.

If frequency of modulation f_2 coincides with frequency of adjustment of filter Φ_2, then on terminals a and b of relay P will appear voltage u and the relay will switch on solenoid $З_2$, ensuring thereby the movement of the control vanes of the missile to the other side.

On the phase principle of control signal emanation was developed the infrared homing device "Linden-I," an indicator type with a 20° angle of sight.

In this system the modulating disk was made in the form of an Archimedes spiral (see Fig. X.6) and made it possible to obtain, in a polar system of coordinates,

signals of errors, differing from each other in phase, depending upon the position of target relative to the optical axis of the coordinator.

Synchronously with the modulating disk revolved an a-c generator which was the generator of support sinusoidal voltage. The phase of pulses of photocurrent, issued by the coordinator, was equalled with the phase of support voltage. The phase difference, separated as a result of comparison, was used to create a control signal removing the error between the direction to target and the optical axis of the coordinator.

An example of the practical use of infrared homing devices on combat rockets are missiles of the "air - air" class, the "Sidewinder" and the "Falcon" GAR-2A (the United States), the "Firestreak" (England), C-7 (Italy), "Matra" R-510 (France) [12]. The most wide-spread of this series, the "Sidewinder," is intended for action on air targets and has a length of 2.75 m and a diameter of nearly 0.125 m.

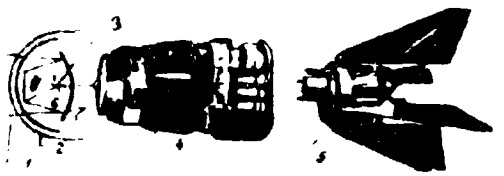

Fig. X.8. Infrared homing device of the "Sidewinder".

The infrared homing device (Fig. X.8) is placed in the nose part of the missile and is covered by a spherical cowl 2. The coordinator of the head occupies a section nearly 10 cm long. For gathering and focusing infrared radiation of target 1 is applied mirror objective, consisting of parabolic 7 and flat 8 mirrors. Diameter of parabolic mirror is 8.9 cm. Angle of sight of objective, in the focus of which is placed uncooled lead sulfide photoresistor 3, is equal to 4°. Before lock-on the optical system accomplishes a scanning motion. Thermal radiation of the target is modulated by a disk-modulator, revolving with a speed of 30 rpm. From the photoresistor is removed the error signal, proceeding to amplifier 4 and, after adjustment of coordinates to the actuating servo-motors 5 which control the control vanes of the missile. Weight of the head is 9 kilogram.

In the missile is applied a noncontact electro-optical detonator, exploding the warhead during flight near the target at a distance not more than 10 m.

As shown in literature [8], the "Sidewinder" (Fig. X.9), in spite of its simplicity and the small dimensions of the homing device, possesses high accuracy of hit and in a number of cases knocked off flares, secured on a flying target, without damaging the actual target.

Fig. X.9. The "Sidewinder" knocks off a flare during tests.

Effective range of the infrared homing device constitutes a magnitude of the order of 3,300 m.

The English missile "Firestreak" is supplied with a more complicated thermal head with mirror optics. The nose cone of the head is made in the form of an octahedral pyramid from thin plates of optical glass (Fig. X.10).

In the press it was reported that the infrared homing device of the "Firestreak" has a range for aircraft of the "Meteor" type at low altitudes by day - 8 km, and at night at 3000 m - 18 km [8].

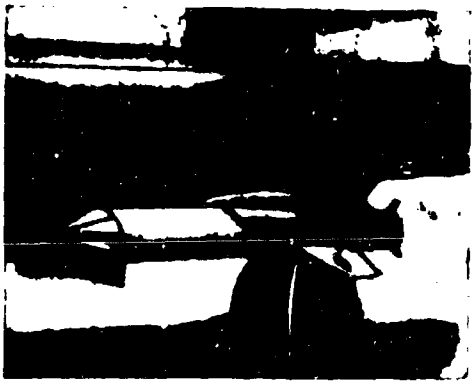

Fig. X.10. The "Firestreak" with thermal head.

The great range of the homing device makes it possible to accomplish lock-on before launch of missile from carrier aircraft. After launching of missile the carrier aircraft can pull out of attack, since further tracking of target is carried out by the self-contained infrared homing device.

3. Noncontact Electro-Optical Detonators (NOV)

To increase probability of striking target with inaccurate guiding of missile, noncontact exploding of warhead in direct proximity of target is applied. Usually the distance to target, in which the detonator must automatically fire, is determined by the type of missile, the power of the warhead, the radius of striking action of fragments, and it varies within 15-50 m for different types of missiles.

The application of noncontact detonators makes it possible to obtain a comparatively high probability of hitting even such maneuvering targets as air targets. According to data available in literature [11], the probability of striking an air target with a missile equipped with a noncontact detonator attains 80-90%, whereas the probability of a direct hit constitutes a magnitude of the order of 60%.

As a source of information about the flight of the target can be used different physical criteria (separating, by contrast, the target relative to the surrounding background); radio emission reflected from the target, proper radio emission of the target, intensity of magnetic or electrostatic field around the target, sonic or ultrasonic radiation, and also thermal radiation of the target and optical contrast of the target with the surrounding background.

At present, most widely used for air and ground (above water) targets are radar and electro-optical noncontact detonators.

For the case of application of electro-optical noncontact detonators, in Fig. X.11 is shown the change of a physical parameter, which is a source of information, and the signal which determines the moment to explode the ammunition.

In principle of action electro-optical noncontact detonators (NOV) can be broken down into three groups:

a) using as a source of information about flight of target the thermal radiation of the target (passive systems),

b) using (reflected from target) modulated radiant flux, radiated by the missile itself (active or optical-radar systems),

c) reacting to visible contrast of the target relative to the surrounding background (contrast principle of action).

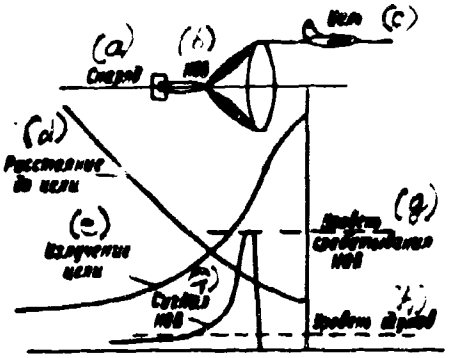

Fig. X.11. Change in time of distance to target, its radiation, and NOV signal. KEY: (a) Missile; (b) NOV; (c) Target; (d) Distance to target; (e) Radiation of target; (f) NOV Signal; (g) Level of NOV operation; (h) Level of noises.

In Fig. X.12 is depicted one of the diagrams of a passive electro-optical detonator (first group), consisting of receiver of radiation 2 placed in the focus of a toroidal lens with circular scan 1, unit of amplification of photoelectric signal 3, thyratron relay 4 and cartridge 5.

As a receiver, as a rule, are applied photoresistors with sensitivity in a range of wave lengths corresponding with the spectral curve of radiation of the target. For a guarantee of circular scan the film of the photoresistor is on a sublayer of cylindrical form.

The form of toroidal lens and position of the photoresistor are calculated so as, first, to ensure the necessary field of sight and, secondly, the slope of it forward along the flight of the missile. The angle of inclination of the axis of the radiation pattern is chosen depending upon the flight speed of the missile and the time lag of the detonator circuit with such calculation that after information enters and before exploding the ammunition the missile does not pass the target.

The unit of amplification of photocurrent constitutes, as a rule, a single-tube amplifier of alternating current with a large pass band (pulse amplifier of signal). From the output of the amplifier a pulse of amplified signal joins the control grid of the thyratron, in the anode circuit of which are included the cartridge and battery. After ignition of the thyratron in the anode circuit will move current, which will trigger the cartridge and explode the ammunition.

In the absence of a heat-radiating target, on the photoresistor falls radiation from a uniform background (for instance, the sky). The current in the circuit of the photoresistor will change little; consequently, from the output of the amplifier will move to the control of the thyratron voltage, insufficient for his operation.

The distance of operation of such an NOV is determined by its sensitivity, the emissive power of the radiation of the target in a given direction, and the meteorological conditions.

It is natural that when outside thermal sources of sufficient power fall in the field of sight of the NOV there can occur false operation of the detonator and premature explosion of the warhead.

Therefore, to increase operational reliability of the detonator it is necessary to apply a series of measures decreasing the probability of premature explosion of the missile on various kinds of heterogeneities of background (clouds illuminated by the sun, solar and moon radiation, radiation of certain ground heat-radiating objects, etc).

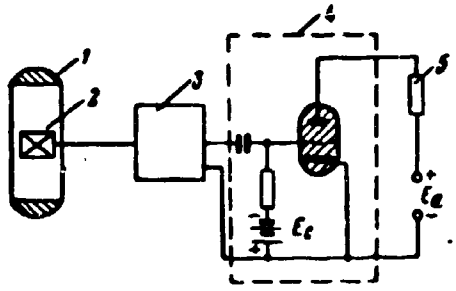

Fig. X.12. Fundamental diagram of a noncontact electro-optical detonator.

Among such measures are:

a) use of narrow-band infrared filters in front of the photoresistor, which separate only the radiation characteristic of a given target,

b) connection of two photoresistors by bridge circuit in opposition. In this case radiation from heterogeneities of the background, as from the areal object, will get on the two photoresistors and compensate one another. When in the field of sight there will appear a target (point object), then on one photoresistor will fall radiation from the target and background, and on the other - only from the background. As a result, in the diagonal of the bridge will appear differential current, sufficient after amplification, for operation of the thyratron relay.

c) application of timed blocking of power supply to NOV circuit so that the detonator goes into operation after a definite time necessary for approach of the missile to target. Such blocking may be carried out either with help of a time relay or with the help of a forced feed of electrolyte to the storage batteries through porous partitions after launch of missile. The latter method has found application in a detonator for an antiaircraft missile of the United States. In it the power supply battery is in a dry state, and the electrolyte is kept in a vessel with porous walls. After the shot, as a result of accelerations developed, the electrolyte under pressure passes through the pores of the walls to the storage battery and brings the detonator into operation.

An example of an active or optical-locating noncontact detonator (second group) can be the electro-optical detonator "Pistole," developed in Germany in the period of the Second World War.

The detonator "Pistole" (Fig. X.13) had source of infrared radiation 1, placed inside revolving cylinder with slots 2. Modulated radiation spread in a radial direction (perpendicularly to the direction of motion). When the missile flew near the target, a modulated reflected signal from the target was perceived by the receiving optics of the detonator 3 and headed to the receiver (photocell) 4. To amplifier 5 proceeded variable photocurrent with a frequency equal to the frequency of modulation of the source of radiation. After passage through electrical filter 6 the signal brought into action executive relay 7 of the detonator and caused explosion of warhead. The presence of modulated radiation and narrow-band electrical filter, tuned to the frequency of modulation, ensured heightened noise immunity of the circuit of detonator, since variable signal from oscillations of the radiation of the background was held back by the electrical filter and did not enter the executive relay.

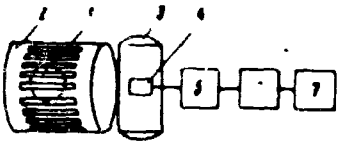

Fig. X.13. Block-diagram of active electro-optical detonator "Pistole".

Electro-optical detonators of the third group constitute the usual photo-relay and work, as a rule, in the visible region of the spectrum. Their essential deficiency is low noise immunity due to operation on the boundaries of objects having various brightness or colorfulness. Due to this, such detonators have not found practical application, although they allow noncontact explosion of the warhead near the target.

Literature

1. V. V. Solodovnikov. Bases of automatic adjustment. Mashgiz, 1954.
2. A. S. Lokk. Missile control. State Technical Press, 1958.
3. Flight, 1958, Vol. 74, No. 2602.
4. F. Mueller. Remote control. Publishing House of foreign literature, 1957.
5. Ya. G. Varaksin. Radio electronics in military matters. Publishing House "Soviet Radio", 1956.
6. Electronics, 1950, Oct., No. 10.
7. V. [illegible] Marisov, I. K. Kucherov. Guided missiles. Voyenizdat, 1959.
8. Aeroplane, 1958, Vol. 95, No. 2462.
9. Aviation Week, 1958, Dec., Vol. 69, No. 23.
10. Electronics, 1958, Nov., No. 11.
11. Interavia, 1958, 1 Apr., No. 3950.
12. Jane's All the World's Aircraft, 1961-1962.

C H A P T E R XI

EFFECTIVENESS AND RANGE OF INSTRUMENTS OF INFRARED TECHNOLOGY

1. Peculiarities in the Construction of Passive Instruments of Infrared Technology

When designing and operating instruments of infrared technology of the passive principle of action, we encounter, mainly, three groups of factors determining the effectiveness of the application of instruments in practice, namely:

a) radiation of the target and background,

b) propagation of radiation energy in the atmosphere,

c) parameters of the receiving device converting radiation energy into a corresponding electrical signal.

It is possible, actively, to influence only the parameters of the receiving device, including the optics, the scanning device, the sensitive element, and the electronic circuit. Also here, more or less, the choice breaks down only to the characteristics of the sensitive element and, to a certain degree, of the optics. By selection of characteristics of the sensitive element and the optics one can determine optimum range of spectral sensitivity of the receiving device, its integral sensitivity, time lag, and overall dimensions of the entrance pupil of the optics.

It is necessary also to know the radiant flux proceeding from the target and determining the integrity of the action of the instrument on the whole and also to estimate the harmful, interferring radiation of the background, in order to decrease it in the appropriate way and to make the instrument serviceable in interference conditions.

During appraisal of radiations of target and background usually is determined spectral density of radiation of target (r_λ), the radiation ability of its surface (ε_λ) and the wave length of maximum radiation (λ_{max}). The last is interesting by the fact that near λ_{max} spectral density of radiation is proportional to the fifth degree of temperature, while the total radiation is proportional to the fifth degree of temperature, while the total radiation is proportional only to the fourth degree.

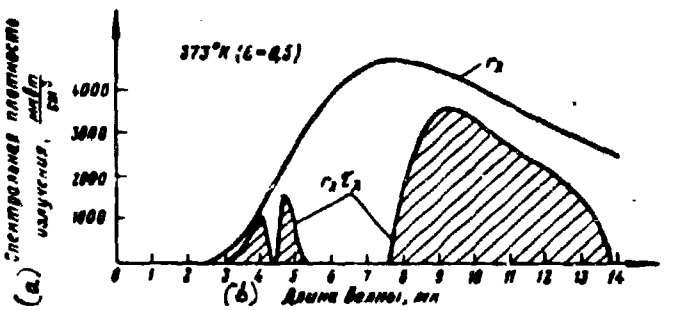

Fig. XI.1. Radiation of a gray body with T -100°C before and after passage through an atmospheric layer of 1.85 km (H_2O — 18 mm).

KEY: (a) Spectral density of radiation, $\frac{\mu w}{cm^3}$; (b) Wave length, μ.

Having obtained the necessary data about radiation of the target, it is necessary to estimate its weakening in atmosphere at the required range of the instrument. This may be carried out by plotting a curve of spectral transmittance of the atmosphere on a curve of spectral density of radiation and multiplying the corresponding ordinates. If curve r_λ is plotted in absolute energy units, then the area limited by curve $r_\lambda \tau_\lambda$, characterizes qualitatively and quantitatively the radiant flux (during calculation of unselective weakening) proceeding to the objective of the receiving device. As an example, in Fig. XI.1 are given curves of radiation of a gray body ($\varepsilon = 0.5$) with temperature of the surface 100°C before and after passage through a layer of atmosphere.

As can be seen from the given curves, after passage through the atmosphere radiation energy enters the receiving device practically at two spectral intervals 3.0-5... and 7.5-13.5 μ. As temperature of radiating surfaces decrease an even

greater specific gravity is apportioned to radiation in the range of waves 7.5-13.5 μ .

Such a graphic construction makes it possible to determine the optimum region of sensitivity of the developed instrument based on the possibilities of the sensitive element and the spectral transmission of the optics.

Frequently it is necessary to resolve another problem: to choose the spectral range of waves in which sensitivity of the equipment to change of temperature would be the highest. Such a problem, in particular, is encountered during the development of radiation pyrometers and receiving head of heat detection equipment.

In this case, while differentiating Planck's equation with respect to temperature and dividing the obtained expression term by term by r_λ, we have

$$\frac{1}{r_\lambda}\frac{dr_\lambda}{dT}=\frac{C_2}{\lambda T^2}\frac{e^{\frac{C_2}{\lambda T}}}{e^{\frac{C_2}{\lambda T}}-1}. \qquad (XI.1)$$

If $\frac{C_2}{\lambda T}$ is large as compared to the second member, then formula (XI.1) can be rewritten in the form

$$\frac{dr_\lambda}{dT}=\frac{r_\lambda C_2}{\lambda T^2}. \qquad (XI.2)$$

The obtained expression considers rate of change of spectral intensity of radiation density with change of temperature of the body with a precision of 1%, if $\lambda T<0.30$ cm·degree, and 10%, if $\lambda T<0.60$ cm·degree.

In Fig. XI.2 are plotted curves of spectral intensity of radiation density of an ideal black body with a temperature of 500°K ($w\cdot cm^{-2}\cdot\mu^{-1}$) and the rate of its change ($w\cdot cm^{-2}\cdot\mu^{-1}\cdot degree^{-1}$).

From curve r_λ it is clear that on it are several paired points with identical spectral intensity of radiation density at various wave lengths (for instance, at 3.5 and 11 μ). If one were now to turn to curve $\frac{dr_\lambda}{dT}$, then it would become evident that the most profitable region is the region near 3.5 μ , since here, during a change of temperature the same number of degrees, the change rate of spectral density of radiation will be higher than nearly 11.0 μ . The final selection of

spectral interval in this case it is possible to make only be considering the operational peculiarities of the instrument, its purpose, the influence of the atmosphere and the possibilities of the sensitive element.

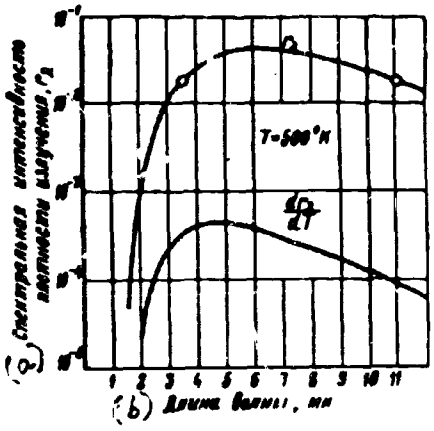

Fig. XI.2. Spectral intensity of radiation density of an ideal black body with T = 500°K and the rate of its change with change of temperature.
KEY: (a) Spectral intensity of radiation density r_λ ; (b) Wave length, μ .

There may be loss of energy in the atmosphere, and it would not present serious obstacles for the development of instruments of infrared technology, if there were available corresponding, highly sensitive elements with wide spectral characteristic. In practice it is necessary to work with sensitive elements possessing either high sensitivity in a narrow spectral band (photoresistors, photodiodes) or comparatively low sensitivity in a wide range of wave lengths (thermoelements, bolometers).

Selection of a sensitive element after effective value of receivable radiant flux has been established should be made, while considering its spectral sensitivity, volt sensitivity (v/w), threshold of sensitivity (w), time lag and utilization factor of a given radiation. Moreover in each concrete case it is necessary to go into a compromise solution. It is not obligatory to select a sensitive element with a wide spectral characteristic or with maximum integral sensitivity (by minimum equivalent power of noises), since this can lead either to complication of construction (to demand deep cooling) or to an increase in time lag of the system (as in the case of PbS). Frequently it is necessary also to consider the necessity of filtration of interferring radiation of the background.

One of the basic requirements during selection of a sensitive element is

maximum conversion of radiant flux reaching it:

$$\mathcal{R}_{\text{э}\Phi} = \int_0^\infty r_\lambda \varepsilon_\lambda S_\lambda \tau_{\text{оп}\lambda} d\lambda, \qquad \text{(XI.3)}$$

where $\tau_{\text{оп}\lambda}$ - spectral transmittance of optics, including filter.

Calculation of this integral may be performed graphically. For that, for instance, on curves $r_\lambda \varepsilon_\lambda$ (see Fig. XI.1) are put curves of spectral sensitivity of the photoresistor and spectral transmission of the optical system. Multiplying ordinates for each wave length, we will obtain curves limiting areas proportional to the output of the sensitive element $\mathcal{R}_{\text{э}\Phi}$ for a given radiation.

Such a method of appraisal allows us to compare the effectiveness of a sensitive element to radiation with a given temperature or the effectiveness of a sensitive element to radiations with various temperatures.

In Fig. XI.3 is given the calculation of $\mathcal{R}_{\text{э}\Phi}$ for lead sulfide (-78°C) and lead telluride (-185°C) photoresistors with respect to the radiation of a gray body with a temperature of 100°C ($\varepsilon = 0.5$).

During the appraisal of effective radiation, the effect of the transmission of optical components of the receiving device, including the filter was not considered. Therefore, the given curves characterize only effective spectral intensity of radiation density of target (w/cm^3), perceived by the sensitive element after passage by radiant flux through the atmosphere.

As can be seen from the given example (see Fix. XI.3), the effectiveness of lead telluride is higher than (area σ_2) lead sulfide photoresistors (area σ_1) because of its large region of spectral sensitivity. Effectiveness of PbTe grows with increase of radiation temperature of target and increase of cooling depth of sensitive element. The latter is illustrated by data of [illegible] S. Lakk [1], which presents the following relationships of output signals for PbS and PbTe during the reception of radiation of an ideal black body with a temperature of 500°K at a distance of 1850 m:

PbS(90°K): PbS (293°K) = 4.5;
PbTe(90°K): PbS (90°K) = 5.2;
PbTe(90°K): PbS (293°K) = 24.

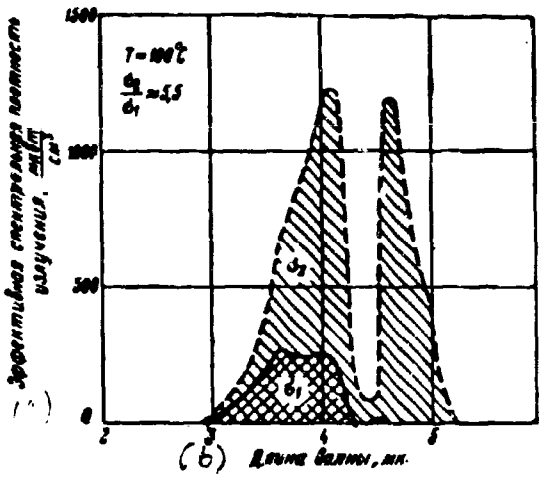

Fig. XI.3. Reaction of PbS(-78°C) and PbTe (-185°C) to radiation with T = 100°C.
KEY: (a) Effective spectral density of radiation, $\frac{\mu W}{cm^3}$; (b) Wave length, μ.

Thus, if PbTe and PbS have identical sensitivity on wave lengths corresponding to maximum sensitivity, then PbTe will be approximately 24 times more sensitive than PbS at room temperature for the registration of total radiation with a temperature of 500°K. In reality integral sensitivity of PbTe is somewhat less than the sensitivity of PbS and, therefore, such an advantage is not obtained.

With such an appraisal of a sensitive element, naturally, the question appears about the expediency of changing to systems with wider bands: lead selenide, indium antimonide and germanium, especially for registration of low-temperature radiation. Such a transition may be justified only if the spectral curve of sensitivity of the photoresistor and its maximum are inside window of transparency of the atmosphere 7.5-13.5 μ. Otherwise, expansion of the region of spectral sensitivity of the photoresistor as compared to PbTe gives no advantages, since in the region of 5.2-7.5 μ the atmosphere in its lower layers is absolutely opaque*. Growth of effectiveness of sensitive elements with longer wave lengths during registration of low-temperature radiation at great heights and in space will take place in any case.

The considered criterion for the appraisal of receiving devices of infrared technology, founded on the calculation of the effectiveness of using the spectrum of radiation, allows us to estimate the effect of target and background radiations

*Application of a broad-band sensitive element can give a well-known advantage when its sensitivity in a wave range of 3-5.2 μ is higher than for PbTe.

on any sensitive element, and also to determine the most optimum conditions of filtration of background.

If one were to construct the dependency of spectral effectiveness of radiation energy for any sensitive element (for instance, PbS) on the temperature of a black body, then one can determine not only optimum target temperatures for a given system, but the degree of interferring action of radiation sources with other temperatures (Fig. XI.4).

In the case of a system with PbS optimum temperature is 1700°K, since the system obtains 22% total energy. The system does not react to intrinsic emission of clouds (273°K), and the reaction to targets such as a jet nozzle of an aircraft (700°K) is sufficiently high. However, it possesses almost the same sensitivity to reflected solar energy and, consequently, is subject to significant influence of background.

When designing infrared equipment the problem of weakening the interferring radiation of the background is the most difficult, since the background can be various sources of proper or reflected radiations: sunlight, light reflected from clouds, from the surface of Earth and the Moon, radiation of objects [illegible], and the atmosphere.

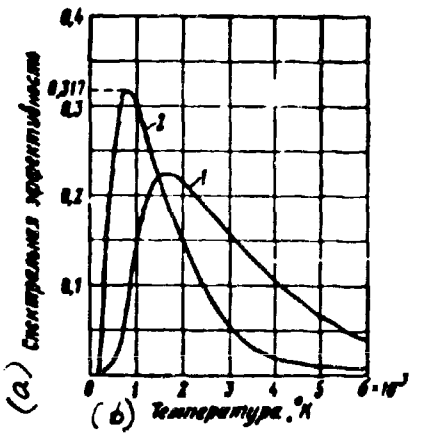

Fig. XI.4. Reaction of PbS to targets with different temperatures: 1--system with PbS; 2--system with optimum filtration.
KEY: (a) Spectral effectiveness; (b) Temperature, °K.

Control of harmful background radiation can be produced by various methods: a means of isolating target by its dimension, isolation of intensity of radiation, or a method of optical filtration [2].

The method of optical filtration is the most widespread in instruments and consists

of the following. If spectral characteristics of target and background radiations are known, then it is possible to select filters which will pass a large part of target radiation and almost completely cut out background radiation.

In the case of the application of instruments by day, basic interferring background it is possible to consider reflected or scattered sunlight, the spectral composition of which is near to straight solar radiation. Sun at a temperature of $T_{\text{с}} = 6000°K$ radiates a spectrum with wave length $\lambda_{\text{макс}} = 0.5\ \mu$, 50% of the energy in which belongs to the infrared range with wave lengths more than $0.7\ \mu$, 25% - to the region over $1\ \mu$ and 2% - over $3\ \mu$. Therefore, the basic problem of filtration in this case is cutting out the visible and near-wave infrared radiations during simultaneous transmission of maximum target radiation. Since the temperature of the target is always significantly lower than the temperature of the Sun, this method is sufficiently effective if transmission of the atmosphere and the optics is known.

In the case of the application of equipment at night or on targets with maximum radiation on waves over $4\ \mu$ the interferring background may be the radiation of the actual medium, earth and atmosphere. In this case it is necessary to cut out long-wave radiation that may be attained by means of a corresponding combination of photoresistor an long-wave filter.

Using the method of optical filtration, it is possible significantly to increase effectiveness of the receiving device during work on comparatively low-temperature targets. Thus, in Fig. XI.4 is given the curve of spectral effectiveness of an infrared system during optimum filtration, from which it is clear that in this case reaction of the system is maximum (0.317) for radiations with temperature near 883°K during sharp suppression of sensitivity to interferring background.

However, this method in practice will not apply if the temperature of the target is close to the temperature of the background or when radiation reflected from the background and radiation of the target possess similar spectral characteristics.

For isolation of a target in this case it is possible to use differences in dimensions of target and background. Many diagrams of target isolation, founded on this principle, have been developed, some very complicated; however, in the basis there is assumed always the assumption about the point character of target image on the sensitive element and about heterogeneities of the background having finite length.

This allows the modulation of target image without modulating image of background, or the development of an analyzer in the form of a system of an opaque element (periodically introduced in the field of sight) with dimensions equal to the dimensions of target image. Then, if infrared radiation, after introduction of the opaque element, attains the sensitive element, this indicates that the surface radiating the infrared beams is larger than the surface of the target and, consequently, is a heterogeneity of the background.

2. Criterion for Appraisal of Effectiveness of Passive Infrared Systems

The efficiency of infrared systems it is possible to estimate by different parameters. However, in instruments of military assignment and, in particular, in instruments of detection, fire control and homing guidance system, from which a large range is required, a criterion for appraisal of effectiveness can be the ability to reveal the target in the presence of noises. Therefore as a criterion during appraisal of the efficiency of passive instruments of military assignment one should consider the minimum signal which may be revealed on a background of noises camouflaging the useful signal.

Noises in instruments of infrared technology are basically from two causes:

a) noises of electronic systems during mechanical vibrations or during the work of follow-up systems. These noises are changed in time, and in correctly designed systems the basic sources of noises will be the sensitive element and the amplifying circuit;

b) noises appearing from a heterogeneity of atmospheric radiation, background of sky or earth. These noises are the result of either direct radiation of the Sun, reflection or scattering of solar energy, or the intrinsic emission of the natural background. They endure comparatively slow changes in time and, therefore, are estimated by their space distribution.

Chaotic fluctuations of radiant flux perceived by the sensitive element, in character, little differ from set noises in the receiving device. We cannot separate them until the level of receivable infrared energy exceeds the level of set noises of the sensitive element. Therefore, sensitivity of equipment it is possible to estimate also by the level of its set noises - the threshold of sensitivity (in foreign literature - equivalent power of noises). Under threshold of sensitivity we understand the power of the infrared radiation in watts on entrance of the sensitive element, which creates on output a signal equal to the average-quadratic value of the level of noises in a corresponding band of frequencies.

The idea "threshold of sensitivity" (equivalent power of noises) pertains to the sensitive element. Since infrared systems include other sources of noises, then for an operational characteristic of the instrument on the whole (in conditions of detection or tracking) an idea about the minimum threshold of sensitivity of the equipment is expedient for the guarantee of reliable work. The ratio of these magnitudes determines the signal noise value, at which the system will work reliably. Usually when designing infrared passive systems with scanning, the signal-to-noise ratio is equal to 3-5.

The signal-to-noise ratio allows us, by the known magnitude of noise, to estimate the range of the infrared equipment.

If we completely disregard noises of the background and radiation of components of the equipment before the sensitive element, then the range of the

passive infrared system may be determined from relationship

$$\frac{S}{N}\overline{N}(\Delta f)=\frac{S_ц S_0}{\pi L_ц}\int_0^\infty r_\lambda \tau_\lambda \tau_{0\lambda} S_\lambda d\lambda, \qquad (XI.4)$$

where $\frac{S}{N}$ - signal-to-noise ratio,

$\overline{N}(\Delta f)$ - average-quadratic value of noises of the sensitive element in a given Δf band of frequencies,

$S_ц$ - area of target, cm^2,

S_0 - area of entrance pupil of objective,

r_λ - spectral density of radiation, w/cm^3,

τ_λ - transmission of atmosphere,

$\tau_{0\lambda}$ - transmission of optical system,

S_λ - spectral sensitivity of receiver,

L - distance to source of radiation.

3. Range of Passive Infrared Systems

Range of passive infrared systems depends on many factors, which sometimes cannot be considered. However, tentatively, the range of a passive infrared system may be estimated if it is possible to estimate the radiant flux reaching from the target to the sensitive element and compare it with the threshold of sensitivity of the equipment $\Phi_ш$ (equivalent power of noises), expressed in watts. Such calculation of range, valid in the absence of background radiation, may be performed by the formula

$$L=\sqrt{\frac{\varepsilon\sigma}{\pi}T_ц^4\frac{S_ц S_0}{\Phi_ш}\tau_0\tau_a\cos\alpha\cos\beta}, \qquad (XI.5)$$

where α,β - angles (Fig. XI.5) between line of observation, normal to radiating surface $S_ц$, and normal to plane of objective S_0, respectively.

In expression (XI.5) enter integral magnitudes of emissivity ε, transparency of atmosphere τ_a and optics τ_0 with respect to radiation with temperature $T_ц$ and for a given sensitive element. Therefore, the magnitude of threshold sensitivity $\mathcal{D}_ш$

should be determined based on the given spectral distribution of target radiation, transmission of the atmosphere, and sensitivity of the receiver, which presents known inconveniences, since rated value Φ_q always is given with respect to radiation with a fully defined temperature. Furthermore, for a given radiation and spectral characteristic of the sensitive element it is necessary to determine effective transmission of atmosphere and optics.

The complexity of such calculation consists in the determination of effective radiant flux acting on the sensitive element. A method of calculating effective flux by graphic means was considered in Section 1. As a result of graphic integration, the limits of which, in practice, are restricted by the spectral interval of sensitivity of the receiver and the transparency of the optics (λ_2—λ_1), there is determined the effective value of radiant flux acting on the receiver (w/cm^2).

The given method is acceptable for calculating range of passive infrared systems intended for work at night when the equivalent power of noises of the sensitive element (average-quadratic value of noise) is determined by set noises of the sensitive layer and is close to the rated values. By day, when value $\bar{N}$ is determined basically by noises of the background and cannot be sufficiently accurately considered, such a calculation can give noticeable errors.

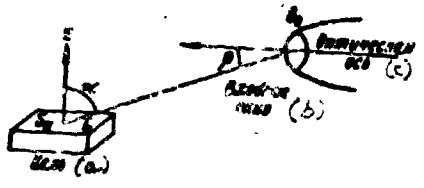

Fig. XI.5. Calculation of range of passive system.
Key: (a) Target; (b) entrance window; (c) Optical axis.

In the considered methods of appraising the range of passive infrared systems, transparency of the atmosphere is practically considered for a limited layer along corresponding curves. The error will not be too great if one remembers that the greater the layer of absorber, the less the additional absorption causes increase of layer of atmosphere. Experimentally, it is established that a noticeable change of atmospheric transmission (especially at great heights)

with increase in its thickness over 2 km is not observed. This allows us to use Jerby's experimental curves of transparency of atmosphere without introduction of noticeable error in calculation of range of infrared systems.

Calculating the range of passive infrared systems by the considered formulas is sufficiently labor-consuming. Therefore, attempts to construct nomographs for the calculation of the range of passive infrared systems were undertaken. One such nomograph (Seymour's nomograph) is presented in Fig. XI.6 [3].

The nomograph is plotted in accordance with formula (XI.6) under following assumptions:

1) radiation of target is modulated with a frequency not exceeding a limit determined by the time constant of the receiver;

2) sensitivity of receiving device is limited by set noises of the receiver of radiation, and the signal-to-noise ratio is 4;

3) image of target is completely inscribed in the dimensions of the sensitive element:

$$L=K\sqrt{\int_0^\infty \frac{J_\lambda \tau_{o\lambda}\tau_{a\lambda}}{N}\,d\lambda \frac{D}{F}\left(\frac{nt_s}{\omega t}\right)^{\frac{1}{2}}}. \qquad (XI.6)$$

where $\int_0^\infty \frac{J_\lambda \tau_{o\lambda}\tau_{a\lambda}}{N}\,d\lambda = A$ - spectral factor;

K - proportionality factor;

J_λ - radiation intensity, w/sterad;

$\tau_{a\lambda}$ - spectral transmittance of atmosphere, averaged for spectral wavelength interval of sensitivity of the radiation receiver;

$\tau_{o\lambda}$ - spectral transmission of optics;

N - limiting sensitivity of receiver (equivalent power of noises) w;

$\frac{D}{F}$ - relative aperture of optics of system;

$\Gamma=\frac{nt_s}{\omega t}$ - parameter of scanning;

n - number of sensitive elements;

t_s - time of frame, sec;

ω - field of sight with respect to frame, sterad;

t - time constant, sec.

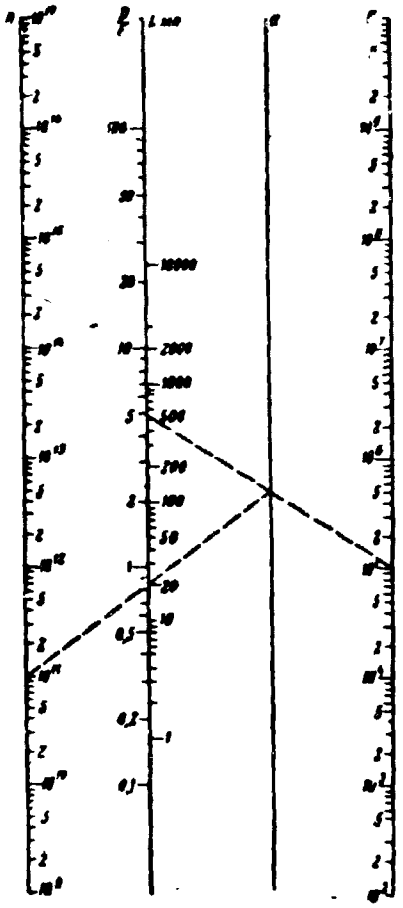

Fig. XI.6. Nomograph of calculation of range of passive infrared system.

Having determined the scanning parameter of the infrared system, we connect corresponding point of scale Γ with value of relative aperture. Then we connect point of intersection of a given curve with auxiliary line a with definite value of spectral factor A. Range of the infrared system in miles is calculated on scale L.

If on the receiver simultaneously act fluxes from target and surrounding background, whose radiation cannot be filtered, then it is said that the system works on thermal contrast. Range of the system may be determined based on the following consideration.

Effective radiant flux, perceived by the receiver from target and background*, obviously, will be defined as

$$\Phi_u = \varepsilon_u \sigma T_u^4 S_u \frac{S_o}{\pi L^2} \tau_{o.u} \tau_{a.u} \cos\alpha \cos\beta;$$

$$\Phi_\phi = \varepsilon_\phi \sigma T_\phi^4 S_\phi \frac{S_o}{\pi L^2} \tau_{o.\phi} \tau_{a.\phi} \cos\alpha \cos\beta.$$

Useful signal on output of passive infrared system will be proportional to the difference between the total flux from the target and the part of the background,

*Indices «ф» and «u» in expressions pertain to radiation of background and target, respectively.

not covered by the target, and the flux from the background is

$$\Delta\Phi = \Phi_{\text{ц}} + \Phi'_{\phi} - \Phi_{\phi}, \qquad \text{(XI.7)}$$

where

$$\Phi'_{\phi} = \varepsilon_{\phi} \sigma T_{\phi}^4 (S_{\phi} - S_{\text{ц}}) \frac{S_{\text{о}}}{\pi L^2} \tau_{\text{о}.\phi} \tau_{\text{а}.\phi} \cos\alpha \cos\beta,$$

consequently,

$$\Delta\Phi = \sigma S_{\text{ц}} \frac{S_{\text{о}}}{\pi L^2} \cos\alpha \cos\beta (\varepsilon_{\text{ц}} \tau_{\text{о}.\text{ц}} \tau_{\text{а}.\text{ц}} T_{\text{ц}}^4 - \varepsilon_{\phi} \tau_{\text{о}.\phi} \tau_{\text{а}.\phi} T_{\phi}^4).$$

If one were to take $\Delta\Phi = \Phi_{\text{п}}$, then by analogy with expression (XI.5) one can determine maximum range of such a system

$$L = \sqrt{\frac{\sigma}{\text{п}} S_{\text{ц}} S_{\text{о}} \cos\alpha \cos\beta \left(\frac{\varepsilon_{\text{ц}} \tau_{\text{о}.\text{ц}} \tau_{\text{а}.\text{ц}} T_{\text{ц}}^4}{\Phi_{\text{п}}} - \frac{\varepsilon_{\phi} \tau_{\text{о}.\phi} \tau_{\text{а}.\phi} T_{\phi}^4}{\Phi_{\text{п}}} \right)}. \qquad \text{(XI.8)}$$

If difference $\Delta\Phi$ is less than the threshold sensitivity of the receiving device of the infrared system, then the latter will lose the target.

4. Range of Active Infrared Systems

Active infrared systems find wide application in instruments of night vision, rifle night sights, and range finders. Such systems include sources of radiation of either pulse action or continuous burning.

The principle of action of active systems, independent of the type of radiation source picked up by them, consists of the following. A high-intensity source of radiation, placed in the focus of a reflector and covered by an infrared filter, irradiates the target. The radiation energy reflected from the target is perceived by a receiving system and is focused on the sensitive element which [illegible] a corresponding signal.

The effectiveness of active systems, to a very strong degree, is determined by the weakening of radiant flux in the atmosphere and, consequently, by meteorological visual range D.

Range may be determined based on the following considerations. If radiation intensity of a searchlight is designated by $J_{\text{п}}$, then irradiance of object $\mathfrak{E}_{\text{о}}$ at

distance L from the searchlight may be calculated from relationship

$$\mathcal{E}_0 = \frac{J_\Sigma}{L^2} e^{-\beta L}, \qquad \text{(XI.9)}$$

where β - attenuation factor of atmosphere, averaged for the spectral interval of sensitivity of the system.

As a result of the reflection of radiant flux from an object in the plane of the objective of the observation instrument, there is created irradiance

$$\mathcal{E}_{\Sigma p} = \frac{J_0}{L^2} e^{-\beta L} = \frac{J_\Sigma}{L^2} S_{0p} e^{-\beta L}, \qquad \text{(XI.10)}$$

where $J_0 = S_0 \mathcal{E}_{0p} \frac{1}{\pi}$ - radiation intensity of radiant flux reflected from the object in the direction of the observation instrument.

If one were to produce corresponding conversion and to replace magnitude of attenuation factor by effective visual range (visual range in a given range of wave lengths, for which it is possible to take value of attenuation factor β), then expression (XI.10) after taking the logarithm will take the form

$$\log \frac{J_\Sigma}{\mathcal{E}_\Sigma} = 4 \log L - \log (S_{0p}) + \frac{1{,}45L}{D}, \qquad \text{(XI.11)}$$

where $\mathcal{E}_\Sigma$ - threshold sensitivity of observation instrument;

D - effective distance of meteorological visibility.

Certain authors define the logarithm of ratio $\frac{J_\Sigma}{\mathcal{E}_\Sigma}$ as a quality of an infrared active system G, characterizing how many times greater the order of magnitude of radiation intensity of a searchlight is than the threshold sensitivity of an observation instrument.

Solving equation (XI.11) with various values of system quality, it is possible to construct the dependency of the range of an infrared active system on the meteorological visual range with various values of G.

From Fig. XI.7 it is clear that during quality of system G = 8 an increase in meteorological visual range from 100 to 500 m gives the same increase in range of system as an increase in quality from 8 to 18, which corresponds to an improvement of the system 10^{10} times. With increase in meteorological visual range this effect

is lowered. In the case of a change in meteorological visual range from 10 to 100 km the increase in range of system with G = 8 constitutes only 5 km which corresponds to a growth in quality from 8 to 9.

The range of active electron-optical systems is also noticeably affected by the brightness of the background on the screen of the converter, caused by thermoemission of electrons from the photocathode and its gating by radiation of the searchlight reflected and scattered in the thickness of the atmosphere. Brightness of the background on the screen may be noticeably lowered by rational location of the searchlight and observation instrument, and also by cooling of photocathode. In the last case, gain in free-space range may be calculated from expression [4]:

$$\frac{L_1}{L_2} = \sqrt{\frac{\frac{\eta}{\Gamma_0^2}\frac{1}{4\lambda^2}\mathcal{B} + R_\Phi}{\frac{\eta}{\Gamma_0^2}\frac{1}{4\lambda^2}\mathcal{B}}}, \tag{XI.12}$$

where L_1, L_2 - free-space range of target in an instrument with cooled and uncooled photocathode, respectively;

η - conversion factor;

Γ_0 - electron-optical magnification;

$\mathcal{B}$ - density of radiation of observed surface;

R_Φ - density of radiation of background of screen.

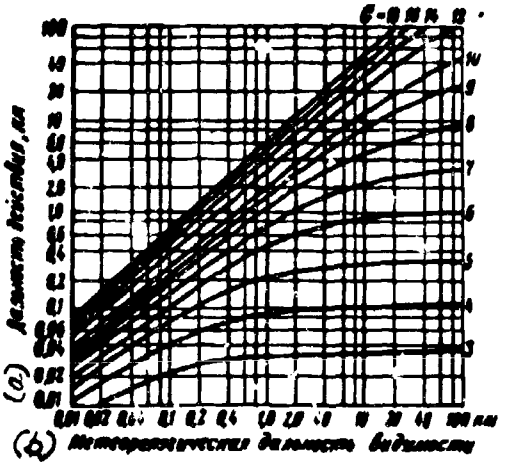

Fig. XI.7. Range of active electron-optical systems depending upon meteorological visual range and quality of systems.
KEY: (a) Range, km; (b) Meteorological visual range.

If active systems are intended not for construction of image, but for obtaining some kind of information about the presence of a target (for instance, in range finders), then, as a rule, pulse irradiation of target is used. Repetition rate of pulses is determined by maximum permissible dissipated power in tube and circuit

$$P_{av}=\frac{CU^2}{2}f, \qquad (XI.13)$$

where f - frequency of repetition of pulses;

C - discharge capacity;

U - voltage to which capacitor is charged.

If radiation intensity of pulse searchlight is $J_п$, then radiance of target will be determined by expression

$$B_ц=\frac{\rho_ц B_п}{\pi}=\frac{\eta_п B_п S_п \rho_ц}{\pi L^2}\tau^L, \qquad (XI.14)$$

where $\eta_п$ - efficiency of optics of searchlight;

$S_п$ - area of light aperture of searchlight;

$B_п$ - brightness of pulse tube;

$\rho_ц$ - coefficient of diffuse reflection of target surface.

Since radiation intensity of target due to reflected radiant flux is $J_ц=S_ц B_ц$, then on the sensitive element of the receiver falls radiant flux $\Phi_с$, causing, on output of system, a definite useful signal

$$\Phi_с=J_ц\frac{S_{пр}}{L^2}\mu\tau^L=\frac{\eta_п\mu S_п S_{пр} S_ц B_п \rho_ц \tau^{2L}}{\pi L^4}, \qquad (XI.15)$$

where μ - efficiency of receiving optics;

$S_{пр}$ - area of entrance window of receiving optics;

$S_ц$ - area of projection of the irradiated part of the target in a direction to the receiver.

Expression (XI.15) is basic for determining range of pulse optical systems. However, simultaneously with useful radiant flux $\Phi_с$ on the receiving device falls also radiant flux from the background, causing noises on output of system, on the background of which it is necessary to separate a useful signal

$$\Phi_ф=\frac{\mu S_{пр} B_ф S'_ц}{L^2}, \qquad (XI.16)$$

where $\mathscr{B}_\phi$ - brightness of background;

S'_n - area of spot entering into the geometric dimensions of target.

The magnitude of noises is proportional in general to the angle of sight of the receiving system θ, the area of the receiving window of optics $S_{вх}$ and the brightness of the background $\mathscr{B}_\phi$

$$N = K\theta S_{вх}\mathscr{B}_\phi^{1/2}. \qquad (XI.17)$$

Consequently, effectiveness of a pulse optical system S/N is determined by parameters of target, source of radiation, transmitting and receiving optics, atmosphere, background, and distance

$$S/N = K\frac{S_n S_{пр}\mathscr{B}_n\rho_n\tau^{2L}}{\theta L^4\mathscr{B}_\phi^{1/2}}. \qquad (XI.18)$$

Let us consider expression (XI.18) for a case when, as a sensitive element, is applied a photomultiplier (FEU).

The current of the FEU, because of useful signal Φ_c and signal from background Φ_ϕ is proportional to the corresponding radiant fluxes,

$$i_c = K\Phi_c,$$
$$i_\phi = K\Phi_\phi.$$

The current of noises on output of the amplifier of the receiving system may be expressed by the following formula:

$$i_ш = \sqrt{2ei_\phi\Delta f}. \qquad (XI.19)$$

where e - electron charge;

Δf - pass band of amplifier.

Consequently, the ratio of useful signal to noises may be expressed in the following manner:

$$\frac{i_c}{i_ш} = \frac{K\Phi_c}{\sqrt{2eK\Phi_\phi\Delta f}}.$$

Substituting corresponding values Φ_c and Φ_ϕ and considering that

$$S_n = \frac{S_n L^2}{f_n^2},$$

where S_n - area of radiation source;

f_n - focal length of optics of searchlight,

we will obtain the following relationship between signal and noises in a pulse

optical system with a photomultiplier as a sensitive element,

$$\frac{i_c}{i_{\text{ш}}} = \frac{\eta_{\text{к}} S_{\text{и}} \rho_{\text{ц}} \Phi_{\text{и}} \tau^{2L}}{\pi L^4 f_{\text{и}}} \sqrt{\frac{S_{\text{эр}} \mu K S_{\text{ц}}}{2e \Delta f \Phi_{\text{ф}}}}. \qquad \text{(XI.20)}$$

Setting up a signal-to-noise ratio necessary for reliable work of the system, from expression (XI.20) one can determine also its range.

From expression (XI.18) it is clear that noises are proportional the angle of sight of receiving system θ. So that the receiving system completely perceives the useful radiant flux, its angle of sight should be equal or larger than the angle of radiation of the searchlight. However, in the latter case noises are increased, and, therefore, it is desirable to have field of sight minimum, so that the receiving device takes the smallest possible radiant flux from the background.

If angular dimension of the target (spot) is larger than the angle of sight of the receiving device, then dimension of spot affecting the receiving device is $S_{\text{ц}} = \theta L$ (during small angles of sight). Substituting this value in formula (XI.18), we will find that effectiveness of a pulse optical device is inversely proportional to the third power of distance, and not to the fourth,

$$\frac{S}{N} = K \frac{S_{\text{и}} \Phi_{\text{и}} \rho_{\text{ц}} \tau^{2L}}{L^3 \Phi_{\text{ф}}^{1/2}}. \qquad \text{(XI.21)}$$

Literature

1. A. S. Lokk. Missile control. State Technical Press, 1957.
2. Proc. IRE, 1959, Sep., Vol. 47, No. 9.
3. Aviation Age, 1958, Vol. 28, No. 7.
4. Z. angew. Math und Phys., 1958, 25 Sep., No. 3.

C H A P T E R XII

COUNTERACTION TO INFRARED MEANS OF AN ENEMY

1. Methods of Counteraction

Above it was indicated that passive infrared means of detection, observation, aiming, and guiding are more noise-immune as compared to active. Actually, an enemy is not able to detect the work of a passive system since it does not radiate any energy into surrounding space. This is one of the disputable advantages of passive systems in general, and infrared, in particular, as compared to active, which for their operation are forced to irradiate target with electromagnetic energy and perceive an echo-signal reflected from the target.

In connection with this, it has long been considered that counteraction to infrared means of an enemy is difficult, although it has been indicated that infrared equipment, as compared to radar, has a disadvantage with respect to sensitivity to false thermal targets [1, 2, 3]. Actually, the presence of a large quantity of bodies radiating infrared beams around a target can lead to the fact that an infrared system, intended for detection and tracking of a certain target, will turn to tracking a false target. This is especially dangerous, if the infrared system is designed for autonomous guiding of missile to target, with which it is no longer possible to correct trajectory of missile flight.

The second possibility of lowering the effectiveness of instruments of infrared technology is caused by their basic deficiency - the great dependency of efficiency

[illegible] state of the atmosphere. As already was noted, in strong fog and in clouds instruments of infrared technology give practically no noticeable advantage over the visual method of detection and, therefore, cannot be effectively used. Precisely therefore, in a number of reports [4, 5], for use as measures of counteraction there are suggested such natural camouflaging means as fog and overcast.

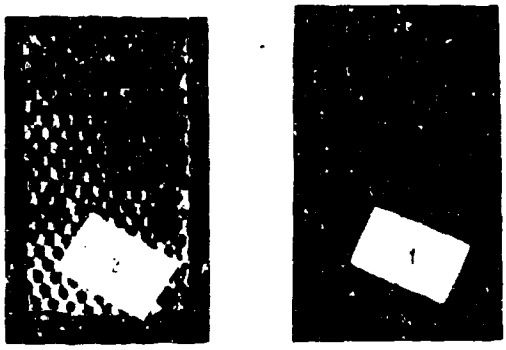

Fig. XII.1. Image of normal camouflage net in light 1 and infrared 2 beams.

Long and successful has been the work conducted on the creation of camouflage means for protection of objects from their detection by photographic infrared equipment. There have been developed and used specially colored materials and camouflage nets, and also paint for the camouflage of objects, whose spectral reflectivities in the visible and infrared regions of the spectrum coincide with the spectral reflectivities of the surrounding background [6, 7, 8] (Fig. XII.1).

This method of counteracting the operation of a narrow group of infrared instruments can give positive results in the case of camouflage of stationary objects or moving objects on a uniform background (for instance, ships on a background of water). The proper thermal radiation of bodies is impossible to mask by such a method.

Concealing proper thermal radiation of certain objects may be carried out by a method long known in heat-technology: application of coverings from thermo-insulational materials and screen devices around protected objects. However, this method, in spite of its cumbersomeness and high costs, does not resolve completely the problem of camouflaging even the majority of stationary objects, not mentioning moving objects. Moreover, it can, in a number of cases, lead to the disturbance of thermal conditions of the protected object and as a consequence, to prematurely

[illegible] of false radiating targets around a protected object, although possible in stationary conditions, is not always effective. For instance, to create interferences for the operation of the optical homing guidance system SOLO it is necessary, preliminarily, in direct proximity to the protected object to place a system of radiation sources, which after drop of bomb it is necessary to transfer slowly away from the object [9], which in practice is very difficult to carry out.

The wide development of means of infrared technology, especially sighting systems and infrared homing devices of rocket missiles, has made necessary a more radical resolution of the old problem of "lance and shield", i.e., creation of a more effective means of protection from instruments of infrared technology.

The entire complexity of the problem at hand consists in the fact that for the creation of effective interference to infrared instruments of detection and aiming, it is necessary to simulate the thermal radiation of the protected object both with respect to the intensity and the spectral composition of the radiation [10]. This, even if it may be carried out in ground conditions, will demand huge expenditures, since in practice the false target should be equivalent to the protected object in temperature rate, dimensions, and emissivity of material.

The most complicated is the problem of protecting flying or moving objects, since on them or near them we can establish bulky installations of counteraction to infrared instruments.

The first method of protecting such objects consists in lowering thermal radiation, i.e., in lowering the temperature of departing gases, decreasing the surfaces of high-speed aircraft and rockets, and also decreasing their emissivity. However, this method is in contradiction to the tactical requirements of aircraft and their durability and may be applied only in certain specific cases. Actually, the continuous growth in aircraft speed of flight requires increase in engine power,

[illegible] which causes skin temperature increase, and, therefore, from the point of view of guaranteeing durability of construction, it is necessary to have high a radiation factor of skin material. In practice it is possible to lower the thermal radiation of aircraft with artificial cooling of their surface by means of the introduction of a refrigerant.

Up to now there have been published very few materials shedding light on the state of works in the region of counteraction to infrared instruments. However, available short reports about tests of rockets with infrared homing devices and separate fragmentary expressions on questions of counteraction allow us to outline basic ways of solving the problem at hand. These ways are:

a) improved methods of scattering heat [11];

b) maneuvering of target [3, 6];

c) application of small-size, high-intensity sources of radiation in the form of pyrotechnic rockets [12, 13, 14, 15, 16];

d) application of low-temperature sources of interference [10, 13, 14, 17, 18];

e) application of high-speed rockets, released in the direction of an attacking enemy [13, 14, 15, 19];

f) application of artificial dimming of atmosphere [6, 20];

g) creation of special flying apparatuses supplied with radiators and accompanying bombers during their flight above enemy territory [3, 15, 21].

2. Lowering of Thermal Radiation

In the foreign press there have been published several theoretical and experimental works, considering the possibility of lowering the temperature of the aircraft surface heated both because of the work of the motors because of aerodynamic braking [22, 23].

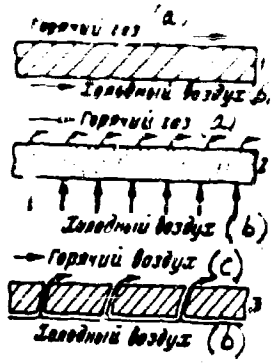

Fig. XII.2. Diagram of convection (1) transpiration (2) and film (3) cooling. KEY: (a) Hot gas; (b) Cold air; (c) Hot air.

The application of air as a refrigerant for cooling surfaces of aircraft, since it is always possible to obtain it at all heights where application the use of airbreathing-jet and turbojet engines is still possible, and it is not necessary to have special reserves of refrigerant on board, since even without that the specific gravity of the motor and the fuel is sufficiently great (for contemporary aircraft it constitutes 50-70% of the total gross weight). The sucking in of air and its preliminary cooling, naturally, cause additional consumption of power and somewhat increase weight of the motor. As compared to other methods of cooling this method is more economical.

There are three methods of cooling external and internal surfaces of an aircraft with the help of air (Fig. XII.2): convection, transpiration, and film.

With the convection method of cooling the flow of the air coolant heads along a cooled surface of wall. Optimum conditions of cooling, in this case, are determined by temperature of wall T_c, at which the necessary durability of material is still ensured. Cooling of walls to lower temperatures requires significant flow rate of air and, consequently, additional expenditures of power.

Effectiveness of convection cooling at various relative flow rates of air is represented in Fig. XII.3.

In Fig. XII.3, as on all subsequent graphs, there is designated:

T_c - temperature of cooled wall, T_B - temperature of air, $T_г$ - temperature of gas, $\rho_в v_в$ - average mass speed of air coolant, $\rho_г v_г$ - average mass speed of gas flow, $\eta_т$ - thermal efficiency of cooling.

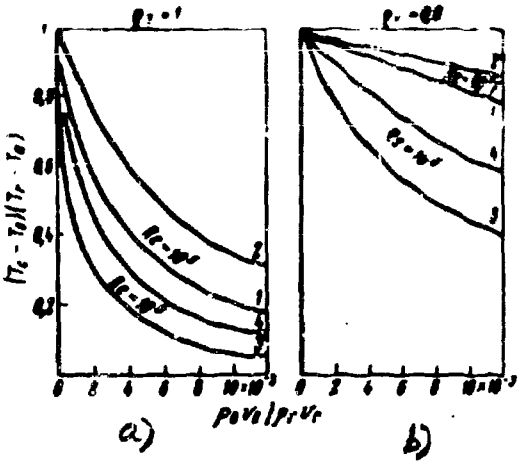

Fig. XII.3. Effectiveness of convection cooling.
a) 1--laminar with radiation; 2--without radiation; 3--turbulent without radiation; 4--with radiation; b) 1--laminar without radiation; 2--with radiation; 3--turbulent without radiation; 4--with radiation.

From curves shown in Fig. [illegible] it is clear that effectiveness of convection cooling is increased with an increase in relative flow rate of air and an increase in Reynolds number and thermal efficiency. Furthermore, effectiveness of cooling in the case of laminar gas flow is higher than during turbulent flow. From the curves one may see also that with growth of relative flow rate of air the slope of curves decreases. Consequently, during achievement of a definite magnitude of relative flow rate of air its increase will not give a noticeable increase in effectiveness of cooling.

During transpiration cooling walls have to be prepared from porous materials, but air coolant should pass through the pores to the hot gas. In this case protective and cooling films are formed on the side of the hot gas, where air coolant is washed off by gas flow from the surface, just as it emerges from the pores. This creates a condition of countercurrent between heat removed from the surface by the air coolant and heat transferred from the hot gas to the wall. The effectiveness of cooling by such a method increases due to the fact that the area of contact between the air and the cooled wall is very large. Therefore, the temperature of the wall will be equal to the temperature of the air, at which it is washed off from the surface.

Results of research on transpiration cooling, shown in Fig. XII.4, show that with this method of cooling the required relative flow rate of air decreases with an increase of Reynolds number. Thus, to obtain identical effectiveness of cooling

of gas is more effective than during turbulent flow.

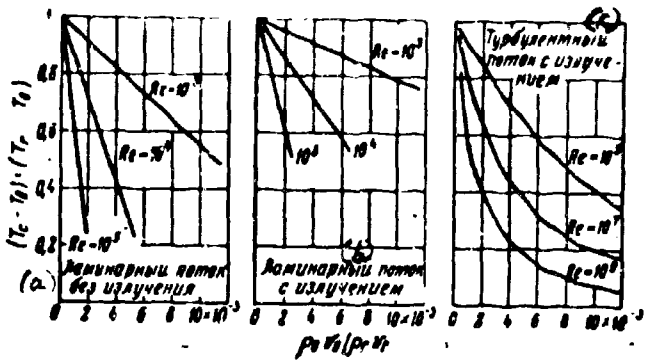

Fig. XII.4. Effectiveness of transpiration cooling.
KEY: (a) Laminar flow without radiation; (b) Laminar flow with radiation; (c) Turbulent flow with radiation.

During film cooling air flows through parallel slots of a cooled surface, forming a cold film. This film gradually is destroyed, as a consequence of which the wall remains cold only near the slot, gradually increasing its temperature downstream of the gas. Decrease in irregularity of temperature of walls may be attained by increasing the number of slots, which is clear from Fig. XII.5, where there is given the dependency of flow rate of air coolant with growth in the number of slots at fixed temperature of wall T_c.

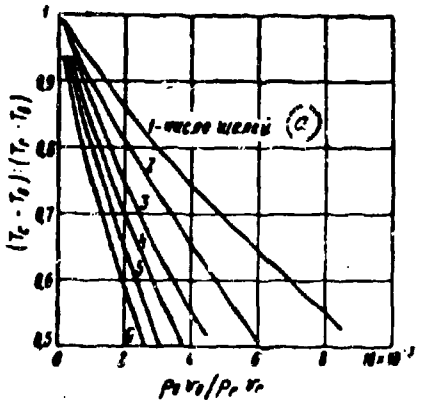

Fig. XII.5. Effectiveness of film cooling.
KEY: (a) Number of slots.

Comparison of the considered methods of cooling allows us to make the following conclusions:

1. With thermal cooling efficiency $\eta_T = 1$ and for comparatively good cooling $(T_c - T_в):(T_г - T_в) = 0.4$, during convection cooling is required almost three times more air than during transpiration.

2. Film cooling has, over other methods, the advantage that it may be applied in a majority of practical constructions.

During convection cooling air can be under any pressure, whereas during transpiration and film cooling there is required a surplus of air pressure above the pressure in the gas flow. It is true, during convection cooling there is required preliminary cooling of air heated by aerodynamic braking.

Effectiveness of cooling, from the point of view of thermal radiation of the aircraft, it is possible to estimate in the example of the convection method of cooling during turbulent flow of gases, taking into account radiation at Reynolds number $Re = 10^9$. For simplicity of calculation we take $\eta_T = 1$. Then for $T_r = 1000°K$ and $T_a = 373°K$ with ratio $(T_c - T_a) : (T_r - T_a) = 0.4$ we obtain temperature of cooled surface $T_c = 624°K$. Consequently, with all other conditions equal, thermal radiation intensity will decrease 6.5 times, and free-space range of the aircraft - in 2.55 times.

If, however, under these conditions we attain an increase of flow rate of air of 2.5 times, then there can be obtained an effectiveness of cooling equal to 0.2 (Fig. XII.3 curve 4a). For that case $T_c = 498°K$, which corresponds to a decrease in emissive power of radiation of 16 times, and free-space range of 4 times.

3. Counteraction by Maneuver

Counteraction by maneuver, attacking the means of the enemy, as a means of aircraft protection has long been well-known. Therefore, naturally, this method began to be considered as one of the possible variants of protection even in the case of enemy use of instruments of infrared technology.

The possibility of using (as a measure of counteracting infrared means of the enemy) maneuvering of the attacked target-aircraft is increased by certain peculiarities of the application of these means, namely:

a) the diagram of thermal radiation of contemporary jet aircraft has a sharp-directed character;

[illegible] of infrared technology, as well as other instruments for tracking the target-aircraft, have a limited field of sight and to assess rapidly the

time lag;

c) attacking aircraft of an enemy, equipped by infrared instruments of detection, aiming, and guiding, as a rule, have to execute attack of an air target from the side of its rear hemisphere, i.e., in pursuit. Consequently, their speed must significantly exceed the speed of the target, and, therefore, their maneuvering qualities will be worse than for the attacked aircraft;

d) the sharpness of maneuver of high-speed apparatuses is limited by the G-forces which appear (especially at low altitudes) and the effectiveness of carrier surfaces and controls (at great heights).

Thus, the maneuvering of the target-aircraft should follow, first, the creation of conditions of flight for the attacking object, at which G-forces would be created, causing either operational breakdown of instruments of infrared technology or disturbance of integrity of the separate structural units of the flying apparatus, and, secondly, the creation of conditions of flight for the flying apparatus with which the effectiveness of controls and its carrier surfaces would not ensure repetition of the maneuver of the target-aircraft.

Furthermore, maneuvering of the target-aircraft should be aimed at the problem of maximum lowering of thermal radiation in the direction of attack, since this still, to a larger degree, will create the prerequisite for appearance of a breakdown in the work of instruments of infrared technology. In some works [6] it is suggested, before fulfillment of maneuver, to turn off motors, which, naturally, will lead to breakdown of the work of the infrared equipment and to loss of target after second starting of motors, already on a new course (the target goes from the field of sight of the instrument of infrared technology).

Maneuver of the aircraft includes three basic elements, unequally valued from the point of view of their effectiveness as a method of counteracting the work of

instruments of infrared technology: change of speed, height, and course of flight.

Thus, a speed change of contemporary heavy bombers of 100-150 km/hr occurs for 2-2.5 min, when a rocket flies to target after its pick-up by an infrared homing device for only several seconds.

During maneuvering by height with preservation of the former flight course, rate of climb of the aircraft will not ensure a fast change of angular direction to target and will not lead to decrease of thermal radiation in the direction of attack. Furthermore, even if a rocket does not produce a direct hit on an aircraft, it will pass near it at a distance sufficient for operation of noncontact electro-optical detonators and the strike of a target-aircraft by fragments.

Obviously, the most effective maneuver should be a sharp change in the course of flight of the aircraft with maximum permissible bank for a given variant of aircraft load and height of flight. In this case a rocket supplied with an infrared homing device and having a significantly greater speed of flight than the aircraft must accomplish a turn with a significantly larger radius and, furthermore, there appears the real possibility of loss of target by the infrared homing device due to the sharp decrease of its thermal radiation.

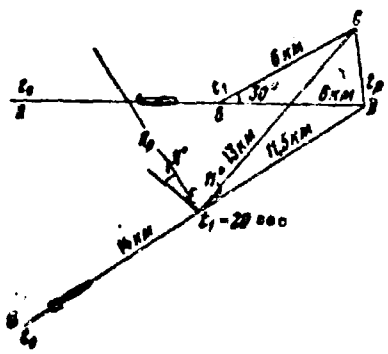

Fig. XII.6. To calculate guiding of rocket to a maneuvering target.

We will consider as an example (Fig. XII.6) the possibility of intercepting a maneuvering target with the help of an antiaircraft guided missile under the following conditions:

height of flight of aircraft H = = 20,000 m;

speed of flight of aircraft v_c = = 300 m/sec;

speed of rocket v_p = 700 m/sec;

weight of rocket P = 1000 kg;

thrust of motor F = 2000 kg;

permissible G-forces n = 1000 g.

20 sec after launching rocket, aircraft at point B makes a 30° turn, continuing flight in direction BC. Rocket during this time was at point E at distance 11.2 km from calculating point of encounter D. The homing device affecting rocket controls deflects its flight trajectory by an 11° angle in direction EC. If one were to consider approximately the length of the arc along which flight of the rocket continues as equal to chord EC, then it is possible to calculate the necessary radius of turn of the rocket so that it gets to new point of encounter C:

$$R_n = \frac{13 \cdot 57,3}{22} = 34 \text{ км}.$$

Permissible radius of turn of rocket can be calculated by the formula

$$R_g = \frac{v_p^2 P}{P \sin \alpha g},$$

where α - angle of displacement of rocket from initial direction of flight, at which G-forces are developed not higher than permissible.

In case n = 1000 g $\alpha = 15°$. Then

$$R_g = \frac{700^2 \cdot 1000}{516 \cdot 9,81} = 95 \text{ км}.$$

Comparing permissible radius of turn of rocket with necessary, it is possible to say that during maneuver of target with a 30° turn, in given conditions an encounter of missile and target will not occur.

From all considered it is clear that in certain cases maneuvering of aircraft can render counteraction to an attacking enemy using instruments of infrared technology.

It is necessary, however, to consider that time in making the maneuver and its sharpness are determined by speed and height of flight and gross weight of aircraft. With growth of speed and height of flight maneuver of aircraft becomes all the more inert and is characterized by a large radius of turn. This, in a number of cases, can set up a more profitable position for the attacking apparatus, and the attacked finds it all the more difficult to depart from under the blow by an energetic maneuver.

Considering the above-stated, maneuvering allows us, in a number of cases, to break up enemy attack, but not always can it lead to the required effect.

4. Artificial Sources of Infrared Radiation

In the process of tests of rockets of the "air - air" class with infrared homing devices in the United States and England it was noted that rockets, with great accuracy (up to direct hit), were led by these heads to an imitator of thermal radiation of an aircraft, utilized during tests as a target. Thus, during tests of the rocket "Sidewinder" its thermal head led the rocket to target with such accuracy that the last one knocked off an illuminating rocket secured on a wing cantilever of a flying target F-9-F, without striking the actual target [12]. Furthermore, a large quantity of "Falcon" missiles GAR-2A with an infrared homing device was tested with illuminating rockets as targets [15].

These tests allow us to make the conclusion that an aircraft subjected to attack by rockets with infrared homing devices, can protect itself by releasing some kind of powerful source of light and thermal energy [13, 14], which will force the deviation of the follow-up system of the missile and lead it away from the bomb run. It is characteristic that in literature dedicated to the counteraction of infrared means [16], there is noted a necessity for the creation of small-size, high-temperature sources of interferences, whose radiation intensity (integral) would simulate the radiation of jet engines and liquid-fuel rocket engines, even though they have a very short time of action.

Naturally, such high-intensity radiators as illuminating or signal rockets with small burning time, whose purpose is to attract the attacking rocket, must not be in operation while on board the protected aircraft. They must, while burning, be outside the aircraft, more correctly - between the aircraft and the attacking rocket, and at a distance that will protect the aircraft from being hit by fragments during explosion of rocket.

In 1957 there was launched an English rocket with an infrared homing device, the "Firestreak," on a heat source simulating the radiation of an aircraft with a turbojet engine [17]. As a source of radiation, on the towed target was applied a wire frame through which current was passed. Although the emissive power of the radiation of such an "electrical stove" is unknown, the launch of the rocket passed successfully, since there was a direct hit on the target with the heat source.

With a known relationship of distances between an aircraft, the heat source, and the rocket, irradiance of an infrared homing device from a comparatively low-capacity heat source will be larger than from the powerful heat source which is the aircraft, remote from the rocket at a comparatively large distance. Not accidentally, therefore, in the article "Development of Rockets of the "Air - Air" Class in the United States" [3] is it indicated that, along with other methods, counteraction of a bomber to rockets will be carried out by setting up thermal baits. Moreover, in the United States [10] the firm United States Flare Association has begun the serial manufacture of light weight, small-size sources of infrared radiation, intended for installation on target airplanes. The power of these sources in a wave range of 0.75-7 μ constitutes, depending upon dimensions, 500-2,500 w with duration of action 4 minutes.

Having now data on emissive power of radiation of a heat source of radiation (2,500 w) and estimating, tentatively the power of thermal radiation of an aircraft at 25,000 w, it is possible to estimate from what distance the effectiveness of the heat source with respect to its effect on the infrared homing device will become larger than the effectiveness of the radiation of the towing aircraft. We will assume that the distribution of radiation energy in space at the source of heat and for the aircraft is equal, and the ratio of their radiation intensities in the direction of attack is equal to the ratio of emissive power of radiation (Fig. XII.7).

During equality of irradiance of the infrared homing device from the towed heat source and the aircraft, equality is valid (if one ignores the coefficient of transparency of the atmosphere)

$$\frac{J_1}{L_1^2}=\frac{J_2}{L_2^2},$$

since

$$J_1=0J_2,$$

then

$$L_2=\frac{L_1}{3.3}.$$

Consequently, if one were to take L_1 = 660 m, then L_2 = 220 m, and towing distance of the source of thermal radiation will be equal to 440 m. Starting at this distance (660 m) from the aircraft, effectiveness of the action of the thermal radiation source will be continuously increased as compared to the effectiveness of the radiation effect of the aircraft. Thus, for instance, at a distance of 540 m from the aircraft (L_2 = 100 m) irradiance of the infrared homing device from the towed heat source will be 29 times larger than from the radiation of the aircraft.

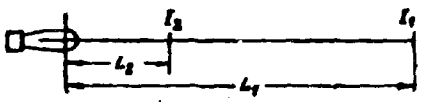

Fig. XII.7. Calculation of the effectiveness of the towed thermal trap.

Aerodynamic heating of the surface of high-speed rockets and also the powerful thermal radiation of their torch in the active section of flight have allowed the assumption that aircraft subjected to the attack of missile with infrared homing devices can render counteraction to them by releasing in the direction of the nearing rocket a counter-rocket whose thermal radiation will force the infrared homing device to deviate from the basic course of tracking [13, 14]. In practice this assumption has been confirmed during tests of the "Falcon" rocket GAR-2A with respect to high-speed rockets and "Matador" missiles [15]. Moreover, the sensitivity of infrared homing devices to the thermal energy of radiation of high-speed rockets

allowed an assumption on the possibility of using their heat for guiding anti-missile missiles [19].

While evaluating the data of the report and recognizing the possibility of clearly pronounced counteraction to infrared means of an enemy with the help of high-speed rockets released in the direction of the nearing enemy, it is impossible not to note the fact that the high cost of rockets and their very limited supply on board the aircraft, obviously, will limit their application as a means of counteraction to only exceptional cases.

Simpler and the least expensive of all the considered artificial sources of radiation may be the method of creating artificial dimming of atmosphere between the aircraft and the attacking enemy with the help of substances, which upon combining with atmospheric oxygen separate a large quantity of heat. In one of the reports [20] there was indicated the creation of a special tracer for tracking flight of the target-missile "Aeromarker", giving a bright flash and a cloud of dense smoke, by which occurs tracking of the flight trajectory of a target-missile. It is noted that the forming cloud well reflects the electromagnetic oscillations of radar range and serves as a source of thermal radiation, useful for guiding infrared systems.

If one were to consider that with this, thermal radiation of the aircraft is simultaneously camouflaged, then the possibility of using tracers for counteracting infrared means of the enemy will become evident since under the cover of such a "smoke curtain" an aircraft can accomplish a maneuver and emerge from under attack.

As a disadvantage of such a form of counteraction one should consider the dependency of the stability of a cloud of smoke on the dimensions of the generators of its particles and the speed of flow of air masses. In spite of this, such artificial smoke clouds, simultaneously camouflaging thermal radiation of an object and being a source of thermal radiation, obviously, will nevertheless be able to find application because of their simplicity, cheapness, and the possibility of

of multiple setting. It is known that in the United States there has been developed a cheap method of obtaining pure titanium tetrachloride, which is an effective smokegenerating substance with good weakening of radiation to 6 μ [27].

Of interest also is research in the region of protection from rockets and reconnaissance artificial earth satellites by means of atomizing in their way clouds of sand or small steel pellets. During collision at great speed of a missile or satellite with such particles destruction should occur, in the first place, of the least durable cowl of the thermal head of the missile or the actual body of the satellite [30, 9] which will lead to their destruction (Fig. XII.8).

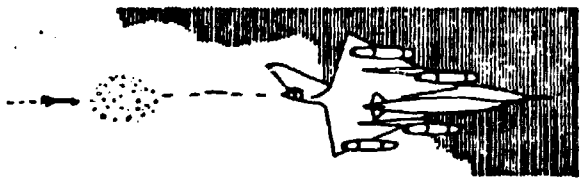

Fig. XII.8. Protection of a bomber with the help of a cloud of small steel pellets.

Bringing to a close consideration of the question about the application of artificial sources of radiation as measures of counteracting infrared means of an enemy, one should mention the intense developments in pilotless carriers of these interferences. Such carriers, at the needed moment, are released from aboard an aircraft and distract to themselves missiles with infrared homing devices.

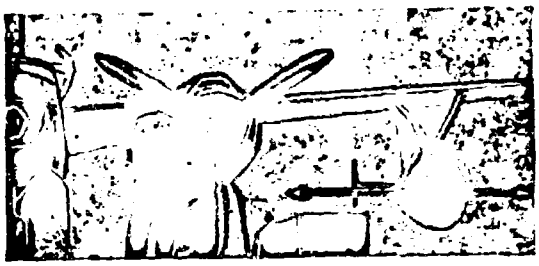

Fig. XII.9. False thermal target "Firebee," suspended under aircraft.

In the United States there has been developed the false thermal target "Firebee," a gliding or remotely controlled flying apparatus launched from land, the deck of a ship, or an aircraft with the help of solid-propellant boosters. Thermal radiators are placed on consoles and are switched on automatically at the moment of launching target (Fig. XII.9).

It is known also that in the United States there has been developed a special missile XKDT-1 as a high-speed flying target for tests of "air - air" missiles with

infrared homing devices [28]. It may be used also as a false thermal target for the protection of ground and air objects.

Literature

1. American Aviation, 1954, 25 Oct.
2. Aeronautics, 1957, Jan., No. 1
3. Missiles and Rockets, 1957, Vol. 2, No. 7; Vol. 2, No. 8.
4. Aviation Week, 1957, Mar.
5. Flight, 1957, Vol. 70, No. 2498.
6. Aviation Week, 1957, 25 Mar., No. 12.
7. Textil-Praxis, 1957, Vol. 12, No. 1.
8. M. A. Ango. Infrared Radiations. State Power Engineering Publishing House, 1957.
9. Aviation Week, 1958, 8 Dec., Vol. 63, No. 23.
10. Aviation Daily, 1958, 28 Nov., Vol. 119, No. 17.
11. Interavia, 1957, Aug., No. 12.
12. Flight, 1957, 7 Jul.
13. Aviation Week, 1957, 6 May, Vol. 66, No. 18.
14. Aircraft, 1957, Jun., Vol. 19, No. 6.
15. Aviation Daily, 1957, 26 Jul., Vol. 111, No. 19.
16. Astronautics, 1958, Mar., No. 6.
17. Aeroplane, 1957, 3 May, Vol. 92, No. 2382.
18. Elektrotechnik, 1955, Sep., No. 3.
19. Interavia, 1956, Oct., Vol. 11, No. 10.
20. Interavia Air Letter, 1957, 30 Apr., No. 3716.
21. Flight, 1957 6 Dec., Vol. 72, No. 2550.
22. "Bulletin NACA", 1954, No. 1182.
23. J. Brit. Interplanet. Soc., 1954, Vol. 13.
24. Flight, 1957, Vol. 71, No. 2512.

25. Aviation Week, 1956, Vol. 65, No. 20.

26. J. Commerce, 1957, 15 Jul.

27. Missiles and Rockets, 1957, Jul.

28. Missiles and Rockets, 1958, Vol. 3, No. 7.

29. Interavia Air Letters, 1960, 26 Feb., No. 4431.

30. Missiles and Rockets, 1959, 31 Aug., No. 36.

DISTRIBUTION LIST

DEPARTMENT OF DEFENSE	NR. COPIES
HEADQUARTERS USAF	
ARL (ARB)	1
OTHER AGENCIES	
CIA	5
DIA	4
ATD	2
NASA (ATSS-T)	1
OAR	1
OTS	2
NSA	6
ARMY (FSTC)	3
NAVY	3
NAFEC	1
AEC	2
RAND	1

MAJOR AIR COMMANDS	NR. COPIES
DDC	20
AFSC	
SCFTC	1
TDBTL	5
TDBDP	2
TDGS	1
TDBMT	5
TDBXP	1
TDT	2
TDBDP (Mrs. Webb)	1
SSD (SSF)	2
TDEED (Bisson)	1
APGC (PGFR)	1
RADC (EMYS)	1